



## Development and application of a milliliter-scale bioreactor for continuous microbial cultivations

**Bolic, Andrijana**

*Publication date:*  
2018

*Document Version*  
Publisher's PDF, also known as Version of record

[Link back to DTU Orbit](#)

*Citation (APA):*  
Bolic, A. (2018). Development and application of a milliliter-scale bioreactor for continuous microbial cultivations. Kgs. Lyngby: Technical University of Denmark (DTU).

## DTU Library

Technical Information Center of Denmark

---

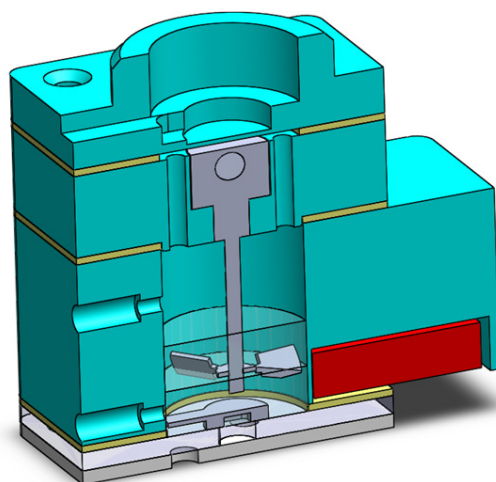
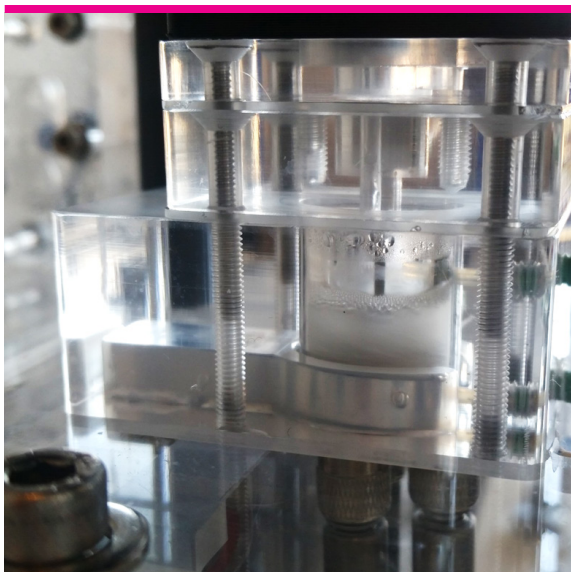
### General rights

Copyright and moral rights for the publications made accessible in the public portal are retained by the authors and/or other copyright owners and it is a condition of accessing publications that users recognise and abide by the legal requirements associated with these rights.

- Users may download and print one copy of any publication from the public portal for the purpose of private study or research.
- You may not further distribute the material or use it for any profit-making activity or commercial gain
- You may freely distribute the URL identifying the publication in the public portal

If you believe that this document breaches copyright please contact us providing details, and we will remove access to the work immediately and investigate your claim.

# Development and application of a milliliter-scale bioreactor for continuous microbial cultivations



**Andrijana Bolić**

PhD Thesis

February 2018

Copyright©: Andrijana Bolić

February 2018

Address: Process and Systems Engineering Center (PROSYS)

Department of Chemical and Biochemical

Engineering Technical University of Denmark

Building 229

Dk-2800 Kgs. Lyngby

Denmark

Phone: +45 4525 2800

Web: [www.kt.dtu.dk/forskning/prosys](http://www.kt.dtu.dk/forskning/prosys)

Print: STEP

**DTU Chemical Engineering**

Department of Chemical and Biochemical Engineering

---

**DTU Chemical Engineering**

Department of Chemical and Biochemical Engineering

# Development and application of a milliliter-scale bioreactor for continuous microbial cultivations

---

**Andrijana Bolić**

PhD Thesis

Kongens Lyngby, 2018

The workhorses of process development, optimization and characterization in the biotech and the pharmaceutical industry are microtiter plates, shake flasks and bench scale bioreactors. They are widely used in academia as well, and with a good reason. Beside inherent benefits, they have standardized properties and have been studied extensively, and thus they offer the possibility to compare research results and to rely on an already collected knowledge base. However, they also have shortcomings, which were emphasized in a recent past and today by development of genetic engineering techniques that enable genetic manipulation of microorganisms, producing more strains and thereby creating a need for even more processes that need to be evaluated than ever before. In order to provide a high-throughput solution to this issue and cut the cost, time spent and the general labor intensity per experiment, a new experimental approach is necessary. Micro- and milliliter scale bioreactors are considered as an adequate solution to address this experimental challenge, since they unite the possibility of parallelization with better control and sensing performance.

Current state of the art research on micro and milliliter scale bioreactors shows a spectrum of different approaches in providing an adequate environment for microbial cultivations with small footprint. Currently, there is no consensus on the choice of best suited working volume for the small scale bioreactors, ranging from nanoliters, over microliters to milliliter scale, which raises a question of potential application and what is the aim or purpose of the developed tool. Examining commercial solutions, it is clear that two design directions are adopted for submerged microbial cultivations: (1) microtiter plate modifications to gain a more controlled environment and better sensing performance in each well (usually up to 2 mL volume); and (2) small scale stirred tank bioreactors for better scale up performance (10-15 mL volumes).

Adequate sensing and mixing with an impeller that enables a good oxygen transfer rate at 1-2 mL scale was investigated and addressed in this thesis, by designing and fabricating two prototypes of milliliter scale bioreactors (MSBR). The engineering design process methodology was utilized to answer the question: "How to go from idea to prototype?" and to find ways to evaluate and materialize ideas. The designed milliliter scale bioreactors aimed to provide the middle ground between the two established bioreactor design directions mentioned above and explore benefits and drawbacks of milliliter scale bioreactors during batch and continuous microbial cultivations.

The first prototype (MSBR I) consisted of a reusable platform containing heater, gas connections, temperature sensor and three optical fiber bundles, and a milliliter scale bioreactor with special stirrer and sensors for measurement of dissolve oxygen, pH and scattered light intensity. A modular approach in design and fabrication provided high flexibility in the choice of working volume (0.5 – 2 mL), aeration type (sparger or surface aeration) and mixing possibilities (one- and bi-directional). The MSBR I exhibited short

mixing times and a high oxygen transfer rate at higher mixing speeds. On-line measurement of the scattered light intensity was based on a transfectance measurement where light was sent through the MSBR bottom and sample to a mirror-like surface in the MSBR and returned back to a fiber bundle. Aerobic and anaerobic batch cultivations were performed with *Saccharomyces cerevisiae* and *Lactobacillus paracasei*, respectively. A high evaporation rate was experienced during cultivations as a penalty for the lack of a proper humidifier and control of gas flow rates.

The second prototype (MSBR II) had a similar modular concept to the previous one, however heater, temperature sensor and gas connections were moved from the platform to the bioreactor, while the three optical fiber bundles and the heating element that was in contact with the heater were part of the platform. The MSBR II also had a sensor for dissolved oxygen and a small stainless steel element that was used for acquiring a scattered light intensity measurement via transfectance. The stirrer had four impeller blades and a simplified structure compared to the stirrer in the previous prototype. The mixing time was longer than in the MSBR I, but efficient mixing was still obtained. A humidifier was developed for this platform and evaporation was reduced substantially.

The interaction between end user and small scale bioreactor platforms is usually challenging if not automated, due to practical issues that the small scale brings along. Connectivity between the small bioreactor and the macro world is troublesome without standardized solutions. Furthermore, any additional equipment required to complete bioreactor functionality usually comes in regular lab size, which then transforms a small scale bioreactor platform to a regular size experimental set up. To address this issue, effort was placed in developing 2 push/pull pumps that were able to deliver gas and medium in a controlled manner as a part of the MSBR II platform design.

Cultivations with *Saccharomyces cerevisiae* as model organism were performed in the MSBR II where batch mode produced sustainable and reproducible results and displayed the expected growth profile while continuous mode cultivations were performed with limited success. With few further design improvements, the MSBR II platform has the potential to become an experimental tool that will sustainably support microbial cultivations at milliliter scale. Afterwards, implementation of parallelization should be relatively straightforward.

Hovedparten af procesudvikling, optimering og karakterisering i den bioteknologiske og farmaceutiske industri bliver udført i mikrotiter plader, rystekolber og laboratorie bioreaktorer. Det samme gør sig gældende i forskningsverdenen, og med god grund. Foruden umiddelbare fordele, er disse reaktorer standardiseret og studeret grundigt, hvilket muliggør sammenligning af forskningsresultater med historisk data. De har dog også en række ulemper, hvilket blev tydeliggjort ved udviklingen af nye teknologier til gensplejsning af mikroorganismer, der fører til mange flere evalueringer af stammer og processer end hidtil. I et forsøg på at levere effektive løsninger til denne udfordring og sænke udgift og arbejdsbyrde per eksperiment, er det nødvendigt at udvikle nye eksperimentelle procedure. Bioreaktorer med en kapacitet i mikro- og milliliter størrelsesordenen ses som en mulig løsning på denne eksperimentelle udfordring, da de forener parallelisering og bedre proces analyse end traditionelle teknologier.

Nuværende teknologi indenfor bioreaktorer i mikro -og milliliter størrelsesordenen indikerer et bredt spektrum af løsninger hvilket leverer et tilfredsstillende system til kultivering af mikroorganismer med en lille miljøbelastning. I øjeblikket findes der ingen konsensus omkring det bedste udgangspunkt i forhold til kapacitet indenfor små bioreaktorer, hvilket spænder fra nanoliter over mikroliter til milliliter størrelsesordenen. Dette sætter spørgsmålstegn ved potentialet og målet for det udviklede værktøj. Kommercielle løsninger går tydeligt i to retninger indenfor kultivering af mikroorganismer: (1) modificerede mikrotiter plader som giver mulighed for bedre kontrol og monitorering af processen (normalt omkring 2 mL); og (2) mindre omrørte reaktorer, som skalerer bedre (10-15 mL).

Tilstrækkelig måling og omrøring med et rørværk der giver god overførsel af oxygen i reaktorer størrelsesordener af 1-2 mL er undersøgt i denne afhandling, ved at designe og konstruere to milliliter skala bioreaktor (MSBR) prototyper. Den ingeniørmæssige designfremgangsmåde blev valgt ved at svare på spørgsmålet: "Hvordan går man fra idé til prototype?" og ved at udvikle metoder til at evaluere og konkretisere idéerne. De udviklede bioreaktorer var beregnet til at give et kompromis mellem de to veletablerede design retninger beskrevet ovenfor og udforske fordele og ulemper ved milliliter bioreaktorer under batch og kontinuert kultivering af mikroorganismer.

Den første prototype (MSBR I) var opbygget af en platform med varmelegeme, gasfittings, termometer og tre optiske fibre, samt en bioreaktor ved et specielt designet rørværk og sensorer til måling af ilt, pH og optisk densitet. En modulær fremgangsmåde i design og konstruktion gav stor fleksibilitet i fyldningsgrad (0.5- 2 mL), gas tilførsel (sparger eller ilt tilførsel via overflade) og omrørings mulighed (envejs eller tovejs). MSBR I viste korte blandetider og høje iltoverførselshastigheder ved høje omrøringshastighed. Online måling af optisk densitet var baseret på måling af transflektans, hvor lys sendtes gennem bundten

af reaktoren og media til en reflekterende overflade hvorefter det sendes tilbage til den optiske fiber. Aerobe og anaerobe batch fermenteringer blev udført med henholdsvis *Saccharomyces cerevisiae* og *Lactobacillus paracasei*. Fordampning af vand var meget udpræget gennem fermenteringen grundet dårlig befugtning af gasflowet og begrænset kontrol af gastilførsel.

Den anden prototype (MSBR II) benyttede samme modulære opbygning som den forrige, dog var varmelegeme, termometer og gasfittings flyttet fra platform til bioreaktoren, medens de tre optiske fibre og varme element forblev på platformen. MSBR II har ligeledes en sensor til måling af ilt og et rustfrit stål element der blev benyttet til at måle optisk densitet vha. transflektans. Omrøreren havde fire blade og en forenklet struktur sammenlignet med den forrige prototype. Blandetiden var længere end for MSBR I, men det var dog stadig muligt at opnå effektiv blanding. En befugter var endvidere udviklet til denne platform og fordampningen var derfor reduceret drastisk.

Interaktionen mellem bruger og bioreaktor er normalt en udfordring når der arbejdes med mikroskala og milliliter skala reaktorer, medmindre interaktionen er automatiseret, grundet de praktiske problemer i den lille skala som er undersøgt i denne afhandling. Forbindelse mellem den lille bioreaktor og omverdenen er besværligt uden standardiserede løsninger. Endvidere fås alt funktionelt udstyr til bioreaktorer kun til bioreaktorer der bruges til normal laboratorie fermentering, hvilket gør at en lille bioreaktor opstilling næsten fylder det samme som en almindelig laboratorie skala fermentor. For at omgå dette problem blev der udviklet to stempelpumper som kunne levere gas og media på en kontrolleret måde. Dette blev en del af platformen i designet af MSBR II.

Kontinuert fermentering blev udført i MSBR II, med *Saccharomyces cerevisiae* som "model organisme", hvor batch fasen gav reproducerbare resultater og viste den forventede vækstprofil, hvorimod den kontinuerte fase havde begrænset succes. Ved få forbedringer har MSBR II potentialet til at blive et holdbart eksperimentelt værktøj der kan supportere kontinuert kultivering af mikroorganismer i milliliter skala. Derefter vil parallelisering være relativt nemt.



To Vuk, Anja and Nenad

The work described in this thesis was conducted at the Process and Systems Engineering Center (PROSYS), Department of Chemical and Biochemical Engineering, Technical University of Denmark (DTU) from March 2010 until February 2017 in partial fulfillment of the requirements for acquiring the Ph.D. degree in Chemical Engineering. It was supported by the Danish Council for Strategic Research in the frame of the project “Towards robust fermentation processes by targeting population heterogeneity at microscale” (project number 09-065160). Originally, this PhD project was supposed to last until February 2013, however during the course of the project time life happened twice, meaning I was on two maternity leaves. Although longer breaks during the research process are not ideal, they were useful to me, since they gave me the possibility to look at my work from a unique perspective. As a result, I was able to quickly find better and more optimal solutions to occasional problems, to make a compromise when needed and set realistic goals toward the end of this project, considering time was a valuable asset which is not abundant when there is a toddler and a baby mixed in the equation.

Professor Krist V. Gernaey (Department of Chemical and Biochemical Engineering) was the principal supervisor and Associate Professor Anna Eliasson Lantz (Department of Chemical and Biochemical Engineering) together with Professor Karsten Rottwitt (Department of Photonics Engineering) were co-supervisors on the project.

The story of how this thesis came into being starts with me reading a description of a PhD vacancy at the DTU website. At that time I was vaguely familiar with the concept of miniature reactors and their purpose, since my previous project was in Unilever and related to Lipton tea. Considering that sustainability and the concept ‘less is more’ are desperately needed in the world today, small scale reactors seemed as a right topic to be tackled by science and me. I visited DTU and after seeing a reactor with 100  $\mu\text{L}$  volume, I was enticed. The mentioned microreactor was part of PhD work done by Daniel Schapper and it was the starting point of my project.

The main hypothesis of the overall project was based on the research that has shown the existence of heterogeneity in microbial populations during a fermentation process. The idea of the project was to find out what would be the optimal population heterogeneity to be able to obtain maximal yields, productivity and robustness of the fermentation process. In order to study this topic in detail, a microreactor was observed as a tool that could provide insight into the effect of cultivation parameters on growth and productivity. Furthermore, it could also be coupled with on-line spectroscopic measurements providing more details on the correlation between essential variables.

My work started immediately in the lab where I was being introduced to in-house manufacturing practice of the microreactor, learning how to use a Computer Numerical Control (CNC) milling machine and go from an assembly made in the software

SolidWorks to a Computer Aided Design (CAD) drawing and afterwards to a G-code - language for the CNC milling machine. I became acquainted with different materials e.g. polydimethylsiloxane (PDMS) and poly(methyl methacrylate) PMMA, their properties and possible applications. During the learning process I was trying to reproduce work based on the 100  $\mu$ L microreactor, mostly focusing on improvement and mastering of the manufacturing process. Afterwards, a first fermentation was run with limited success.

As with anything in life, there is always space for further development. Based on the difficulties that I encountered during work with a 100  $\mu$ L volume microreactor I decided to abandon the submilliliter design constraint. By increasing the volume of the microreactor I dived in a design process with new specifications that were supposed to address the difficulties encountered in the previous design and obtain a reactor that is more user-friendly and robust. The product of this decision, and the work performed during this project, is presented in this thesis.

Kgs. Lyngby, February, 2017

Andrijana Bolic

## Acknowledgements

---

My PhD study at DTU happened to be quite a long journey with many expected and unexpected life events. It was not an easy journey, and not without obstacles in the scientific realm as well, but then again progress and development in personal or professional life comes with a lot of hard work, perseverance, passion and challenging yourself on a daily basis. I was lucky to be surrounded with great people that empowered me to always move forward.

Krist V. Gernaey, I am grateful for your belief in me through all this time, for all the support and enormous patience. It was nice to have a supervisor with open, clear and honest communication style as well as being open-minded and responsive to different needs of the project and challenging situations.

Anna Eliasson Lantz, thank you for good discussions regarding cultivation results and your guidance and knowledge during experimental work. With your help, experimental procedures related to the biological part of the project were effectively implemented without any issues.

Francesco Christino Falco and Katrin Pontius thanks for being great lab buddies. Experimental work and long hours in the lab were more fun in good company. Francesco, thank you for your knowledgeable inputs and all the practical help in the lab.

Aleksandar Mitic, cheers for all the lunch breaks we had together where you patiently listened to all my complaints when experiments didn't go well. Thanks for being supportive in the lab searching for chemicals and different pieces of equipment when I needed them.

Special thanks go to Ivan Horst Pedersen and his workshop team for fruitful collaboration and their readiness to help me promptly with practical problems, when I needed solutions not for today or tomorrow, but for yesterday.

PROCESS, then CAPEC-PROCESS and now the Process and Systems Engineering Center (PROSYS) would not be such a nice place to work without positive, friendly and outgoing colleagues, with whom I enjoyed many coffee breaks. Big thanks go to all people that I worked with in recent and distant past in our research center.

Biggest gratitude goes to my family, to my husband Nenad for constant and selfless support and encouragement, for being my academic sparring partner and technical support when needed; to Vuk and Anja for being understanding and patient when mom needed to work instead of playing.

Hvala ti mama za svu podrsku i ljubav. Od malena pa do danas uvek si bila uz mene, verovala u moje sposobnosti, bila ponosna na svaki moj uspeh i bodrila me u teskim trenucima.

<b>Abstract</b> .....	i
<b>Resumé</b> .....	iii
<b>Preface</b> .....	vi
<b>Acknowledgements</b> .....	viii
<b>Table of Contents</b> .....	ix
<b>List of Figures</b> .....	xii
<b>List of Tables</b> .....	xv
<b>Chapter 1 Introduction</b> .....	1
1.1 Application is a key starting point.....	1
1.2 Why small scale?.....	2
1.3 Outline of the thesis .....	4
1.4 Dissemination of accomplished results.....	5
<b>Chapter 2 Review of small scale bioreactors developed for cultivation processes in academy and industry</b> .....	7
2.1 Overview of small scale bioreactors and their application in microbial and cell cultivations .....	7
2.2 High throughput small scale platforms for cultivation processes .....	6
2.3 Cultivation modes and <i>Saccharomyces cerevisiae</i> as a model organism .....	10
2.4 Scope of the thesis and specific objectives of the project.....	12
<b>Chapter 3 The engineering design process methodology</b> .....	14
3.1 Introduction.....	14
3.2 Step 1: Problem formulation .....	15
3.3 Step 2: Gather required knowledge .....	17
3.4 Step 3: Brainstorm and develop solutions .....	18
3.5 Step 4: Evaluate and select possible solution .....	21
3.6 Step 5: Build a prototype .....	23
3.7 Step 6: Test prototype .....	25
3.8 Step 7 and 8: Evaluation of the prototype performance (7) and redesign if needed (8) .....	26
<b>Chapter 4 Milliliter scale bioreactor design - Prototype I</b> .....	27
4.1 Introduction.....	27
4.2 Materials and Methods.....	29

4.2.1	Milliliter scale bioreactor platform – Prototype I.....	29
4.2.2	Milliliter scale bioreactor design – Prototype I.....	30
4.2.3	Stirrer design and fabrication – Prototype I.....	32
4.2.4	Control algorithm and mixing profiles.....	33
4.2.5	Measurement of scattered light intensity (SLI) for biomass monitoring...	36
4.2.6	Determination of mixing time.....	37
4.2.7	Residence time distribution.....	38
4.2.8	Oxygen transfer rate - $k_{La}$ measurement.....	39
4.2.9	Evaporation .....	41
4.2.10	CFD .....	41
4.2.11	Microbial Strain.....	43
4.2.12	Medium Composition .....	43
4.2.13	Batch Cultivation .....	44
4.2.14	Monitoring and control.....	45
4.3	Results and Discussion .....	47
4.3.1	Measurement of scattered light intensity (SLI) for biomass monitoring...	47
4.3.2	Mixing time.....	48
4.3.3	Residence time distribution.....	51
4.3.4	Oxygen transfer rate - $k_{La}$ measurements.....	53
4.3.5	Evaporation .....	56
4.3.6	CFD .....	57
4.3.7	Batch cultivation in the MSBR .....	60
4.4	Conclusion.....	65
	<b>Chapter 5 Milliliter scale bioreactor design – Prototype II.....</b>	<b>67</b>
5.1	Introduction.....	67
5.2	Materials and Methods .....	68
5.2.1	Milliliter scale bioreactor platform – Prototype II.....	68
5.2.2	Humidifier – Prevention of evaporation.....	69
5.2.3	Syringe pump system.....	71
5.2.4	Milliliter scale bioreactor design– Prototype II .....	75
5.2.5	Temperature .....	79
5.2.6	Measurement of scattered light intensity (SLI) for biomass monitoring...	80
5.2.7	Determination of mixing time.....	81
5.2.8	Microbial strain .....	81
5.2.9	Medium composition .....	81
5.2.10	The MSBR II preparation for cultivation.....	83
5.2.11	Cultivation conditions.....	84
5.2.12	Monitoring and control.....	85

5.3	Results and Discussion .....	91
5.3.1	Temperature .....	91
5.3.2	Measurement of scattered light intensity (SLI) for biomass monitoring...	95
5.3.3	Mixing time.....	100
5.3.4	The MSBR II platform hardware performance during continuous cultivations	104
5.3.5	Initial batch phase of the cultivations in the MSBR II (first part of the continuous cultivation) .....	108
5.3.6	Continuous mode of cultivation in the MSBR II .....	111
5.4	Conclusion.....	115
	<b>Chapter 6 Conclusion and future perspectives .....</b>	<b>117</b>
6.1	Conclusion.....	117
6.2	Future work.....	119
	References.....	123
	<b>Appendix A .....</b>	<b>133</b>
	<b>Appendix B.....</b>	<b>137</b>
	<b>Appendix C.....</b>	<b>145</b>
	<b>Appendix D .....</b>	<b>168</b>
	<b>Appendix E.....</b>	<b>171</b>

## List of Figures

---

Figure 1.1. Different vessels (microtiter plates, shake flasks and bench scale bioreactor) and their positioning according to achievable throughput (experiments/ tests performed simultaneously) and data quality (sets of data that are accurate, consistent, comprehensive, relevant and accessible). .....	2
Figure 1.2 The structure of the PhD thesis presented in graphical form. ....	4
Figure 2.1. Schematic representation of monitoring and control strategies for important process parameters (temperature, dissolved oxygen and CO <sub>2</sub> , pH and cell concentration) at small scale. ....	5
Figure 2.2. Example of a growth curve of a microbial culture in a batch cultivation adapted from [89]. ....	10
Figure 2.3. The glycolysis pathway (left side picture); fermentation and respiration pathways (right side picture) are same until pyruvate, after they split to fermentative or respiratory pathway. Pictures are adapted from [92]. ....	12
Figure 3.1. Iterative steps in the design process of a milliliter scale bioreactor with the problem formulation step as the starting point. ....	14
Figure 3.2. Photo of the 100 $\mu$ L microbioreactor reproduced from the PhD thesis of Daniel Schapper [100]. ....	16
Figure 3.3. Representation of the complexity of the microbioreactor design. Green bubbles represent the main functions that are pillars of the microbioreactor design, while orange bubbles present what needs to be included in each function so it can be complete. ....	19
Figure 4.1. The millilitre-scale bioreactor supporting platform is made of a PMMA plate with 4 metal rods as plate holder. In the middle of the plate, a pocket is made with designated islands for the temperature sensor, the heater, three optical fibre bundles used for measurement of OD, DO and pH, and finally openings for aeration tubes. Around the pocket, 4 electromagnetic coils are positioned. A technical drawing of the platform is presented in appendix B. ....	29
Figure 4.2. The MSBR designs with one (maximum volume 1 mL) and two polymer block chambers (maximum volume 2 mL) (Dassault Systèmes SOLIDWORKS Corp., DTU licence). Both reactors have the same features, except for the working volume that is bigger in the reactor with two PMMA block chambers. The light purple plate in the exploded view of the MSBR shows areas where heater and optical probes are placed when the MSBR I is positioned on the platform. The tube used for aeration is ending in a small microchannel that is connected with the cultivation chamber (visible in the wall of the MSBR and enlarged in the lower part of the figure). The yellow layer is made from PDMS and it is used to seal the reactor. Another PDMS layer is used when an additional PMMA block is added on top (it is not shown in the figure). A technical drawing of the reactor is presented in appendix B. ....	31
Figure 4.3. Mixer design (Dassault Systèmes SOLIDWORKS Corp., DTU licence). The stirrer consists of two cylinder pockets where a ring-shaped magnet is encapsulated.	



Each cilinder has two forks for holding two blades, so the impeller blades can be placed at two levels. A technical drawing of the stirrer is presented in appendix B. .	33
Figure 4.4. Position of the four coils around the microbioreactor. The principle of magnetic stirring is presented in the right picture showing interaction between the magnetic field created by the magnetic coils and the magnet that is magnetised across its diameter. ....	34
Figure 4.5. Signal flow from end user to the power supply. End user uses Labview interface to set impeller speed by adjusting rpm on a provided scale (left picture). This information is translated by the puls-width modulation technique to a signal (middle picture) that is applied to the magnetic coils by switching the power supply mode (right picture). ....	35
Figure 4.6. Scattered light intensity (SLI) measurement. An LED (light-emitting diode) is used as a source of light at 600 nm wavelength. Light was guided by an optical fibre to the beam splitter that divided the light intensity to two light paths with 70% and 30% intensity, respectively, compared to the incoming light. 30% light was sent directly to a photodiode as reference signal while 70% light was used to measure the current condition in the MSBR. The resulting light from the MSBR was guided to another photodiode. ....	37
Figure 4.7. Conductivity probe used during residence time distribution experiments. The solution passed through plastic tubing and it entered to brass tubes (electrodes) while a voltage was applied on the electrodes. The created current together with the applied voltage were used for the calculation of resistance and indirectly the electrical conductance (1/resistance). ....	39
Figure 4.8. (a) The unstructured mesh used for the simulations; (b) The geometry setup showing the rotating element and the steady shaft and holder. The position of the gas-liquid interface at rest is indicated (turquoise), as well as the position of the source point (red octahedron) and the monitoring point (blue ball) that were used in the transient mixing simulations. ....	42
Figure 4.9. The LabView program overview. A high speed card was used for handling dissolved oxygen and pH measurement while a low speed card was used for measurement of the SLI and temperature. ....	46
Figure 4.10. Module for mixing control is added to the Labview program made by Daniel Schapper [100]. ....	46
Figure 4.11. Principles of transmission, reflection and transfection measurements. Incident light that illuminates samples is marked with $I_0$ , while the transmitted light is presented by $I_T$ , reflected light is presented by $I_R$ and the resulting light in case of the transfection measurement is presented by $I_{TR}$ . ....	47
Figure 4.12. Principle of the scattered light intensity (SLI) measurement and calibration curve. Detail explanation of the SLI measurement is presented in figure 4.6., section 4.2.5. ....	48
Figure 4.13. Mixing time determination experiment, here for determining the mixing time at 600 rpm stirring speed. At time = zero seconds, HCl is added in the MSBR that was filled with water, NaOH and phenolphthalein. Stirring disperses the HCl all over the	

MSBR and enables acid-base neutralization to occur which resulted in a color transition of the liquid from pink to transparent in less than 2 seconds.....	49
Figure 4.14. Decrease of the mixing time with the increase of the stirrer speed (rpm) during unidirectional mixing in the MSBR with 1 mL working volume. ....	50
Figure 4.15. The experimental results showing distribution of a tracer measured at the outlet of the MSBR.....	51
Figure 4.16. (a) The volumetric mass transfer coefficient - $k_{L,a}$ at different mixing speeds and for different aeration modes; (b) Influence of MSBR working volume on $k_{L,a}$ (c) Effect of viscosity change on $k_{L,a}$ . Results presented here are average values of 3 to 5 experiments per condition evaluated. ....	55
Figure 4.17. The simulated gas-liquid interfaces at the different rotational speeds in the MSBR. ....	57
Figure 4.18. The simulated versus the experimental $k_{L,a}$ values for different rotational speeds. ....	58
Figure 4.19. The simulated versus the experimental mixing times. Mixing time was defined as the time when the concentrations entered within the $\pm 5, 10$ or $15\%$ interval of their final (average) value, i.e. the concentration that is achieved once the additional variable was homogenously distributed in the liquid. ....	59
Figure 4.20. (a) The distributions of the additional variable over time for 800 and 1000 rpm simulation. The coloring scheme is applied, i.e. additional variable values higher than the $\pm 10\%$ interval are displayed as red and values lower than this interval are blue. Values within the interval are turquoise. (b) The concentrations of the additional variable in the 800 and 1000 rpm mixing simulations. The maximal values and the values in the monitoring point are displayed as well as the $\pm 10\%$ interval from the final value. ....	60
Figure 4.21. Cultivation with <i>L. paracasei</i> in the MSBR. Temperature, DO, pH and scattered light intensity data during 11 h cultivation time are shown. ....	61
Figure 4.22. Process parameters during cultivation with <i>L. paracasei</i> in the 2 L bioreactor scale. Off-line OD, temperature, pH and added base per time and total added base during 16 h cultivation time are shown on the first graph. OD and HPLC results from the cultivation with <i>L. paracasei</i> in the 2 L scale are presented in the second graph [133].....	62
Figure 4.23. Aerobic cultivation with <i>S. cerevisiae</i> , strain CEN.PK-113-7D. Temperature, DO, pH and scattered light intensity data during 40 h cultivation time.....	64
Figure 5.1. The MSBR platform with heat exchanger 2 (Dassault Systèmes SOLIDWORKS Corp., DTU licence). Technical drawings of the platform can be seen in appendix C. ....	68
Figure 5.2. Psychrometric chart [137]. Dry bulb temperature (measured by a dry thermometer); Wet bulb temperature (measured by a wetted sensor tip); Dew point temperature (when moist air sample reaches water vapor saturation); Relative humidity (ratio of the fraction of water vapor in air to the fraction of water in saturated moist air at the same temperature and pressure); humidity ratio (the mass	

of water vapor per unit mass of dry air); enthalpy (total heat energy of the moist air); specific volume (volume per mass of air sample). When air at room temperature (22°C) and relative humidity of 30% (point A on chart) enters to the MSBR at temperature 30°C (point B on chart), relative humidity decreases to 20%. If air stays long enough in the MSBR at 30°C, relative humidity will increase to a certain value, e.g. 80% and a certain amount of water will be lost due to evaporation. In order to prevent this process, it is important to increase the relative humidity in the headspace as much as possible (point E on chart). Ideally, humidified air at slightly higher temperature than the one in the MSBR (point D) can be introduced to the MSBR to reduce evaporation to a minimum. Moving from point D to point E along the green line in figure 5.2 it can be seen that the water content in the air is not lost due to evaporation and the relative humidity of air is increased. However, increasing further relative humidity, point D would move above the current point and will be above dew point temperature in the MSBR and condensation would occur. ....70

Figure 5.3. Pre-humidifier – red heating element (aluminum plate, copper wires and thermocouple encapsulated in epoxy from the bottom side) and grey shaft with stirrer in turquoise box (Dassault Systèmes SOLIDWORKS Corp., DTU licence). Technical drawings of the humidifier can be found in appendix C. ....71

Figure 5.4. Syringe pump – push pull working principle (Dassault Systèmes SOLIDWORKS Corp., DTU licence). Three positions of the pump with syringe groups A and B are presented in the figure and are indicated with numbers 1, 2 and 3. The figure illustrates a process where fluid is pumped in to the syringes from the group B while fluid is pumped out from the syringes in the group A. During this process, the slider (pink element in the middle, connected to the linear bearings and the shaft of the motor) is moving its position from the closest to the motor in step 1, to the furthest away from the motor in a step 3. With this motion, the volume of the group B syringes will increase from 0 to max, while opposite will be true for the group A. Technical drawings of the pump can be found in appendix C. ....73

Figure 5.5. One-way valves bridge configuration (Dassault Systèmes SOLIDWORKS Corp., DTU licence). Four one-way umbrella valves are arranged in a “bridge” configuration. This configuration ensures the one-way flow from the inlet port to the outlet port of the part, assuming the syringes from two groupes are used on the pump ports. Technical drawings of the one-way valves bridge configuration can be found in appendix C. ....74

Figure 5.6. The MSBR prototype II – assembly, cross section and exploded view (Dassault Systèmes SOLIDWORKS Corp., DTU licence). The milliliter scale bioreactor had two inlets and two outlets (for medium and air), a magnet attached to the shaft and stirrer, DO sensor spots, a stainless steel element for OD and T measurement and a heater. PDMS layers were used between PMMA blocks for sealing purposes. ....76

Figure 5.7. The MSBR experimental set-up: A and B - the milliliter scale bioreactor during cultivation; C – the MSBR before being assembled; D - the stirrer with two impellers; F - the whole platform with both pumps. ....78

Figure 5.8. Block diagram of the cascade regulation. ....79

Figure 5.9. End-user interface of the Labview control routine. ....85

Figure 5.10. Sequence of steps performed in the Labview program in order to measure and control process parameters during cultivation in the MSBR. ....	86
Figure 5.11. Communication between software and peripheral units. ....	87
Figure 5.12. The DC drive converts a constant 12 V input voltage and generates output voltage in the range -12 to +12 V based on the control inputs. ....	88
Figure 5.13. The stepper drive generates two phase output voltages with phase shift of 90 deg in order to drive the stepper motor. The input voltage is 12 V and the control inputs are the step rate input and the direction of the rotation input. ....	90
Figure 5.14. Temperature profile in the MSBR and control capabilities during multiple set point changes (heating and cooling). T sp is the temperature set point; T msbr is the temperature recorded in the MSBR. Temperature control was more effective during heating than during the cooling process. At temperatures closer to the room temperature, the cooling step was longer, which can be seen in the last T set point change from 30°C to 26°C. ....	92
Figure 5.15. Temperature profile of heat exchangers and the MSBR during the set-point change from 32 to 35° C. When the set point for temperature in the MSBR was changed, also the set point for temperature of the heating element was changed due to the action of the cascade controller. T msbr is the recorded temperature in the MSBR; T he represents the recorded temperature of the heating element that is in direct contact with the heater in the MSBR; T sp is the set point for the temperature in the MSBR; T sp he is the set point for the temperature of the heating element. ....	93
Figure 5.16. Heat exchanger II – 2 aluminium plates (orange and grey blocks) and Peltier element (red block) placed in plastic casing (two blue blocks) with heat sink (grey block with yellow fan). ....	93
Figure 5.17. Cascade regulation response to introduction of a temperature disturbance in the MSBR. With introduction of the disturbance (cold water) in the MSBR, temperature of the liquid in the reactor dropped from 30 to 25°C. Consequently, the temperature of the heating element increased to compensate for the disturbance. T msbr is the recorded temperature in the MSBR; T he is the recorded temperature of the heating element that is in direct contact with the heater in the MSBR. ....	94
Figure 5.18. Influence of light intensity on measurement range and sensitivity of biomass concentration. ....	96
Figure 5.19. Exponential correlation between OD determined in the MSBR and by the spectrophotometer at 600 nm corrected for sample dilution. ....	97
Figure 5.20. Linear correlation between OD determined by the spectrophotometer and cell dry weight. ....	97
Figure 5.21. Exponential function used to establish a direct correlation between OD determined in the MSBR and dry cell weight. ....	98
Figure 5.22. Light pathway in two prototypes: MSBR II (left) and MSBR I (right). ....	99
Figure 5.23. Determination of mixing time in the MSBR for an experiment with 200 rpm mixing speed. ....	101

Figure 5.24. Mixing times at different mixing speeds in the MSBR (2 mL). For different string speeds 3 – 5 experiments were performed to determine mixing time in the MSBR. With increase of stirrer speed, mixing time decreased. Also, addition of another impeller to the existing one decreased the mixing time substantially which can for example be seen for the data obtained at 200 rpm stirring speed.....	102
Figure 5.25. Batch phase of the last cultivation performed with <i>Saccharomyces cerevisiae</i> ..	109
Figure 5.26. Initial batch phase of three different cultivations with <i>Saccharomyces cerevisiae</i> . .....	110
Figure 5.27. Continuous mode MSBR operation for three different cultivations with <i>Saccharomyces cerevisiae</i> .....	112

## List of Tables

---

Table 2.1. Overview of different micro- and milliliter- scale bioreactors (in chronological order).....	9
Table 2.2 Scale influence on bioreactor characteristics and bioprocess condition.....	3
Table 3.1. Decision matrix for heater design. Three criteria are used and a certain importance is assigned to each of them. Seven ideas presented in the text above are assessed against these criteria and rated according to a 5- point scale. Each assigned number from the 5-point scale was multiplied by a weight. The sum of the resulting values gave the main scores for each idea, which were then compared in order to choose the best idea.....	22
Table 3.2. Specifications for the prototype I.....	24
Table 4.1. Four different ratios between a 3% CMC solution and water produced four model solutions with different viscosities. ....	40
Table 4.2. Mean residence time and dimensionless variance of the mean residence time at different rpm and air flow rates. ....	53
Table 4.3. Performance comparison between cultivations at 2 L and 2 mL scale [133]. ....	63
Table 5.1. Mixing times for different stirrer speeds in prototype I and II. ....	103
Table 5.2. Summary of problems that occurred and solutions that were implemented during cultivations in the MSBR .....	104
Table 5.3. Growth rate comparison between three different cultivations. ....	111

### 1.1 Application is a key starting point

In the last decade rapid technological progress has brought about new alternative ways of thinking about old problems, and as a result major breakthroughs occur in a blink of an eye in many different industries. Particularly this phenomenon takes place when a cross-over between fundamentally different and usually segregated disciplines occurs. Suddenly semiconductor manufacturing methods find an important role in applications such as fuel and solar cells, disposable blood testing cartridges, ink jet print heads, different micro sensors and medical components. 3D printing allows complex shapes to be produced using different types of materials, and as a result we can suddenly enjoy eating printable food or wearing printable clothing. Moreover, 3D printers provide fast and cost effective solutions for building prototypes and durable models in dental and medical applications, in architecture, and in the aerospace and automotive industries. Consequently, development of such new technologies is creating fields of various novel applications nowadays. In order to find a way in today's advanced world of knowledge and possibilities, it is important to have a clear goal as a starting point, and thus we look at the application. Do we think about disruptive innovation or technology? What do we want to accomplish? Which goals do we want to achieve? How to materialize these goals? These commonly applicable questions are also important when the topic of small scale high-throughput screening systems comes to one's mind. There is a broad range and variety of applications that involve small scale systems. Application requirements give direction for design and size of the small scale system ranging from a modified microtiter plate, microfluidic chip, (bio)microreactor, milliliter-scale (bio)reactor, to integrated microfluidic systems. All of these configurations have a distinctive characteristic which makes them better suited for a certain application than for others. For example, microfluidic chips and integrated microfluidic systems are beneficial tools for polymerase chain reaction (PCR) and deoxyribonucleic acid (DNA) sequencing, glucose strip tests, drug discovery and in-vitro diagnostic [1]. Microreactors are used in a wide variety of applications e.g. hydrogen production, catalytic reaction, organic synthesis and many other chemical reactions; microreactors are especially useful for these reactions that are fast and highly exothermic since microreactors have excellent heat and mass transfer capabilities [2,3] which is the consequence of their large surface to volume ratio. Microbioreactors and small scale bioreactors have played a main role in applications involving biocatalysis, microbial and cell cultivation. Micro- and milliliter scale reactors are also the main topic of this thesis, but with focus on microbial cultivations.

## 1.2 Why small scale?

Microbial cultivations and mammalian cell cultures are frequently used for production of so-called biopharmaceuticals, e.g. human insulin, human growth hormone, vaccines, other therapeutic proteins, monoclonal antibodies, etc. In the early process development stages, genetic manipulation of a biological host system results in a large number of potential production strain candidates during the development of new biologics. Also, once a promising candidate strain has been selected, there is a long development time necessary for the bioprocess itself to be transferred to the large scale.

Usually bench-scale reactors, flasks and tubes are used for obtaining relevant experimental data of microbial cultivations. Although bench-scale reactors allow efficient control of process variables and yield valuable data, they are expensive, labor intensive and they generate a relatively small amount of data [4,5]. Regarding microbial cultivations in flasks and tubes, there is a lack of control and the amount of data collected per experiment is usually limited [5,6]. Beside the above-mentioned vessels, today, microtiter plates are becoming the dominant technology for screening experiments considering that they provide easy handling, low cost and high throughput. Nevertheless, the control of the process conditions in microtiter plates is often not reliable enough, which is affecting the overall quality of generated data, and as a result the microtiter plates have difficulties with producing realistic data that can form the basis for scale up [4,5]. Different reactor configurations and their positioning according to throughput and data quality are presented in Figure 1.1.

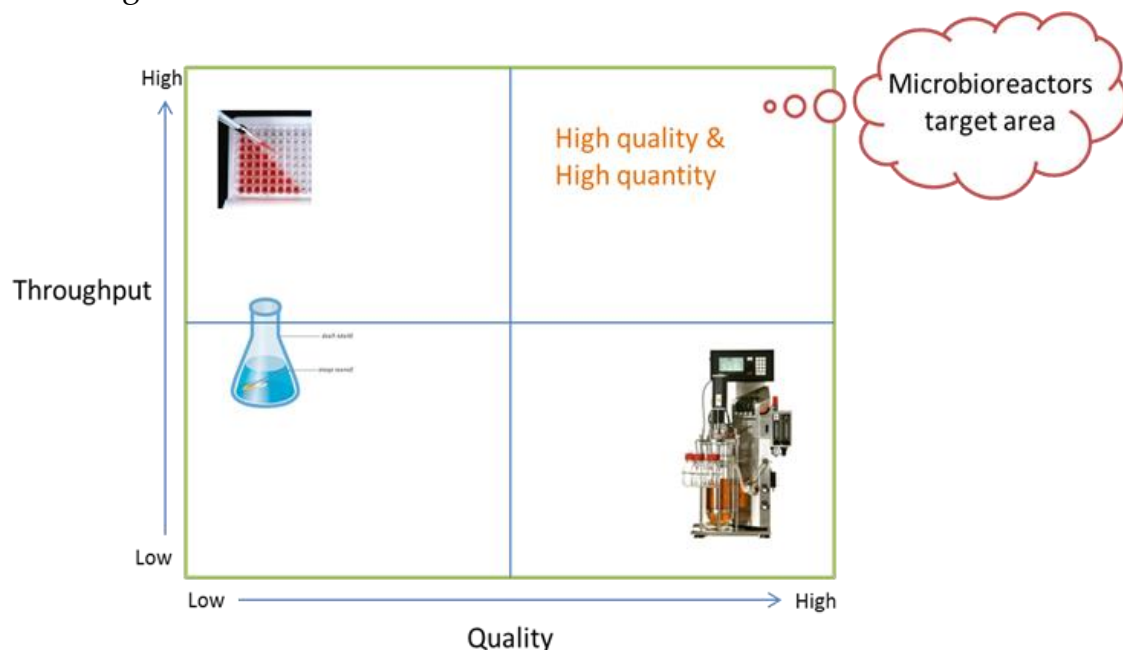


Figure 1.1. Different vessels (microtiter plates, shake flasks and bench scale bioreactor) and their positioning according to achievable throughput (experiments/tests performed simultaneously) and data quality (sets of data that are accurate, consistent, comprehensive, relevant and accessible).



In Figure 1.1., throughput indicates the number of experiments/tests performed simultaneously, and data quality refers to the relative ability of the different technologies to produce a set of data that are accurate, consistent, comprehensive, relevant and accessible.

Thus, there is a driving force and interest in the last decade for development of new techniques which could provide both high quality experimental data and also a high quantity of the experimental data. Microtiter plates with improved process control (e.g. BioLector technology) present one of the development directions [7]. As an alternative to microtiter plate systems, in recent years microbioreactors have been researched intensely due to their potential advantages like small volume, little or no need for cleaning (one time usage), high throughput (multiple microbioreactors in parallel), high information content per experiment and excellent control capabilities [8]. Microbioreactors together with analytical methods are providing the opportunity for a potentially automated and well-defined experimental system, which can deliver results that are more comparable to bench-scale reactors in comparison to e.g. a shake flask or a microtiter plate.

For bioprocess development, it is of interest to follow the dynamics of different substrates and metabolites during microbial cultivation, besides measuring process variables like temperature, pH, optical density (OD) and dissolved oxygen (DO). A modular approach could be applied here for combining different monitoring possibilities with the microbial cultivation. From the moment when a module or a platform for cultivation is well established, NIR or Raman modular spectrophotometers that are available on the market could be used to extend the real time information content per cultivation. This year, Musmann et al. [9] provided an overview and evaluation of existing spectroscopic methods and their applicability for high-throughput bioreactor systems and mammalian cell cultures, pointing out benefits and advantages as well as potential obstacles of this fusion.

With each technological breakthrough that is relevant for application in the area of biotechnology at small scale, the microbioreactors and small scale bioreactors will become better and more established as commercially acceptable tools for industry. One example of a crucial advancement in a recent past was the development of optical sensor spots which made it possible to obtain continuous, on-line and non-invasive measurements of dissolved oxygen and certain pH ranges, which gave a boost in the development of the first commercial high-throughput systems for cell and microbial cultivations. Similarly, this advancement had an impact on the scientific community as well, which provided many different studies featuring microbioreactors and small scale bioreactors which included sensor spots as a sensing choice.

The selection of the optimal strain for production of a specific product, and subsequently the choice of an appropriate process, is a procedure that requires a tremendous number of cultivations which are costly. In general, labor and time contribute significantly to the total cost of cell cultivation. Planning the cultivation, setup preparation (reactors, pumps, etc.), sampling, sterilization and cleaning procedures per cultivation, and - last but not least -

analysis of the obtained process data are major contributors to the experimental cost. In addition, the costs linked to raw materials and infrastructure, like single-use components, media, supplements, electricity, lab gas, incubators, sterilization equipment, contribute significantly to the overall cost of cultivations. High-throughput platforms for microbial fermentation and cell cultures aim to reduce the total cost per cultivation by employing small volume single-use systems with automation as mentioned earlier, which eliminates the need for cleaning, shortens the time from planning an experiment to performing the fermentation, and drastically reduces the need for manhours and raw material.

If microbioreactors and small scale bioreactors are to become viable and cost effective solutions for process development and strain screening, high throughput and the cost per cultivation/informative data set are the key points. Using high-throughput microbioreactor platforms, design of experiments can be employed, where several process parameters are varied in a systematic manner and experiments are executed in parallel. This can drastically reduce the time necessary to gain valuable experimental data (shorter time-to-market in the industry realm) and hence improve process understanding with a potential future production cost reduction as a result.

### 1.3 Outline of the thesis

The PhD thesis consists of 6 chapters, which are presented as a graphical list in Figure 1.2.

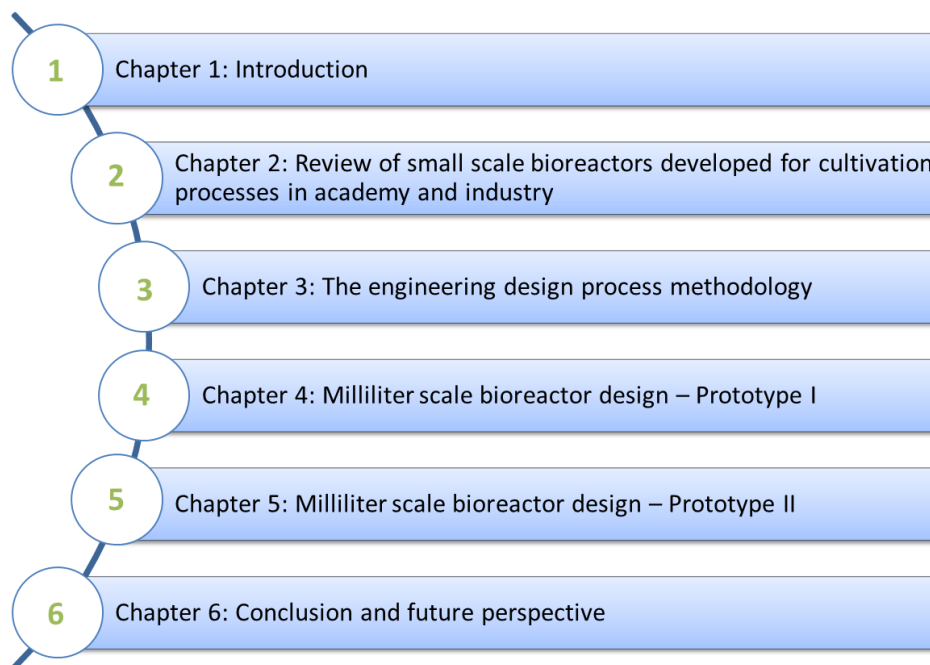


Figure 1.2 The structure of the PhD thesis presented in graphical form.

**Chapter 1** provides the introduction to the PhD thesis by explaining the motivation behind the work, and the purpose of the research project. The chapter ends by providing the structure of the thesis.

**Chapter 2** gives an overview of existing small scale bioreactors used for microbial cultivations. The chapter ends by providing the objectives of the thesis.

**Chapter 3** provides the operational framework of the research project. In other words, chapter 3 focuses on the methodology applied to structure the research activities and to organize the overall work in cohesive tasks.

**Chapter 4** presents a detailed design of the first prototype. The milliliter-scale bioreactor with supporting platform is described together with an array of different experiments used to characterize the whole system, troubleshoot potential issues and determine the working range. Focus of the tests was mainly on the mixing performance and the oxygen transfer. Results of batch cultivations in the milliliter scale bioreactor were reported as well.

**Chapter 5** continues with a description of the second prototype, which was designed and built to overcome the limitations of the previous model. It demonstrates the capability of prototype II to provide a suitable environment for continuous microbial cultivations. Experimental results are presented and discussed in detail.

**Chapter 6** concludes the thesis, summarizing the main findings and providing a more detailed discussion on the challenges related to further development in the area of small scale bioreactors.

## **1.4 Dissemination of accomplished results**

### *Publications*

**Bolic A**, Kensy F, Zainal Alam M. N. H, Perozziello G, Di Fabrizio E, Krühne U, Gernaey KV. (under review) Chapter: Microbioreactors and their application in bioprocess development and optimization. Book: Novel Bioprocessing Technology for Production of Biopharmaceuticals and Bioproducts. John Wiley & Sons, Inc., Hoboken, New Jersey, U.S.A.

**Bolic A**, Larsson H, Hugelier S, Eliasson Lantz A, Krühne U, Gernaey KV. 2016. A flexible well-mixed milliliter-scale reactor with high oxygen transfer rate for microbial cultivations. Chem. Eng. J. 303: 655–666.

Formenti LR, Nørregaard A, **Bolic A**, Quintanilla-Hernandez D, Hagemann T, Heins A-L, Larsson H, Mears L, Mauricio-Iglesias M, Krühne U, Gernaey KV. 2014. Challenges in industrial fermentation technology research. *Biotechnology Journal*. 9(6):727-738.

Gernaey KV, **Bolic A**, Svanholm B. 2012. PAT tools for fermentation processes. *Chimica Oggi*. 30(3):38-43.

Lencastre Fernandes R, Nierychlo M, Lundin L, Pedersen AE, PuentesTellez PE, Dutta A, Carlqvist M, **Bolic A**, Schäpper D, Brunetti AC, Helmark S, Heins A-L, Jensen AD, Nopens I, Rottwitt K, Szita N, van Elsas JD, Nielsen PH, Martinussen J, Sørensen SJ, Eliasson Lantz A, Gernaey KV. 2011. Experimental methods and modeling techniques for description of cell population heterogeneity. *Biotechnology Advances*. 29(6):575-599.

### *Oral presentations and posters*

**Bolic A**, Eliasson Lantz A, Rottwitt K, Gernaey KV. 2011. Uniform and reproducible stirring in a microbioreactor. Abstract from the 8<sup>th</sup> European Congress of Chemical Engineering, Berlin, Germany. (Oral presentation)

**Bolic A**, Krühne U, Prior RA, Vilby T, Hugelier S, Eliasson Lantz A, Gernaey KV. 2012. One-millilitre microbioreactor with impeller for improved mixing. Poster session presented at the 12<sup>th</sup> International Conference on Microreaction Technology, Lyon, France. (Poster)

## Chapter 2

### **Review of small scale bioreactors developed for cultivation processes in academy and industry**

---

The chapter gives an overview of the small scale bioreactors that have been developed for microbial cultivation and cell culture thus far. A table format was used to present developed micro- and mini-bioreactors that have been described in detail in the literature in the last two decades. The short discussion in this chapter results from analyzing and summarizing the key process parameters for the bioreactors presented in the table. Afterwards, some of the most well-known high-throughput bioreactor systems, which are commercially available and have been reported in the open literature, are described in detail.

#### **2.1 Overview of small scale bioreactors and their application in microbial and cell cultivations**

At present, research in bioprocess science and engineering requires fast and accurate analytical data (rapid testing) that can be used for investigation of the interaction between bioprocess operating conditions and the performance of biological systems, which consequently can provide better and faster process development and optimization. Conventional microbial cell cultivation techniques are not sufficient anymore considering the fast development of tools for genetic manipulation of biological systems resulting in a large number of strains and conditions that need to be screened. Naturally, the academic community saw an opportunity and need to make a contribution in the rising niche of high-throughput bioreactor systems as they became indeed a necessity. A number of reviews address this topic, emphasizing different aspects of small scale applications. Kumar [10] characterized small scale bioreactors up to 100 ml volume by type of mixing and application area in 2004, dividing them in shaken, stirred and specially designed small scale bioreactors for microbial cultivations and animal cell cultures. Similar reviews were made by Betts and Baganz in 2006 [11], whilst Micheletti and Lye [12] focused on engineering fundamentals of microwell bioreactors and the role of microfluidic systems. The same year, Fernandes and Cabral [13] published a review analyzing only the engineering features of shaken small scale systems. In 2007, Duetz [14] put most emphasis on fundamental issues of microtiter plates and their application areas at the time. In 2009, Marques et al. [15] highlighted the hydrodynamic behavior in a microfluidic environment and the use of microreactors in biocatalysis. In the same year, Schapper et al. [8] provided a comprehensive overview about the application of microbioreactors (up to 1 mL volume) in fermentation processes with the main emphasis on materials, mass and heat transfer,

sensing and control. Hortsch and Weuster-Botz [16] wrote a review on the status of milliliter-scale stirred tank reactors for bacteria, yeast and filamentous microorganisms in 2010. Afterwards, in 2011, Bareither and Pollard [17] highlighted the importance of cost control by application of high throughput bioreactor technology during the process development phase and they defined an ideal automated system based on criteria from the large scale cases. Pasirayi et al. in 2011 [18], and Kim et al. in 2012 [19], made reviews regarding the application of mini- and micro-bioreactors for cell based studies, with examples from animal cell cultivation, tissue engineering, single cell analyses, cytotoxicity assays, etc. Furthermore, Gernaey et al. [20] gave an expert opinion on the topic of microbioreactors in 2012 by summarizing the monitoring and control requirements for microbioreactors in bioprocess development and toxicity testing. In 2013, Kirk and Szita [21] provided a detailed description of the oxygen transfer characteristics in the specific case of submilliliter and milliliter scale bioreactors. In the same year Neubauer et al. [22] published an overview about bioprocess development and enabling technologies from a business perspective. Lattermann and Büchs [23] published a short review at the end of 2014 about the latest developments of small scale bioreactors regarding automation, fed-batch systems and on-line sensing, covering the period between 2012 and 2014. Earlier the same year, Long et al. [24] focused on the role of high throughput cultivation in quality by design driven bioprocess development, where commercially available platforms were compared and evaluated.

As can be seen in the previously mentioned reviews, a number of small scale bioreactors have been developed specifically for microbial and cell cultivation processes and they are intensely reviewed addressing different aspects of small scale high-throughput systems. A chronological overview of the different micro- and milliliter- scale bioreactors is presented in Table 2.1, where emphasis is placed on cell line, working volume, sensing and control of important process parameters and finally the capability of a device for parallelization.

### **Micro scale**

From Table 2.1 it is evident that there is no common trend in the choice of working volume, ranging from a few microliters, even nanoliters, up to the milliliter scale, and each scale brings its own advantages and disadvantages. It is important to realize though, that with a considerable decrease in the working volume (e.g. to microliter level), problems with biofilm and bubble formation, evaporation, handling, sampling, providing adequate mixing, aeration and sensing are more pronounced. Furthermore, the physics (mass and heat transfer, shear stress...) of a small scale system could have an impact on the cell metabolism which can lead to wrong conclusions in the choice of the best performing strain or the most optimal process parameters. Balagaddé et al. [25] showed that a microchemostat can only have 16 nL volume and sustain cell growth for 200 - 500 h. This work provides an example of scale influence on the cell behavior, since they observed that cells kept their specific characteristics longer at the nanoscale compared to milliliter scale cultivations.

Table 2.1. Overview of different micro- and milliliter- scale bioreactors (in chronological order).

Type	References	Cell line and Cultivation mode	Working volume	Mixing	Aeration	Parameters monitored	Parameters controlled	Parallelization
Miniature bioreactor	Walther et al., 1994 [26]	<i>S. cerevisiae</i> , continuous	3 mL	Magnetic stirrer	Aeration membrane	pH (ISFET), T, redox potential, flow	pH	1
12-well microtiter plate	Girard et al., 2001 [27]	CHO, HEK 293, batch	2 mL	Rotational shaker	None	pH, cell growth	T, CO <sub>2</sub>	12
Cuvette-based microbioreactor	Kostov et al., 2001 [4]	<i>E. coli</i> , batch	2 mL	Magnetic stir bar	Sparger	pH, DO, OD – by optical sensing	None	1
Stirred tank	Lamping et al., 2003 [28]	<i>E. coli</i> , batch	6 mL	Set of three impellers, mechanically driven	Single tube sparger	pH, DO, OD – by optical sensing, T	T	1
Membrane-Aerated Microbioreactor	Zanzotto et al., 2004 [29]	<i>E. coli</i> , batch	0.005–0.05 mL	None	Polymer aeration membrane	pH, DO, OD – by optical sensing, T	T	1
Microbioreactor	Maharbiz et al., 2004 [30]	<i>E. coli</i> , batch	0.25 mL	Shaken stainless steel bead	Electrochemical gas generation system	T, OD, pH (ISFET)	T	8
Membrane-Aerated Microbioreactor	Szita et al., 2005 [31]; Zhang et al., 2006a [32]; Zhang et al., 2006b [33], Boccazzi et al., 2006 [34]	<i>E. coli</i> , <i>S. cerevisiae</i> , batch, continuous	0.15 mL	Ring-shape magnetic stir bar	PDMS membrane	pH, DO, OD – by optical sensing, T	T, pH (buffered), flow (for contin.)	1-4
Microchemostat	Balagaddé et al., 2005 [25]	<i>E. coli</i> , pseudo continuous	16 nL	None	None	Cell growth by optical microscopy	T, flow	6
Gas-Inducing Milliliter-Scale Bioreactor (2mag bioreactor 48)	Puskeiler et al., 2005 [35], Gebhardt et al., 2011 [36], Weuster-Botz et al., 2005 [37]	<i>E. coli</i> , <i>S. cerevisiae</i> , batch and fed-batch	5-10 mL	Gas-inducing impellers	Surface / head space aeration	pH, DO, OD – by optical sensing (at line), T	pH, T	48

Table 2.1. Overview of different micro- and milliliter- scale bioreactors (continued in chronological order).

Type	References	Cell line and volume	Mixing	Aeration	Parameters monitored	Parameters controlled	Parallelization
<b>BioLector</b>	Funke et al., 2010a [38]; Kensy et al., 2009 [39]; Samorski et al., 2005 [40], Huber et al., 2009 [41]; m2p-labs (Baesweiler, DE)	<i>E. coli</i> , <i>V. natriegens</i> , batch, fed-batch 0.2 mL, 0.1 - 2 mL	Shaken	Surface aeration	Biomass, NADH, GFP, pH, DO, T	O <sub>2</sub> , CO <sub>2</sub> , T, relative humidity	48/96
<b>Robo-Lector</b>							
<b>Microbioreactor arrays</b>		<i>E. coli</i> , batch 0.1 mL	Peristaltic oxygenating mixer		pH, DO, OD	pH, DO, T	8
<b>Miniature stirred tank</b>	Harms et al., 2006 [43]	<i>E. coli</i> , batch 1 mL	Mechanically driven stirrer	Sparger, surface aeration	pH, DO-by optical sensing, turbidity, T	DO	24
<b>Miniature stirred tank - Cellstation</b>	Ge et al., 2006 [44]	SP2/0 myeloma/mouse 30 - 35 mL	Mechanically driven stirrer	Sparger	pH, DO, pCO <sub>2</sub> OD - bv	T	12
<b>Mini-bioreactor</b>	Diao et al., 2007 [45], Kim et al., 2011 [46]	Insect cell- <i>Spodoptera frugiperda</i> batch, fed-batch 2.5 - 3 mL	Pressure shuttling between the two chambers	Molecular diffusion through 50 mm thick membranes	T, CO <sub>2</sub>	T, humidity, pH, CO <sub>2</sub>	8
<b>Twenty-Four well plate miniature bioreactor system</b>	Chen et al., 2009 [47]; Isett et al., 2007	<i>S. cerevisiae</i> , <i>E. coli</i> , <i>P. pastoris</i> , CHO, batch, fed-batch 3-7 mL	Shaken		pH, DO, T	pH, DO, T	24
<b>Hollow fiber microbioreactor</b>	Villain et al., 2008 [49]	<i>E. coli</i> , batch 2 mL	Magnetic stirrer	PVDF membranes	DO, OD, T	T, flow	1



Table 2.1. Overview of different micro- and milliliter- scale bioreactors (continued in chronological order).

Type	References	Cell line and Cultivation mode	Working volume	Mixing	Aeration	Parameters monitored	Parameters controlled	Parallelization
Miniature stirred bioreactor	Gill et al., 2008 [50]	<i>E. coli</i> , <i>B. subtilis</i> , batch	100 mL	Magnetically driven six-blade miniature turbine impeller	Sintered sparger	pH, DO, T, OD - probes	pH, DO, T	4-16
Microbioreactor arrays	Buchenaer et al., 2009 [51]	<i>E. coli</i> , fed-batch	0.5 - 0.7 mL	Shaking	Surface aeration	pH, conductance, biomass	pH	48
Microbioreactor	Rahman et al., 2009 [52]	<i>Pseudomonas aeruginosa</i> DS10-129, batch	1.5 mL	Shaking	Diffusion through porous PTFE	OD - offline, T	T	3
Diffusion-based microreactor	Edlich et al., 2010 [53]	<i>S. cerevisiae</i> , continuous	0.008 mL	Rapid diffusive mixing	PDMS membrane	DO, OD - by optical sensing	T	1 - 2
Milliliter-scale stirred tank	Hortsch et al., 2010 [54]	<i>Streptomyces tendae</i> , batch	10 mL	Magnetically driven one-sided paddle impeller	Surface aeration	pH, DO, T, cell growth	T, DO	48
SimCell™ System	Seahorse Bioscience, Amanullah et al., 2010 [55]; Legmann et al., 2009 [56]	CHO cell, batch, fed-batch	0.6 - 0.7 mL	By motion of an air bubble during rotation	Gas permeable membrane	DO, pH, and total cell density - by optical sensing	T, pH, pO <sub>2</sub> , pCO <sub>2</sub> , OD, relative humidity, feed and growth rate	1260
Single used microbioreactor	Schäpper et al., 2010 [57]	<i>S. cerevisiae</i> , batch	0.1 mL	Free floating stirrer bar	PDMS membrane	T, pH, DO, OD	T, pH	1
Disposable parallel PDMS microbioreactor	Demming et al., 2011 [58]	<i>Aspergillus ochraceus</i> , batch, continuous	0.009 mL	None	Passive aeration	T, germination behavior	T	5

Table 2.1. Overview of different micro- and milliliter- scale bioreactors (continued in chronological order).

Type	References	Cell line and volume	Mixing	Aeration	Parameters monitored	Parameters controlled	Parallelization
Microfluidic chemostat	Lee et al., 2011 [59]	<i>E. coli</i> , continuous 1 mL	Liquid movement by inflation and deflation of reactor chambers	PDMS membrane	T, DO, pH, flow	T, cell density, DO, pH.	1
	Au et al., 2011 [60]	<i>E. coli</i> , <i>S. cerevisiae</i> , <i>C. cryptica</i> , batch ~0.07 mL	Manipulating mother drop in a circular path	None	OD, T	T	1
Advanced Microscale Bioreactor System-Ambr	Moses et al., 2012 [61], Frédéric et al., 2013 [62], Rameez et al., 2014 [63]	Cell culture, batch, fed-batch 10 - 15 mL	Impeller	Sparge tube	pH, DO, T	T, pH, DO, DCO <sub>2</sub>	24/48
	Bower et al., 2012 [64]	<i>E. coli</i> , fed-batch temperature- 1 mL	Liquid movement by inflation and deflation of reactor chambers	PDMS membrane	T, DO, pH, OD	T, DO, pH	1
Automated microscale platform	Baboo et al., 2012 [65]	<i>E. coli</i> , batch 0.5 mL	Shaking	None	T, OD	T	96
Vertical microbubble column	Demming et al., 2012 [66]	Generation of microbubbles				T	1

Table 2.1. Overview of different micro- and milliliter- scale bioreactors (continued in chronological order).

Type	References	Cell line and Cultivation mode	Working volume	Mixing	Aeration	Parameters monitored	Parameters controlled	Parallelization
Miniaturized stirred bioreactors	Klein et al., 2013 [67]	Schizosaccharomyces pombe, continuous	10 mL	Disc-like magnetic bar	Passive aeration by negative pressure	DO, Off-gas analysis, flow	T, flow	8
High-throughput cultivation and screening platform featuring Tecan Freedom Evo 200 pipetting robot	Tillich et al., 2014 [68]	Synechocystis sp., fed batch, semi-continuous	1.8 mL	Orbital shaking with three glass beads	Gas diffuser	T, DCO <sub>2</sub> , light, OD <sub>750nmv</sub> absorption spectrum, chlorophyll content, vitality	T, DCO <sub>2</sub> , light	192
Milliliter - scale chemostat system	Schmideder et al., 2015 [69]	<i>E. coli</i> , continuous	10 mL (8 - 14 mL)	Magnetic driven gas-inducing stirrers	Surface / head space aeration	T, DO, pH, OD at-line	T, pH	48
Parallel miniature bubble column	Kheradmandnia et al., 2015 [70]	<i>E. coli</i> , batch	20 mL, batch	Generation of bubbles	Gas diffuser made of sintered glass	T, DO, pH	T, pH	3

A potential explanation for this observation, according to the authors, lays in the assumption that a smaller population size could provide genetically homogeneous populations for a longer time. This immediately raises an important question: will information required in the genetically homogeneous environment (nL scale) be applicable to an environment where the mutation rate is higher (mL - L scale)? It has been observed that cultures with programmed behavior lost their regulation within 70 h at 3-50 mL scale, while they kept this behavior much longer at nanoscale [25]. As mentioned earlier, the reason for this observation could be the smaller population size at nanoscale compared to larger scale. Alongside population size, population heterogeneity at larger scale is also closely related to conditions that the cells experience in their surroundings, which are not uniform. In order to survive, cells can adapt to the new environment by expressing certain genes that will help them to overcome adversity [71]. Consequently, nanoscale cultures could be used to acquire more information at the cell level and to acquire understanding on how cells react at different conditions, and one could afterwards apply that knowledge for process optimization at larger scale.

Edlich et al. [53] developed a microreactor with 8  $\mu$ L volume for the growth kinetic study of *Saccharomyces cerevisiae*. Liquid behavior in this system is described as extremely laminar and creeping, and the inoculation procedure for the microreactor was demanding in order to avoid bubble formation. Even though cultivation results from the microreactor showed a certain level of agreement with lab scale results, the potential formation of biofilm as well as the importance of a correlation between cell vitality and cell position (closer or further from the PDMS membrane throughout which oxygen was supplied) are important issues that should not be overlooked. Reproducibility of the same cultivation conditions at microliter scale is frequently appearing as an issue, as well as the quality of the acquired data (laminar vs turbulent environment) which should be sufficiently good in order to be compared to larger scale cultivation results.

However, submerged cultivations at micro - and nano - liter scale make sense and most impact, especially if they highlight some behavior which cannot be obtained or studied with already available tools at different scales by focusing, for example, on enhancement of single cell resolution [72]. Microfluidic devices with a volume of a few microliter and laminar flow provide a platform for controlled cell growth with focus on a single cell or a small populations of cells, allowing precise feeding, sample retrieval, cell manipulation as well as analysis [73]. Demming et al. [58] used the microliter scale (9  $\mu$ L) to obtain a better understanding of *Aspergillus ochraceus* by performing cost effective morphology screening of cells. Implementing a grid matrix in 5 parallel chambers of a microfluidic device allowed imaging of spores for counting and morphology studies via a normal microscope. Thus, an inverted microscope was not needed as is the case for microwell plates. Going further in the simplification of screening tools on a cellular level, there is the emerging field of digital microfluidics (DMF) based on the droplet manipulation technique [74]. Liquid movement in DMF is obtained by an electric field and multi-step operational

microfluidic devices containing a number of pumps, channels, micromixers and valves could be potentially replaced with these devices. Au et al. [60] displayed DMF potential by growing bacteria, algae and yeast in an integrated microbioreactor that had a reactor, sample and reservoir region, while liquid manipulation was based on the movement of mother and daughter droplets by the potential between two electrodes.

### **Milliliter scale**

Compared to microliter scale, there are a considerably larger number of design options at milliliter scale where one tries to mimic large scale cultivations. Up to 10 mL volume, the bioreactors are big enough to accommodate higher cell density and still small enough to be considered for parallelization. Moreover, achieving adequate mixing and aeration is less challenging since there is available space for a stirrer, a sparger and baffles that contribute to fluid behavior similar to larger scale. Besides, sampling during submerged cultivations is also easier at milliliter scale and general handling of the cultivation is less challenging.

To understand better the influence of different length scales, different aspects of bioreactor performance at micro- and at milliliter scale are presented and compared in Table 2.2.

### **Cell line and cultivation mode**

From Table 2.1, it can be seen that the majority of the small scale reactors reported in the literature have been used for microbial cultivations with bacteria (*E. coli*) and yeast (*S. cerevisiae*), while fewer have been used for mammalian cells. An obvious reason is the different process requirements for mammalian cell cultures regarding sensitivity to shear and nutrient and oxygen supply in the stirred systems and sterility and large sample size (due to lower cell density) in the shaken systems. In addition, the fed-batch and perfusion cultivation mode are predominant in large scale mammalian cultivation, while at small scale these two modes are less preferable since they have a lot of issues related to the establishment of proper connections and high throughput [19]. Nowadays, companies like BioSilta and Kuhner offer slow release technology for glucose which gives the potential for establishing a fed-batch process at small scale without the need for tubing and pumps.

Furthermore, there is an important application area with filamentous and pellet forming microorganisms, strains that have not been investigated that often at small scale, due to the microorganism's morphology and its effect on the process (shear forces, non-Newtonian shear-thinning behavior of the culture broth, viscosity, mass transfer challenges, wall growth). One successful example of the application of small scale reactors for studying filamentous organisms is the 10-milliliter scale stirred tank bioreactor with a one-sided paddle impeller and surface aeration, designed for mycelium forming microorganisms [38, 39]. This system can be run in parallel with up to 48 bioreactors, and is now also commercially available (bioREACTOR 48, 2mag AG, Munich, Germany).

Table 2.2 Scale influence on bioreactor characteristics and bioprocess condition.

	<b>Microliter scale bioreactors(&lt; 1mL)</b>	<b>Milliliter scale bioreactors (&gt; 1mL)</b>
<b>Biofilm formation</b>	Biofilm formation is enhanced by usually employed porous and hydrophobic PDMS as a reactor fabrication material as well as hydrodynamic conditions at microliter scale.	Less probable due to active liquid mixing and different choice of reactor material.
<b>Bubble formation</b>	Reoccurring problem due to trapped air in microfluidic devices caused by device configuration, temperature change, leakage produced by fitting issues, material like PDMS.	Doesn't have a negative role at milliliter scale due to increased space, good mixing and possible presence of a sparger.
<b>Evaporation</b>	Rapid, due to high surface to volume ratio.	Evaporation is present and needs active prevention. However, the evaporation rate per unit volume is lower than in the case of the microliter scale due to lower surface to volume ration compared to the microscale.
<b>Handling</b>	If an integrated microfluidic platform with micro-valves, micro-pumps and micromixers is not developed, than the handling is quit problematic due to differences between regular size (=lab) equipment and the microliter scale bioreactor.	It is possible to use chromatographic fittings and multichannel peristaltic pumps with milliliter scale bioreactors. Also introduction of automation in liquid handling makes handling much less difficult. However, it also increases the purchase price of such a platform.
<b>Sampling</b>	Problematic. Typically only end point sample.	Sampling is feasible for milliliter scale bioreactors with more than 10 mL working volume. Sample size is limited.
<b>Aeration</b>	Membrane aeration only. Proves to be sufficient for small diffusion lengths when mixing is rapid and the high surface to volume ratio creates a large interfacial area over which oxygen can diffuse.	Headspace is present in milliliter scale bioreactors, so surface aeration is possible. Furthermore, more space in the reactors - compared to microscale - provides opportunities for sparger and stirrer implementation.
<b>Adequate mixing</b>	Surface to volume ratio has a dominant effect, thus surface tension, fluidic resistance and capillary forces play a major role in fluid behavior. Mixing is diffusive and laminar, which is regarded as inefficient. Micromixers are necessary.	It is possible to implement a proper stirrer with different impeller designs, which considerably increases mixing performance and changes it from laminar to turbulent.
<b>Heat transfer</b>	It is rapid, due to the high surface to volume ratio. Precise temperature control of the environment in the reactor is necessary to avoid temperature gradient.	Heat transfer is enhanced by hydrodynamic conditions in the milliliter scale bioreactors created by effective mixing. Nevertheless, temperature control is necessary.
<b>Sensing</b>	Lack of physical space limits comprehensive sensing possibilities.	Milliliter scale bioreactors provide more space for implementation of sensors.

As mentioned earlier in this chapter, most cultivations in the small scale bioreactors were run as batch processes, since fed-batch and continuous mode contribute to the complexity and cost of the system (long tubing, syringe pumps, reservoirs). The continuous cultivations were usually considered as an option in the microfluidic devices with microliter volumes where pumps and valves were an integrated part of the whole design. A good example of a microfluidic bioreactor capable of working in different operational modes is described for the first time by Lee et al. [59] in 2011 as chemostat and turbidostat. Shortly after, Bower et al. [64] presented a modified version of the mentioned microfluidic bioreactor capable of operating in fed-batch mode. Lastly, in 2015 Mozdierz et al. [75] presented a “perfusostat” which presented the previously described microfluidic bioreactor where a perfusion filter was added in the growth chamber allowing continuous perfusion cultivations.

On the other hand, in the last few years it seems that research focus has shifted from design of novel small scale bioreactors to establishment and optimization of feeding strategies in the already existing systems and evaluation of commercially available high-throughput platforms. In 2014, Faust et al. [76] presented the impact of different feeding strategies on achieving high cell density cultivation (dry cell weight above 60 g L<sup>-1</sup>) using *E. coli* in the bioREACTOR 48. They investigated three feeding strategies by intermittent glucose feeding using a liquid handler, by means of a microfluidic device prototype [77] and by using the enzymatic release concept. All three feeding strategies gave similar dry cell weight, while optical density was higher and dissolved oxygen fluctuations were less pronounced in the case of the microfluidic device and the enzymatic glucose release. However, high cell density at small scale brought about issues with high usage of antifoam and reduction in the oxygen transfer capacity. Furthermore, problems were encountered with irreproducible displaced liquid when the microfluidic device was used, which required further technical improvement. In 2015, the bioREACTOR 48 was further modified to accommodate also continuous cultivation which enabled kinetic growth study of *E. coli* [69]. In the same year, Toeroek et al. [78] developed a procedure for fed-batch like conditions for cultivation of *E. coli* in the BioLector by using a synthetic enzymatic glucose release method. The final result of the cultivation was a cell density of 10 g biomass L<sup>-1</sup> without any limitations in the oxygen supply.

### **Monitoring and control of process parameters at small scale**

Independent of the scale, a successful cultivation/cell culture requires certain conditions to be satisfied. As a consequence, our ability to measure and control process parameters in a bioreactor, for example related to supply of nutrients, or dissolved oxygen and pH control, is essential. A schematic representation of the important parameters can be seen in Figure 2.1 together with on-line methods for sensing and control systems that are frequently applied at small scale. In many aspects, sensing at the small scale is a major bottleneck for further advancement of microbioreactor technology.

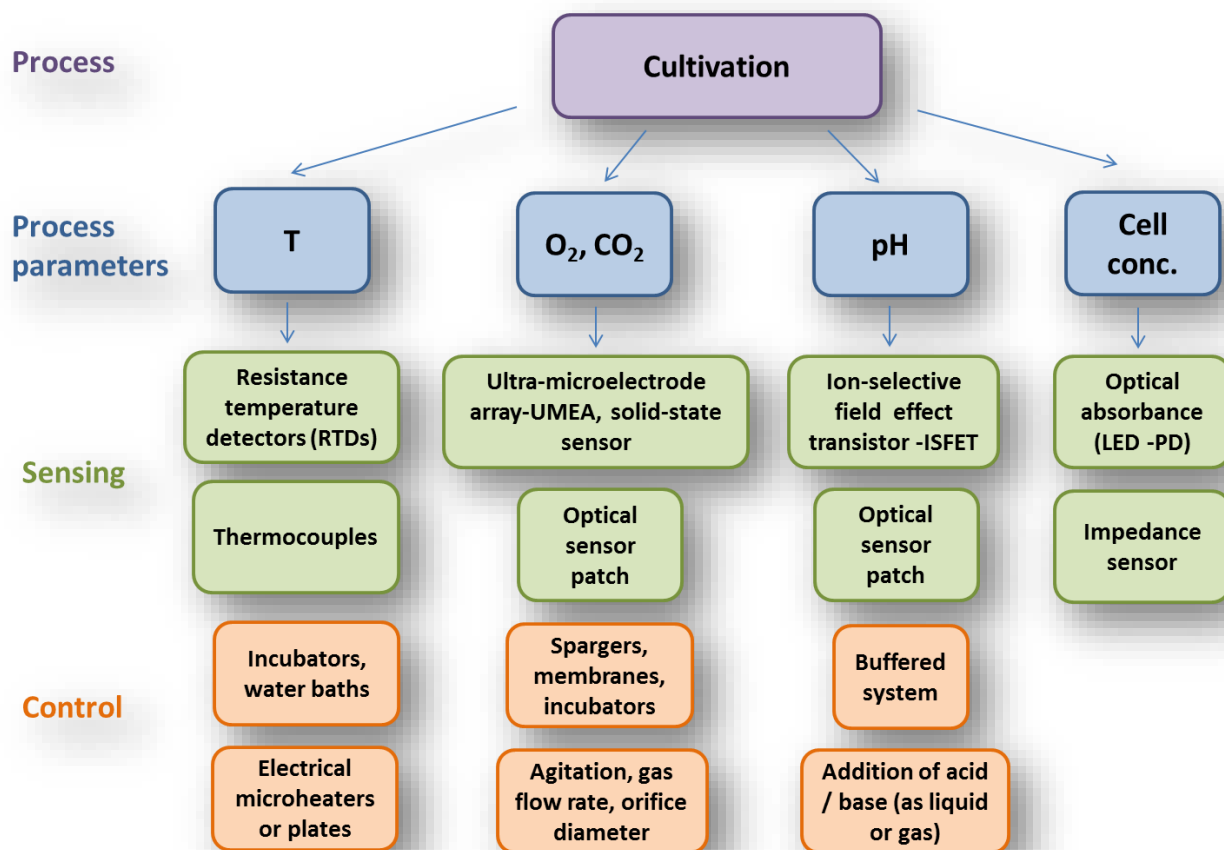


Figure 2.1. Schematic representation of monitoring and control strategies for important process parameters (temperature, dissolved oxygen and CO<sub>2</sub>, pH and cell concentration) at small scale.

Obtaining reliable experimental data is not straightforward and it can be expensive due to lack of commercially available sensing systems. The measurement of important process parameters, e.g. pH, dissolved oxygen and carbon dioxide in many small scale reactors is based on the same optical sensor patches (available from different companies, e.g. PreSens, Ocean Optics, PyroScience...) as they are considered to be state of the art, offering noninvasive measurement in a small footprint. Although they are a popular choice, optical sensors need further improvement, especially the sensor for pH measurement, since it has a far too narrow measurement range and limited long-term stability [8,79]. In addition, optical sensing in high-throughput applications can grow in complexity and cost, considering the number of required connections and the necessary hardware. The first step in extending the pH measurement range was presented by Janzen et al. [80] last year, when they evaluated two prototype fluorimetric pH sensors made by PreSens GmbH, Germany. Tests, performed in the bioREACTOR 48 platform, showed that online measurement of pH is possible between pH 4.0 and pH 7.0. However, they also pointed out that medium fluorescence was a major problem and optical isolation of sensor and reader was necessary in order to restore the characteristics of the pH sensor.



The complexity of small scale bioreactors protrudes not only in sensing and data acquisition of process parameters, but has also major implications on control strategies of these process parameters. The pH control during batch cultivation is a good example of a realistic challenge faced by many microreactor systems, since the small reactor working volume requires an acid/base dispensing system that can dose nanoliters at a time. The need for a very precise dispensing system substantially increases the complexity and cost of a small scale system. However, assuming that different feeding strategies (e.g. fed-batch) are readily available, this issue could in principle be overcome by increasing the buffer capacity of the medium.

## 2.2 High throughput small scale platforms for cultivation processes

Despite all the problems that the operation of a bioreactor at small scale brings about, application of small scale bioreactors in cultivation processes is already a reality. At the moment there are few commercially available high throughput small scale platforms trying to compete with already established systems based on shaken flasks, tubes, and microtiter plates. They are described in more detail in the text below.

**BioLector** is a first and basic model of a high-throughput microbioreactor system that m2p-lab GmbH can offer. It is based on a microtiter plate that can run 48 parallel cultures with the possibility for on-line monitoring of biomass concentration, pH, DO and fluorescent proteins or substrates. Dissolved oxygen and pH are measured by optical sensor spots, while biomass concentration is measured by scattered light. An incubation chamber is used to regulate temperature, humidity and specific gas concentration (O<sub>2</sub>, CO<sub>2</sub>, anaerobic conditions) of microplates with wells (0.1 – 2 mL) that have a specific flower shape which provides a high oxygen mass transfer rate during cultivation. Agitation is maintained by an orbital shaker [81]. The system can be upgraded with different modules for low, high or no oxygen condition, for CO<sub>2</sub> atmosphere and fluorescence resonance energy transfer (FRET) applications. In addition, the system can be integrated into standard liquid handling systems to perform further bioprocess operations such as media preparation, sampling, induction and feeding [41,82]. In order to provide adequate pH control for individual wells and the possibility for running fed-batch processes, the BioLector was upgraded by integration of a microfluidic chip in the system which resulted in a new product called BioLector Pro. This new system has a microfluidic flower plate (0.8 – 2.4 mL) that can run 32 parallel cultivations while the rest of the wells was used as reservoirs for pH control and feeding [7]. Both, the BioLector and the BioLector Pro, when integrated with a liquid handling robot, provide a completely automated platform for up to 48 parallel cultivations – RoboLector® L and RoboLector® XL.

**SimCell** (withdrawn from the market in the meanwhile) is a fully automated system that employs arrays of 210 microbioreactors simultaneously. Each array consists of six gas-permeable reactors with 600-800  $\mu\text{L}$  working volumes, which allows 1260 parallel experiments to be performed. The SimCell system has a modular structure consisting of incubator, sensing, sampling and dispensing module. There can be up to five incubator modules integrated in the system with the main purpose to secure the environmental conditions (temperature, humidity,  $\text{O}_2$ ,  $\text{CO}_2$ ) and provide sufficient mixing by rotational agitation (motion of air bubble). The sensing module is providing optical on-line measurement of cell count, cell growth, pH, dissolved oxygen and  $\text{CO}_2$ . The sampling module allows taking samples (10 to 100  $\mu\text{L}$ ) during and at the end of a cultivation in order to perform further analyses, which are not possible via on-line measurement with the sensing module. For addition of media, base for pH control or inoculation of cells a dispensing module is available. In order to maintain a fully automated platform and have a good coordination between modules, a loading and transfer robot is employed [55].

**2mag-bioreactor-48** platform has 48 milliliter scale reactors with gas inducing impellers, optional baffles and a working volume of 8-15 mL, which are used together with a reaction block. The gas inducing impellers have permanent magnets which are driven by a magnetic field created by four magnets positioned around each reactor in the reaction block, allowing stirring speeds up to 4000 rpm. The reaction block also has two heat exchangers, one for temperature control and one for cooling of the reactor headspace in order to reduce evaporation during cultivation. All 48 reactors are closed with a gas cover that allows sterile gas to come to the headspace of each reactor [35]. In the last few years this bioreactor platform was featured in a few publications where different feeding strategies [69,76,83,84] were tested as well as two prototypes of fluorimetric pH sensors [80].

**Pall Micro-24 Reactor System** consists of a microreactor console and a single-use cassette (deep well plate) that has 24 cylindrical reactors with 3-7 mL working volume. Each reactor has its own gas injection port, thermal heater, temperature sensor, pH and dissolved oxygen optical sensors which allow independent monitoring and control of the mentioned parameters. Oxygen and pH control is obtained through the same gas injection port using defined gas mixtures. Mixing is obtained by orbital shaking of the cassette that is attached to a base located on the microreactor console using vacuum. Beside a gas injection port, aeration can be obtained through surface aeration as well. There are three types of plates: with baffles, without baffles and with a central vent. Also, there are four options for well closure that are used to prevent cross-contamination and reduce evaporation [47,48,85].

**Cellstation HTBR** system consists of 12 disposable miniature stirred tanks in glass with 30-35 mL working volume. Miniaturized motor driven impellers enhance mixing and provide individual control in each reactor. Optical sensors for detection of dissolved oxygen and pH are placed at the bottom of each reactor for non-invasive on-line

measurement of these two important process parameters. A gas distributor (connected to the individual sparger in each mini-scale bioreactor) and a turntable serving as a water bath were also included in the system [44].

**ambr® 15 cell culture and ambr® 15 fermentation** from Sartorius Stedim Biotech forms another high-throughput milliliter scale platform (8-15 mL) that is commercially available. The platform with liquid handling supports both types of disposable bioreactors with integrated impeller for mixing and sparging tubes for gas delivery. Reactors are grouped in culture stations and each station has 12 reactors, with a total of 24 bioreactors per run. Each reactor has a sample and feed port, and has sensor spots attached at the bottom of the vessel for measurement of dissolved oxygen and pH, which allow on-line monitoring and closed loop control of these two process parameters. Independent control of N<sub>2</sub>, O<sub>2</sub> and CO<sub>2</sub> for each reactor is possible. Temperature and stirring speed are controlled per culture station [63]. The main difference between ambr 15 cell culture and ambr 15 fermentation bioreactors lies in the type of stirrer applied. Both bioreactors use the same pH sensors with measurement range between 6 and 8, which limits the ambr 15 fermentation platform to be used only for cultivations in the mentioned pH range, thus excluding cell lines that are cultivated at lower pH values. Automation is obtained by a liquid handling system which allows feeding, base addition and sampling [61]. The ambr platform showed promising features, thus few studies including ambr 15 cell culture were performed in order to evaluate its performance and ability to produce similar results as the ones obtained in bench scale bioreactors [61,63,86]. Moreover, an interesting study was performed by Nienow et al. [87] in which physical characteristic (power number,  $k_L a$  and mixing time) of ambr bioreactors were determined and evaluated. Results showed that physical features of ambr bioreactors were different compared to the ones at larger scale (transitional flow, low superficial gas velocity and high specific power input). However, this work also confirmed that cell growth and productivity were similar in both bioreactors as other studies suggested. Nienow et al. assigned this resemblance to similar control capabilities that enabled similar stress parameters (produced by stirring and aeration) at both scales compared to shake flasks.

In further development of high throughput platforms, Sartorius Stedim Biotech decided to increase the working volume of the bioreactors keeping existing parallelization, so they designed ambr® 250 high throughput where single-use bioreactors have a volume between 100 and 250 mL and the possibility to sustain high cell density cultivation (up to 400g L<sup>-1</sup> wet cell weight) [88].

**micro-Matrix** is a platform made by Applikon Biotechnology that consist of 24 square bioreactors in cassette format (Society for Biomolecular Screening (SBS) micro-titer plate) with the possibility of individual control and measurement of essential process parameters - temperature (10°C - 45°C), pH (6 - 8), dissolved oxygen (0 - 150 % air saturation), liquid addition and up to 4 separate gas (N<sub>2</sub>, O<sub>2</sub>, CO<sub>2</sub>, air) additions. Mixing is performed by an orbital shaker plate (0 - 400 rpm) on which the bioreactor cassette is placed. Total volume

of the bioreactor is 10 mL, while the working volume is 1 - 7 mL and 5 mL is recommended as optimal volume. This platform has very similar features to the previously described platform from Pall Corporation - Pall Micro-24 Reactor System.

Although each high throughput platform described above has its own unique design and different working volumes, there are certain similarities between them. Most of them have similar sensing tools for DO and pH, based on optical sensor spots. The BioLector, Pall Micro-24 Reactor System and micro-Matrix are using microtiter plate technology where mixing is obtained by orbital shaking and humidity is maintained by using an incubation chamber. The main advantage of microtiter plate based platforms is their adaptability and compatibility to existing analytical tools in laboratories. Using robotic handling they can easily become fully automated systems. Nevertheless, the microtiter plate based design has inherent problems with providing an opportunity for variation of process conditions from well to well. Another issue limiting applicability is the fact that cultivations in continuous mode cannot be accommodated in such a system.

The 2mag-bioreactor-48, Cellstation HTBR and ambr 15 are focused on stirred tank reactor design in order to provide better individual monitoring and control of process parameters, which allow easier scalability compared to shaken platforms. However, the complexity of the mentioned systems is not low, and if automation is not obtained by robotic handling, they still require the same amount of manual work as other technologies. In addition, the mentioned systems also don't offer any possibility to run continuous cultivations yet.

Simcell is the only system that provides perfusion mode and full automation for working volumes below 1 mL. Nonetheless the system is complex and it can be used only for mammalian cell culture as the low oxygen transfer rates limit the application for microbial cultivations. The fact that this product is not available anymore on the market is simply showing that the high complexity of the product with limited application potential results in higher cost and difficulties to compete with other products available on the market.

Overall, the design of high-throughput platforms with all the necessary features that will allow for versatile applications still remains a challenge in academia as well as in industry. However, only ten years ago there were hardly any commercial small scale high throughput bioreactors available on the market and the first marketable solutions that came were limited in their possibilities for achieving proper process controls and application of different feeding strategies. Nowadays, fed batch cultivations with high cell densities at 10 mL scale are available, so there is significant progress and probably soon enough continuous cultivations at small scale will become reality and established routine procedures for cell screening and process development. It is just a question if progress will build up on existing small scale bioreactor solutions waiting for other technologies to mature - sensors and pumps - or if some new, different concept will emerge in the future.

## 2.3 Cultivation modes and *Saccharomyces cerevisiae* as a model organism

Microbial submerged cultivation presents the process where microorganisms grow in liquid medium under controlled conditions. Growing microorganisms require nutrients in order to grow, and these are provided via the culture medium that usually contains carbon and nitrogen source, trace metals and vitamins. Beside nutrients, other factors need to be maintained during cultivations as well e.g., temperature, pH, aeration and agitation. Usually, a bioreactor is vessel that can provide adequate process conditions for growth of microorganisms by applying appropriate monitoring and control of the key process parameters. Bioreactors are usually used in three different operating modes dependent on the cultivation process characteristics and requirements: batch, fed-batch and continuous. During batch cultivation all nutrients are provided at the beginning of the cultivation and are used during microorganism growth. There is no addition or removal of liquid feed medium; however gas used for aeration (in aerobic cultivations) is constantly refreshed, and pH control is applied by adding acid/base if required. A typical growth curve of a microbial culture under batch conditions is presented in Figure 2.2.

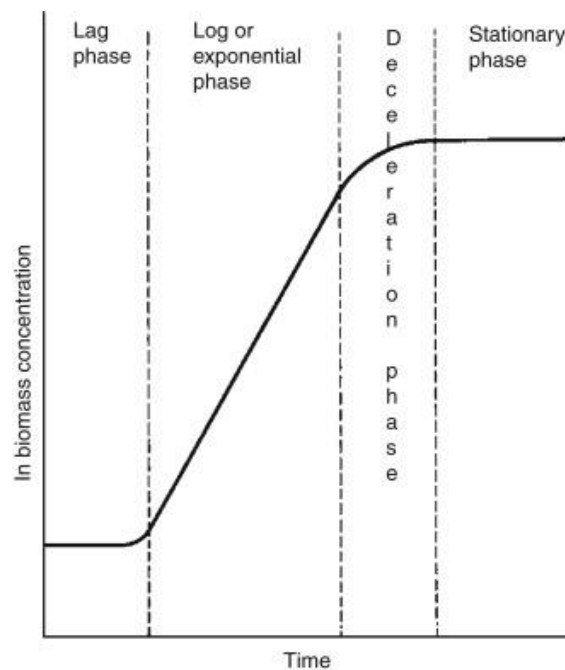


Figure 2.2. Example of a growth curve of a microbial culture in a batch cultivation adapted from [89].

During fed-batch cultivation fresh culture medium is added when the initial batch phase is finished. Liquid is not removed at any point during the cultivation, and thus the total volume increases. Aeration is applied for aerobic cultivations, if needed, as well as pH control. At the end of the fed-batch cultivation, i.e. when the bioreactor is filled with

fermentation broth, feed addition is stopped, the broth is harvested and product can be recovered.

During continuous cultivation (chemostat), fresh medium is provided continuously to the microorganisms and broth is removed from the bioreactor at the same flow rate (after an initial batch phase is finished). In this way constant volume is maintained in the bioreactor. Also the concentrations of substrate, biomass and products are maintained constant during steady state, while the cell growth rate is determined by addition of the limiting nutrient, typically the carbon substrate.

All three modes of cultivation are used in industry and academia, where the chemostat method of operation presents a valuable research tool in academia that enables study of physiological parameters in correlation with growth rate, or to observed the cell response when a sudden change of a process parameter is imposed (e.g., a change in glucose or oxygen concentration), as well as to study mutant behavior and microbial evolution during long-term cultivations (many generations) [90].

To be able to maintain a controlled and well-defined environment during microbial cultivations, monitoring of process parameters is crucial and it is usually categorized as off-line, at-line and on-line monitoring based on the time and place of the measurement.

Off-line measurement requires sampling of the cultivation broth where samples are analyzed later in the lab.

At-line measurement requires sampling of the cultivation broth where samples are immediately treated and analyzed, for example in a room next to the bioreactor.

On-line measurement doesn't require sampling, and measurement and data analysis are performed in real time. Measuring equipment can be located in the bioreactor (probes immersed in the cultivation broth) or outside the bioreactor (flow-through cell) [91].

Application of a chemostat with on-line monitoring is the cultivation mode of main interest in this thesis.

Yeast *Saccharomyces cerevisiae* was chosen as a model organism for this project since it is well known and researched organism in academia and industry and was part of a larger project collaboration that included this PhD project. Also *Lactobacillus paracasei* was chosen in one case study to perform first test of the MSBR I.

*S. cerevisiae* is a facultative anaerobic microorganism; it can metabolize sugar aerobically and anaerobically using two different metabolic pathways that have the same beginning - the glycolysis pathway (see Figure 2.3). Pyruvate is the glycolysis end product, which can be further utilized depending on the employed metabolism. During respiration pyruvate is transformed to carbon dioxide and water, while during fermentation pyruvate is transformed in ethanol and carbon dioxide [92].

*S. cerevisiae* is a Crabtree positive organism. In case of high glucose concentration, it produces ethanol under aerobic conditions, which is later used when all the glucose is utilized, after the diauxic shift [93]. During the diauxic shift cells decrease their growth and make a switch from glycolysis to aerobic utilization of ethanol [94].

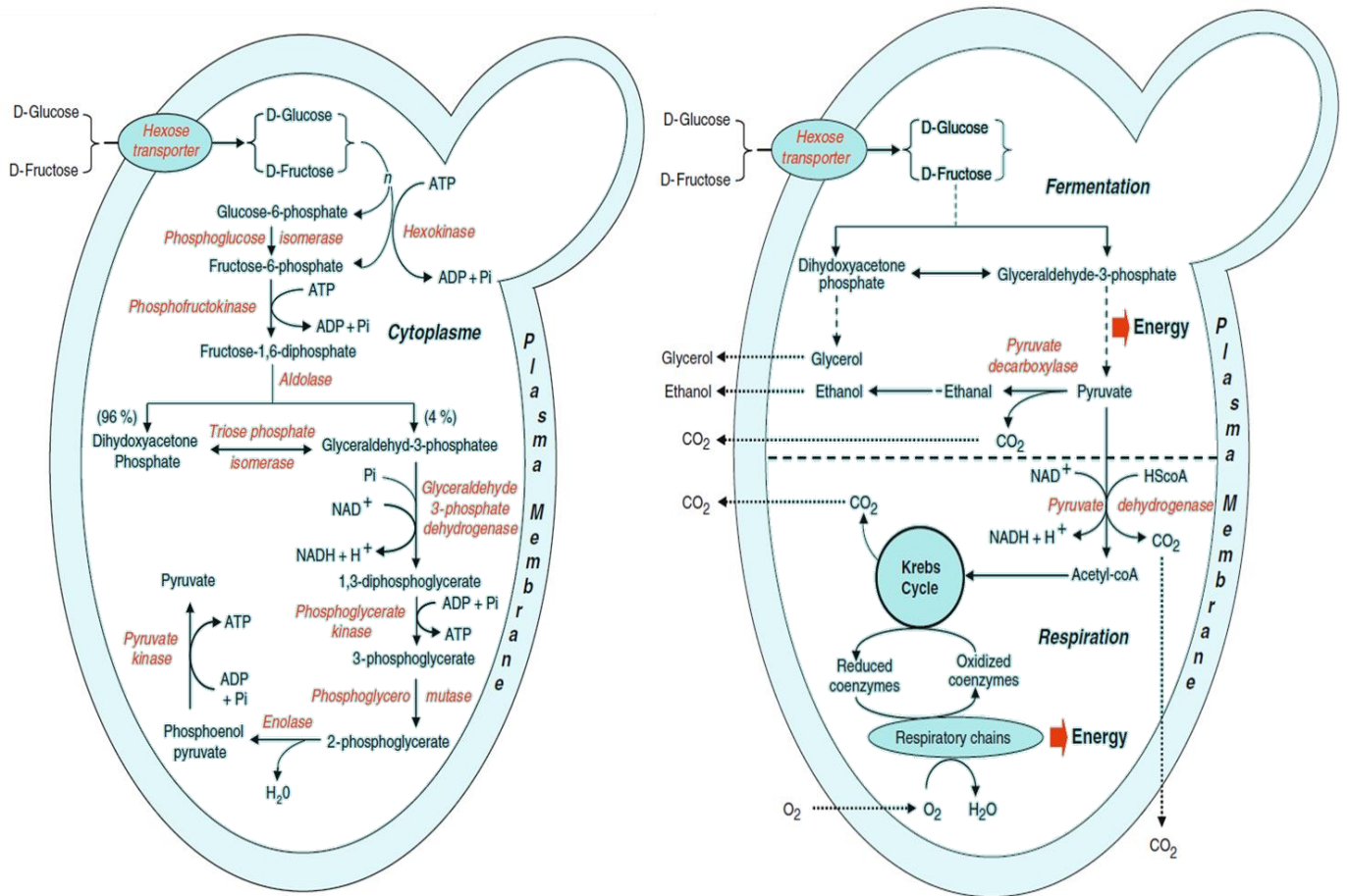


Figure 2.3. The glycolysis pathway (left side picture); fermentation and respiration pathways (right side picture) are same until pyruvate, after they split to fermentative or respiratory pathway. Pictures are adapted from [92].

## 2.4 Scope of the thesis and specific objectives of the project

Even though microbioreactors potentially have many advantages, it is important not to underestimate issues related to their size and handling. Evaporation, proper and reliable stirring, interconnections between micro-scale and the ‘macro world’ are just some of the burning problems that need to be solved. In addition, measurements of several process variables in microbioreactors are far from straightforward to implement. They rely on analytical methods, which are often not sufficiently developed for such a small scale at this point. If the measurements are possible, they are usually not cheap either. Another important issue that needs to be addressed is determining the optimal microbioreactor volume, if it exists at all, while keeping in mind the final objective – the application. There are several potentially interesting targets and cultivation strategies, and they raise a number of relevant questions related to the microbioreactor design. Do we work with

submerged cultivation or cells adhered on a substrate? Do we need to take samples during the cultivations? Which process parameters need to be monitored and controlled? Does the experimental work include expensive raw materials? Do we work with aerobic or anaerobic fermentation? Which  $k_{LA}$  values need to be achieved when we talk about aerobic fermentation? How crucial is a small reactor footprint? It is important to answer these questions in order to find the optimal working volume of the microbioreactor, since the working volume has a major impact on the reactor design and involves finding solutions for problems specifically related to a certain scale of operation. The final microbioreactor design should thus strongly depend on the goal of a specific microbioreactor application as mentioned earlier in section 1.1. In order to narrow down the quest of this research project, the defined application of interest, the scope and the main research project objectives are presented next.

The scope of this thesis is the development and application of a microbioreactor/milliliter-scale bioreactor in the field of submerged microbial cultivations, where the bioreactor design should satisfy typical requirements for such an application. The main goal is to create a tool that provides an adequate environment for cell growth, and to address the problems related to work with small scale bioreactors that are mentioned before. To be able to realize the main goal, the work was divided in specific objectives which are presented and addressed in this thesis:

- Modular design of single-use milliliter-scale bioreactor that can accommodate sensing interface, adequate heating, aeration and mixing conditions. Modularity gives a certain flexibility with regard to the application preferences (working volume, mixing, aeration).
- Integration of a mixing unit that can provide standardized, effective and reproducible mixing at milliliter scale.
- Improvement and characterization of mass transfer in the novel milliliter-scale bioreactor.
- Integration of an evaporation attenuating element as a measure to limit evaporation during cultivation.
- Development and integration of a cost effective syringe pump unit(s) for continuous microbial cultivation.
- Software - hardware interface and communication.

Although this research project produced a single milliliter-scale bioreactor, all design solutions were made with the high throughput possibility in mind. Furthermore this platform could be used and tested for different types of cells, and performances can be compared with bench scale bioreactors.



### 3.1 Introduction

The engineering design process methodology [95,96] is used to give a certain transparency and a structure to the overall research project. It is used as a guide in creating steps and tasks in the attempt to solve the research problem. The design process of the milliliter-scale bioreactor (MSBR) that was applied in this project starts with the problem formulation as a first activity, and it consists of 8 steps with a cyclical flow structure, indicating as well the iterative nature of the design process. An overview of the methodology is presented in Figure 3.1.



Figure 3.1. Iterative steps in the design process of a milliliter scale bioreactor with the problem formulation step as the starting point.

The cyclic structure or iterative nature of the design process gives a certain flexibility, since it allows repeating some steps and implementing improvements along the way. When creativity, prototype building and testing is a major part of the work and the possibility for multiple correctly functioning solutions is present, the cyclic structure helps coping with unforeseen difficulties and changes during the development process. All the steps of the design process will be briefly described and discussed in relation with the development of the MSBR in this chapter.

### **3.2 Step 1: Problem formulation**

*“The mere formulation of a problem is far more essential than its solution, which may be merely a matter of mathematical or experimental skill. To raise new questions, new possibilities, to regard old problems from a new angle require creative imagination and marks real advances in science.” – Albert Einstein*

Problem formulation is a process by itself that requires a certain time, when initial facts and data are gathered.

In general, the problem definition consists of a few stages [97,98]:

- Identify the need
- Recognize requirements and constraints
- Define a problem statement
- Establish a target for success

#### *The need*

The microbial cultures exhibit different environmental conditions at different scale during cultivations. Bench-scale bioreactors provide a uniform and well controlled environment with good mixing, while large-scale bioreactors can display gradients of substrate concentration, dissolved oxygen concentration and pH due to imperfect mixing performance [99]. In the large-scale bioreactor cells are exposed to a constantly changing environment going from nutrient-rich zones to nutrient-poor zones where cells suffer, which has influence on their metabolism and in return promotes population heterogeneity. It is difficult to monitor local process conditions in the large bioreactor due to limiting sensing options. Consequently, these process local conditions experienced by cells, need to be replicated in the environment where monitoring is possible. Ideally, a microbial culture is grown under uniform process conditions and a sudden change of substrate concentration or oxygen level is introduced and cell response is monitored. Micro- and milliliter- scale bioreactors coupled with flow cytometry, NIR or Raman spectroscopy can provide an adequate environment to determine the effect of different process conditions on population heterogeneity in microbial culture. Small scale bioreactors can be a valuable tool in understanding the environmental effects in large scale bioreactors and their influence on population heterogeneity of a microbial culture.

#### *Requirements and constraints*

Microbioreactors have potential to provide a uniform environment for the microbial cultures due to their small size and absence of gradients. The microbioreactor in Figure 3.2 is an illustrative example on how 100  $\mu\text{L}$  can be used efficiently for monitoring of basic process parameters (T, pH, DO, and OD). On the other hand such a small available space in the reactor doesn't allow elaborated stirrer or connection ports for communication with other equipment. Furthermore it is a challenge to maintain aeration high enough so a culture is not affected.

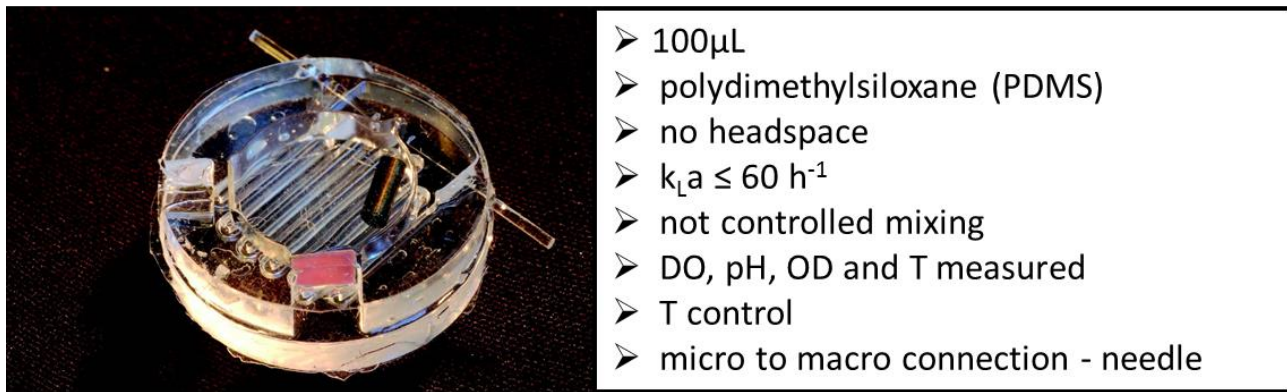


Figure 3.2. Photo of the 100  $\mu\text{L}$  microbioreactor reproduced from the PhD thesis of Daniel Schapper [100].

A small scale bioreactor used to study cell response to changes in the surroundings needs to display a certain level of functionality and uniform culture conditions.

Functionality implies:

- Disposable (no cleaning, no cross contamination)
- User friendly (if reactor and supporting equipment are complex for end user, it is less probable that it will be accepted)
- Low cost (low cost per data point)
- Small footprint (to open a possibility for parallelization)
- Easy communication with external equipment

Uniform microbial culture conditions imply:

- Process parameters being monitored and controlled to achieve fully defined environment for cell growth.
- Working volume small enough to produce a functional platform with absence of gradients in the bioreactor and big enough to accommodate different sensors, a stirrer and the possibility to take a sample for any additional off-line analysis.

Oppositely, constraints can be defined on a case by case basis starting from available design solutions. Development work with a 100  $\mu\text{L}$  scale bioreactor and microbial cultivations in this reactor, gave an indication about the first and most important constraint - working volume. It can be questioned why the working volume is the most

important constraint? As a matter of fact, when designing microbioreactors all other constraints occur as a consequence of the choice of the working volume. It is for example difficult to obtain efficient mixing and a high oxygen transfer rate if there is no sufficient space to place a stirrer and use it in a controlled way. Furthermore, it is challenging to fabricate a bioreactor (bioreactor, not microfluidic channels) with a very small volume.

The previous discussion brings us to the *problem definition*, which is a statement that answers three questions: who has a need, what is needed and why is it needed [101].

**Researchers, scientists and engineers that work in the biotech industries on development and optimization of microbial cultivations and mammalian cell cultures have a great need for tools-bioreactors that provide a low cost, comprehensive, high quality information output per experimental set up. A complete solution to this issue still doesn't exist. The fast growth of new therapeutics is accompanied with a high development cost, pushing companies to look out for new technologies [17] that can give them a competitive advantage in the rapidly changing market.**

In order to conclude the problem formulation and complete the first step in the engineering design process, it is important to *establish criteria for a successful solution* of the previously specified problem statement. The following statements are criteria that apply to the design of a small-scale bioreactor:

- The small-scale bioreactor should be user-friendly with small footprint, and have a low cost with the inherent possibility for mass production of the device.
- The small-scale bioreactor should have efficient and controllable mixing.
- The small-scale bioreactor should have an oxygen transfer rate similar to a bench scale bioreactor.
- The small-scale bioreactor should be robust and capable of providing reproducible cultivation conditions in the bioreactor.
- The small-scale bioreactor should have robust and tight connections from the bioreactor to other equipment.
- The small-scale bioreactor should be able to operate in batch and continuous mode.

### **3.3 Step 2: Gather required knowledge**

When the problem formulation is completed, the scope of the research is defined and that brings us to step 2 - background research. Obtaining the information and a comprehensive understanding about the problem at hand is of outmost importance for creating a successful solution. It requires time to gather information, learn and allow knowledge to be absorbed.

The study of small scale bioreactors has a multi-disciplinary character, so many different areas of expertise were considered during the learning process and the data collection, e.g.

on-line monitoring at small scale, fluidics, fabrication and material choice, software, the microbioreactor itself, etc.

An extended literature survey was performed. Figures and facts were collected regarding the history and past research on the topic of small scale bioreactors. Existing solutions in academia and industry were carefully examined and compared. The gathered information provided confirmation that the problem formulation stated in step 1 was correct and valid.

All the information collected from journal articles, books and the internet is presented in the Chapter 3 as a review of the current status of small scale bioreactors.

### **3.4 Step 3: Brainstorm and develop solutions**

The starting point for generating potential solutions was an existing solution. The design of a 100  $\mu$ L bioreactor within our research center [100] generated ideas on how to address certain limitations that are the consequence of performing a cultivation at such a small scale. Development and design of the microbioreactor and the supporting platform is a complex undertaking and it was divided in smaller tasks with specific functions in mind. The solutions of the different tasks needed to work together in a modular way, and accomplish the final goal. In Figure 3.3 the complexity of the problem is presented graphically in the form of a tree.

Green bubbles in Figure 3.3 present features that the microbioreactor is supposed to have and orange bubbles are specifications that need to be addressed for each feature. It was essential to develop a solution that is self-sufficient, since a small scale bioreactor in combination with regular size laboratory equipment cannot provide the possibility for high throughput experimentation.

Two main decisions provided a direction for future design:

- The volume of the microbioreactor changed from microliter to milliliter scale (1-2 mL).
- The fabrication material of the microbioreactor was changed from Polydimethylsiloxane (PDMS) to poly(methyl methacrylate) PMMA.

Increased volume of the microbioreactor had multiple effects, allowing different design solutions to be considered for different features:

- *Mixing* – change from chaotic mixing with a stirrer bar at the bottom of the microbioreactor to a versatile, fully controlled stirrer mounted on a shaft. This induced a change in the secondary equipment, and thus the typical laboratory magnetic stirrer could be replaced by a tailor-made device with a smaller footprint.

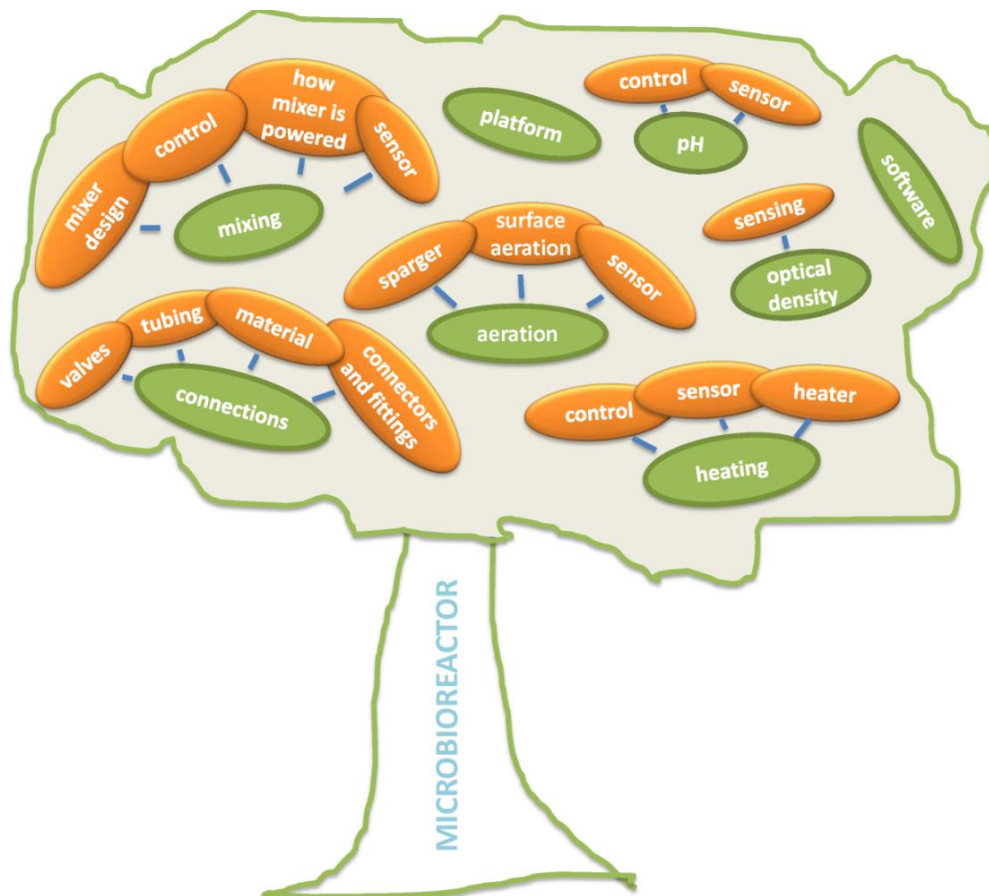


Figure 3.3. Representation of the complexity of the microbioreactor design. Green bubbles represent the main functions that are pillars of the microbioreactor design, while orange bubbles present what needs to be included in each function so it can be complete.

- *Aeration* – move from a completely filled microbioreactor to a bioreactor with a headspace, which gave the opportunity for surface aeration and sparging. Bubbles were not an issue any more, but rather a positive and wishful appearance.
- *Sensing* – with a bigger diameter of the bioreactor base, it was possible to arrange standard size fiber bundles, a temperature sensor and heater with minimal interference between each other which was important for temperature control and precise, reproducible sensing.
- *Connection* – enough space was created to introduce a number of openings on the top or on the walls of the microbioreactor which allows making a move from needle type connections to standard size fittings and an appropriate number of openings.

The change of the fabrication material of the microbioreactor had an effect on:

- The oxygen permeability of PMMA is  $0.155 \times 10^{-10} \text{ cm}^3(\text{STP}) \text{ cm}/\text{cm}^2 \text{ s cmHg}$  [102], while PDMS has an oxygen permeability of  $800 \pm 20 \times 10^{-10} \text{ cm}^3(\text{STP}) \text{ cm}/\text{cm}^2 \text{ s cmHg}$  [103] which it is about three orders of magnitude higher. Consequently, aeration in the microbioreactor is shifting from a membranes-without-headspace

principle for the 100 µl microbioreactor [57] to direct contact between gas and liquid phase.

- *Manufacturing* – change from mold-shaped silicon parts connected by silicon glue to micro-milled plastic parts connected by applying the ‘Lego’ plug and play principle and chromatography fittings.
- *Connection* – switch from needle type connections to standard size fittings and an appropriate number of openings, which in turn gave rapidly established, reusable (no glue) and leak-tight connections.
- *Reproducibility and ease of use* – non-permanent (no glue or adhesion) assembly that can be put together or disassembled according to the need with the same reproducible result.

The brainstorm process evolved around the main idea that the microbioreactor should resemble a bench scale stirred tank bioreactor in order to obtain a similar physical environment for the cells. Different possibilities were considered for each feature of the microbioreactor. Below a few examples are provided:

Heating – incubators, jackets, coils inside or outside of the microbioreactor.

Mixing – shaking, stirring with stirrer on the shaft, two or one impellers on the shaft, presence of baffles, non-rotational stirring by moving liquid up and down.

Temperature sensor – distance from the heater, inside or outside of the microbioreactor, etc.

Aeration – sparger type (porous, orifice, nozzle) and location, combined sparger-stirrer, bubble size.

Vessel – size and shape (cylindrical, square) to accommodate all the other features, position of the openings.

Scattered light intensity measurement – location of optical fibers from side to side or from top to bottom, using the shaft of a stirrer, using a mirror in the reactor.

Platform – small or large footprint, rectangular, round or square plate adjusted to fit the microbioreactor.

The mentioned ideas are just a few examples of the brainstorm results. They were evaluated in a systematic way that is described in step 4, and then combined together to create the microbioreactor with the platform. Potential solutions for each feature were further developed to be compatible with the rest of the system, hence the whole system went through 7 design iterations until it reached the version of the first prototype model.

### 3.5 Step 4: Evaluate and select possible solution

Even a few ideas for each subsystem of the microbioreactor platform can give a considerable number of possible solutions for the overall design. To be able to select the best solution and decide which one to keep and which one to disregard, all ideas needed to be analyzed and evaluated. The main tool used in this step was the decision matrix. The decision matrix has the form of a table where different options/solutions/ideas are evaluated based on different attributes/criteria [96]. Each carefully chosen criterion was assigned an importance/weight factor on a scale from 0 (low importance) to 100 % (high importance) which is reflecting how significant an attribute is in the overall classification. Throughout the evaluation and selection process, each option/solution/idea was ranked on a scale from 0 to 4 and adjusted for the importance factor, for all the selected attributes. A 5-point scale is used for rating different ideas against a set of design criteria, where 0 = inadequate, 1 = poor, 2 = satisfactory, 3 = good and 4 = excellent. Also this 5-point scale can be translated to an 11-point scale (0-10) when there are fewer unknowns and more details of the design are available. The sum of the rankings was then compared and the idea with the highest score selected as the winner.

Let's consider the evaluation and selection process for the heater design as an example of the earlier explained procedure. In section 3.4 certain ideas are proposed for heating in the MSBR and here, in this section, they will be assessed according to the specific design criteria.

The main function of a heater is to warm up liquid to the required temperature set point in the reactor and to maintain it at a given temperature set point. There are a few ways to achieve heating in the MSBR:

- Heating from the bottom
  1. heating element
  2. heating plate
  
- Heating the walls of the MSBR
  3. jacket filled with water
  4. jacket made of coils
  5. solid jacket inside of the MSBR
  6. solid jacket outside of the MSBR
  
- Heating the whole MSBR
  7. Incubator

When ideas are created, it is important to also establish certain success criteria which can be evaluated and rated. In the example presented here, 3 criteria are considered important for achieving a functional design of the heater:



- Simple implementation - the heater should be implemented such that it is compatible with other units with different functions e.g., mixing and online monitoring, and still be close enough to the liquid in the reactor.
- Effective control - the contact surface between heater and the reactor needs to be large enough to provide an adequate heater response to disturbances and does not create a large temperature gradient.
- Parallelization - the possibility for individual heater settings with impact per reactor should be included.

After generating ideas and establishing evaluation criteria, the decision matrix is made in the form of a table (see table 3.1) and the 5-point scale ranking is applied based on available knowledge, experience and engineering reasoning. In this example, the heating element / microheater is a winning idea among the 7 ideas that are proposed, based on the following requirements: simple implementation, effective control and parallelization. Heating elements are small and can be placed at different places in the reactor based on the overall design. They allow parallelization since each microheater can be controlled separately. However effective temperature control will depend on the size of the reactor and heater, the working volume and the mixing efficiency.

Table 3.1. Decision matrix for heater design. Three criteria are used and a certain importance is assigned to each of them. Seven ideas presented in the text above are assessed against these criteria and rated according to a 5- point scale. Each assigned number from the 5-point scale was multiplied by a weight. The sum of the resulting values gave the main scores for each idea, which were then compared in order to choose the best idea.

Criteria	Weight (%)	1	2	3	4	5	6	7
Simple implementation	45	4/180	1/45	1/45	2/90	1/45	2/90	1/45
Effective control	35	3/105	3/105	2/70	2/70	4/140	3/105	3/105
Parallelization	20	4/80	4/80	1/20	2/40	2/40	2/40	1/20
Score		<b>365</b>	230	135	200	225	235	170

Size and position of the heater in the platform is important when ideas are ranked according to the criterion: simple implementation. The heating plate could be simply implemented if the bottom part of the reactor is free. However, if sensing is applied through the bottom plate, implementation of the heating plate suddenly becomes a

complex problem. Also implementation of a jacket filled with water around the reactor increases the complexity of the whole platform, the risk of leakage and it can interfere with sensing and mixing processes. A jacket with coils is a slightly better solution since it doesn't require water, however it has a more complex geometry and its positioning on the wall and the size of the contact surface can produce a temperature gradient. A solid jacket inside of the reactor can interfere with the mixing by creating dead zones and preventing installation of baffles and reducing the available space for the stirrer. Moreover it can create pockets that are difficult to clean, and thus contamination can be a frequent problem if this type of heater is chosen. An alternative to a jacket inside of the reactor is a solid jacket placed outside of the reactor chamber which could be a good option as long as the wall of the reactor chamber is thin and the electromagnetic field used for mixing is above or below the reactor chamber, or if a motor is used for driving the stirrer. Placing a reactor in an incubator seems to be a solution that is simple enough to implement, however the reactors need the sensing platform and different types of connections which are not that easy to implement in the incubator. Also, temperature variation from reactor to reactor, a potential option in a screening design, is not possible using an incubator.

Idea selection and application of the decision matrix is done in the same manner for each subsystem of the MSBR platform, e.g. to choose the sensing principle (optical or electrochemical) or the type of mixing (stirring or shaking) and so on. The final result of this step is a collection of defined main features of the first prototype:

- Non-invasive sensing from the bottom of the reactor.
- DO and pH measurement by sensor spots and an optical fiber bundle.
- T measurement by an RTD sensor (resistance temperature detectors).
- Heating by means of a heating element / microheater.
- Mixing by a rotating electromagnetic field and impeller blades.
- Aeration via the headspace or via a small opening in the wall of the reactor.
- Reusable connections.

### **3.6 Step 5: Build a prototype**

Detailed planning is required during this step. Here, each aspect/feature of the design proposed is elaborated and specifications are made, which are presented in table 3.2. The list of necessary materials and tools is created based on technical drawings as well as the sequence of important fabrication operations.

The first prototype MSBR was made in our laboratory at the Technical University of Denmark (DTU) using a CNC milling machine (CNC micromill, Minitech MiniMill 3/Pro, Minitech Machinery Corporation, Norcross, GA, USA). First, an assembly was created using the software Solidworks and each part was converted to a technical drawing which

was then translated to a numerical control language G-code, which the CNC milling machine was able to understand.

Table 3.2. Specifications for the prototype I

<b>Bioreactor</b>	
<b>Maximum working volume</b>	1 mL (2 mL)
<b>Minimum working volume</b>	0.5 mL
<b>Bioreactor inner diameter</b>	16 mm
<b>Bioreactor height</b>	11 mm (18 mm)
<b>Bioreactor material of construction</b>	PMMA, PDMS
<b>Impeller</b>	Top-mounted, magnetically-driven (0-1200 rpm)
<b>Impeller type</b>	Custom made impeller with 4 blades at two levels
<b>Impeller diameter</b>	14 mm
<b>Impeller location</b>	Centered
<b>Sparger / Headspace aeration</b>	Opening at the bottom of the bioreactor wall / inlet and outlet opening above liquid level
<b>Process instrumentation</b>	
<b>DO sensor</b>	SP-PSt3-NAU-D5-YOP (0-250% air sat.)
<b>pH sensor</b>	SP-HP5-D5-US (pH5-8)
<b>T sensor</b>	PT100 (0-100°C)
<b>OD sensor</b>	Transflectance with specular reflection
<b>Heater (T control unit)</b>	Custom made from copper wire and aluminum casing

Values between parentheses apply in case two polymer blocks were used for the taller reactor (2 mL volume).

The fabrication involved many trials and errors, especially with the very small pieces used for the stirrer. It involved learning about different milling inserts and tools, the behavior of plastic under aggressive milling, fixing plastic plates on the milling surface and establishing the x, y and z axis to the zero position. Also, a mold was made for polydimethylsiloxane (PDMS) seals that were used between plastic parts to prevent potential leakage. Full details of the MSBR prototype I and the fabrication procedure are described in Chapter 4.

The second prototype design was fabricated in collaboration with the DTU workshop, except for the pump system which was made by milling at DTU Skylab. Details of the MSBR prototype II are described in Chapter 5.

Even with the latest prototype, fabrication constraints were still present. We would frequently encounter various limitations in the workshop as well, since most of the regular, commercial fabrication tools are used for larger elements. It is of outmost importance to have access to proper fabrication technology when working with very small structures. It simply gives more freedom in creating diverse and better solutions. Here micromilling was used as the main fabrication technology; however production at larger scale would demand a more effective way to make a prototype, e.g. hot embossing and injection molding. Further, 3D printing is becoming established technology as well, which is capable of producing structures whose production is hardly feasible with already established fabrication technologies. These more advanced tools provide an opportunity to have a different approach to the process of making a prototype. So, some ideas in this project that were discarded in the previous steps as too complex, would be considered differently if there was a more effective fabrication technology available at the time.

### **3.7 Step 6: Test prototype**

The most important step in the final phase of the project is testing and evaluating the prototype. Does the prototype work or not? Which parts could work better? Is fine-tuning necessary or is a complete redesign required? Since the MSBR platform is a rather complex system, many different tests and experiments were performed for each subsystem. In addition, this step also included troubleshooting and minor revisions along the way. Eventually, the whole MSBR platform was tested by performing a microbial cultivation.

The performed tests and experiments gave information about the capabilities of the MSBR platform. Tests were performed to check the connection between software and hardware, coils or DC motor performance, leakage possibility, fittings, sensing precision, etc. Afterwards, characterization of the mixing performance, aeration and sensing (establishing the measurement range for the scattered light intensity) was completed with different types of experiments that were used to establish the mixing time, the residence time distribution, the  $k_L a$  correlation with the different process parameters, the scattered light intensity linear range, and the temperature profile. Detailed descriptions of the performed experiments together with results are presented in Chapters 4 and 5 where prototypes I and II are described.

Due to time constraints close to the end of the project and the slightly different configuration of the prototype II, tests and experiments performed to characterize prototype II were not as extensive compared to prototype I. When developing prototype II, emphasis was put on the pump system and the pre-humidifier to be able to obtain continuous cultivations.

### **3.8 Step 7 and 8: Evaluation of the prototype performance (7) and redesign if needed (8)**

During step 7, evaluation of the prototype performance takes place. The assessment is based on the previous testing (step 6) and if the results are positive and the prototype essentially satisfies earlier established performance criteria, then design activities are concluded and the results are communicated.

Step 8 is necessary when the prototype doesn't perform as envisioned. The issue can be small, where a minor modification or optimization of a certain part is necessary and parametric redesign is applied, or medium, where an entire subunit or subsystem has to be modified and adaptive redesign is applied. In the worst case scenario, the prototype has a major flaw which leads to a complete redesign and application of the original redesign [104].

In the case of this research project, after the evaluation and characterization of the first prototype, an overview of the occurring issues during the work was made which indicated that further improvement was needed, but not an overall redesign. Some of the issues are described in Chapters 4 and 5 where the developed prototypes are presented in detail. Consequently, prototype II was made in order to improve the design and make it more robust and reliable. Beside improvements in the already existing design, two new units were designed in the frame of the development of prototype II - a pump system for liquid and gas, and a pre-humidifier for prevention of evaporation, such that it should be possible to perform continuous cultivations.

### Milliliter scale bioreactor design – Prototype I

---

This chapter presents the prototype that was first chosen to be designed and fabricated and its content is mostly based on the article “A flexible well-mixed milliliter-scale reactor with high oxygen transfer rate for microbial cultivations” published in Chemical Engineering Journal in 2016 by Bolic et al. The design of the milliliter-scale bioreactor (MSBR) – prototype I is described in detail together with the fabrication method. Each part of the system is shown as well as its function and role in the overall assembly. Afterwards, the experimental methods used for characterization of the MSBR in terms of mixing performance and oxygen transfer rate possibilities are explained. Computational fluid dynamics simulation of the MSBR configuration, work that has been performed by PhD student Hilde Larsson, is also presented in this chapter to complement the experimental results. The results are presented and discussed showing the MSBR capabilities to provide effective mixing and a sufficient oxygen transfer rate. In conclusion, the results of microbial cultivations performed in the MSBR are presented as well as short overview of the problems encountered during work with prototype I.

#### 4.1 Introduction

For an aerobic cultivation at any scale mixing performance and effective oxygen supply are crucial. Many research studies are performed in order to have a better understanding about transport processes in bioreactors, particularly related to oxygen transfer to the liquid phase. Performing cultivation studies in small scale bioreactors brings many benefits (reduce overall cost, footprint, cleaning, substrate consumption and labor), but then again adequate mixing and achieving a sufficiently high oxygen transfer rate becomes considerably more difficult as well as maintaining process conditions similar to the ones at larger scale. Moreover, solving this issue at microliter (< 1 mL) and milliliter scale (> 1 mL) essentially requires a different approach, and the solution is also dependent on the device geometry. Scale effects (micro vs. milliliter) on the conditions in the bioreactor are discussed in section 2.1. Microfluidic devices where the mixing is governed by diffusion processes using active or passive mixing principles in microchannels are an entirely different area which is not the topic of this discussion and the thesis. Capretto et al. [105] and Lee et al. [106] provide a detailed overview of the micromixing field and the different types of mixers that can be used in different applications at the mentioned scale.

Mixing, applied at submilliliter (< 1 mL) and milliliter (> 1 mL) scale during microbial cultivations in tank/well chamber geometry, is mostly based on shaking [38,47,48,51,52] or stirring with some sort of custom made impeller or magnetic ring

[4,26,28,33,35,43,49,50,54,57]. There are also some less traditional solutions presented in the literature as well, where mixing is obtained by inflation and deflation of the reactor chamber [59], pressure shuttling between the two chambers [45] or by using a peristaltic oxygenating mixer [107]. In submilliliter bioreactors oxygen is mostly delivered by surface aeration while in bioreactors with bigger volumes (6 -12 mL) sparging is often a plausible option. Overall, microbioreactors up to 1 mL do not usually have a proper stirrer (i.e. a stirrer that is not a modified magnetic stirrer bar) and a sparger, which gives a limitation to the maximal achievable oxygen transfer rate. Furthermore, many solutions for submilliliter bioreactors are simply not stand-alone solutions since they rely heavily on supporting lab equipment e.g. magnetic stirrers and incubators [8].

To study and evaluate performance of microbioreactors, experimental characterization can be performed or computational simulation techniques can be employed. Computational fluid dynamics (CFD) simulations are used for analysis of mass and heat transfer, fluid behavior and energy dissipation rates among others, which helps in design, analysis and optimization of the simulated operations and applications [108]. CFD simulations can contribute to reducing cost and process development time compared to experimental work [109]. However, the main prerequisite for further model applicability is model validation which initially involves experimental work. CFD simulations are successfully used for microscale bioreactors with laminar flow and absence of rotational parts, due to the smaller number of elements in the CFD mesh and the absence of turbulence model. On the other hand, simulations become more complex and require more computing time when impellers (rotating element), a turbulence model and gas-liquid mass transfer modeling are used [110], and including these features in the model is necessary if conditions in bioreactors are simulated.

In the current study a milliliter-scale bioreactor (MSBR) design with a supporting platform is presented. The MSBR is equipped with a novel stirrer that enables good mixing and a high oxygen transfer rate at milliliter scale and below. Overall the MSBR system is made to be robust and user-friendly with certain degrees of freedom regarding the use of different working volumes (from 0.5 ml to 2.0 ml), application of one- and bi-directional mixing and two aeration modes (surface aeration and sparging). The MSBR is considered to be a disposable tool since material and fabrication are inexpensive and all reusable parts of the system are items of the supporting platform. In the present work, mixing performance is demonstrated and characterized in the MSBR by evaluating mixing time, residence time distribution and oxygen transfer rates at different conditions in the system.

## 4.2 Materials and Methods

### 4.2.1 Milliliter scale bioreactor platform – Prototype I

The supporting platform for the milliliter-scale bioreactor is made of a polymethyl methacrylate (PMMA) plate (75 mm x75 mm dimension) and 4 stainless steel threaded rods that are used for height adjustment. Four electromagnetic coils, used to generate a controlled magnetic field, are placed on the plate with 90 degrees angle between each other, surrounding the MSBR. In the middle of the plate, a base (25 mm x 25 mm x 3mm dimension) is made by means of a CNC milling machine (CNC micromill, Minitech MiniMill 3/Pro, Minitech Machinery Corporation, Norcross, GA, USA) as a negative to the bottom of the MSBR. The milliliter-scale bioreactor supporting platform is presented in Figure 4.1.

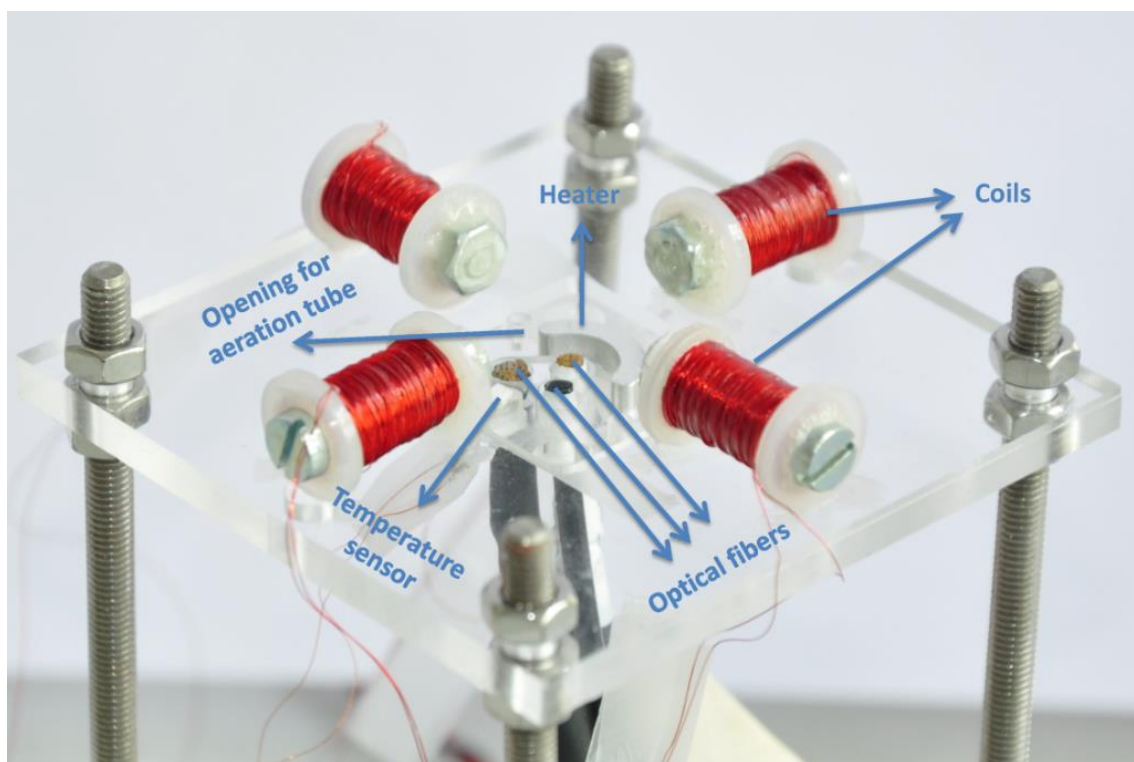


Figure 4.1. The millilitre-scale bioreactor supporting platform is made of a PMMA plate with 4 metal rods as plate holder. In the middle of the plate, a pocket is made with designated islands for the temperature sensor, the heater, three optical fibre bundles used for measurement of OD, DO and pH, and finally openings for aeration tubes. Around the pocket, 4 electromagnetic coils are positioned. A technical drawing of the platform is presented in appendix B.

A temperature sensor, a heater and three custom made optical fibers (for pH, dissolved oxygen and the scattered light intensity) are located in the base and arranged in a complementary way to the MSBR bottom. The temperature sensor is a PT 100 resistance



thermometer (chip dimensions 2 x 2.3 mm). The aluminum heater is custom made by the CNC milling machine as a pocket in the shape of a banana, where a bundle of copper wire is placed inside the pocket and sealed by glue. The heater and the temperature sensor are located furthest away from each other to maintain a reliable reading of the temperature in the MSBR. The three optical fiber bundles are used for on-line monitoring of dissolved oxygen, scattered light intensity and pH during the cultivations. Two small cylindrical holes, placed on the opposite sides in the base, are made to facilitate passage of aeration tubes across the platform. They are also used as guidance for positioning of the MSBR on the platform.

Overall, the platform is compact and reusable which allows the MSBR to be disposable, since all expensive parts of the system are located on the platform. The MSBR uses the modular 'Lego' plug and play approach to be placed on the platform.

#### **4.2.2 Milliliter scale bioreactor design - Prototype I**

The milliliter-scale bioreactor itself is fabricated from a transparent plastic - PMMA, the same material that is used for the supporting platform. It has a design that allows for flexibility in working volume (0.5 - 2.0 mL), mixing pattern (one- or bi-directional stirring) and aeration mode (sparging or surface aeration).

The bottom part of the MSBR is a 3 mm thick plate with outer dimensions 25 x 25 mm on which two PreSens sensor spots for measurement of pH (SP-HP5-D5-US) and dissolved oxygen (SP- PSt3- NAU- D5-YOP) were glued. They are glued on the side which is in contact with the cultivation broth. The side of the bottom plate facing the platform has a specific pattern that permits optical fibers, heater and temperature sensor to be very close (0.25 mm) to the fluid inside the MSBR (see Figure 4.2). In other words, the bottom part is made as a negative to the platform and had a thin optically transparent layer to ensure that measurements based on optical properties were possible (pH, dissolved oxygen, scattered light intensity).

The top part of the MSBR is made in two versions: either consisting of one or two blocks of polymer, where the reactor chamber and the stirrer are fit inside; those two versions are presented in Figure 4.2. This approach provides flexibility in choosing the appropriate working volume for different applications.

Between each PMMA part, a 1 mm thick polydimethylsiloxane (PDMS) layer is placed for sealing purposes. The silicone layer is custom made using PDMS (Sylgard 184, Dow Corning Corp., Midland, MI, USA. Mixing ratio of 10 parts silicone: 1 part curing agent) and a micro-milled mold with a structure defined by the MSBR design. The mold is also fabricated using the CNC milling machine. The MSBR is sealed by four screws when all parts were assembled together.

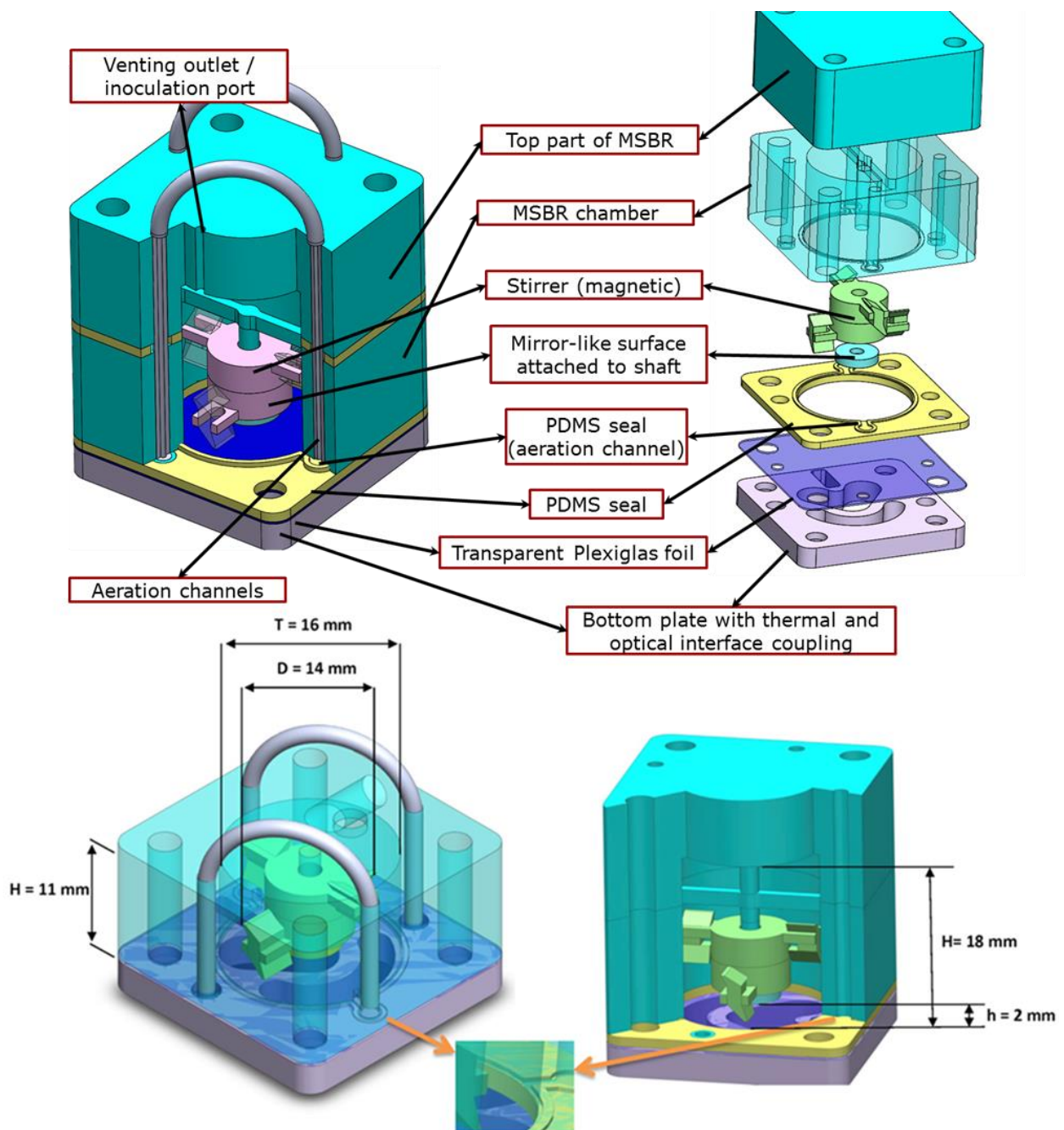


Figure 4.2. The MSBR designs with one (maximum volume 1 mL) and two polymer block chambers (maximum volume 2 mL) (Dassault Systèmes SOLIDWORKS Corp., DTU licence). Both reactors have the same features, except for the working volume that is bigger in the reactor with two PMMA block chambers. The light purple plate in the exploded view of the MSBR shows areas where heater and optical probes are placed when the MSBR I is positioned on the platform. The tube used for aeration is ending in a small microchannel that is connected with the cultivation chamber (visible in the wall of the MSBR and enlarged in the lower part of the figure). The yellow layer is made from PDMS and it is used to seal the reactor. Another PDMS layer is used when an additional PMMA block is added on top (it is not shown in the figure). A technical drawing of the reactor is presented in appendix B.

Both versions of the MSBR have holes in the wall allowing the connection with aeration tubes. The holes are ending in small microchannels that are connected with the MSBR chamber. This can be seen in the small picture in Figure 4.2. Consequently, air is coming through a tube into the microchannel and the air ends up as bubbles in the MSBR chamber. In this way aeration by sparging is obtained.

On the other hand, surface aeration is achieved by direct placement of air tubes in the headspace through connecting ports with thread. The same principle is used for the inlet tube.

Mixing is performed by a specifically designed stirrer (see section 4.2.3 for a detailed description) which is mounted on a shaft and secured by a small plate with a diameter of 6 mm. The side of the plate facing downwards is covered with aluminum tape that is acting as a mirror for the scattered light intensity measurement.

#### **4.2.3 Stirrer design and fabrication – Prototype I**

The general idea of stirring in the MSBR was revolving around the same principle that is applied in the case of stirred tank bioreactors where shaft and impeller blades exist. In order to achieve this in the MSBR, the shaft was made as a part of the PMMA block which was housing the bioreactor chamber. Considering that the mixing principle applied was based on a revolving electromagnetic field, it was necessary to attach a magnet to the stirrer, and more specifically to the impeller blades but not to the shaft such that it would be possible to freely rotate the impeller part. Design of the stirrer emerged around one main constrain – the size and shape of the magnet. It was necessary to use a ring shaped magnet, so it can freely rotate around the shaft. The magnet needed to be isolated from the fermentation broth, and thus two PMMA cylinders with pockets inside were made to encapsulate it. Both cylinders included fork shape parts that were sticking out and that served as carriers for impeller blades that were separately produced by micromilling. In other words, the stirrer consists of a cylinder made up of two separate parts, which has two pairs of impeller blades placed at different levels. An illustration of the stirrer is presented in Figure 4.3. A permanent magnetic ring, magnetized across its diameter, is placed inside the cylinder and it is driven by a magnetic field. The size of the cylinder is determined by the dimension of the magnetic ring ( $d_{OUT}=6.5\text{mm}$ ,  $d_{IN}=3.1\text{mm}$ ).

Both parts of the cylindrical structure have an opening in the middle which allows the placement on the shaft. On the opposite side of each cylinder part, two holders for the impeller blades are located. The impeller blades are broad and they have a zigzag geometry. The position of the impeller blades at two levels enabled to work with different volumes in the MSBR whilst the two upper impellers also had the purpose to break the

liquid surface and enhance the oxygen transfer from the headspace to the liquid. All parts of the stirrer, except the magnet, are made of PMMA using the CNC milling machine.

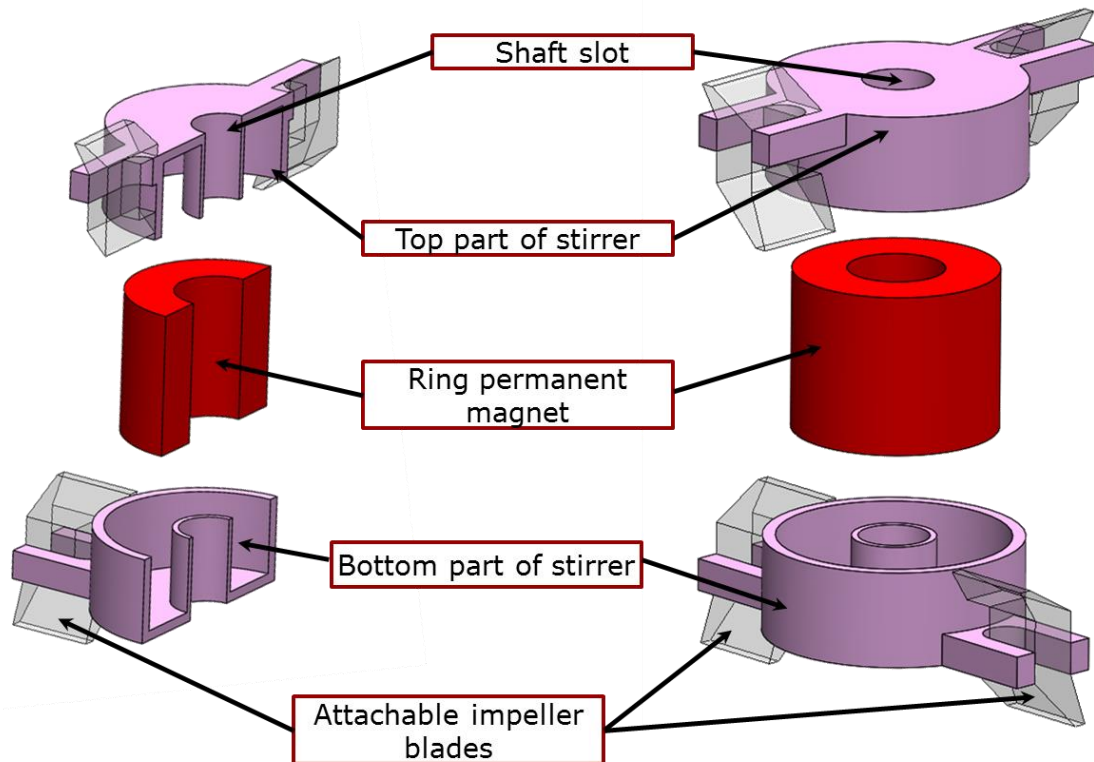


Figure 4.3. Mixer design (Dassault Systèmes SOLIDWORKS Corp., DTU licence). The stirrer consists of two cylinder pockets where a ring-shaped magnet is encapsulated. Each cylinder has two forks for holding two blades, so the impeller blades can be placed at two levels. A technical drawing of the stirrer is presented in appendix B.

#### 4.2.4 Control algorithm and mixing profiles

A stand-alone mixing system with a control algorithm was developed in order to obtain reliable and reproducible mixing in the reactor. The magnetic field, used to rotate the stirrer, is generated by four electromagnetic coils of copper wire. The coils and their position in relation to the MSBR and the permanent magnetic stirrer are presented in Figure 4.4 which in essence constitutes a 2-pole stepper motor operational principle. The coils are powered and controlled with a custom made power electronic module consisting of two 'H' bridges, MOSFET transistors and corresponding drivers.

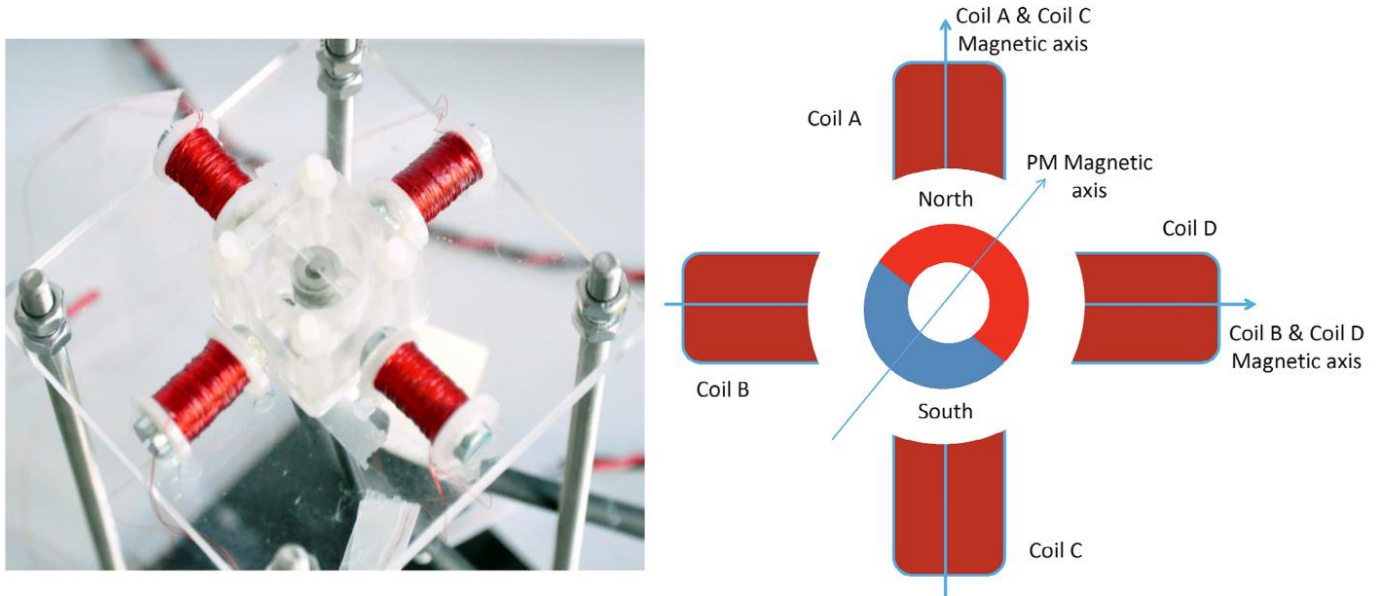


Figure 4.4. Position of the four coils around the microbioreactor. The principle of magnetic stirring is presented in the right picture showing interaction between the magnetic field created by the magnetic coils and the magnet that is magnetised across its diameter.

All control inputs are generated by a National Instrument USB6229 IO card and connected to the power module where all inputs are galvanically insulated via opto-couplers. The power stage of the power electronic module works with voltages from 5V to 30V, which complies with the safety requirements of most laboratories, and is capable of delivering currents of 2A.

The control algorithm written in LabView generates a Pulsed Width Modulation (PWM) signal which in turns controls average value and polarity of the output DC voltage, hence the user can set the speed and direction of the stirrer as desired. The operation of the stirrer is based on the proper sequence of coil excitation such that the position of the created magnetic field can revolve in the specified direction and with the specified speed, which is as well the working principle of a stepper motor. An illustration of this principle is shown in Figure 4.4 (right).

The user interface in LabView includes the possibility of varying the rotational speed of the stirrer. It is possible to create a speed profile as a function of time such that the stirrer will not only rotate at constant rotational speed, but will also have periods with acceleration and deceleration. The profiles of the stirrer speed as a function of time can also be expressed as time varying functions like a sine wave or a sine wave with offset. This working principle and signal flow - from the end user to the power electronic module - is presented in Figure 4.5. In this way, an additional aspect of mixing control could be achieved where the stirring speed could be a function of process parameters such as oxygen transfer rate or temperature. At this stage of the design when everything was

tested for the first time, mixing control was left as an open loop control with the possibility to change the mixing speed manually according to the need. The next step would be the implementation of mixing control based on the measurement of the dissolved oxygen concentration level.

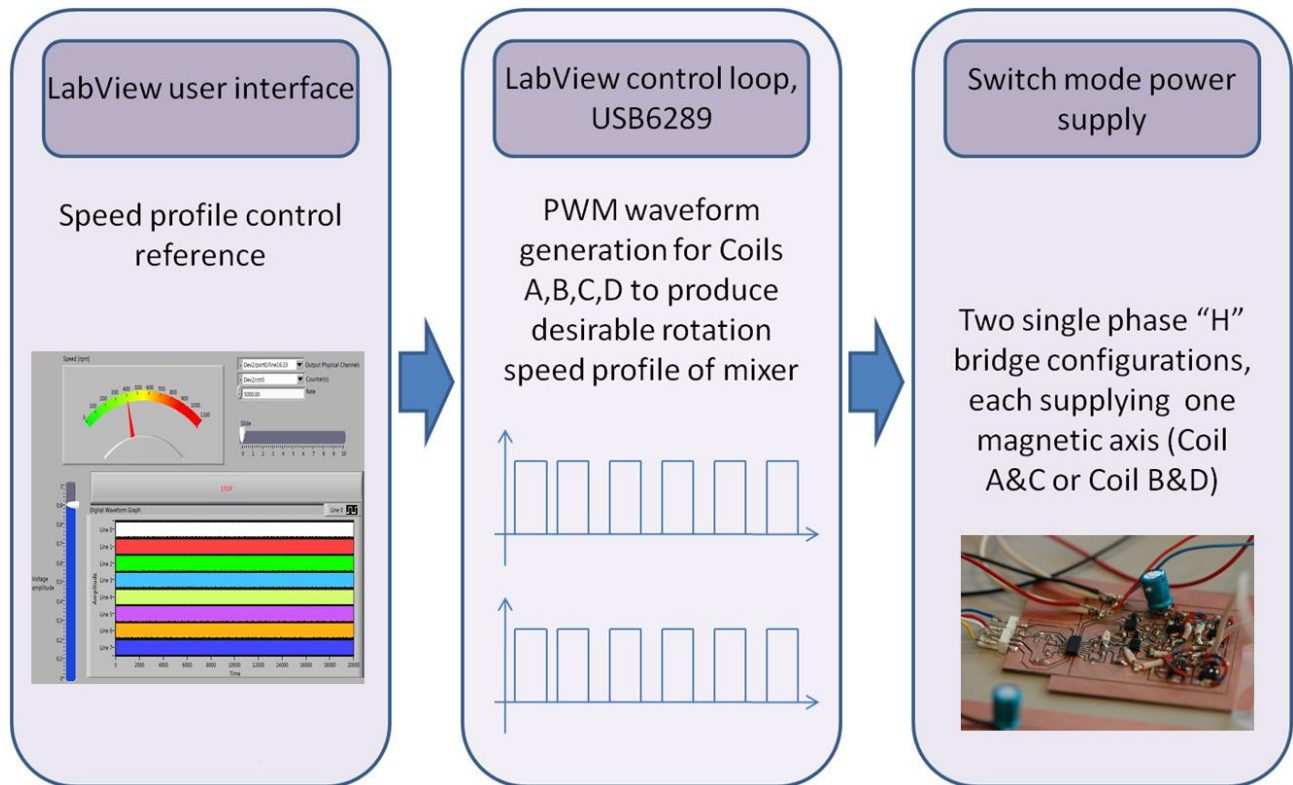


Figure 4.5. Signal flow from end user to the power supply. End user uses Labview interface to set impeller speed by adjusting rpm on a provided scale (left picture). This information is translated by the puls-width modulation technique to a signal (middle picture) that is applied to the magnetic coils by switching the power supply mode (right picture).

Furthermore, there is a possibility for the stirrer to change direction during operation which facilitates bidirectional mixing and provides another level of flexibility in the bioreactor design, e.g. removal of baffles. Bidirectional mixing has the advantage that it avoids vortex formation.

#### 4.2.5 Measurement of scattered light intensity (SLI) for biomass monitoring

In order to follow cell growth in the MSBR, on-line monitoring of cell density was established via non-invasive optical sensing, since sampling was not an option with only 1 mL working volume. Besides, the idea was to obtain process parameters in real time without direct contact with the cultivation broth. At small scale, usually the Lambert-Beer law is applied, and optical density is obtained by means of light that is guided to the reactor via optical fibers from an orange/yellow emitting diode; the light passes through the microbioreactor (vertically or horizontally) and is eventually captured onto a photo diode – transmittance measurement. Of course, this is a feasible approach when the bioreactor is small enough such that the pathway of light is short enough to allow reasonable detection of cells. In milliliter scale bioreactors (10 mL) sampling is necessary in most of the cases. For the MSBR presented here, both options were not feasible, neither sampling nor measuring light over the length or the height of the chamber. To solve this issue, the working principle of a transreflectance probe with specular reflection (mirror - like reflection) was applied where both transmission and reflectance mode are taken into account during measurement of scattered light intensity [91,111,112]. The signal flow during the transreflectance measurement is presented in Figure 4.6.

An LED (light-emitting diode) was used as a source of light at 600 nm wavelength and it was led to a beam splitter which created two light paths with light intensity ratio 70 % - 30 % relative to the intensity of the light entering the beam splitter. The beam splitter device was custom made by PhD student Daniel Schäpper for his experimental set up used with the 100  $\mu$ L microbioreactor and it is described in detail elsewhere [100]. The path with 30 % of light intensity was directly guided by an optical fiber to a photodiode as the reference signal, while the light path with 70 % of light intensity first was directed to the MSBR by a bifurcated optical fiber bundle, and the resulting light was returned through the same optical fiber bundle toward another photodiode. Both photodiodes provided voltages and ratio of these voltages presented the scattered light intensity, which was correlated with cell concentration during offline calibration.

To apply and test this measuring method and determine the correlation between biomass concentration and the SLI measurement, a calibration was performed by placing and mixing solutions with different cell concentrations (baker's yeast) in the MSBR. Light was guided through a bifurcated optical fiber bundle, passing the PMMA plate (bioreactor bottom) and the sample, then reaching the mirror-like surface, from which light was reflected passing the same pathway back towards the same bifurcated optical fiber bundle, after which light was collected by a photodetector.

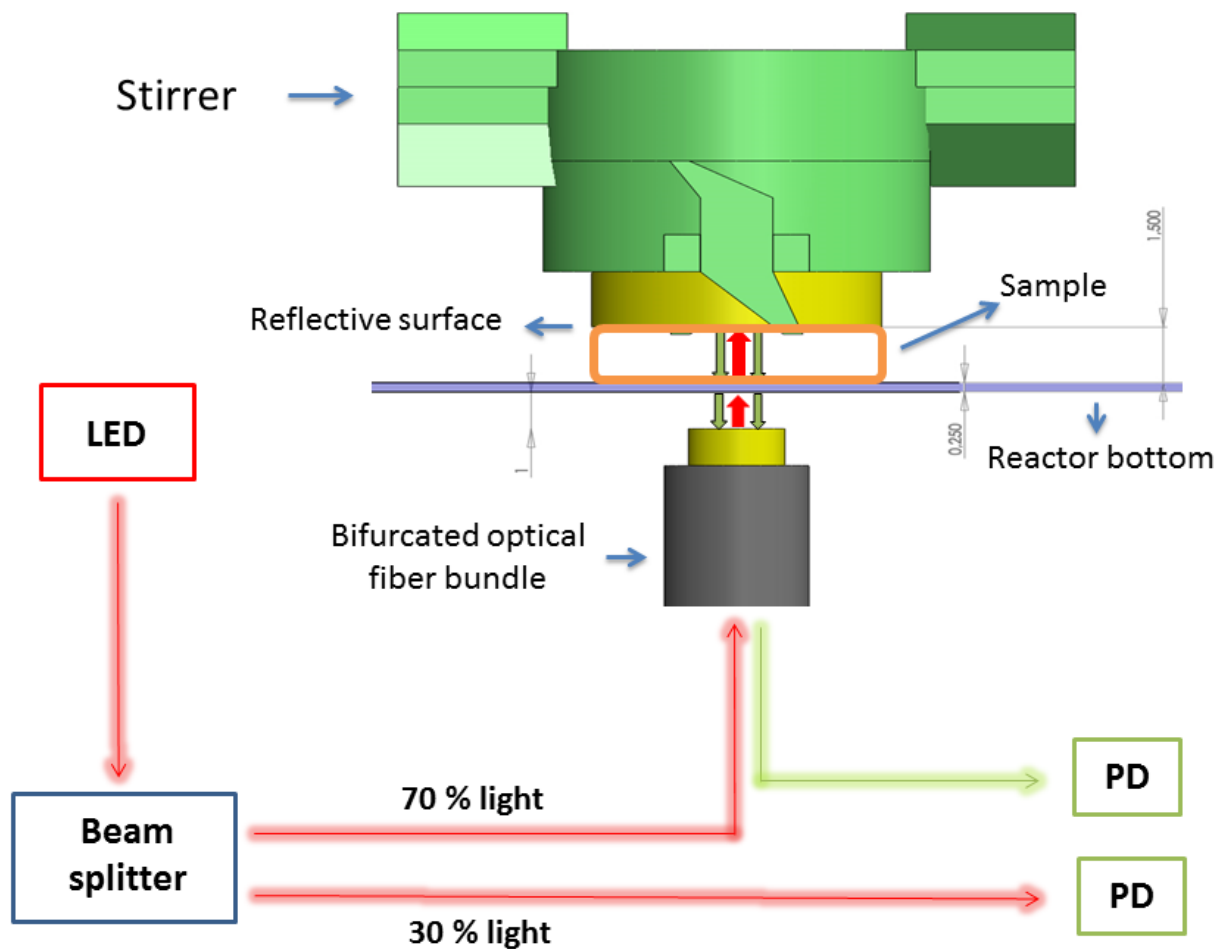


Figure 4.6. Scattered light intensity (SLI) measurement. An LED (light-emitting diode) is used as a source of light at 600 nm wavelength. Light was guided by an optical fibre to the beam splitter that divided the light intensity to two light paths with 70% and 30% intensity, respectively, compared to the incoming light. 30% light was sent directly to a photodiode as reference signal while 70% light was used to measure the current condition in the MSBR. The resulting light from the MSBR was guided to another photodiode.

#### 4.2.6 Determination of mixing time

The acid-base color change method is used to determine a mixing time in order to characterize mixing performance at milliliter scale. The mixing time was defined as the time needed to observe a change in color from pink to transparent during the acid-base neutralization using phenolphthalein as indicator [113]. Aqueous solutions of 0.1 M hydrochloric acid (HCl), 0.1 M sodium hydroxide (NaOH) and 1% phenolphthalein were prepared. 10  $\mu$ L of the 0.1 M NaOH solution and 10  $\mu$ L of the phenolphthalein solution



were then mixed with 1 ml water in the milliliter-scale bioreactor. Afterwards 10  $\mu\text{L}$  of the 0.1 M HCL solution was added while mixing was performed. For these experiments the reactor chamber was modified by making an opening at the top of the reactor chamber in order to allow the physical and visual access to the liquid that was needed for solution injection and video capture. To prevent and avoid subjectivity in the interpretation of the measured results, experiments were filmed with a Nikon D5000 camera and a stopwatch was employed next to the reactor chamber. This arrangement allowed for frame by frame analyses of the captured videos using Free Video to JPG Converter v.2.1.1 software. In the analysis the change of color was correlated with the registered time displayed by the stopwatch.

#### **4.2.7 Residence time distribution**

Further characterization of mixing in the MSBR was done by determining the residence time distribution in the liquid. Experiments with a tracer-response technique using a pulse input were used to determine the residence time distribution. The MSBR was filled with 2 ml of water, which was continuously pumped and withdrawn by syringe pumps (Harvard Apparatus Model 11 Plus Syringe Pump) at specific flow rates. In the inlet stream of the MSBR, 20  $\mu\text{L}$  of 1 M NaOH was suddenly injected. Very small conductivity probes were not readily available on the market, so the inlet and outlet concentrations dynamics of the tracer were monitored by custom made probes that were constructed from materials and equipment available in our laboratory. Each probe consisted of two brass tubes positioned at a certain distance (4 mm) from each other, and such a probe was then located at the inlet and the outlet of the MSBR. Two brass tubes were attached to the wires and they acted as electrodes. Their outer diameter was smaller than the inner diameter of plastic tubing, and thus it was possible to place them in the inlet and the outlet stream of the MSBR. Schematic presentations of the probe as well as a picture of the device are presented in figure 4.7.

When the conductivity measurement was performed, a voltage was applied on the two brass tubes through which the solution was passing, and the resulting current was measured. Based on Ohm's law, the resistance was calculated by dividing voltage by current ( $R = V/I$ ; [ $\Omega = V/ A$ ]). From there, the electrical conductance is calculated as the reciprocal of the resistance ( $G = 1/R$ ; [ $S = 1/\Omega$ ]) and afterwards the signal is used for determination of the residence time distribution.

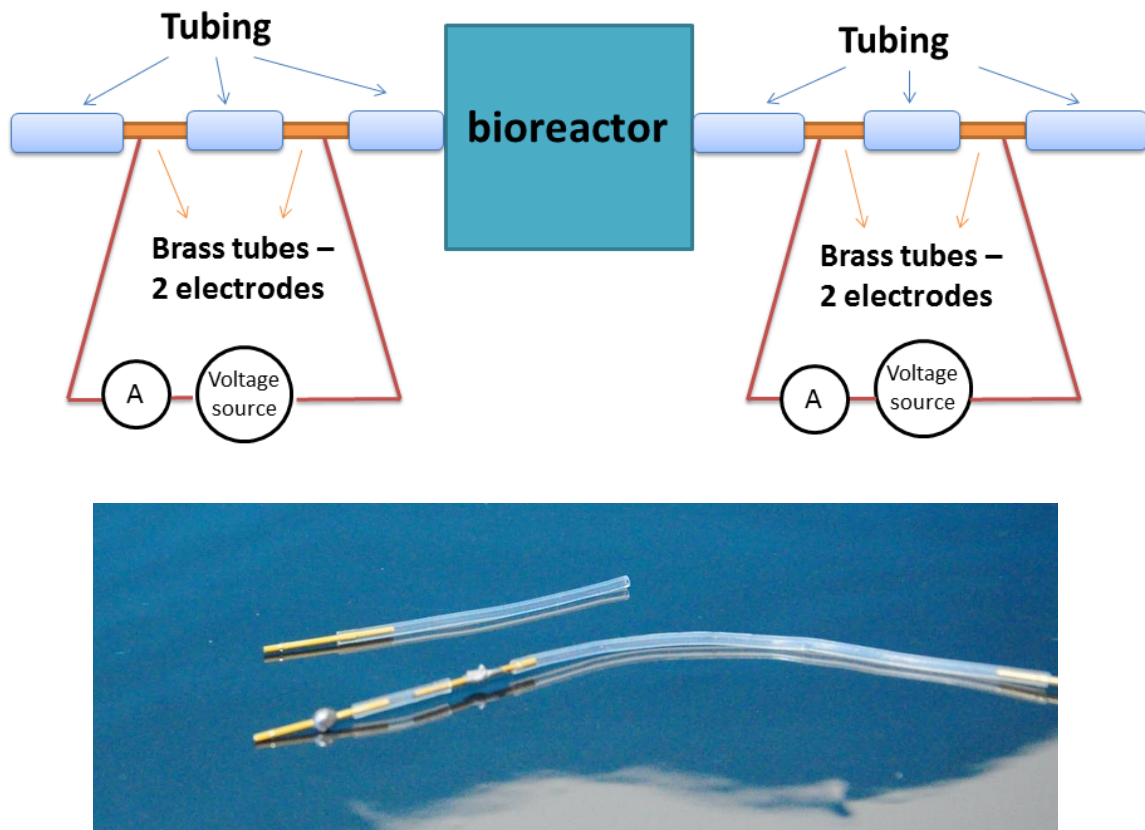


Figure 4.7. Conductivity probe used during residence time distribution experiments. The solution passed through plastic tubing and it entered to brass tubes (electrodes) while a voltage was applied on the electrodes. The created current together with the applied voltage were used for the calculation of resistance and indirectly the electrical conductance ( $1/\text{resistance}$ ).

#### 4.2.8 Oxygen transfer rate - $k_La$ measurement

In order to characterize the maximum oxygen transfer capacity in the system for a range of process conditions, the gassing-out method was employed [89,114]. The MSBR was first filled to working volume (0.5-1 mL) with CBS medium (described in section 4.2.12), without microbial cells and a step change in the oxygen concentration was introduced by starting surface aeration with a  $30 \text{ mL min}^{-1}$  gas flow rate or by sparging (bubble aeration) with a  $40 \text{ mL min}^{-1}$  gas flow rate, depending on the type of experiment that was performed. First, nitrogen was continuously flushed through the medium until the oxygen concentration dropped to zero in the reactor. Subsequently, air was introduced and the change in the oxygen concentration was measured with help of the optical fiber and a PreSens sensor spot at the bottom of the reactor.

In general, to be able to determine the mass transfer coefficient correctly, it is necessary to take into consideration the response time of the sensor, since it can have a major influence on the  $k_{LA}$  values if the response time of the sensor is in the same order of magnitude as the response time of the system during  $k_{LA}$  determination [115].

The response time of the Presens sensor was determined by transferring a sensor from an oxygen-free solution to one saturated with air, and it was assumed that the response is following a first-order model. Consequently, the oxygen concentration measurements corresponded to a second-order process due to the influence of the sensor dynamics, which can be represented by the following equation [116]:

$$C_P(t) = C_L * [ 1 + (k_{LA}/(k_P - k_{LA})) * e^{-k_P t} - (k_P / (k_P - k_{LA})) * e^{-k_{LA} t} ] \quad [4.1]$$

where  $C_P$  is the concentration of oxygen in the liquid ( $\text{mol L}^{-1}$ ), measured by the dissolved oxygen (DO) sensor,  $C_L$  is the concentration of oxygen in the liquid in equilibrium with the gas phase ( $\text{mol L}^{-1}$ ),  $k_{LA}$  is the volumetric mass transfer coefficient ( $\text{s}^{-1}$ ),  $k_P = (1/\tau_P)$  ( $\text{s}^{-1}$ ),  $\tau_P$  is the time constant of the DO sensor (s).

The described procedure was used to determine  $k_{LA}$  values during experiments with surface and with bubble aeration, as well as to investigate the influence of viscosity, and one- and bi-directional mixing on the oxygen transfer.

In order to evaluate the influence of viscosity on the oxygen transfer rate during mixing and aeration in the MSBR, four solutions with different viscosities were made. For this purpose 3% carboxymethylcellulose (CMC) solution was used and it was diluted with water to get a range of different viscosities (Table 4.1). The numbers in the table are not exact, but rather an estimation due to difficulties of obtaining the exact amount of CMC solution [117].

Table 4.1. Four different ratios between a 3% CMC solution and water produced four model solutions with different viscosities.

Volume of CMC (ml)	Volume of water (ml)	Measured viscosity (mPa.s)
5	45	13.30
10	40	17.01
15	35	27.73
20	30	34.80

The viscosity of each solution was measured with the advanced rheometer AR 2000 at 21°C. Also, solutions with different yeast concentrations were made (10 - 50 g/L) and their viscosities were measured with an Anton Paar AMV 200 Viscosity Meter [117]. In this way information was obtained on how the viscosity of the model solutions compared to the viscosity of solutions with up to 50 g/L yeast concentration.

#### 4.2.9 Evaporation

Mixing and aeration are used as main drivers to enable better oxygen transfer during aerobic cultivations at elevated temperature, which also creates good conditions for the evaporation process to occur, unfortunately. Temperature has a direct impact on the kinetic energy of the molecules in the liquid phase enabling them to move from the liquid surface to the vapor phase. In addition, air entering the MSBR with a lower temperature and humidity than air in the reactor will allow continuous evaporation to occur during the cultivation in the bioreactor. At small scale all these effects are enhanced due to the larger surface to volume ratio, so evaporation becomes a pronounced problem. In order to estimate how big evaporation in the MSBR is, the evaporation rate was determined for 1 mL working volume by measuring the mass of the reactor without and with water during a period of 20 h at 30°C and 800 rpm, with and without active aeration [118]. An analytical balance AX200 from Shimadzu Medical System was used for the measurements of the reactor mass without and with liquid. Water was used as model liquid since its density was similar to the density of the medium (the difference was 1.8 %) [118].

In addition, three evaporation control strategies were tested by application of:

- A pre-humidifier (300 mL Pyrex bottle with stirrer bar and active air flow placed on a heating plate)
- A condenser (small metal pipe placed on the air outlet from the MSBR with active chilling of the metal pipe)
- A closed saturated chamber without active gas flow (similar to the pre-humidifier, but just without active aeration of the Pyrex bottle).

#### 4.2.10 CFD

Computational fluid dynamics (CFD) was employed in order to simulate the mixing times, the oxygen transfer rates and the appearance and size of the gas-liquid interfaces in the MSBR. The selected case for modeling was the one with 1 ml liquid, one-directional stirring and surface aeration. The CFD simulation software ANSYS CFX 15.0 was used for all simulations, and a 150,000 nodes large unstructured computational mesh was created in ICEM CFD 15.0. The mesh is shown in Figure 4.8a and the simulated geometry in Figure 4.8b. The symmetry of the MSBR design was utilized by applying rotational symmetry, so only half of the bioreactor was needed to be simulated.

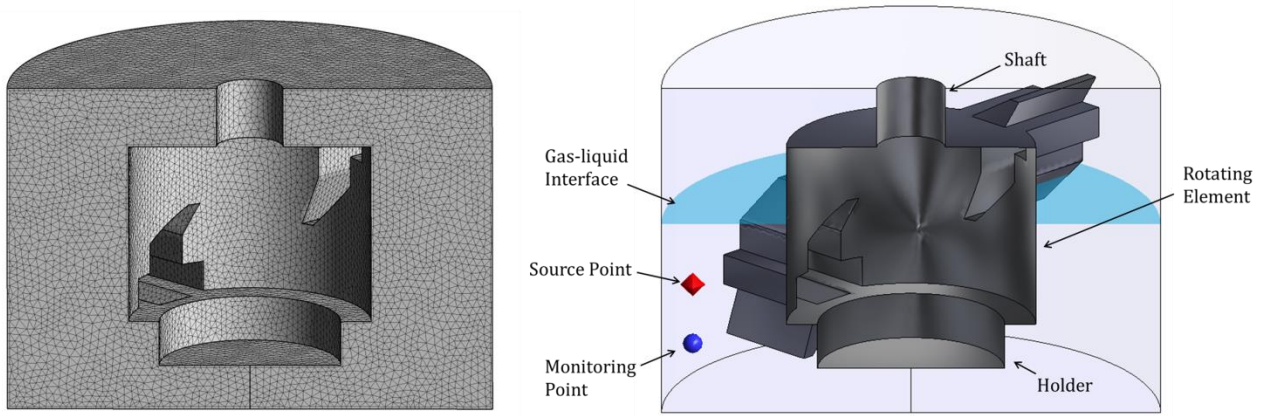


Figure 4.8. (a) The unstructured mesh used for the simulations; (b) The geometry setup showing the rotating element and the steady shaft and holder. The position of the gas-liquid interface at rest is indicated (turquoise), as well as the position of the source point (red octahedron) and the monitoring point (blue ball) that were used in the transient mixing simulations.

Two-phase simulations were performed with the two continuous fluids: water (density 997 [kg m<sup>-3</sup>], dynamic viscosity 9.899×10<sup>-4</sup> [kg m<sup>-1</sup> s<sup>-1</sup>]) and air (density 1.885 [kg m<sup>-3</sup>], dynamic viscosity 1.831×10<sup>-5</sup> [kg m<sup>-1</sup> s<sup>-1</sup>]). The free surface interphase model and the  $k-\epsilon$  turbulence model implemented in CFX 15.0 were selected for the simulations.

The mass transfer coefficient  $k_L$  was modeled according to the eddy cell model [119] shown in Equation 4.2, where  $D_L$  is the diffusion coefficient of oxygen at 20 degrees Celsius (1.98×10<sup>-9</sup> [m<sup>2</sup> s<sup>-1</sup>]),  $\nu$  the kinematic viscosity of the liquid and  $\epsilon$  the turbulent energy dissipation rate in the fluid. The turbulent energy dissipation was directly modeled by the turbulence model, while the diffusivity and kinematic viscosity were held constant.

$$k_L \propto \sqrt{\frac{D_L}{\nu}} (\epsilon \nu)^{0.25} \quad [4.2]$$

The specific interfacial area 'a' was calculated based on the size of the simulated interface between the water and the air, and the oxygen transfer rate  $k_{LA}$  was calculated as the product of a,  $k_L$  and a proportionality constant  $Ck_{LA}$  fitted to the experimental data. Oxygen transfer rate results in similar systems have been previously published in [120] and [121], where the  $Ck_{LA}$  values 0.167 and 0.36 were used respectively. Equation 1 has also been extensively used to model  $k_L$  values in larger and aerated reactor systems e.g. in [122].

Mixing time simulations were performed by the introduction of a liquid-phase bound additional variable from a source point in the beginning of transient simulations. The maximal values of the additional variable in the liquid, as well as its concentrations in a virtual monitoring point were observed over the course of the simulations. Mixing time was defined as the time when the concentrations entered within the  $\pm 5, 10$  or 15% interval

of their final (average) value, i.e. the concentrations once the additional variable was homogeneously distributed in the liquid. The location of the source point and the monitoring point can be seen in Figure 4.8b.

#### 4.2.11 Microbial Strain

The prototrophic laboratory strain *Saccharomyces cerevisiae* CEN.PK-113-7D [123] was used for aerobic yeast cultivation, while *Lactobacillus paracasei* (DSM 5622) was used in anaerobic bacterial cultivations. Both organisms are well known, research relevant strains and they will be shortly described here.

*Lactobacillus paracasei* is a gram-positive, rod-shaped, non-spore forming, non motile and facultatively heterofermentative microorganism that belongs to a group of lactic acid bacteria (LAB). The strain grows at temperatures between 10 °C and 40 °C. It can be found in the human gastrointestinal tract and other mucosal membranes, fermented milk products and sewage [124,125]. *L. paracasei* is commonly used in food and as a dietary supplement due to its beneficial probiotic properties to boost the immune system and reduce problems with an upset stomach.

*Saccharomyces cerevisiae* is a single cell eukaryotic microorganism that can be found in nature on plants, fruits and grains. It is a facultative anaerobe and heterotroph that is extensively researched [126]. It is frequently used as a model organism due to its easy genetic manipulation, robustness, rapid growth and the fact that its genome is known [127]. *S. cerevisiae* is also an industrial relevant organism with applications ranging from winemaking, baking, brewing to production of insulin.

#### 4.2.12 Medium Composition

##### *Anaerobic cultivation with Lactobacillus paracasei*

Difco Lactobacillus MRS Broth medium (BD Diagnostics) was used in cultivations with *Lactobacillus paracasei*. The medium contains the following: 10 g/L proteose peptone no.3, 10 g/L beef extract, 5 g/L yeast extract, 20 g/L glucose, 1 g/L polysorbate 80, 2 g/L ammonium citrate, 5 g/L sodium acetate, 0.1 g/L magnesium sulfate, 0.05 g/L manganese sulfate, 2 g/L dipotassium phosphate. For maintaining a constant pH, 1.95 g of biological buffer MES (2-(N-morpholino)ethanesulfonic acid) was added to the medium.

#### *Aerobic cultivation with Saccharomyces cerevisiae*

The CBS medium (CBS stands for Centraalbureau voor Schimmelculturen, or in English Central Office for Fungal Cultures) was used for yeast cultivations [128]. It is a defined mineral medium with the following composition: 5 g/L glucose, 5 g/L ammonium sulfate, 3 g/L monopotassium phosphate, 0.1 g/L magnesium sulfate, 1 ml/L trace metal solution, 1 ml/L vitamin solution, 50 µL Sigma 204 antifoam. For maintaining pH constant, the biological buffer MES (2-(N-morpholino)ethanesulfonic acid) (0.12 mol/L ) was added to the medium.

#### **4.2.13 Batch Cultivation**

##### *Anaerobic cultivation with Lactobacilli paracasei*

As inoculum, two different glycerol stock cryo tubes (1 mL size) were transferred to a 200 mL bottle with MRS medium, which then was incubated overnight in the incubator at 37°C. The working volume of the bioreactor was 2 mL and it was inoculated with 1 volume% of the overnight culture. The cultivation was kept at 37°C, 300 rpm and pH 6.0. MES buffer (2-(N-morpholino)ethanesulfonic acid) was used for keeping pH constant at 6.0. The easiest way to obtain an anaerobic environment is by purging the headspace with nitrogen. However, to avoid problems due to excessive evaporation, another strategy was taken to maintain anaerobic conditions. The bioreactor was purged with nitrogen until all oxygen was removed and the outlet of the bioreactor was closed. The inlet was still open and filtered nitrogen had access to the headspace of the bioreactor. Overpressure was avoided by introduction of a Y connection in the inlet tube. End point samples were taken and analyzed by spectrophotometer and HPLC to determine cell mass concentration by optical density, and furthermore also the concentration of lactic acid and glucose.

##### *Aerobic cultivation with Saccharomyces cerevisiae*

For propagation, the yeast strain was grown on an agar plate (6.7 g/L yeast nitrogen base (Difco, USA), 20 g/L glucose and 20 g/L agar) for two days at 30°C and then stored at 4°C until usage (maximum for 1 month). Inoculum was prepared by transferring a yeast colony from an agar plate to a 500 mL Erlenmeyer flask containing 100 mL CBS medium adjusted to pH 6.5. The flask was incubated for 10 h at 30°C on an orbital shaker set at 150 rpm. The milliliter-scale bioreactor, filled with 1 ml CBS medium, was subsequently inoculated with 1% v/v inoculum size. The temperature in the reactor was kept at 30°C during the cultivation and the stirrer was set to 800 rpm. Aerobic conditions were achieved by headspace aeration.

#### 4.2.14 Monitoring and control

In both cultivations a custom LabVIEW program, made by PhD student Daniel Schäpper, was the interface between the end user and the MSBR. Control of temperature and mixing, together with monitoring of dissolved oxygen, pH and the scattered light intensity were managed by the LabVIEW program and two data acquisition cards.

For dissolved oxygen measurement, a blue-green LED at 505 nm wavelength was used as input to a DO sensor located at the bottom of the MSBR I. The DO sensor produced fluorescent light at 652 nm peak wavelength. The working principle of the detection method relies on the fact that the resulting light has the same frequency as the input light, but with a certain phase lag that is dependent on the measured oxygen concentration, and this phase lag was detected by a silicon detector (Thorlabs PDA36A). The final information obtained from this measurement was a voltage that was registered in LabView where a lock-in amplifier was programmed to measure the phase shift between input and output signal and convert it to the dissolved oxygen concentration based on a set of calibration data [100]. More detailed information about the DO measurement set-up can be found in [100].

The principle of the pH measurement was similar to the one for oxygen that was described above. Here, a blue LED at 465 nm was used as an input signal to the pH sensor that was located at the bottom of the MSBR I. Fluorescent light emitted from the pH sensor at 520 nm wavelength was emitted with the same frequency as the input light but with a certain phase lag. A Thorlab PDA36A silicon detector was used to receive the light emitted from the pH sensor and the resulting voltage was registered in LabView. The created phase shift between input and output light was registered by a programmed lock-in amplifier in LabView and it was correlated with the pH values based on a set of calibration data [100]. More detailed information about the pH measurement set-up can be found in [100].

Input and output signals used by the LabView program were handled by two National Instruments A/D cards : PCI-4461 (high speed card) and USB-6229 (low speed card). Measurement of different process parameters was done sequentially. Dissolved oxygen and pH were processed in one loop with the high speed card while temperature and the SLI data were collected in another loop that was assigned to the low speed card. The generated data were registered as text files by the LabView program and were later analyzed by means of other software according to the need. An overall summary of the developed LabView program is presented in figure 4.9 that was reproduced from [100]. Considering that the lock-in amplifier function was part of the LabView program, a high speed card was necessary to perform pH and DO measurements and enable a high sampling frequency [100].



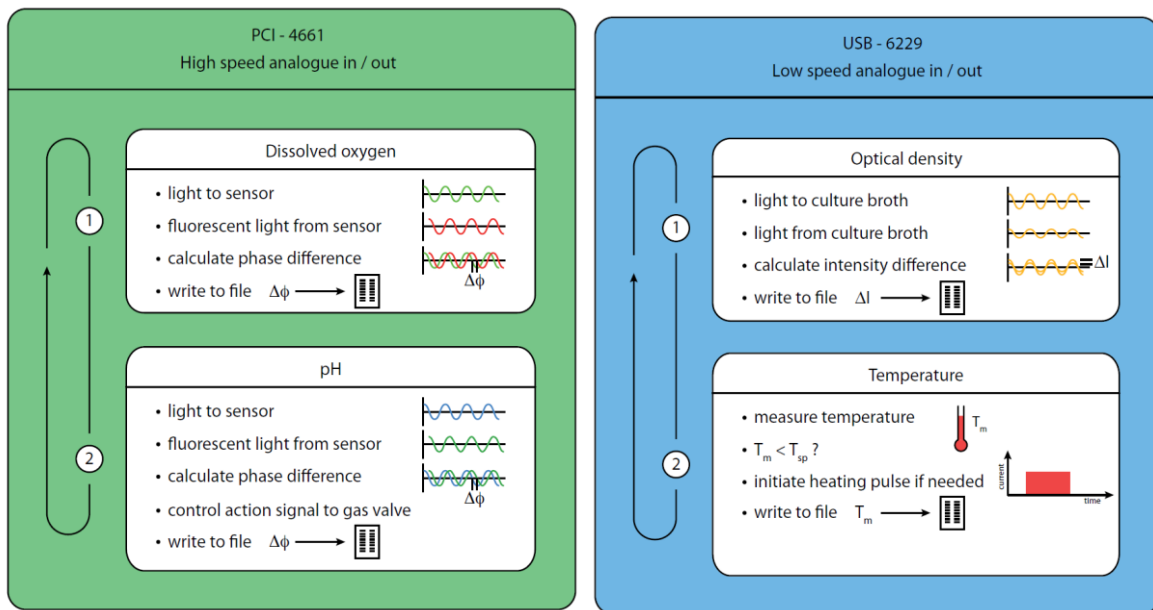


Figure 4.9. The LabView program overview. A high speed card was used for handling dissolved oxygen and pH measurement while a low speed card was used for measurement of the SLI and temperature.

The described Labview program was only used for pH, DO, OD and T and didn't have any module made for mixing control, consequently the LabView program was modified by addition of control algorithm for mixing that is previously described in section 4.2.4. The modification of Labview routine is presented in figure 4.10 while LabView end-user interface with block diagram are presented in appendix D.

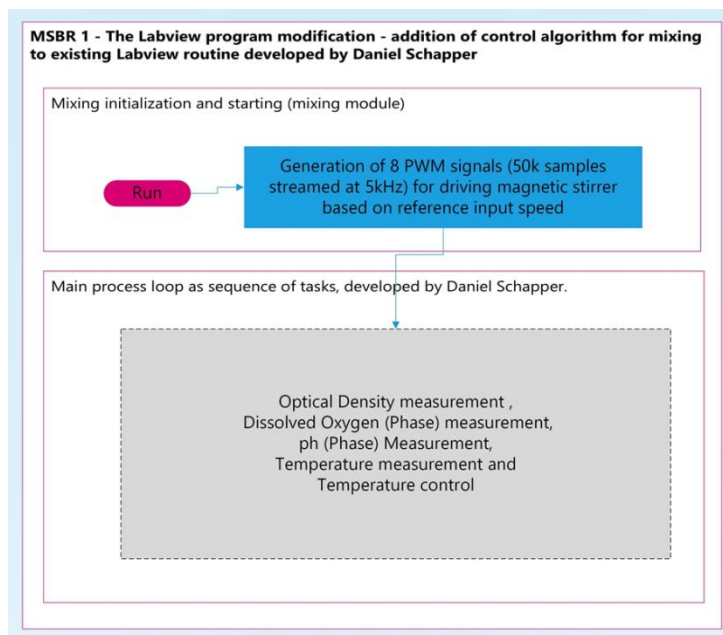


Figure 4.10. Module for mixing control is added to the Labview program made by Daniel Schapper [100].

## 4.3 Results and Discussion

### 4.3.1 Measurement of scattered light intensity (SLI) for biomass monitoring

There are three modes how light can be introduced to and collected from the sample: transmission, reflection and transfection mode (presented in figure 4.11) [129]. Transmission mode is obtained when a beam of light from one probe is passed through a sample to the second probe which guides the transmitted light to a detector on the other side.

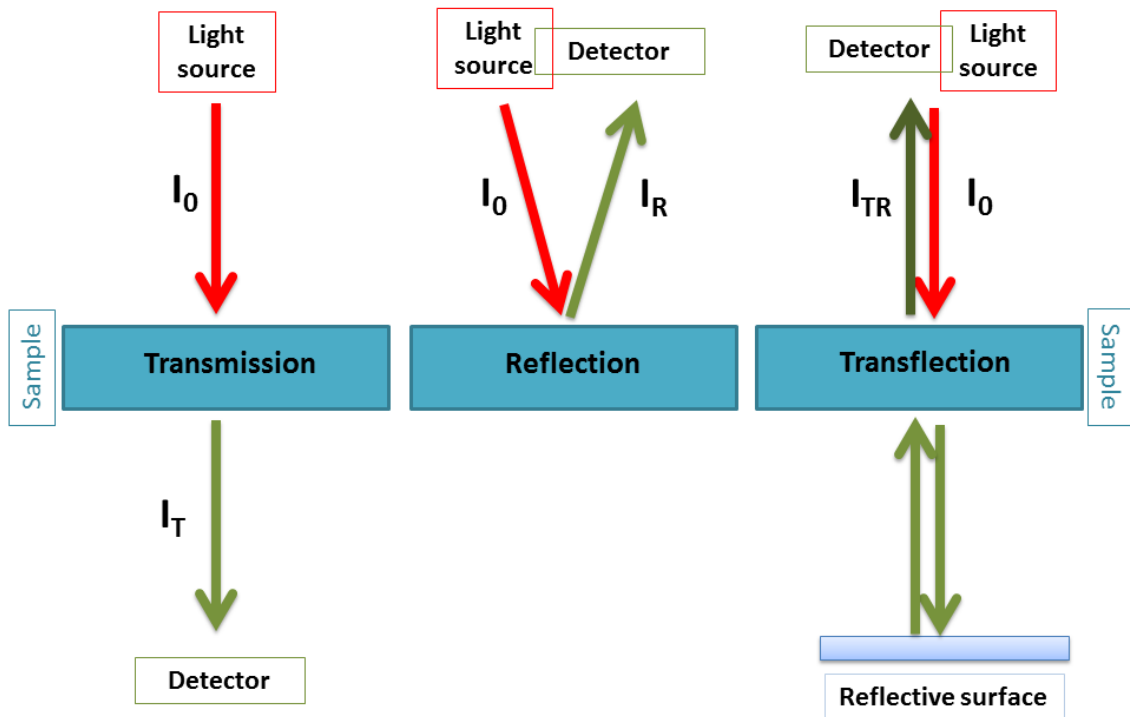


Figure 4.11. Principles of transmission, reflection and transfection measurements. Incident light that illuminates samples is marked with  $I_0$ , while the transmitted light is presented by  $I_T$ , reflected light is presented by  $I_R$  and the resulting light in case of the transfection measurement is presented by  $I_{TR}$ .

Reflection mode is achieved when a bifurcated fiber bundle is used to introduce light into a sample as well as to collect returning light. Transfection is a hybrid mode that consists of transmission and reflection. Besides the bifurcated fiber bundle, it involves a reflector – a mirror that is placed behind the sample, so the light pathway throughout the sample and back is in fact doubled [129]. Due to the size and structure of the MSBR, it was chosen to measure the SLI via the transfection mode as mentioned in section 4.2.5. The working principle is presented in Figure 4.12 together with the calibration curve for the MSBR.

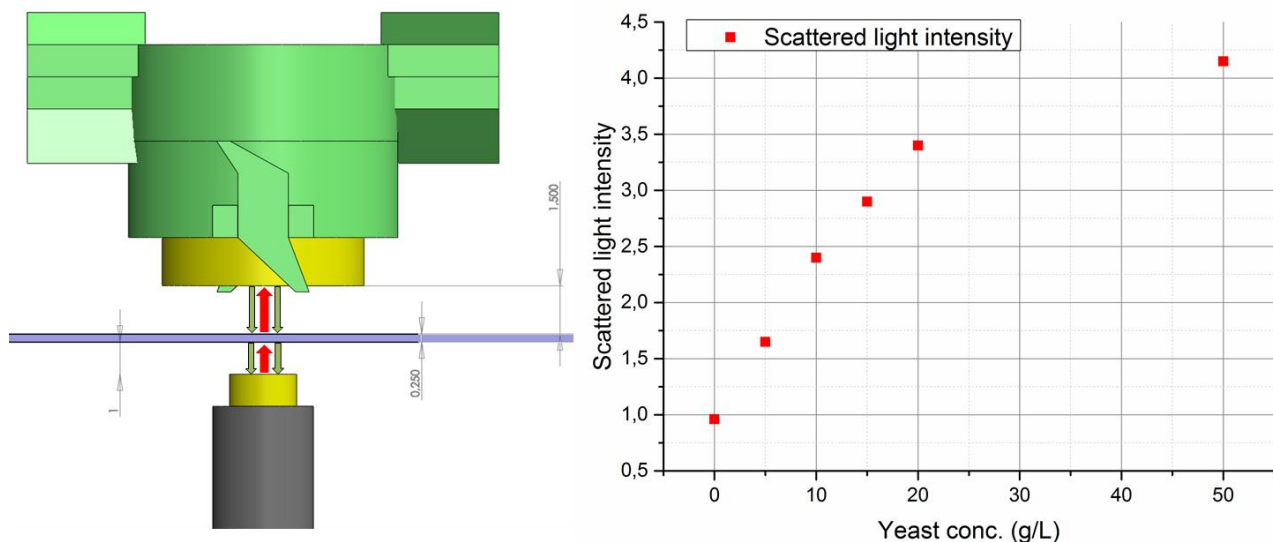


Figure 4.12. Principle of the scattered light intensity (SLI) measurement and calibration curve. Detail explanation of the SLI measurement is presented in figure 4.6., section 4.2.5.

The experimental set-up was tested with different concentrations of baker's yeast solutions (5, 10, 15, 20, and 50 g L<sup>-1</sup>), as can be seen in the calibration curve. Results showed a linear correlation up to 20 g L<sup>-1</sup> of biomass concentration.

### 4.3.2 Mixing time

The mixing time is an important parameter in the evaluation of the liquid phase behavior and the stirrer effectiveness. It helps quantifying how well and how fast the liquid is mixed in the vessel. Mixing at milliliter scale is a challenging task since there is not much space for the stirrer and baffles in the bioreactor, and still there is a volume of liquid that needs to be actively mixed. The MSBR doesn't have baffles and the novel stirrer has impeller blades at two levels which ensure that all liquid is included in the mixing process. The geometry of the impeller blades enables upward and downward flow dependent on the direction of the shaft rotation.

Considering that the MSBR working volume was 1 ml and it was possible to have direct access to the MSBR, the dye decolorization technique proved to be a good method for evaluating the mixing time. The mixing time was determined for different rotational speeds in order to characterize the mixing efficiency of the novel mixing device and identify potentially poorly mixed regions that would show as a pocket of color in the videos.

As mentioned in section 4.2.6, mixing in the MSBR was filmed by means of a camera (24 frames per second) and videos were converted to frames in order to determine the

moment when color disappeared and the liquid became completely transparent. An example of this analysis is presented in figure 4.13 where the mixing time was obtained for a stirrer speed of 600 rpm. At the beginning of the experiment a known volume of an acid (HCl) is added to the MSBR and the pink colored liquid (originating from using a mixture of phenolphthalein and NaOH in water as buffer) slowly starts changing color due to the mixing capability of the presented experimental set up. Complete mixing and acid-base neutralization were achieved after 1.3 s, which was detected by occurrence of a transparent color of the liquid in the MSBR.

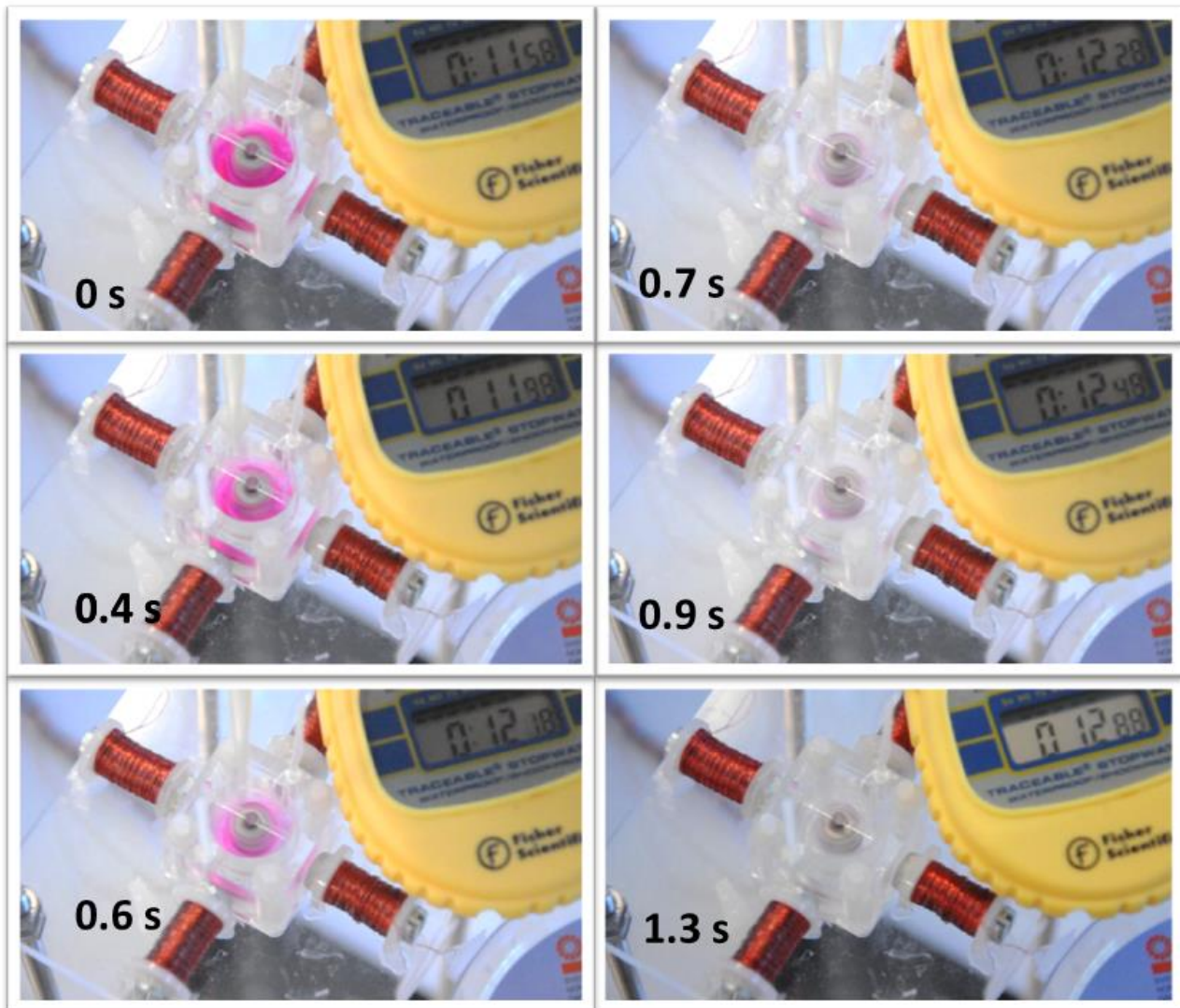


Figure 4.13. Mixing time determination experiment, here for determining the mixing time at 600 rpm stirring speed. At time = zero seconds, HCl is added in the MSBR that was filled with water, NaOH and phenolphthalein. Stirring disperses the HCl all over the MSBR and enables acid-base neutralization to occur which resulted in a color transition of the liquid from pink to transparent in less than 2 seconds.

As the camera had 24 frames per second, the time resolution of the recording was around 40 milliseconds. For the mixing speed of approximately 0.5 s (12 frames), the uncertainty level of the mixing time estimation corresponded to approximately 8%. Mixing times

obtained at different stirrer speeds together with error bars ( $\pm 8\%$ ) are presented in Figure 4.14.

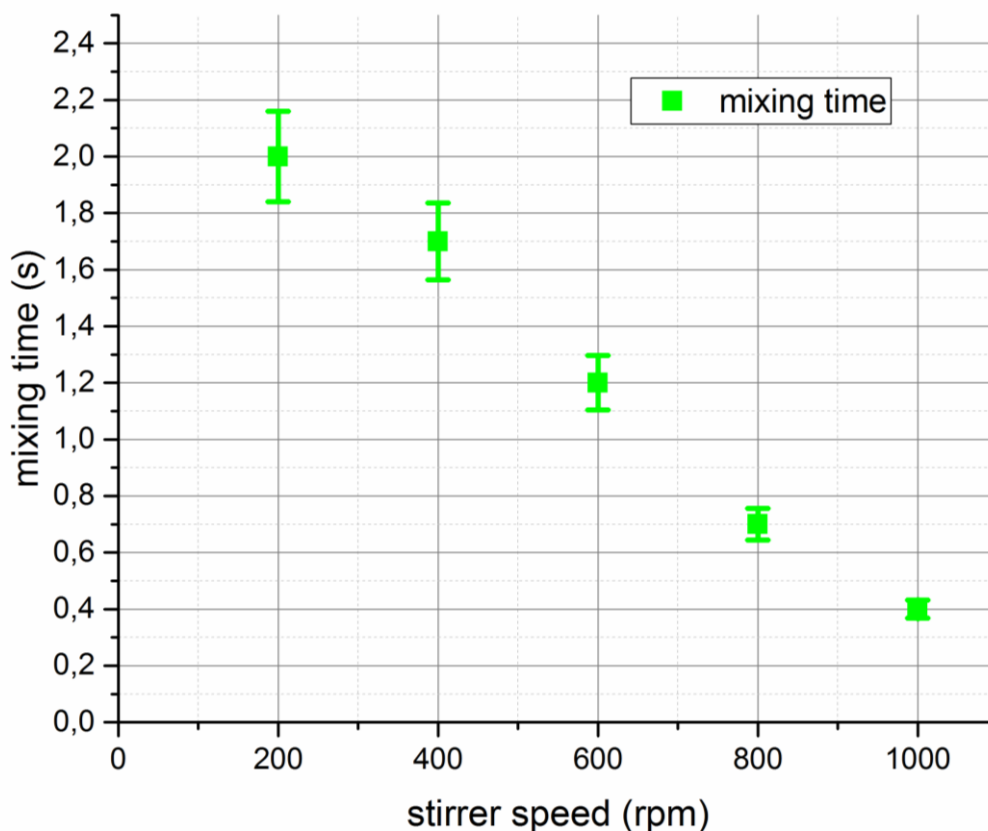


Figure 4.14. Decrease of the mixing time with the increase of the stirrer speed (rpm) during unidirectional mixing in the MSBR with 1 mL working volume.

The mixing time at 200 rpm was determined to be 2 s. The mixing time decreased with an increase of the rotational speed, as expected. The decrease was 5-fold, since the mixing time was reduced from 2 s at 200 rpm to 0.4 s at 1000 rpm. Considering mixing times were short and some were lower than 1 s, one should keep in mind that the equipment capabilities e.g., the speed of the camera, dispensing speed of a pipette and the experimenter's capability to recognize and define when color in the MSBR is transparent play a limiting and important role in the achieved accuracy of the experimental results. However, very exact mixing time determination was not crucial for this type of experiment. It was essential to determine whether the mixing time range was in order of ten minutes, 100 seconds or below 10 seconds, and to observe areas of the reactor where mixing was not good and could be improved. Poorly mixed zones were not detectable by visual inspection, and thus it was concluded that the reactor was well-mixed. However, the observation was made at higher stirring speeds that splashing can occur due to vortex formation caused by the absence of baffles in the reactor. Splashing can influence the

specific interfacial area between the gas and the liquid, which in turn has an effect on the achievable  $k_{L,a}$  values, which is the topic of section 4.3.4.

### 4.3.3 Residence time distribution

The residence time distribution study was performed to further characterize the mixing in the MSBR. The whole system was operated in a continuous operation mode for this study. The purpose of the experiments was to observe how much mixing deviates from ideal, and to perform diagnostics regarding the potential presence of dead zones, bypassing or recirculation zones. The experimental results are presented in figure 4.15.

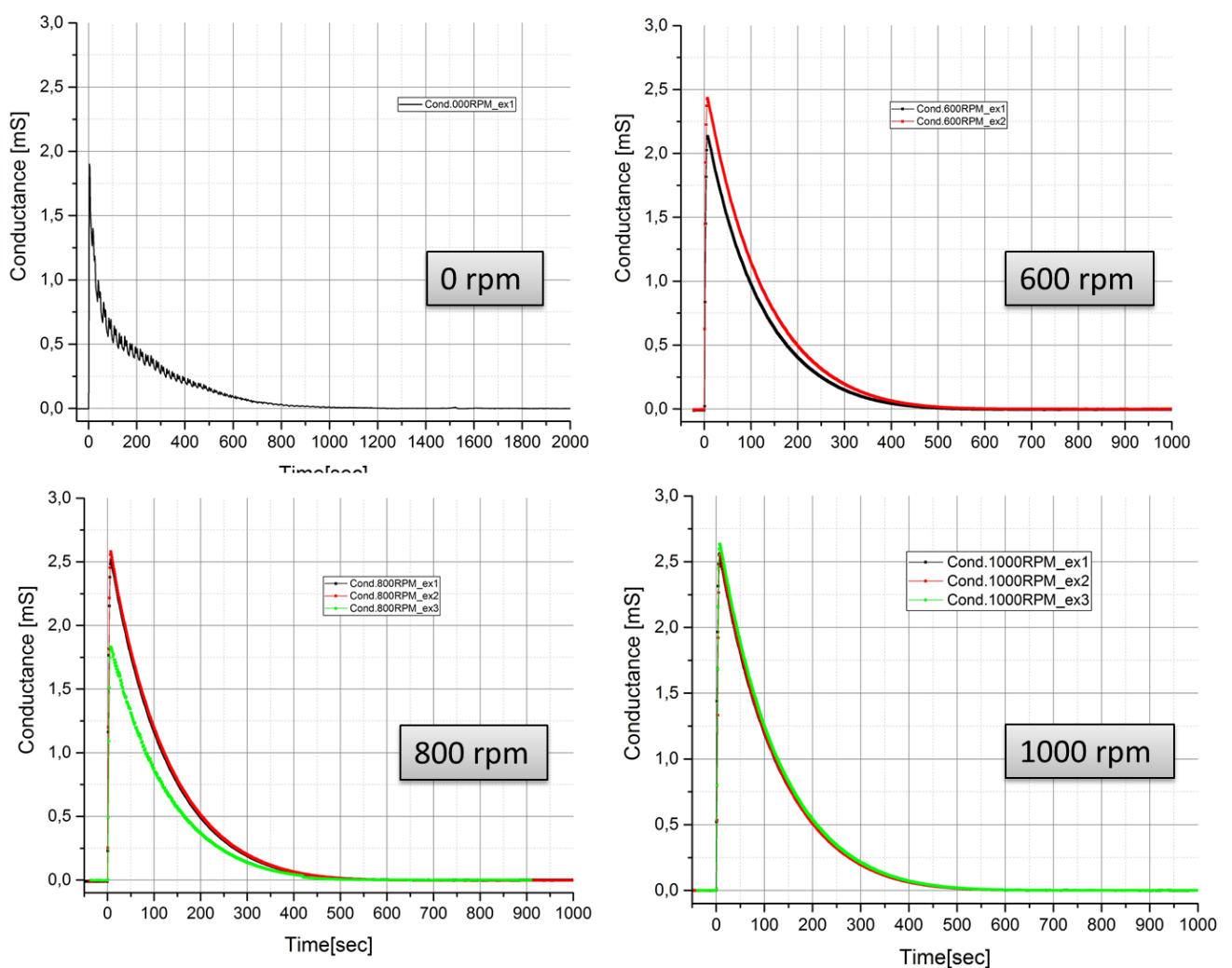


Figure 4.15. The experimental results showing distribution of a tracer measured at the outlet of the MSBR.

The mean residence time and the dimensionless variance of the mean residence time are shown for different stirrer speeds and for three different flow rates in Table 4.2.

The mean residence time was calculated from equation 4.3 [130]

$$\bar{t} = \frac{\int_0^{\infty} tC dt}{\int_0^{\infty} C dt} \quad [4.3]$$

and the dimensionless variance of the mean residence time was obtained from equation 4.4 [131]

$$\sigma^2 = \frac{\int_0^{\infty} (t-\bar{t})^2 f(t) dt}{\bar{t}^2} \quad [4.4]$$

The Reynolds number for the impeller is also presented in Table 4.2, and it was calculated using equation 4.5

$$Re_{Impeller} = \frac{ND^2}{\nu} = \frac{\rho ND^2}{\mu} \quad [4.5]$$

where N is the rotational speed [rps],  $\rho$  is the density [ $\text{kg m}^{-3}$ ],  $\mu$  is the dynamic viscosity [ $\text{kg m}^{-1} \text{s}^{-1}$ ] and D [m] is the diameter of the stirrer. Considering that the presented stirrer has a shape and size that are very far from the turbine or propeller stirrers that are typically used in pilot or full scale, the calculated Reynolds numbers should be taken only as an indicator. In the presented experimental work, high flows and low stirring speed were chosen in order to test the stirrer performance in extreme conditions and test the whole system.

The mean residence time and the dimensionless variance describe the size and the shape of the residence time distribution, respectively. The dimensionless variance has a range from 0 (characteristic for plug flow reactor) to 1 (characteristic for continuous flow stirred tank reactor). In well-designed reactors with turbulent flow, the dimensionless variance ( $\sigma^2$ ) has a value between 0 and 1, while a laminar flow reactor can have a  $\sigma^2$  value higher than 1 [131].

From the results presented in Table 4.2, the dimensionless variance of the residence time distribution is between 0.7 and 0.8 for different flow rates and stirrer speeds. Therefore, it can be concluded that the mixing performance of the MSBR is closer to a perfectly-mixed continuous flow stirred tank reactor than to a plug flow reactor.

In all experiments, the mean residence time was slightly lower than ideal which could suggest fouling or retention of some tracer in the reactor [131]. This could be the case, since the bioreactor volume was small compared to the available surface area, and surface tension could play a role in retaining a certain amount of tracer at the wall, which would have an effect on the mass balance and results. Furthermore, there was a possibility of electrolysis to occur on the custom made conductivity probe since it was made of brass tubes. Keeping that in mind, the experiments were kept short (13 - 120 s) and AC current was applied to reduce the risk of electrolysis and polarization to occur.

Table 4.2. Mean residence time and dimensionless variance of the mean residence time at different rpm and air flow rates.

Flow rate = 1 mL min <sup>-1</sup> ; V = 2 mL; RTD <sub>average</sub> = 120 s			
Stirrer rpm	Mean residence time [s]	Dimensionless variance of the RTD	Re <sub>impeller</sub>
200	112.3	0.74	732
400	114.2	0.78	1464
600	113.8	0.74	2196
800	112.6	0.76	2928
1000	113.6	0.75	3660
Flow rate = 5 mL min <sup>-1</sup> ; V = 2 mL; RTD <sub>average</sub> = 24 s			
Stirrer rpm	Mean residence time [s]	Dimensionless variance of the RTD	Re <sub>impeller</sub>
100	22.8	0.69	366
200	23.1	0.79	732
400	23.4	0.75	1464
Flow rate = 9 mL min <sup>-1</sup> ; V = 2 mL; RTD <sub>average</sub> = 13.3 s			
Stirrer rpm	Mean residence time [s]	Dimensionless variance of the RTD	Re <sub>impeller</sub>
50	11.9	0.82	183
100	13.2	0.75	366
200	12.7	0.71	732

Overall, experimental results were comparable and different flow rates and mixing speeds didn't have a major influence on the resulting residence time distribution. Although the applied flow rates were quite high compared to the ones normally used in cultivations, the mixing system had a good, constant performance and it was still not forced into non-ideal behavior.

#### 4.3.4 Oxygen transfer rate - k<sub>l</sub>a measurements

The amount of dissolved oxygen that can be transferred to a liquid (usually aqueous environment) has an influence on the dissolved oxygen concentration that can be obtained, which is one of the critical process parameters for aerobic cultivations and bioreactor performance evaluation. It is influenced by the aeration mode and mixing, the type of fluid involved and the reactor geometry. The high surface to volume ratio is a



beneficial aspect of small-scale bioreactors, especially when dealing with processes with adhered substrates and cells. However, in submerged cultivation at small scale there is a need to further increase the surface to volume ratio and to obtain efficient mixing in order to avoid substrate gradients, dead zones and oxygen limitation. The novel stirrer has a specific design, which helps in dispersing gas in the liquid in different ways dependent on the aeration mode. When surface aeration is applied, the stirrer – due to its size – works at two levels: below and at the liquid surface. At the liquid surface, the stirrer works according to a similar principle as surface aerators employed in biological waste-water treatment and aquaculture: the stirrer breaks and increases the contact surface between liquid and gas phase. Below the surface the stirrer is providing good blending and distribution of the gas drawn in from the liquid surface. In case of sparging, the stirrer increases the time of contact between gas and liquid by breaking bubbles and distributing them all over the liquid volume before they can reach the surface of the liquid.

In order to evaluate the performance of the MSBR, an effort was made in determining the volumetric mass transfer coefficient  $k_{LA}$  at different conditions. Oxygen transfer from air to the liquid is achieved by surface aeration or/and sparging at different mixing speeds, and it was characterized by means of a set of experiments exploring the influence of different mixing speeds, working volumes and viscosity on the oxygen transfer. The measurement of the dissolved oxygen concentration in the MSBR was based on non-invasive optical measurement with a PreSens sensor spot, which had an average response time of 11s.

Figure 4.16a illustrates the correlation between mixing speed and  $k_{LA}$  for three different cases. The working volume of the MSBR was 1 ml for these experiments. As expected, there was an increase in  $k_{LA}$  value with an increase of the mixing speed for all cases. For surface aeration, the  $k_{LA}$  had a range from 72 to 382  $\text{h}^{-1}$ , while sparging gave a  $k_{LA}$  range from 124 to 450  $\text{h}^{-1}$  for mixing speeds between 200 and 1000 rpm. It was expected that sparging will give much higher  $k_{LA}$  values compared to the surface aeration. However there was a design constraint regarding the manufacturing of a tiny sparger-hole in order to create small size bubbles. The stirrer was able to disperse the bubbles until a certain point, but many were anyhow not caught by the impeller blades since the sparger was positioned at the side of the bioreactor wall.

Considering that the MSBR doesn't have baffles, it was expected that, at higher rotational speeds, a vortex would be created and this was confirmed. Although the appearance of a vortex during mixing in larger reactors is characterized as poor and inefficient mixing, at milliliter scale this was not an issue. It was even considered beneficial due to the resulting increase of the interface between liquid and gas, and thus the possibility to transfer more gas to the liquid. Vortex formation is not an indication of poor mixing at small scale, since mixing occurs rather quickly due to the small distances and the high rotational speeds.

Also any vibration of the stirrer as well as friction at the wall of the bioreactor can easily produce secondary flows and improve the mixing. That being said, the oxygen transfer

rate was also evaluated when the vortex was not present. The occurrence of a vortex was avoided by introduction of bi-directional mixing, since there was no available space for adding baffles in the MSBR.

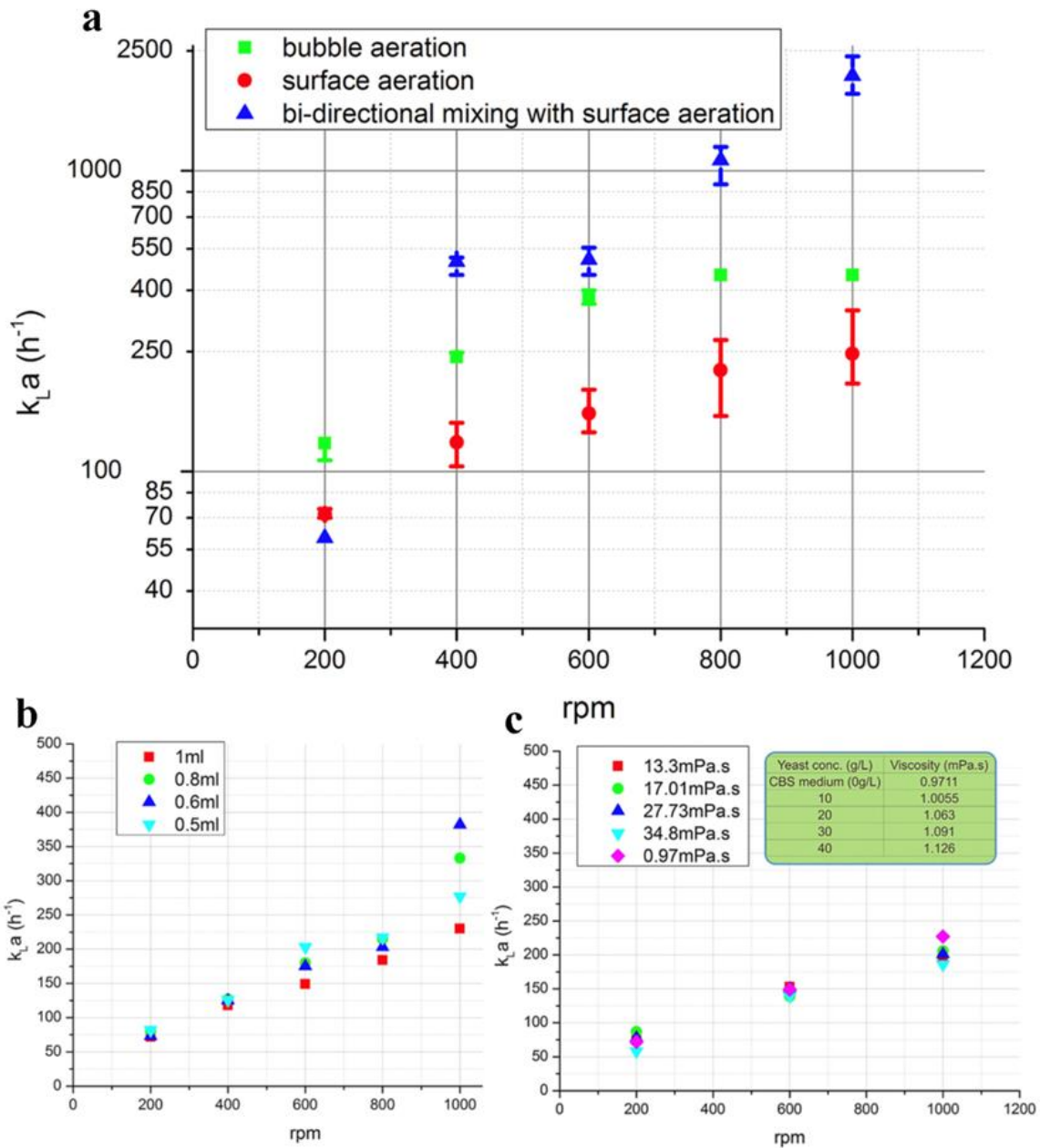


Figure 4.16. (a) The volumetric mass transfer coefficient -  $k_{La}$  at different mixing speeds and for different aeration modes; (b) Influence of MSBR working volume on  $k_{La}$  (c) Effect of viscosity change on  $k_{La}$ . Results presented here are average values of 3 to 5 experiments per condition evaluated.

Every half a second the rotation direction was changed, such that a vortex would not have time to be created or – if it was present – it would disappear almost instantaneously by the change of the direction of the impeller rotation.

Results are presented in Figure 4.16a, where bidirectional mixing was applied in combination with surface aeration. An increase in mixing speed resulted in this case in a  $k_{La}$  increase from 60 to 2067  $h^{-1}$ . Bidirectional mixing was very effective at higher rpm, from 400 rpm and up as visible in the Figure 4.16a. It resulted in  $k_{La}$  values of more than 1000  $h^{-1}$  at milliliter scale, as an effect of the increased liquid – gas contact area. At low mixing speed - 200 rpm (3.3 rps), the stirrer was only able to make 1.5 turns before the direction was changed, so it didn't have sufficient time to gain momentum. Consequently, the stirrer was in vibrational instead of rotational mode, which resulted in a low volumetric mass transfer coefficient (60  $h^{-1}$ ).

The influence of working volume on the oxygen transfer rate was evaluated as well (Figure 4.16b). Different rotational speeds were applied during surface aeration experiments with different volumes (0.5 – 1 mL). It would be expected that lowering the working volume results in a higher oxygen transfer rate due to an increase of the surface to volume ratio. However, results presented in Figure 4.16b demonstrate that there is no added value to the working volume decrease for the milliliter scale bioreactor presented here. One explanation is that the stirrer doesn't participate in the mixing process with the whole geometry for low reactor volumes, so a 0.5 mL working volume is mixed with two instead of four impeller blades. In other words, the mixing efficiency is decreased with a reduction in the volume. Still, the amount of oxygen transferred to the liquid is sufficient for cultivation and has a similar range for the 0.5 mL and for the 1 mL working volume.

The change of viscosity during the cultivation is an important parameter since both the mixing and the oxygen transfer rate are directly influenced by it. The MSBR was designed for application with yeast cells, although different bacteria could be used as well. It was not designed for highly viscous processes, for example with filamentous organisms [132]. In line with this, experiments were performed to evaluate the influence of viscosity on the volumetric mass transfer coefficient, where the tested range of viscosities went up to 35 times more viscous than the values obtained in the yeast cultivation (1.126 mPa.s for 40 g/L yeast conc.). Results are presented in Figure 4.16c. The results demonstrate that a viscosity up to 35 mPa.s didn't have a major influence on the oxygen transfer rate and the mixing in the MSBR.

In conclusion, the volumetric mass transfer coefficient in the presented milliliter-scale bioreactor was mostly influenced by the mixing and the aeration mode, where changes in working volume and viscosity didn't have a profound impact.

#### **4.3.5 Evaporation**

The average evaporation rate of water in the MSBR at 30 °C and 800 rpm without active aeration was 0.0030 mL/h, which means that approximately 6 % of the water present in the reactor evaporated after 20 h [118]. When active surface aeration (22 mL/h) was

applied during the same conditions in the MSBR, the evaporation rate showed a tenfold increase to 0.0339 mL/h [118]. These results are hardly surprising when high air flow rate, mixing and elevated temperatures are applied to such a small volume. Consequently, a few evaporation control strategies were evaluated as mentioned in section 4.2.9. Although they showed a certain potential in prevention of the evaporation during first tests, eventually they failed to provide adequate evaporation control during aerobic cultivations [118]. Specific reasons for evaporation control failure were lack of temperature control in the long tubing between the blue cap bottle (humidifier) and the MSBR, and the adaptation of lab-scale equipment to perform functions for which they are not made in the first place.

#### 4.3.6 CFD

The appearances of the gas-liquid interfaces at the different rotational speeds can be seen in Figure 4.17, together with the simulated specific interfacial areas 'a' and the mass transfer coefficients  $k_L$ . The mass transfer coefficients are based on the averaged value for the turbulent energy dissipation rates in the liquids.

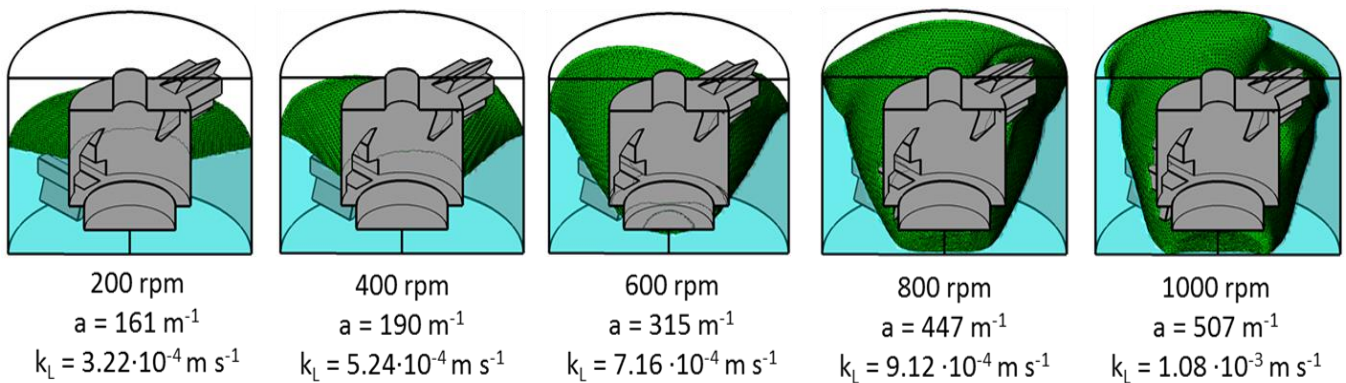


Figure 4.17. The simulated gas-liquid interfaces at the different rotational speeds in the MSBR.

The calculated interfacial area for 1000 rpm is more than three times larger than the area for the 200 rpm simulation, and the values for the mass transfer coefficient follow a similar trend.

The simulated oxygen transfer rates, i.e. the product of 'a',  $k_L$  and the proportionality constant  $Ck_La$  that was found to be 0.13, are plotted together with their corresponding experimental values in Figure 4.18 for the different rotational speeds. It can be seen that the model under-predicts the mass transfer rates for the lower rotational speeds (200-600 rpm) and over-predicts the mass transfer rates slightly for 800 and 1000 rpm. It is however

very hard to draw any conclusion if the reason for this lies in a miscalculation of 'a' or  $k_L$ , since they are very hard to determine experimentally.

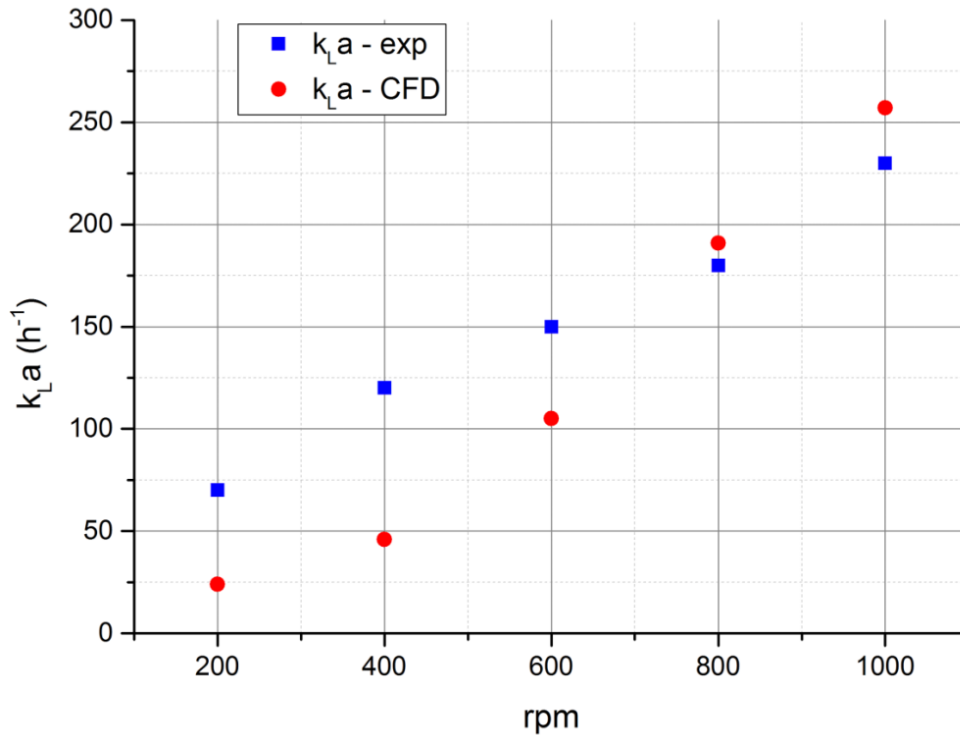


Figure 4.18. The simulated versus the experimental  $k_L a$  values for different rotational speeds.

Figure 4.19 shows good agreement between simulated and experimental data for mixing times at different rotational speeds. It can be observed that the simulated values are in the same range as the experimental ones, but underestimated for all rotational speeds except for 1000 rpm. One probable explanation for this trend is that the turbulence model applied within the CFD model overestimated its effect on the diffusion of the additional variable. The reason why the simulated mixing time for 1000 rpm is so unexpectedly high is shown in Figure 4.20, where the mixing behavior between the 800 and 1000 rpm simulations is compared. In Figure 4.20a the concentrations of the additional variable, i.e. the compound that is being virtually mixed in the fluid, are shown at different time steps during the transient mixing simulations. The red volumes are indicating volumes where the concentrations of the additional variable are exceeding the final (average) homogenous concentration by more than 10%, whereas the blue volumes indicate a concentration lower than 90% of the final one. The turquoise volumes indicate volumes with a concentration within the  $\pm 10\%$  interval from the final concentration.

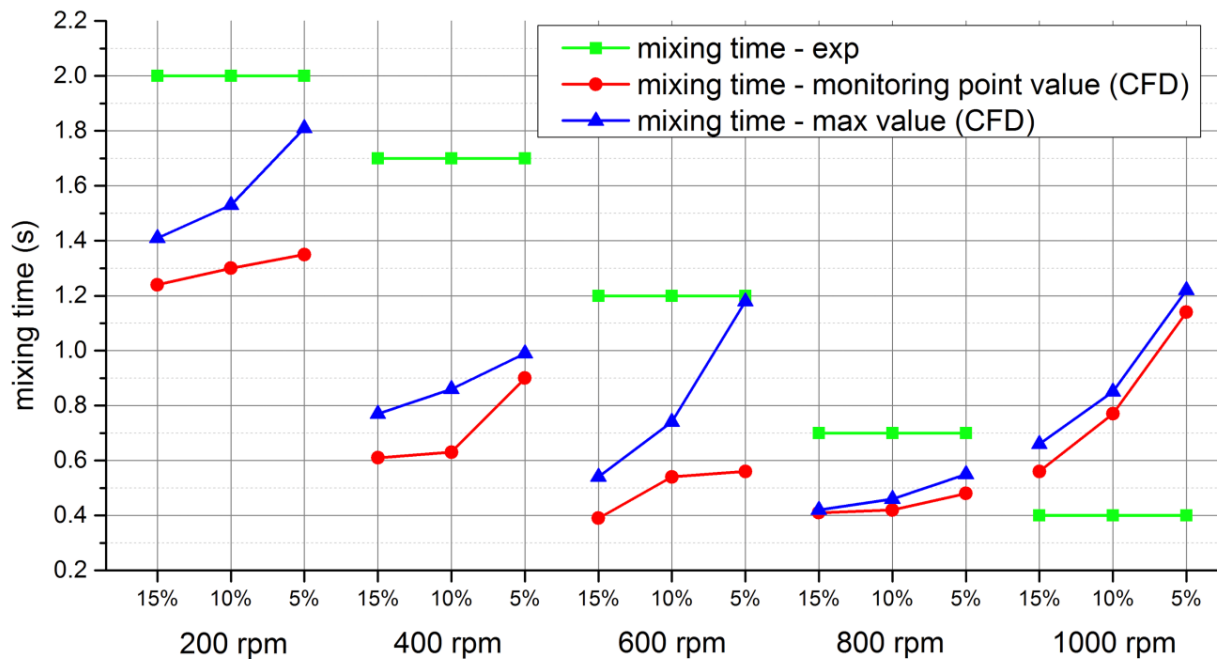


Figure 4.19. The simulated versus the experimental mixing times. Mixing time was defined as the time when the concentrations entered within the  $\pm 5, 10$  or  $15\%$  interval of their final (average) value, i.e. the concentration that is achieved once the additional variable was homogeneously distributed in the liquid.

The illustrations at 0.1 and 0.4 s in Figure 4.20a show that the additional variables are spreading in the lower part of the reactor first before this dissolved compound is transported upwards. This behavior is most apparent for the 1000 rpm case, and as can be seen there is still a zone of poorly mixed liquid present in the top of the volume after 1 s. The impact, which this poorly mixed zone has on the overall mixing times, can be found in Figure 4.20b, where the concentrations of the additional variable over time are plotted. As can be seen both the curves associated with the 800 rpm simulation, i.e. the maximal value and the monitoring point value, enter the turquoise area just after 0.4 s, while it takes up to around 0.8 s for the two 1000 rpm curves to do the same. This behavior could be a consequence of the definition of the monitoring point (average vs. max) or its location. Furthermore, the explanation for a higher predicted mixing time for 1000 rpm that did not appear in the experiments is the thin and stable liquid volume closest to the top of the reactor which might in fact be unstable, i.e. oscillating, in reality. In the simulations, the stirring element is rotating with a constant angular velocity along a perfectly fixed axis, but even small disturbances from this motion might in reality give rise to small alternations in the flow pattern, which in this case might have prevented the less well-mixed zone on the top from forming.

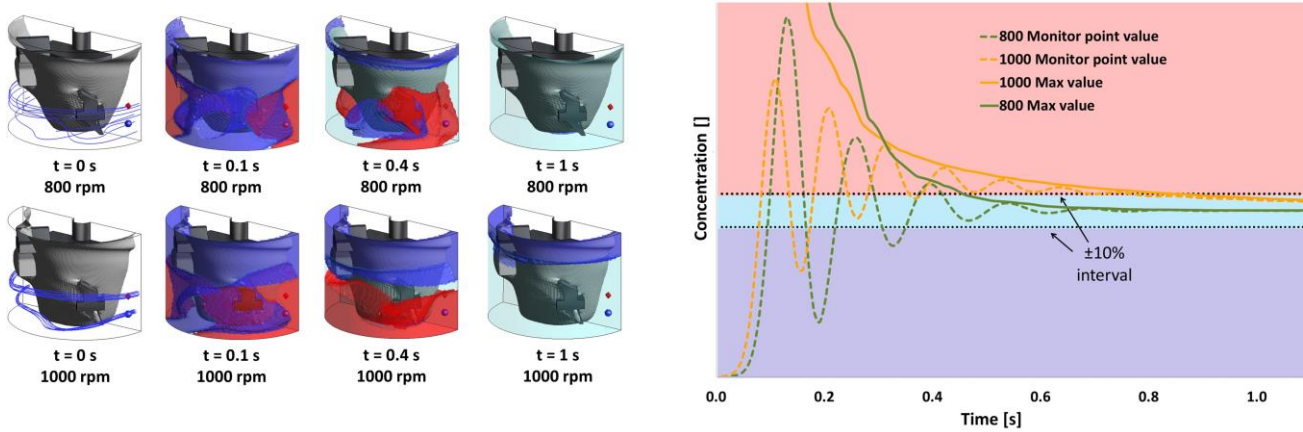


Figure 4.20. (a) The distributions of the additional variable over time for 800 and 1000 rpm simulation. The coloring scheme is applied, i.e. additional variable values higher than the  $\pm 10\%$  interval are displayed as red and values lower than this interval are blue. Values within the interval are turquoise. (b) The concentrations of the additional variable in the 800 and 1000 rpm mixing simulations. The maximal values and the values in the monitoring point are displayed as well as the  $\pm 10\%$  interval from the final value.

#### 4.3.7 Batch cultivation in the MSBR

Anaerobic and aerobic batch cultivations were performed in order to evaluate the capabilities of the first milliliter scale bioreactor prototype. Results of these cultivations are presented in Figures 4.21 and 4.23.

##### *Anaerobic cultivation with *Lactobacilli paracasei**

An anaerobic cultivation with *Lactobacilli paracasei* was performed in the MSBR and in the 2 L bioreactor. Data from both cultivations are compared in order to evaluate the MSBR performance. The lag phase lasted about 3 hours and it was followed by an exponential growth phase. This is in a good agreement with the recorded pH change, since pH starts changing around the same time. The MES buffer didn't have enough buffer capacity to keep the pH constant, so a pH decrease occurred from 6 (phase shift 79) to 4.7 (off-line end point measurement, since the used PreSens pH sensor cannot measure pH values below 5.5). Furthermore, calibration of the pH sensor was unreliable since the phase shift change was very small for each pH unit and the specific position of the optical fiber bundle for pH measurement had a big influence on the calibration process. With a slight movement of the optical fiber bundle the pH phase shift changed several points which in pH units corresponds to a big change [133]. Temperature control was satisfactory as well as mixing, which can be seen in figure 4.21 where cultivation temperature was kept constant at 37 °C until the end of cultivation, and a mixing speed set at 300 rpm was sufficient to avoid a

temperature gradient and settling of cells at the bottom of the MSBR (steady increase of the scattered light intensity). The scattered light intensity (SLI) was recorded on-line (shown in Figure 4.21) and the end point result was comparable with the optical density measured off-line (4.3).

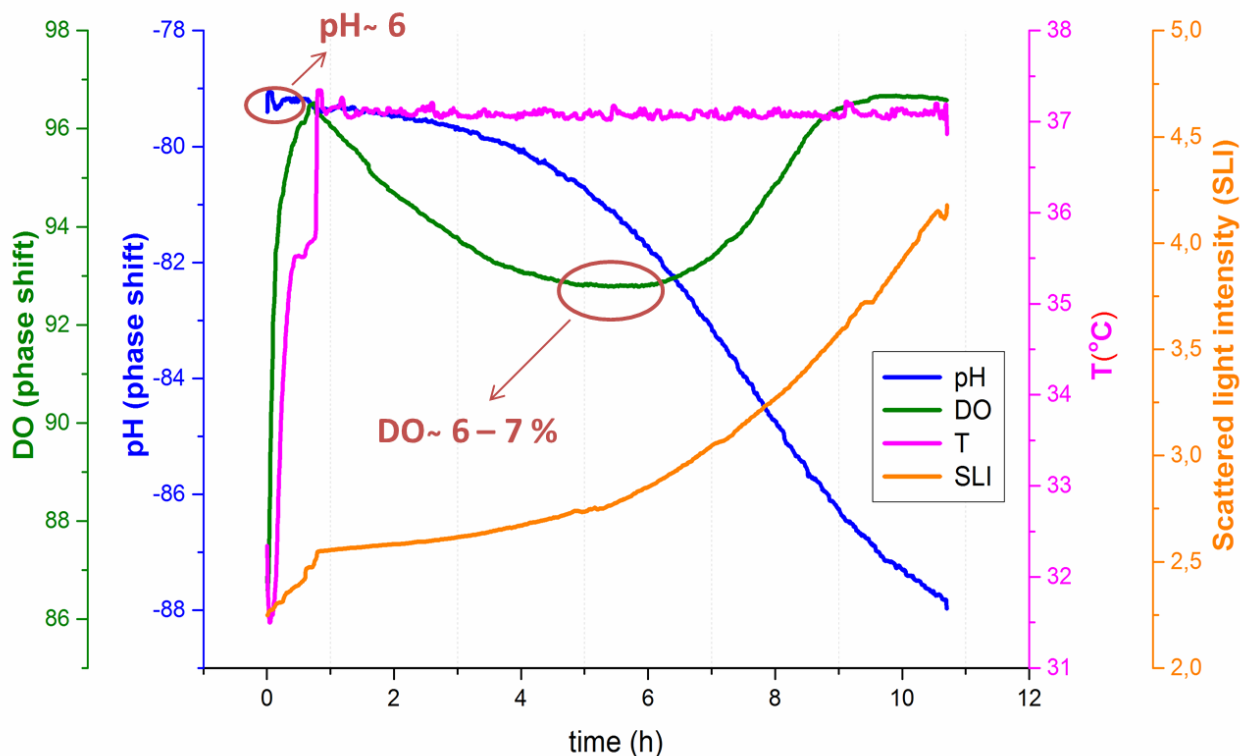
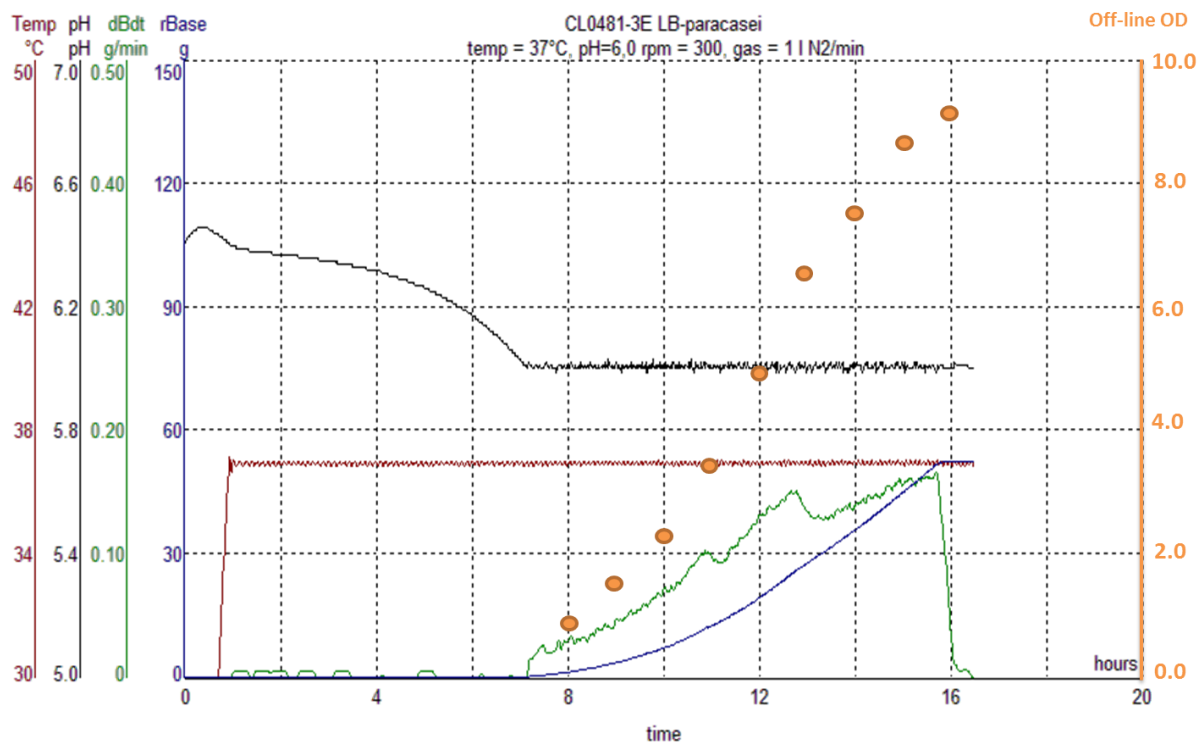


Figure 4.21. Cultivation with *L. paracasei* in the MSBR. Temperature, DO, pH and scattered light intensity data during 11 h cultivation time are shown.

After 11 hours, a decrease in glucose concentration together with an increase in the scattered light intensity and lactic acid concentration (8.7 g/L) indicated that *L. paracasei* was growing in the MSBR. The possibility of contamination was verified using a microscope and there was none detected. In figure 4.21, it can be seen that there was a change in the dissolved oxygen concentration during the cultivation. Apparently there was around 7% oxygen (phase shift 93) present during part of the cultivation which suggests oxygen-limited conditions, but it didn't have a major effect on the growth, probably since *L. paracasei* is aero-tolerant. The end-point measurement from the cultivation in the MSBR was compared to a cultivation performed in a 2 L reactor ( $T = 36^{\circ}\text{C}$ ,  $\text{pH} = 6$ , 300 rpm, 1 L/min nitrogen gas purge of the headspace). Process parameters during cultivation with *L. paracasei* at 2 L scale can be seen in figure 4.22 and cultivation results from 2 mL and 2 L bioreactors are presented together in table 4.3.





### CL0481-3E

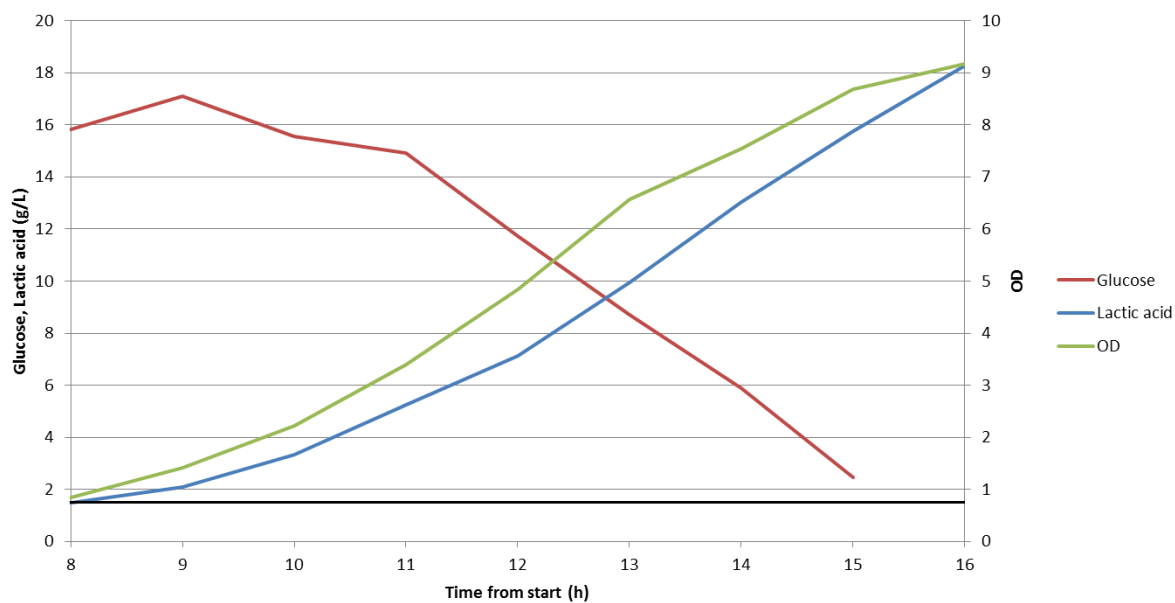


Figure 4.22. Process parameters during cultivation with *L. paracasei* in the 2 L bioreactor scale. Off-line OD, temperature, pH and added base per time and total added base during 16 h cultivation time are shown on the first graph. OD and HPLC results from the cultivation with *L. paracasei* in the 2 L scale are presented in the second graph [133].

Table 4.3. Performance comparison between cultivations at 2 L and 2 mL scale [133].

Fermentation	Sample time (h)	OD (off-line)	Glucose (g/L)	Lactic Acid (g/L)
2 L bioreactor	10	2.2	15.6	3.3
	11	3.4	14.9	5.3
	12	4.8	11.7	7.1
	13	6.6	8.7	9.9
2 mL bioreactor	11	4.3	11.5	8.7
2 mL bioreactor	10	4.6	13.3	9.2

After 11 h of cultivation the optical density in the 2L bioreactors was 3.4, the glucose concentration was 14.9 g/L and the lactic acid concentration was 5.3 g/L in the 2 L reactor, while after 11 h of cultivation in the 2 mL reactor the scattered light intensity was 4.3, the glucose concentration was 11.5 g/L and the lactic acid concentration was 8.7 g/L. Only after 12 - 13 h in the 2 L reactor similar conditions were obtained as for the 11 h sample time in the 2 mL reactor. It thus seems that *Lb. paracasei* growth was slightly faster at 2 mL scale, which can be the consequence of a different pH control strategy (NaOH is added for pH control at 2 L scale and MES buffer is used at 2 mL scale) or inoculation procedure (cold inoculation at 5 - 10 °C in 2 L and hot inoculation at 37 °C in 2 mL reactor) [133]. Still, it can be concluded that both cultivations resulted in rather similar glucose, lactic acid and biomass concentrations, forming a strong indication that the MSBR is a suitable platform for performing cultivations.

#### *Aerobic cultivation with Saccharomyces cerevisiae*

In aerobic cultivations at small scale, the issue of evaporation is pronounced, as a consequence of the aeration. For the yeast cultivation in this study, three different solutions were tested to prevent evaporation: a humidifier for the air used for aeration (with air flow through the humidifier), a condenser (with air flow through the condenser) and a saturation chamber (passive oxygen replenishment). The saturation chamber (a 5000 ml sealed flask containing 700 ml of water at 30°C and 250 rpm) was chosen, since it gave the best results. Besides, the idea was to observe yeast growth and see when oxygen limitation will occur, since the experimental system was a closed system with passive oxygen replenishment.

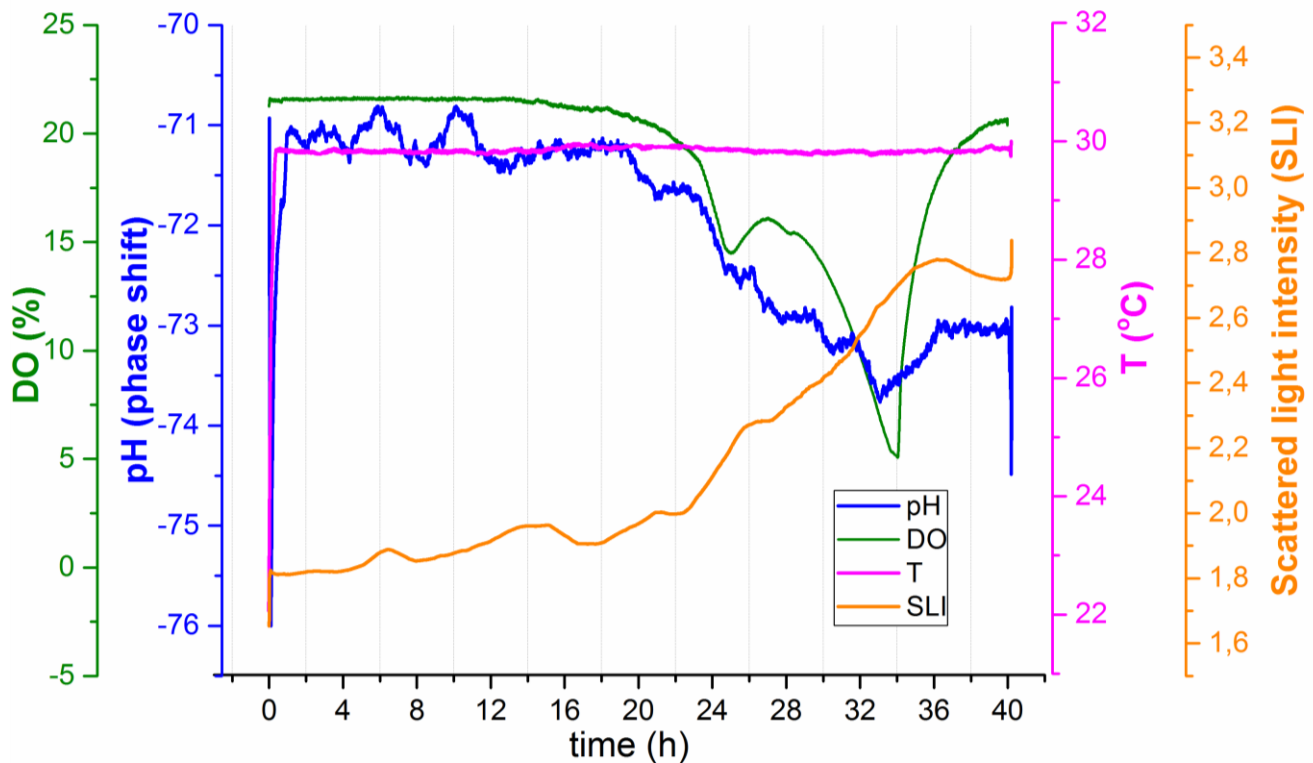


Figure 4.23. Aerobic cultivation with *S. cerevisiae*, strain CEN.PK-113-7D. Temperature, DO, pH and scattered light intensity data during 40 h cultivation time.

Figure 4.23 shows a good agreement between the scattered light intensity and the dissolved oxygen curves during the cultivation with *Saccharomyces cerevisiae*, meaning that when OD started to increase, a drop in dissolved oxygen concentration was seen due to oxygen consumption by the cells. In addition, when growth ceased, judged from the OD measurement, the dissolved oxygen value went back to the same high level as seen before growth started. The lag phase was rather long, which can mean that the inoculum was not large enough or it took a long time for the cells to adapt to the new environment or both. Furthermore, there is a possibility that high shear stress could be responsible for slow growth due to the higher applied stirring speed (800 rpm) during cultivation in the MSBR. Although, this is not very likely, since *S. cerevisiae* is known for its high resistance towards shear stress, and since growth was observed, it proved that cells can survive the applied conditions in the MSBR. After approximately 16-18 h, exponential growth occurred and the concentration of dissolved oxygen began to decrease. Around 26 h and SLI was 2.3, a plateau was seen both in the dissolved oxygen concentration and in the scattered light intensity (Figure 4.23), which is also visible at larger scale cultivations and it is associated with the characteristic diauxic shift due to that yeast exposed to an excess of glucose produces ethanol in parallel to growth. Hence, two growth phases are observed, first glucose is used as carbon source and after diauxic shift, ethanol is used as a second carbon source in aerobic conditions [134]. Although a saturation chamber was used to prevent

evaporation, still a volume change occurred and prevented the possibility of taking a sample to compare results with the off-line analysis. Besides reducing the working volume, evaporation has a strong impact on the ethanol concentration as ethanol is a volatile compound, and if evaporation occurs, it means that less of this second carbon source is available for cellular growth. Note that evaporation of ethanol can also give challenges with lab-scale cultivations, where it might prevent closing a carbon balance over the reactor.

In conclusion, aerobic and anaerobic batch microbial cultivations were performed in order to test the performance of the MSBR. Evaporation and pH control were seen to be major bottlenecks, but with an optimized pre-humidifier and a higher buffer concentration this issue can potentially be solved, which gives promising expectations for further development of the MSBR system. Moreover, the mentioned issues are less problematic in continuous cultivations, which is the next step for the MSBR design.

## 4.4 Conclusion

It was demonstrated that achieving flexible, robust mixing and sufficient oxygen transfer rate is possible at milliliter scale. The MSBR platform has a functionality and design that take into consideration:

- Small footprint
- Disposable reactor
- High level of flexibility
  - Surface aeration or sparging
  - One - or bi- directional mixing
  - Working volume (0.5-2 ml)
- Mixing can be considered nearly instantaneous
- Bi-directional mixing eliminates need for baffles
- $k_{La} > 1000 \text{ h}^{-1}$
- $k_{La}$  obtained by surface aeration is sufficient for standard cultivations.

The standalone mixing system has a unique magnetic stirrer with adjustable geometry and user-defined stirrer speed profiles, which is low cost and maintenance free.

On the other hand the whole MSBR platform was not robust enough to produce reliable results for every single experiment performed due to:

- Optical fiber bundles were handmade and without tread, so it was difficult to fix them to the platform in exactly the same position every time and secure the reproducibility of measurements during experiments.

- The coating on sensor spots for pH measurement frequently disappeared during experiments, i.e. the coating layer was degraded. The sensing range for the pH measurement (5.5 - 8.5) was also inadequate since there was no active pH control, i.e. only buffer solution was used in the culture medium and that could not avoid that pH would drop outside the active measurement range.
- Gas control was difficult and inconsistent due to application of oversized flowmeters and valves that were available in the laboratory, which in return gave problems with evaporation.
- The distance between the reflective surface (aluminum tape) at the bottom of the shaft and optical fiber bundle was not constant due to elasticity of the PDMS layer between the two PMMA parts. Also, aluminum tape was in direct contact with the broth, which was not ideal considering that the reactor needs to enable sterile and leakage free conditions for cultivations.

## Chapter 5

### Milliliter scale bioreactor design – Prototype II

---

This chapter is formulated in a similar manner as the previous chapter, by presenting and explaining the design of the second MSBR prototype. Most emphasis is put on the new solutions that emerged as answers to problems occurring with the first prototype. Beside the MSBR and the platform, two new units are presented as well – a pre-humidifier and a pump unit.

#### 5.1 Introduction

As presented and discussed earlier the MSBR prototype I showed promising results, however the platform was far from flawless. To be able to show that the whole platform can take as little place as possible, a small plate with four rods is used as a base. However, the weight of the bifurcated fiber bundles and wires was enough to destabilize the supporting structure, and therefore another plate at the bottom was installed for stability, and of course duct tape came in handy as well. Furthermore, three bifurcated optical fiber bundles used for measurement of dissolved oxygen, pH and the scattered light intensity were made in-house without any metal or plastic housing, so it was not possible to use a thread for fixing the fiber bundles in place. Consequently the placement of the fiber bundles in the platform was not reproducible, and with slight pressure from the bioreactor above they would, to some extent, change positions in the platform. This introduced a problem with calibration and consistency of the acquired data per cultivation. Furthermore, the four electromagnetic coils used for mixing, would frequently heat up and influence the whole system, so a fan was installed as a short-term solution. The influence of a high frequency electromagnetic field on cell viability was taken into consideration too. The applied strength of the field was not enough to kill cells, but one could wonder if the cells could display certain changes in the behavior by being exposed to unwanted environmental factors. Another very important issue was the high evaporation rate due to lack of a possibility to obtain very small gas flows in the MSBR. Also, measurement of pH was not reliable enough due to the limiting range and instability of the pH sensors acquired from PreSens. During some cultivations, the coating from the pH sensor would disappear and only the plastic base would stay.

Some of the issues mentioned above are minor and merely representing practical limitations that required some extra work and made the experimental set-up less user friendly. However evaporation, pH sensing and the use of adequate pumps for taking a step further and performing continuous cultivations presented problems that needed to be

addressed in order to obtain full flexibility and adequate performance. The MSBR prototype II was therefore designed with the aim to solve these issues.

## 5.2 Materials and Methods

### 5.2.1 Milliliter scale bioreactor platform – Prototype II

The MSBR platform for prototype II was also made of a PMMA plate and four bars attached to a wide base. The choice of making a bigger platform was related to making every day usage in a laboratory setting more practical and easy, although the footprint of this design would be rather small in a commercial application and the possibility to stack more than one MSBR together would be feasible. Bars used for platform elevation had thread only at the bottom and the top which provided an opportunity to screw them in the base and the PMMA plate without surfacing from the plates. In the middle of the platform a pocket was allocated for the MSBR with threaded openings for 3 bifurcated fiber bundles (30 fibers for excitation and 31 fibers for collection of light) that had a thread and were protected with metal sleeves. On the one side of the pocket, an opening was made to establish a connection between heat exchanger 1, which was part of the MSBR, and heat exchanger 2 that was attached to the platform and used to indirectly heat liquid in the bioreactor. The heat exchanger 2 consisted of a Peltier element which on one side has a heat sink and ventilation fan and on the other side has an aluminum element that has a contact surface with heat exchanger 1 to transfer the heat efficiently. The platform and heat exchanger 2 are presented in Figure 5.1.

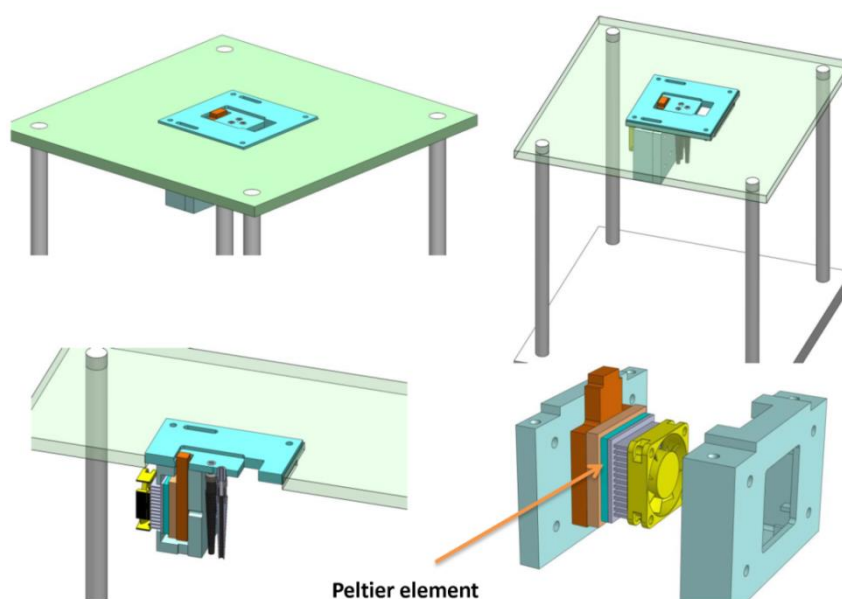


Figure 5.1. The MSBR platform with heat exchanger 2 (Dassault Systèmes SOLIDWORKS Corp., DTU licence). Technical drawings of the platform can be seen in appendix C.

On the left side of the Peltier element there are two aluminum plates. The reason for having two of them is to gain flexibility regarding the contact surface (top part of the orange element in Figure 5.1) with the MSBR by moving the element up or down according to the experimental needs.

### **5.2.2 Humidifier – Prevention of evaporation**

It is expected for an evaporation process to occur in any system where liquid is warmed up and mixed for a long time, no matter the scale. However, the evaporation rate can be lowered, if air above the liquid would contain a certain amount of water. If the MSBR was a closed system, water would evaporate from the liquid phase until the headspace reached 100% humidity which would reduce the evaporation rate to zero. When active aeration is applied in the MSBR, humid air is actively removed from the headspace and therefore the evaporation rate increases much more. The evaporation process is very pronounced in the small scale bioreactors where surface-to-volume ratio plays an important role, so active prevention is necessary. Prevention of evaporation is most often performed by application of sealing tape or different kinds of lids [135,136], PDMS membranes [29,32,107], incubators when possible [31], pre-humidifiers [57], by cooling the headspace or gas outlet [35], and by applying passive [31] or active replenishment.

In case of the MSBR prototype I, a few concepts (pre-humidifier, condenser and closed saturated chamber without active gas flow) were tested with a limited success due to adaptation of lab equipment with limited control capabilities. Consequently, sufficient time was devoted to design a proper pre-humidifier for the second prototype. It seems a rather simple task to design a chamber that increases the humidity of air. However, there are a few things to be taken into account in the frame of the entire set-up e.g. sterilization, condensation and temperature control in the pre-humidifier. The pre-humidifier should be easy to sterilize, since it is the last element before air reaches the MSBR directly. Also, it should have a good temperature control for fine tuning of the outlet gas temperature since that variable will be responsible for potential condensation in combination with a tube length that is connecting the pre-humidifier and the MSBR. Ideally, a closed-loop control with a humidity sensor in the gas inlet stream would be the best way to prevent condensation and reduce evaporation to a minimum. However, this would increase the complexity of the platform further, and thus an open loop control was applied where a trial and error approach was used to estimate the temperatures at different points in the air stream. To understand the correlation between humidity and temperature and make a good estimate about conditions in the MSBR and the surroundings, a psychrometric chart was used (see figure 5.2 and explanation below figure 5.2).



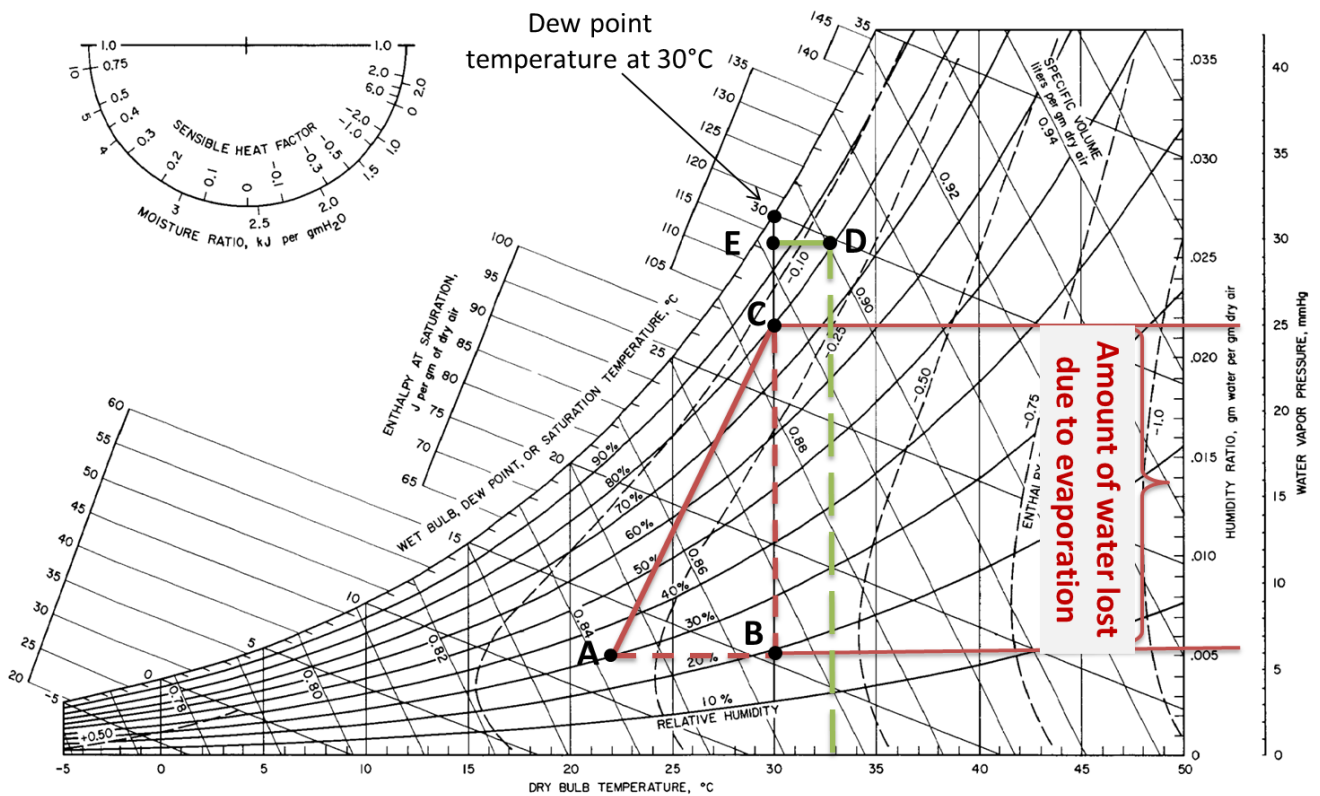


Figure 5.2. Psychrometric chart [137]. Dry bulb temperature (measured by a dry thermometer); Wet bulb temperature (measured by a wetted sensor tip); Dew point temperature (when moist air sample reaches water vapor saturation); Relative humidity (ratio of the fraction of water vapor in air to the fraction of water in saturated moist air at the same temperature and pressure); humidity ratio (the mass of water vapor per unit mass of dry air); enthalpy (total heat energy of the moist air); specific volume (volume per mass of air sample). When air at room temperature (22°C) and relative humidity of 30% (point A on chart) enters to the MSBR at temperature 30°C (point B on chart), relative humidity decreases to 20%. If air stays long enough in the MSBR at 30°C, relative humidity will increase to a certain value, e.g. 80% and a certain amount of water will be lost due to evaporation. In order to prevent this process, it is important to increase the relative humidity in the headspace as much as possible (point E on chart). Ideally, humidified air at slightly higher temperature than the one in the MSBR (point D) can be introduced to the MSBR to reduce evaporation to a minimum. Moving from point D to point E along the green line in figure 5.2 it can be seen that the water content in the air is not lost due to evaporation and the relative humidity of air is increased. However, increasing further relative humidity, point D would move above the current point and will be above dew point temperature in the MSBR and condensation would occur.

The pre-humidifier is envisioned as a plastic container in the shape of a cube that has lower and upper parts which are pressed together on a seal to completely close the container. It is presented in Figure 5.3.

In the upper part of the pre-humidifier a stirrer is placed to stir the air and liquid (it was omitted during experimental work, since it became apparent that the pre-humidifier worked well without mixing). The bottom part of the pre-humidifier was covered with an aluminum plate that was used as a heating element. Three temperature sensors were placed in the pre-humidifier for temperature measurement of the heating element, liquid and gas phase, respectively. Inlet and outlet ports for gas are placed on the top of the pre-humidifier.

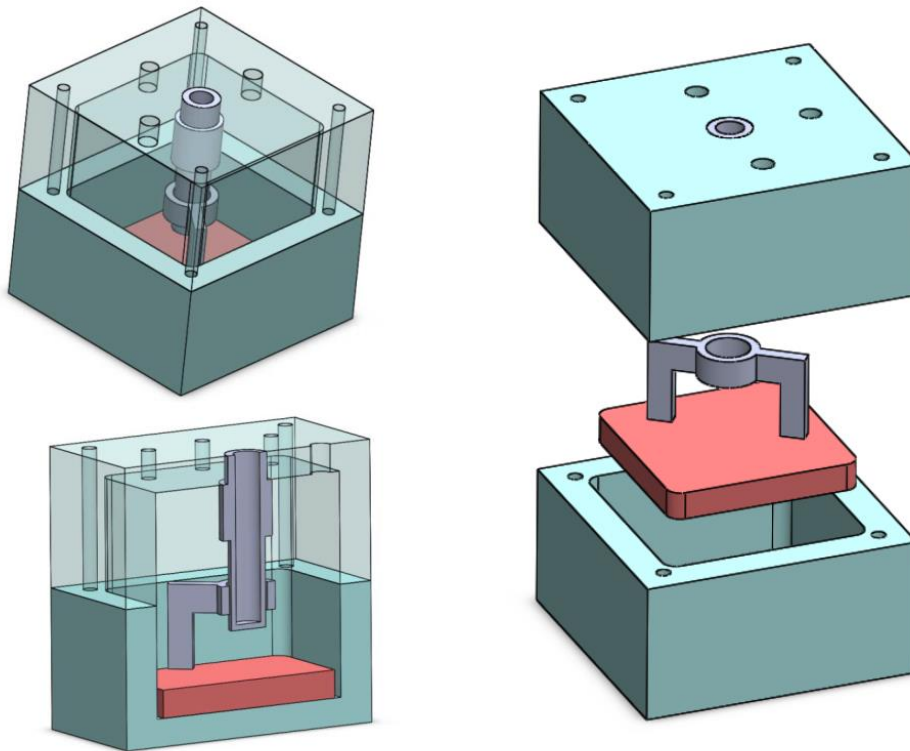


Figure 5.3. Pre-humidifier - red heating element (aluminium plate, copper wires and thermocouple encapsulated in epoxy from the bottom side) and grey shaft with stirrer in turquoise box (Dassault Systèmes SOLIDWORKS Corp., DTU licence). Technical drawings of the humidifier can be found in appendix C.

### 5.2.3 Syringe pump system

The continuous cultivation at milliliter scale is still a challenge in academia and industry. A partial explanation for this lies in the pump system - the unit that enables a continuous flow at different flow rates. In small scale applications obtaining low flow rates with a certain precision is important and often a challenging task. There are a number of possibilities when it comes to pumps intended for flow control at micro-scale, mainly pressure controllers, peristaltic, recirculation and syringe pumps. Each type of pump has

its own strengths and weaknesses that could be more or less pronounced based on the requirements of the application.

To get an idea about the flow rates necessary for continuous cultivations, looking at the requirements of a frequently used model organism such as *Saccharomyces cerevisiae* is a good starting point. In the range of dilution rates applied, a commonly used dilution rate in continuous cultivation of *Saccharomyces cerevisiae* is  $0.2 \text{ h}^{-1}$  [138–140]. For a cultivation with 1 mL working volume, the flow rate that needs to be delivered by the pump for such a continuous cultivation can be derived from the definition of dilution rate  $D = F/V \rightarrow$  i.e. flow rate / volume. If all known values are inserted in the previous equation ( $0.2 \text{ h}^{-1} = F / 1 \text{ mL}$ ), the result is  $F = 0.2 \text{ mL h}^{-1} = 3.3 \mu\text{L min}^{-1}$ . For 2 mL working volume of the MSBR, the necessary flow rate would of course double for the same dilution rate. Consequently, pumps that can deliver flow rates with  $0.1 \mu\text{L min}^{-1}$  resolution would be required for this milliliter scale cultivation platform.

Peristaltic and recirculation pumps don't have precise flow control compared to syringe pumps or pressure controllers. The syringe pumps are frequently and extensively used in laboratories since they are inexpensive, simple, easy to use, and they can provide a certain level of precision. They easily can change their working range by application of different sizes of syringes, since the flow rate  $F [\mu\text{L min}^{-1}]$  is directly correlated to the diameter of the syringe and its cross section  $A, [\text{mm}^2]$  by the correlation  $F = v * A$  where  $v [\text{mm s}^{-1}]$  is the speed of the piston pushing the liquid to the reactor. However, the typical syringe pumps have flow oscillations at very low flow rates due to the nature of the pump motor choice, i.e., a stepper motor. The issue of flow oscillation can be addressed by proper choice of the syringe size, where smaller volume syringes tend to give better performance at low flow rates. At the system level choice, the selection of pulseless syringe pumps with advanced motor drive equipped with feedback, removes the flow pulsation completely, although pulseless syringe pumps are more expensive.

In order to find the best suited syringe pump for the MSBR there are a few conditions that should be fulfilled:

- adequate performance
- low cost
- adaptable - to fit with the MSBR
- small footprint

It is not possible to obtain a syringe pump that satisfies all these conditions fully, so a compromise was achieved between different requirements. One potential drawback of the syringe pump design presented here is based on the inherent behavior of the stepper motor which produces incremental flow at very low flow rates (as any other classical syringe pump), which means it could deliver the medium in small portions during defined time periods ( $0.025 \mu\text{L}$  per step for 5 mL syringe). Also, mechanical strength of the

supporting frame would be an issue if the application included high pressures and viscous liquids. However, the mechanical strength of the syringe pump, while pumping medium during continuous microbial cultivation, should not be an issue.

Two push pull/continuous syringe pumps were designed for the MSBR. Mechanical parts of the syringe pump were made at the DTU Skylab workshop by milling, while a linear actuator (with step motor and integrated precision screw, Z20000 series) was purchased from HaydonKerk. Afterwards, all the parts were assembled, thus producing a low cost and versatile syringe pump system. Both pumps were attached to the MSBR platform bars with flexible screws that allow a change of the pump orientation. One syringe pump was used for controlled delivery of air and the other one was used to deliver medium into the MSBR. Both pumps follow the same working principle of the classic syringe pump – movement of a syringe piston with user-preset speed is obtained via a motor. The bipolar stepper motor controlled linear motion of the threaded guide rod that is attached to the pump slider, which in turn is attached to the syringes. The working principle of the syringe pump is presented in Figure 5.4.

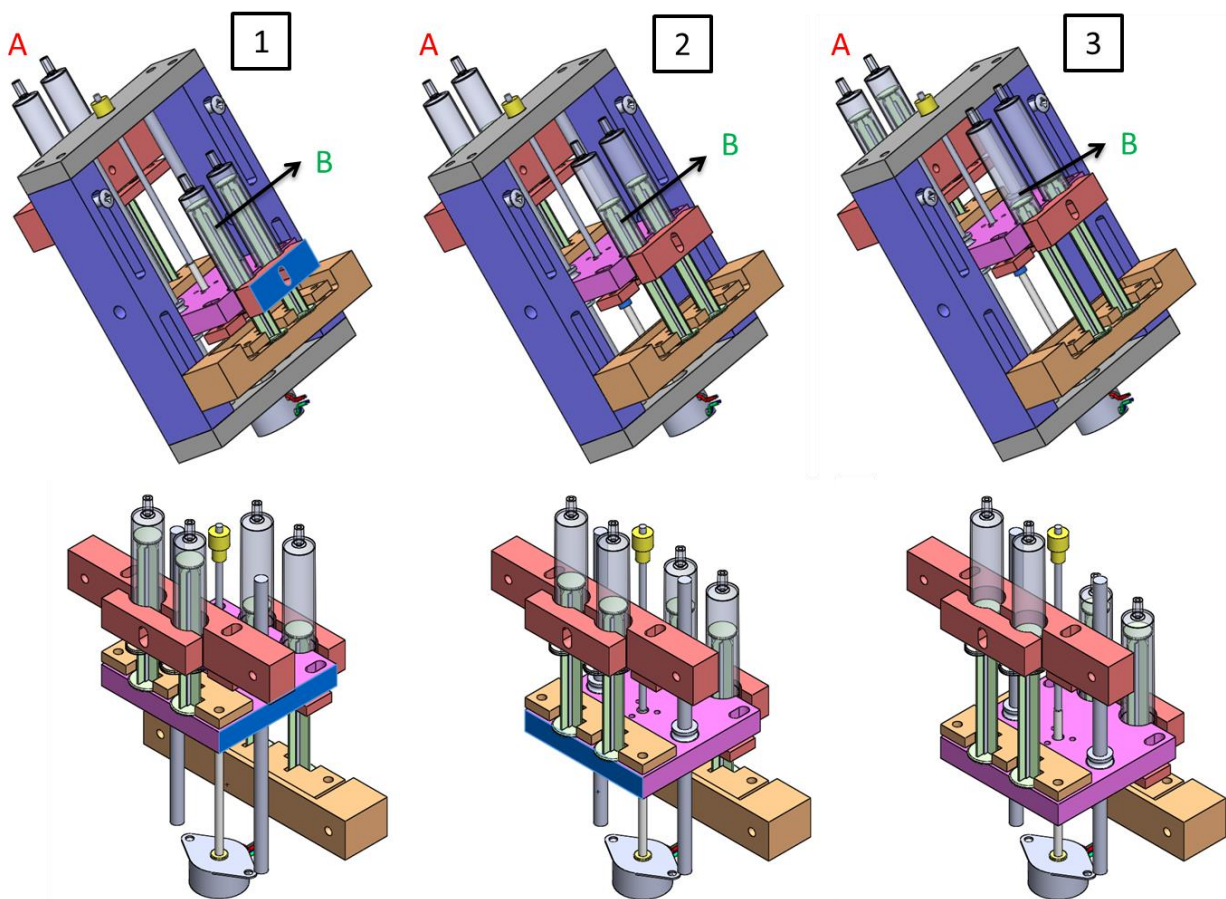


Figure 5.4. Syringe pump – push pull working principle (Dassault Systèmes SOLIDWORKS Corp., DTU licence). Three positions of the pump with syringe groups A and B are presented in the figure and are indicated with numbers 1, 2 and 3. The figure illustrates a process where fluid is pumped in to the syringes from the group B while fluid

is pumped out from the syringes in the group A. During this process, the slider (pink element in the middle, connected to the linear bearings and the shaft of the motor) is moving its position from the closest to the motor in step 1, to the furthest away from the motor in a step 3. With this motion, the volume of the group B syringes will increase from 0 to max, while opposite will be true for the group A. Technical drawings of the pump can be found in appendix C.

In order to extend the pump operation to the continuous flow mode, the pump was made so that controlled bidirectional movement of the slider with four syringes (two for each direction) can be established. This configuration allows simultaneous infusion (with 2 syringes) and withdrawal (2 syringes) of fluid (liquid or gas). With addition of one-way valves, the whole system became a continuous flow syringe pump where the available volume is no longer a limiting factor.

The housing for the one-way valves was made from three PMMA plates stacked together and enclosed with two thicker PMMA plates acting as holders. Each plate had a distinctive structure to enable a defined direction functionality, which can be seen in Figure 5.5. The middle plate had holes in the shape of flowers that featured one-way valves (umbrella valves UM 058.001 SD from miniValve).

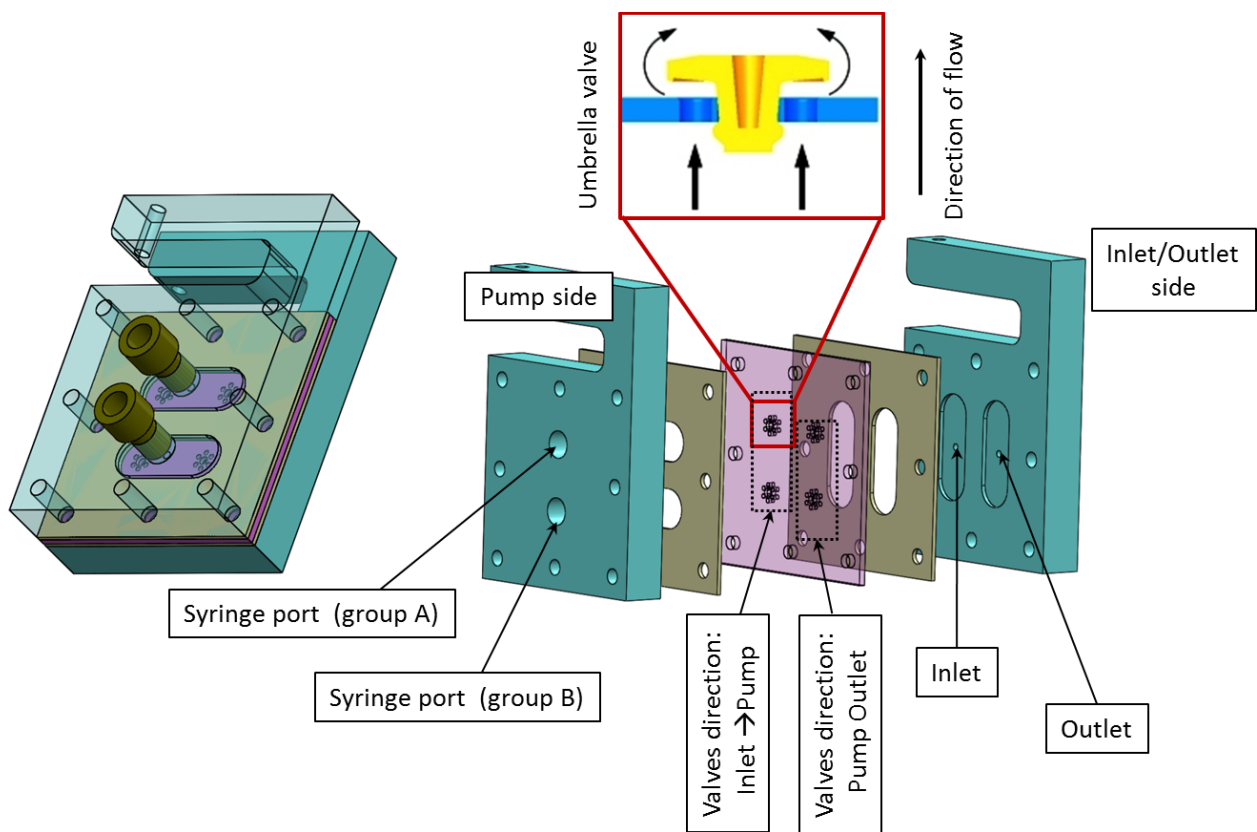


Figure 5.5. One-way valves bridge configuration (Dassault Systèmes SOLIDWORKS Corp., DTU licence). Four one-way umbrella valves are arranged in a “bridge” configuration. This configuration ensures the one-way flow from the inlet port to the outlet port of the part, assuming the syringes from two groups are used on the pump

ports. Technical drawings of the one-way valves bridge configuration can be found in appendix C.

One could of course ask the question why considerable effort was put in designing an own syringe pump when the market is overwhelmed with different types of pumps, and the design/construction task is rather complex. There are however not so many commercial solutions for the microfluidics area and the small scale systems, and even if they are available they were quite expensive since they are not wide-spread products. If commercially available equipment was chosen to use with the MSBR platform, it would require 4 infuse/withdraw syringe pumps like e.g. the Harvard Pump 11 Elite. The average price of each pump is around 2500 euros with its footprint being 23x18x15 cm. Besides being an expensive and bulky solution, unlimited continuous flow would not be an option since syringes would be eventually emptied and application would be limited by the size of the used syringe. Also gas delivery and obtaining small flows in the bioreactor would require a precise mass flow meter that is also expensive.

Nowadays, Harvard Apparatus offers a PHD Ultra syringe pump (<http://www.instechlabs.com/Pumps/syringe/phdultra.php>) that has a rather similar operation principle to the syringe pump developed and presented in this thesis. However they apply a more advanced motor with increased number of steps turning it in a pulseless syringe pump. It is a recent product and the push pull / continuous working mode is provided in a category of special configurations. Beside Harvard Apparatus, there are other companies as well that offer new products and solutions, e.g. Cellix, Tecan, Elveflow, Cetoni, KD Scientific syringe pumps and others. However, price and reliability of these products makes them a less attractive choice.

#### **5.2.4 Milliliter scale bioreactor design- Prototype II**

The prototype II uses the same alternating layer structure between PMMA parts and PMDS seals as in the previous prototype, as can be seen in Figure 5.6. The bottom of the MSBR consists of a 35 x 35 mm PMMA plate with 2 mm thickness. Another layer, made in aluminum, with three openings for light guidance, and a thickness of 1.5 mm, is added to the bottom layer to prevent leakage and bending of the PMMA plate. In the middle of the base plate of the bioreactor, an opening ( $d = 4$  mm) is placed with guiding channel toward an edge of the base plate. The opening allows for wires attached to the temperature sensor PT 100 to exit the MSBR. The opening is covered by a stainless steel element that has a twofold function. It is used for measurement of the scattered light intensity and temperature. The side of the stainless steel element facing the opening has a pocket where the temperature sensor is placed, while the side facing the MSBR has an extended, wide and thin lever - reflector that is placed 1 mm above the position where light enters for

measurement of the scattered light intensity (the SLI). In this way, the reproducibility of the SLI measurement is improved compared to the prototype I where the distance between the optical fiber bundle and the reflector (attached to the shaft) was

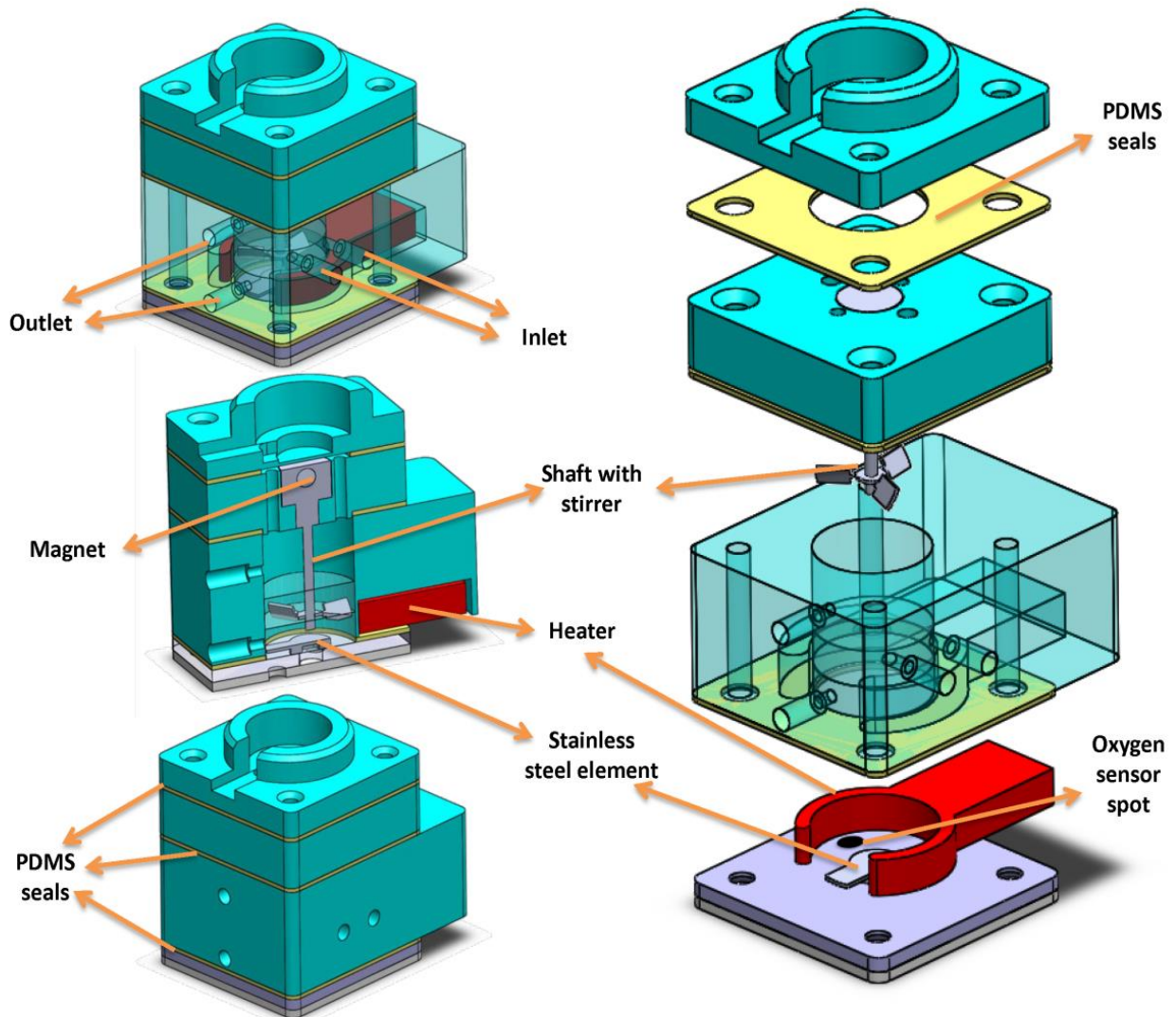


Figure 5.6. The MSBR prototype II - assembly, cross section and exploded view (Dassault Systèmes SOLIDWORKS Corp., DTU licence). The milliliter scale bioreactor had two inlets and two outlets (for medium and air), a magnet attached to the shaft and stirrer, DO sensor spots, a stainless steel element for OD and T measurement and a heater. PDMS layers were used between PMMA blocks for sealing purposes.

somewhat variable due to pressure applied by screws on the adaptable PDMS layer between the bottom part of the reactor and the chamber during assembly. In case of the second prototype, the reflector is attached to the bottom of the MSBR at a fixed distance. Moreover, the temperature measurement is improved as well. In the first prototype the temperature sensor was in contact with a thin PMMA plate, while now it is connected to a stainless steel element that is in direct contact with liquid in the MSBR. Stainless steel has

two orders of magnitude higher thermal conductivity than the PMMA which improves sensitivity and reliability of the temperature measurements.

On one side of the stainless steel element, a sensor spot for the measurement of dissolved oxygen is glued to the bottom of the MSBR and on the other side there was an empty position assigned for other types of measurements according to the needs. All three positions are equidistant from each other (60 degree angle) lying on the same circle and corresponding to the position of three bifurcated fiber bundles placed in the platform. First, the empty position was devoted to pH measurement with the PreSens sensor spot similar to the one used for DO measurement. However the reliability of this measurement was questionable. The coating of the sensor spot had a tendency to disappear during the cultivation and the LabView custom made program for this measurement was not communicating well with the sensor. In light of reading more about these uncertainties, the decision was made to ensure an end point measurement of pH and to use buffer for pH control purposes which ought to be sufficient for continuous cultivations.

The middle PMMA (35x47x20 mm) part was allocated to the reactor chamber, inlet and outlet for medium and gas as well as heat exchanger 1. The heater in heat exchanger 1 is redesigned completely, going from banana shaped to the shape of an external jacket. Even though the heater in the previous prototype covered a certain portion of the bioreactor bottom and successfully managed temperature control, the idea of increasing the contact surface and designing a heater that will resemble the well-known jacketed heating applied at bench scale was pursued. Subsequently, a big portion of the wall was heated up instead of the bottom part, and in return a small heating area and potential temperature gradient were avoided. As a result, the bottom layer of the MSBR was simplified significantly as well. Furthermore, the PMMA middle part was 12 mm longer than the base of the MSBR on one side. This additional space was used as contact surface between heat exchanger 1 and the heat exchanger 2 in the platform (explained earlier in section 5.2.1).

The top two PMMA parts were designed to hold a stirrer and a magnet, and to seal the MSBR. The small cylinder, placed in a designated pocket of the lower top PMMA part, was made with two openings - one for a rod-shaped magnet (horizontal) and one for a shaft (vertical). Thus the shaft was connected to a magnet which was coupled to another magnet attached to the DC motor. The stirrer design also went through a redesign in an attempt to make the MSBR more comparable to traditional solutions. It is made of stainless steel instead of plastic, which reduced its size and complexity compared to the previous stirrer design and also made reactor cleaning easier. The stirrer has four impeller blades which could be categorized as pitched-blade impellers with 30° pitch angle that produce axial flow patterns (up and down).



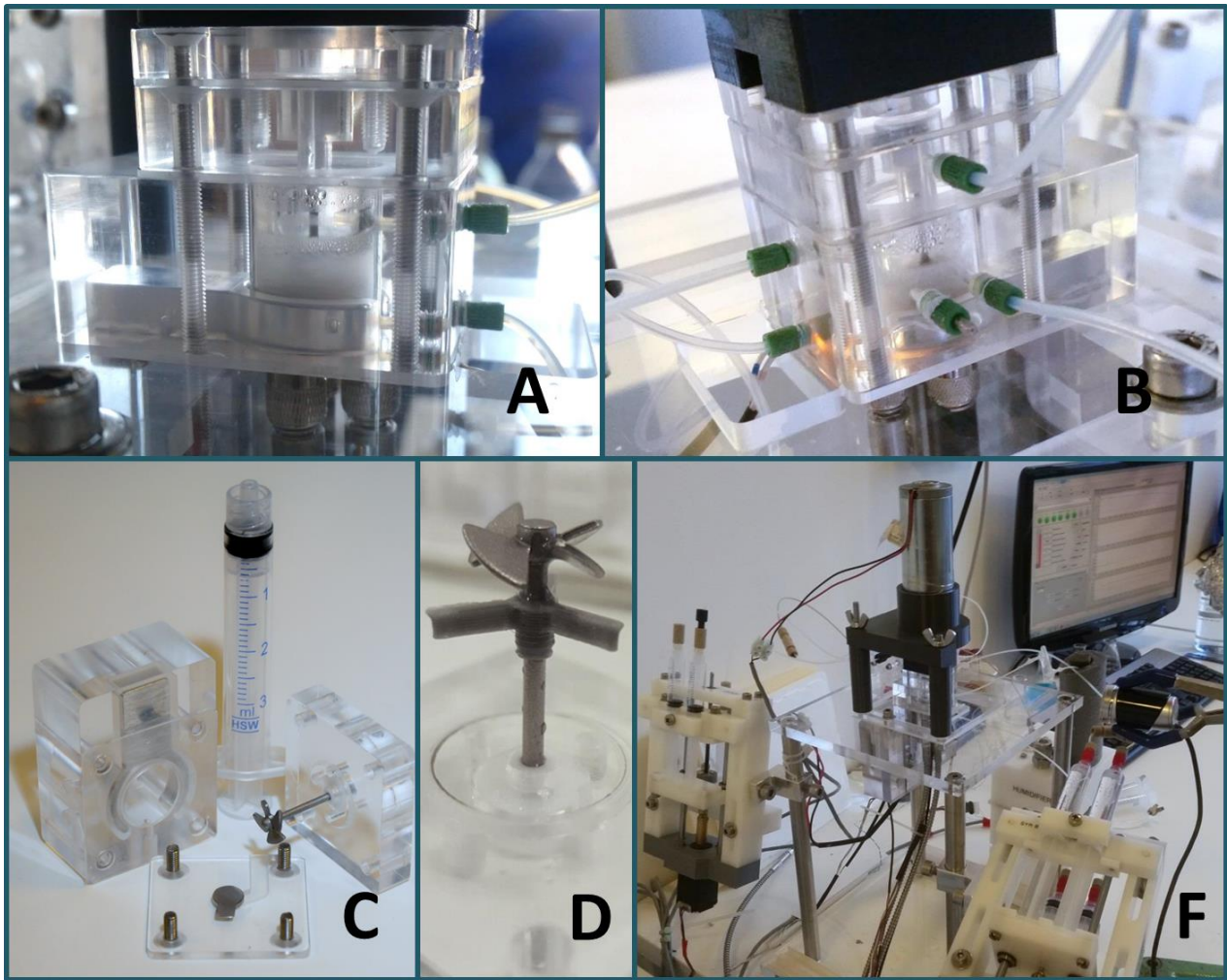


Figure 5.7. The MSBR experimental set-up: A and B - the milliliter scale bioreactor during cultivation; C - the MSBR before being assembled; D - the stirrer with two impellers; F - the whole platform with both pumps.

The upper top PMMA part of the reactor had as main purpose to close the MSBR and prevent potential contamination. The specific geometry with a small channel on one side of the MSBR was designed for the DC motor placed in a cylinder, where the cylinder would be placed on the ring structure on top of the reactor. Thus, the motor would always have the same position and distance from the magnet connected to the stirrer. Unfortunately, this idea was in the end not adopted due to two problems. The small size DC motor was very fast and operating well at higher rotational speeds; however obtaining a speed as low as 200 – 400 rpm was a challenge. Another, important issue was that the DC motor was vibrating during operation and it was transferring this vibration to the MSBR since it was attached to it.

Consequently, another DC motor was selected that was bigger with better performance, and a holder was made to support it which was not directly attached to the MSBR.

However, the small channel on the top part of reactor is still used for the Hall effect sensor measuring the speed of the motor shaft, and thus precise information is acquired about the applied rotational speed of the stirrer in the MSBR.

The MSBR platform experimental set-up with all the features mentioned above is presented in Figure 5.7.

### 5.2.5 Temperature

As explained earlier prototype II has a heater (heat exchanger 1) with slightly more complex design compared to the previous prototype, since heating is based on having a contact surface between heat exchanger 1 and heat exchanger 2 attached to the Peltier element. This allowed for more precise measurement and control capabilities, since both the possibility for heating and cooling were now available. It also introduced the need for a more complex control scheme, involving two temperature sensors and two controllers. The cascade control system seemed to be an appropriate choice for this configuration. A block diagram of the applied cascade regulation is presented in figure 5.8.

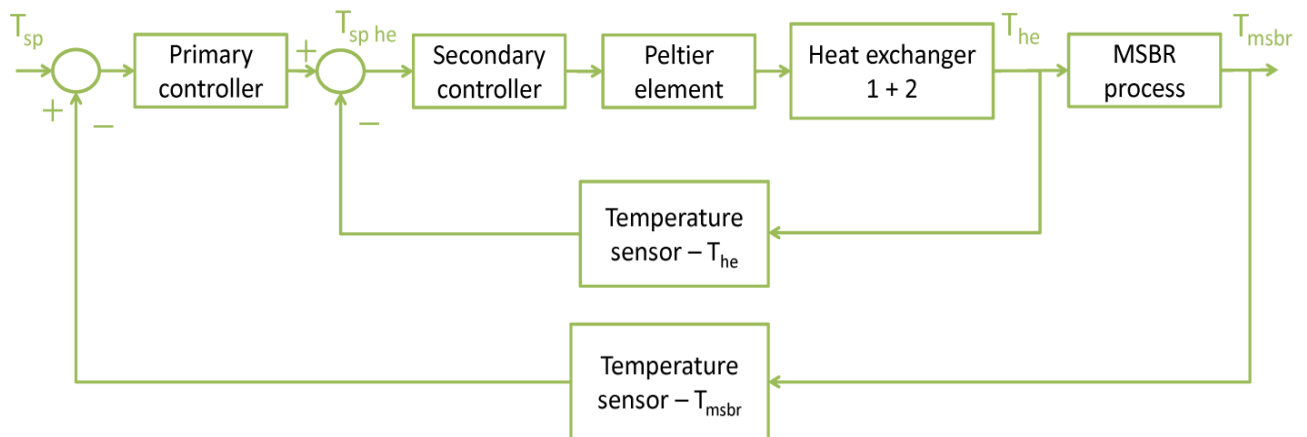


Figure 5.8. Block diagram of the cascade regulation.

The block diagram in Figure 5.8 shows that cascade regulation uses two sensors (in this case, temperature sensors), two controllers and one actuator (Peltier element). There is a certain temperature in the MSBR that is desired and it is represented by the temperature set point  $T_{sp}$  in the block diagram. The primary controller in the outer loop receives information about the difference between the temperature set point ( $T_{sp}$ ) and the temperature measured in the MSBR ( $T_{msbr}$ ) and asks the secondary controller in the inner loop to apply more or less heat based on the calculated deviation from the set point. Afterwards, the secondary controller uses the Peltier element to control the secondary

process (heat exchanger 2, which is in close contact with heat exchanger 1). In general, both the inner and outer loop perform as feedback control loops, where the inner loop acts as an actuator for the outer one. The cascade control requires more tuning than simple feedback control since there are two controllers that need to be tuned. First, the secondary controller is tuned and adjusted until the inner loop performed satisfactory, resulting in a proportional gain set to 10 and an integral time set to 3 min. Afterwards, the primary controller is tuned where the proportional gain is set to 8 and the integral time to 3 min.

Temperature control is tested by performing step changes of the temperature set point in order to see how fast and accurate the temperature control capability can be realized. In addition, cascade control performance is evaluated by introducing a disturbance in the MSBR by suddenly decreasing the temperature of the liquid (30°C), which was done by taking out 50% of the liquid volume and re-introducing the same amount of liquid with different temperature (4°C). The MSBR was filled with 2 mL of water and stirring was maintained at 600 rpm with bidirectional mixing (change of direction every 1 s). The heating capability is tested by introducing the step change from 23°C to 32°C, continuing to 35°C and afterwards to a temperature 40°C. The cooling capability is tested in the same way as the heating, by applying step changes to the temperature set point from 40°C to 36°C, continuing to 30°C and afterwards to 26°C.

### **5.2.6 Measurement of scattered light intensity (SLI) for biomass monitoring**

The principle of the scattered light intensity measurement applied in the first prototype is also used in the design of the second prototype. To obtain transfection measurements, two important components needed to be present in the design – a bifurcated fiber bundle in the platform and a reflector – mirror in the MSBR. As explained in section 5.2.1 the bifurcated optical probe used 30 optical fibers to send light and 31 fibers to receive it back. This probe was fastened to the platform so it kept the same position which allowed repeatability. Considering that the prototype II design changed considerably and it was not possible to have a mirror-like surface at the bottom of the shaft, a solution was provided using a new stainless steel element that was attached to the bottom of the MSBR. This element is described in the section 5.2.4. Calibration of the scattered light intensity measurement in the MSBR is performed with different concentrations of baker's yeast and by growing yeast cells (strain CEN.PK-113-7D) in shake flask and taking samples from different growth phases followed by analyzing them in the MSBR, in the UV-1800 UV-VIS Shimadzu spectrophotometer at 600 nm and by dry cell weight determination. Moreover, different strengths of the orange LED light were evaluated in order to define and adjust the range (between cell concentration and the scattered light intensity) and resolution since the light pathway is fixed by the set up.

### 5.2.7 Determination of mixing time

The method based on acid-base neutralization with phenolphthalein as an indicator is used to evaluate mixing time. It is the same method as the one used for determination of mixing time in the MSBR prototype I. Therefore, the experimental method will not be explained per se in this section to avoid repetition. However, a certain description is necessary to clarify how the tests are performed due to the difference between both set-ups.

As the upper part of the MSBR held the stirrer, the reactor needed to be closed during any test involving the mixing process. Consequently, dispensing 10 - 20  $\mu\text{L}$  volumes of liquid (necessary for determination of mixing time) proved to be more difficult. It was important that the whole amount of liquid is dispensed at once, so acid-base neutralization can be completed and the effect of mixing could be observed. Usage of inlets or outlets was not possible since some liquid volume could be retained in tubes or in the reactor wall. Therefore, the MSBR was adapted by removing the upper part and leaving the bioreactor chamber open for access. The stirrer was directly attached to a shaft of the DC motor using a magnet and it was placed in the chamber by positioning the motor on its own holder, so the location of the stirrer was the same for each experiment. A pipet is used to dispense the allocated volume of acid via an opening from the top of the MSBR chamber.

Another important aspect was to achieve satisfactory visual access to the reactor chamber in order to observe and document the change of color during the mixing experiments. A camcorder (Sony Handycam HDR-CX330, 9.2 megapixels) attached to a support is placed on a side of the reactor chamber wall that is not covered with the heater, and since the reactor chamber wall was transparent and without visual obstacles, capturing the color change was possible in this way.

### 5.2.8 Microbial strain

Considering that the major interest is in the application of the MSBR in aerobic cultivations and in order to make a performance comparison with the previous prototype, the laboratory strain *Saccharomyces cerevisiae* CEN.PK-113-7D is used as well in the MSBR prototype II.

### 5.2.9 Medium composition

The CBS medium [128] was also used for yeast cultivation in the second prototype. However, the medium composition was slightly different compared to the first prototype since the glucose concentration was 20 g/L in the batch part of the cultivations and 5 g/L during the continuous part of the cultivations. Furthermore an increased concentration of

monopotassium phosphate served as a buffer. Stock solutions were made in demineralized water:

$(\text{NH}_4)_2\text{SO}_4$	10 g in 100 mL
$\text{KH}_2\text{PO}_4$	24 g in 200 mL
$\text{MgSO}_4, 7\text{H}_2\text{O}$	5 g in 100 mL

Vitamin and trace metal solutions were received from the Department of System Biology at DTU. They are prepared according to following procedure:

**Solution of trace metals:** The following amounts of salts (-EDTA) are dissolved/suspended in 1000 mL distilled water. Keep the pH at 6 and add the components one by one. The solution is gently heated (lukewarm/hand warm) and the EDTA is added. In the end, the pH is adjusted to 4, and the solution is autoclaved or sterilized by filtration.

$\text{FeSO}_4, 7\text{H}_2\text{O}$	3.0 g
$\text{ZnSO}_4, 7\text{H}_2\text{O}$	4.5 g
$\text{CaCl}_2, 6\text{H}_2\text{O}$	4.5 g
$\text{MnCl}_2, 2\text{H}_2\text{O}$	0.84 g
$\text{CoCl}_2, 6\text{H}_2\text{O}$	0.3 g
$\text{CuSO}_4, 5\text{H}_2\text{O}$	0.3 g
$\text{Na}_2\text{MoO}_4, 2\text{H}_2\text{O}$	0.4 g
$\text{H}_3\text{BO}_3$	1.0 g
KI	0.1 g
$\text{Na}_2\text{EDTA}$	15 g

**Vitamins:**

For 500 mL

d-biotin	25 mg
----------	-------

is dissolved in 10 mL 0.1 M NaOH + approx. 400 mL  $\text{H}_2\text{O}$ . Adjust the pH to 6.5 with HCl, and add the following vitamins one by one.

Ca-Pantothenat	500 mg
Thiamin-HCl	500 mg
Pyridoxin-HCl	500 mg
Nicotinic acid	500 mg
p-aminobenzoic acid	100 mg

Again adjust pH to 6.5. Add 12.5 g m-Inositol and adjust pH to 6.5 while filling up to 500 mL.

Sterilize by filtration and store in a cold environment.

Preparation of 1 L of CBS-medium from stock solutions:

Stock solutions for	
$(\text{NH}_4)_2\text{SO}_4$	75 mL

KH <sub>2</sub> PO <sub>4</sub>	120 mL
MgSO <sub>4</sub> , 7H <sub>2</sub> O	10 mL
Trace metals	2.0 mL
Sigma 204 antifoam (foam control)	50 μL

are poured together and water is added up to 900 mL in a glass bottle. Separately, 5 g of glucose is dissolved in 100 mL water and another glucose stock solution was made by dissolving 20 g of glucose in 100 mL water. These three solutions were autoclaved separately. Afterwards, the 100 mL solution with 5 g of glucose was added to the 900 mL mixture in a laminar flow bench (LAF-bench). Next, the vitamin solution (1 mL/L) was added by sterile filtration in the LAF-bench. 2 M NaOH was used to adjust pH to 5.6. The CBS-medium with glucose concentration of 5 g/L is stored in the refrigerator at 4°C. Also, glucose stock solution with concentration of 200 g/L was stored in the refrigerator. Medium with higher glucose concentration for the batch phase was prepared later by adding 0.1 mL/mL of the 200 g/L glucose stock to the earlier prepared CBS-medium (containing 5 g/L glucose).

#### 5.2.10 The MSBR II preparation for cultivation

Cleaning of the milliliter scale bioreactor is an important step in running a cultivation in order to avoid contamination that can influence the reproducibility of data. A sterilization step of bioreactors at larger scale is part of the standard operating procedure and usually involves an autoclaving step where the applied temperature is 120°C. Of course, this method is not applicable with plastic compounds like the PMMA used for construction of the MSBR. The MSBR consists of diverse materials ranging from different types of plastics (PMMA, PLA), over silicone (PDMS) to stainless steel. Each material has its own specific resistance toward different chemicals, which makes cleaning of the MSBR challenging. After examining different characteristics of the used materials in the MSBR, hydrogen peroxide emerged as the only option for performing a cleaning at room temperature, i.e. chemical sterilization. All materials used in the MSBR were tested by being exposed to 10% hydrogen peroxide solution for 48h and the overall material strength was investigated. Since materials were not affected, the MSBR cleaning is performed with 10% hydrogen peroxide solution according to the following step-wise procedure:

1. The MSBR is disassembled to parts.
2. Each part of the bioreactor is left submerged in a 10% hydrogen peroxide solution in a beaker for 1h in the LAF-bench.
3. All parts are rinsed with sterile water to remove hydrogen peroxide, and are then left to dry in the LAF-bench.
4. The sensor spot for measurement of dissolved oxygen is glued to the bottom of the MSBR in the LAF-bench.

5. The MSBR is assembled in the LAF-bench.
6. Tubes for inlet/outlet of air and medium are rinsed from inside and outside with ethanol and are brought to the LAF-bench where they are rinsed with sterile water and attached to the MSBR. Another cleaning method was to leave the tubes in a 10 % hydrogen peroxide solution for 1 h with the rest of the MSBR parts, and afterwards to rinse them with sterile water. Ends of the tubes are connected to 3 mL sterile syringes before the MSBR with attached tubes is taken out from the LAF-bench.
7. The clean and airtight MSBR is properly positioned on the platform outside of the LAF-bench and the temperature sensor is connected.
8. Medium is pumped through the MSBR and tubing to remove sterile water and to perform DO sensor calibration.
9. 1.5 mL of medium with inoculum is introduced to the MSBR.
10. Syringes placed at the end of the tubes coming from the MBSR are replaced by connectors with tubes that are attached to the pump and humidifier.
11. Similar steps are applied in the cleaning procedure of the humidifier and the tubes that are attached to it, except at the end of the cleaning where sterile water was kept in the humidifier.
12. Syringes used with the pump are filled with medium in the LAF-bench and connected to tubes with a Y connector and closed by means of needles at the open end before leaving the LAF-bench.

### **5.2.11 Cultivation conditions**

In order to perform a continuous cultivation, inoculum was first prepared by growing yeast in 14 mL round bottom culture tubes with closure. 3 mL of CBS-medium (containing 5 g/L glucose) plus 0.3 mL of 200 g/L glucose stock solution was added to a culture tube. A colony was picked from a plate with cells and transferred to the culture tube. The inoculated culture tube was then incubated at 220 rpm shaking speed and 30°C for 10 to 15 h. In the meanwhile, the MSBR was prepared for inoculation. When the preculture was taken from the incubator, a sample was withdrawn aseptically, and OD600 was measured. The inoculum volume was calculated ( $V_{\text{inoculum}} = V_{\text{MSBR}} + 9.5 \text{ mL} \cdot \frac{\text{OD}_{600\text{start}}}{\text{OD}_{600\text{tube}}}$ ) to provide an initial optical density of 0.1. Since the MSBR operated with 1.5 mL working volume, the inoculum would be very small and it would be an issue to inoculate the MSBR in a repeatable manner. Thus, 11 mL medium (containing 20-21 g/L glucose) was inoculated from which then 1.5 mL was transferred to the MSBR through an inlet via a syringe. Afterwards, the process parameters of the MSBR were adjusted to the required values and a cultivation was started in batch mode. The batch part of the cultivation was performed under the growth conditions that are determined by the following set of initial process parameters: pH 5.6, aeration: 3 – 5 vvm, stirring: 500 rpm (every 1s change of stirring direction), 21 g/L glucose as a carbon source, temperature:

30°C. Stirring rate and aeration were changed according to the amount of dissolved oxygen available during the cultivation. When the batch mode of the cultivation was completed, the continuous cultivation mode was started by initiating the pump. For continuous cultivation, the same medium was used but without additional glucose, and thus the available carbon source concentration was about 5 g/L glucose. The dilution rate applied in continuous cultivation of *S. cerevisiae* was 0.2 h<sup>-1</sup> [141-144].

### 5.2.12 Monitoring and control

For the MSBR II prototype, a serious effort has been invested in the development of a user interface of the LabVIEW control routine. The print screen is depicted in Figure 5.9, where the main fields on the user interface can be seen. The nominal control input parameters are positioned at the left hand side while the timespan traces of selected process parameters can be found on the right hand side. Full content of the user GUI (Graphical User Interface) is presented in the Appendix E.

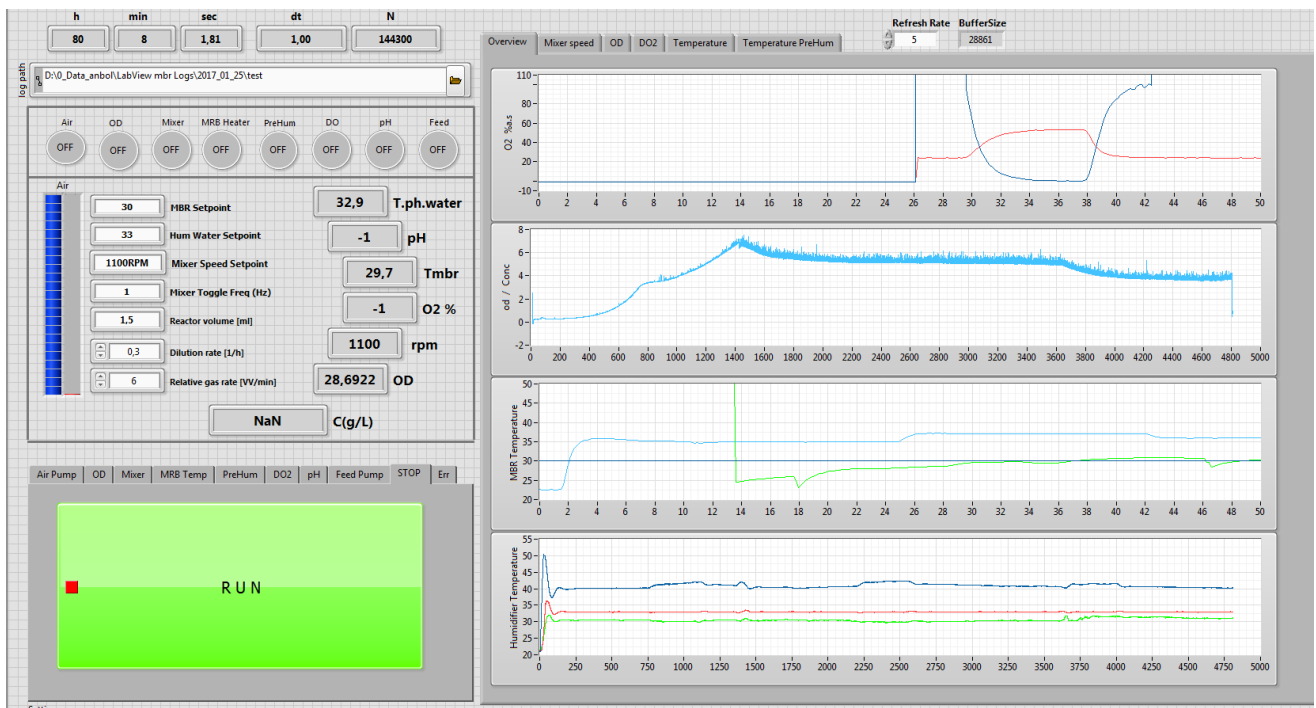


Figure 5.9. End-user interface of the Labview control routine.

The functionality of the control routine with signal flow is presented as a block diagram in Figure 5.10. The control routine consists of three sequential steps which are executed each time the control routine is called.



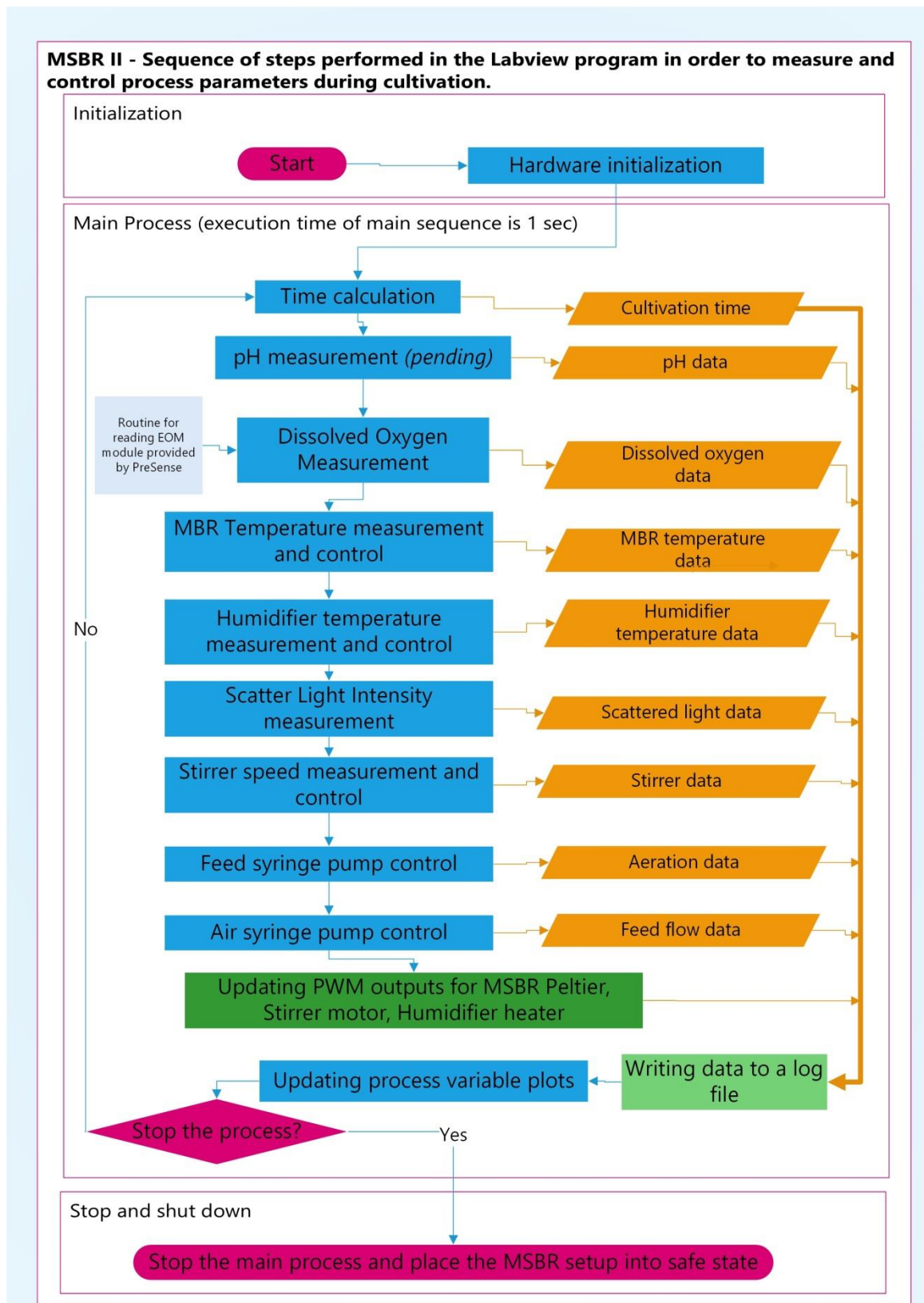


Figure 5.10. Sequence of steps performed in the Labview program in order to measure and control process parameters during cultivation in the MSBR.

The first step is the initialization, where the PC running the control routine, sets up all the communication channels (namely serial communication/ USB) with peripherals. The list

of peripherals includes National Instrument US6229 DAQ cards, DC current supply, thermocouple and PT100 analog input modules and PreSens EOM-O2 module as illustrated in figure 5.11.

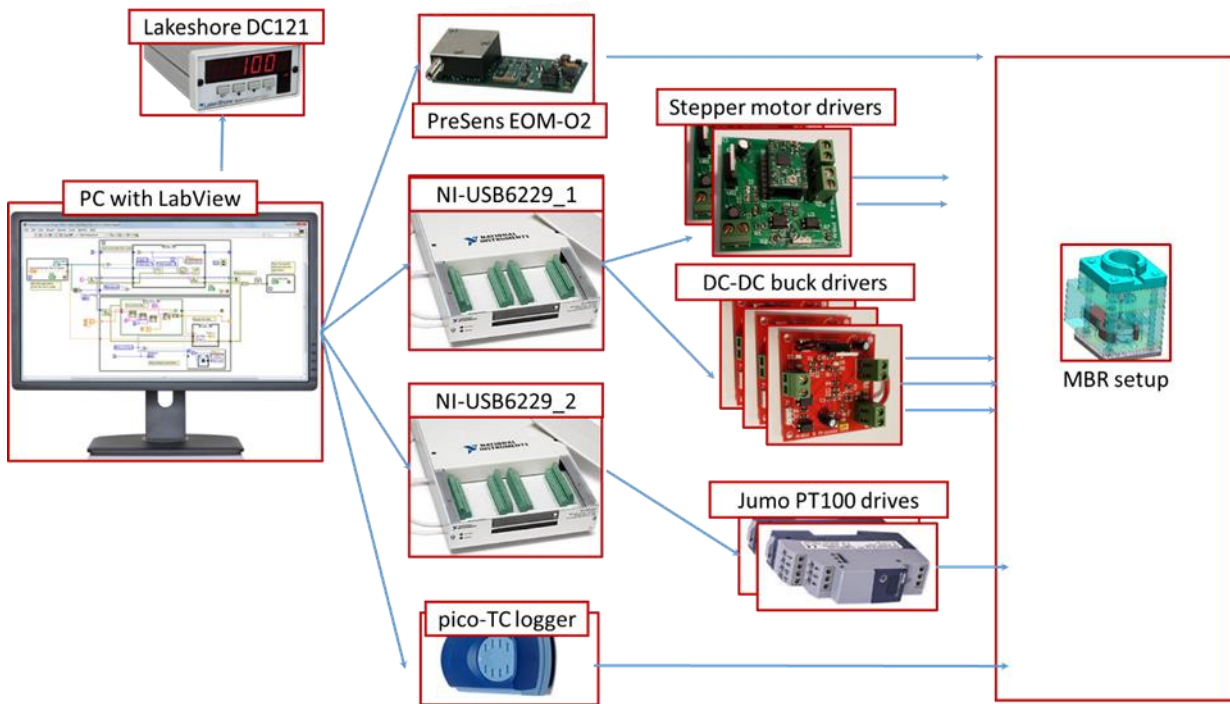


Figure 5.11. Communication between software and peripheral units.

The control routine can be scaled up and easily expanded with any additional modules which could be added at a later stage to the MSBR setup e.g., pH module, CO<sub>2</sub> module, NIR spectrometer etc.

When initialization is completed and no error is found, the control routine will enter into the main loop where all monitoring, data logging and control is executed. Each iteration of the main loop takes approximately 1 second after which it repeats itself until a user stops the execution from the GUI. As illustrated in Figure 5.10, the main control loop consists of a number of sequential steps and each step manages a particular subsystem of the MSBR platform measurement and control system. The block diagrams of the LabView routine are showed in detail in Appendix E.

When time was calculated based on the time of the PC running LabView, the program read the variable which contains the value of the dissolved oxygen concentration and potentially pH (planned but not implemented). It is important to note that a separate LabView routine was obtained from PreSens, and was running in parallel with the main control routine. It was continually communicating with the EOM-O2 module (each ~0.25 sec) and it was receiving the dissolved oxygen, phase and amplitude values from EOM-O2 and it stored them in intermediate variables for further use in the main control sequence.

Next in line was the temperature control of the MSBR, starting with acquiring the temperature values of the MSBR and the aluminum heat exchanger. The values of the resistance of two PT100 sensors placed in the MSBR and at the aluminum heat exchanger have been converted to an analog voltage signal with JUMO-PT100, resulting into a signal with voltage ranging from 0 - 10 V. The JUMO- PT100 module was preset to the 0 - 60 °C range which made the correlation between 0 - 10 V output and temperature rather straightforward, i.e. multiplication with a factor 6. To minimize the signal noise, the voltage output of the JUMO-PT100 module was sampled with USB-6229 over 0.2 s with 1 kHz sampling rate and averaged out into a scalar value. Following the acquisition of the temperatures of the MSBR and the aluminum heat exchanger, the further signal processing is affected by the choice of the type of temperature controller (selected from the GUI). The available temperature controllers include open loop control (constant voltage of the Peltier element), a “thermostat function” closed loop control based on temperatures measurement and a “PID controller” closed loop control based on the temperature measurement, the latter being the default choice in the experimental phase. The output of the controller, regardless of the type, is a supply voltage of the Peltier element as a percentage of 12 V (which is the input voltage to DC/DC Buck Drivers, shown in Figure 5.12). This modulation index is further used to generate appropriate Pulse Width Modulation (PWM) and is streamed to digital output on USB6229.

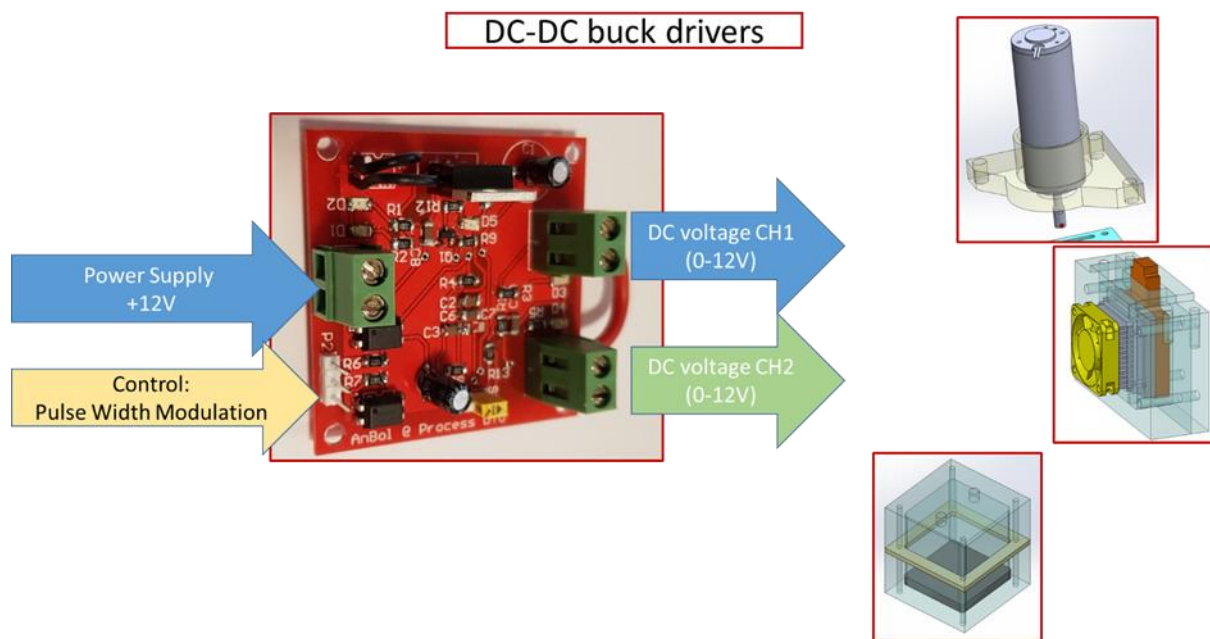


Figure 5.12. The DC drive converts a constant 12 V input voltage and generates output voltage in the range -12 to +12 V based on the control inputs.

Maximal temperatures in the system were limited to 60 °C in order to prevent damage of the Plexiglas parts.

After the MSBR temperature control stage, the temperature control of the humidifier was implemented in a similar manner. Temperatures of the humidifier heater plate, water and

air were measured with thermocouples (type K) and evaluated with pico USB Thermocouple Data Logger. The values of the temperatures were read from the pico USB Thermocouple DL and used in closed loop PID control. As the reference points for the air inlet temperature in the MSBR (hence the outlet air from the humidifier) is typically kept at 3 °C above the MSRB temperature set point, the dynamics of this temperature control was deemed of a lesser importance compared to stability, which resulted in slow but stable control of the inlet air.

Scattered light intensity measurement of the biomass concentration ( $OD_{msbr}$ ) in the MSBR II was the following step in the main operating routine. Implementation of the  $OD_{msbr}$  measurement is done when the LED was supplied with constant current in attempt to eliminate temperature dependence of the LEDs and their light emitting capacity, which is fairly proportional to a supply current. In the GUI, the user could choose between two preset values 10 mA and 30 mA, which were empirically found to produce sufficient light intensity for a successful  $OD_{msbr}$  measurement. Two photo diodes, used to measure the light reflected from the MSBR (70% light after the beam splitter) and the portion of the LED light that served as a reference signal (30% light after the beam splitter), had the voltage output range from 0 - 3V and were sampled with USB6229. The voltage of photodiodes was sampled at 10 kHz for 0.5 sec and averaged to reduce the noise levels. As the light source (LED) used is of a DC nature (constant in time), steps to eliminate potential parasitic light sources (day-night variation, artificial light) interfering with the scattered light measurement was implemented by turning off the LED and sampling the background light levels every 10<sup>th</sup> iteration of the main loop. The background values of the light were used to offset the light intensity values measured while the LED was on. Scattered light from the MSBR, photo diode voltage, was divided with the photo diode voltage of the reference photo diode and effectively multiplied with 30 in order to scale the values in a 0 - 100 range. The derivation of  $OD_{msbr}$  and the signal processing result is presented in the equation below:

$$OD_{MSBR} = \frac{V_{PD70\%|LED=on} - V_{PD70\%|LED=off}}{\frac{V_{PD30\%|LED=on} - V_{PD30\%|LED=off}}{0.3}} 100$$

where  $V_{PD70\%}$  and  $V_{PD30\%}$  are the voltage outputs of corresponding photo diodes (photo diode measuring scattered light of 70% of the LED light flux and one measuring 30% of the LED light flux, respectively). The LED=on and LED=off designates the states when the LED is powered on and when the LED is powered off.

The speed of the stirrer is controlled in the open or closed loop configuration. As the stirrer motor is a permanent magnet DC motor and the motor used in the setup was rather oversized in terms of power, the speed of such motor is fairly constant at constant DC voltage. Hence, calculating the terminal voltage of the DC motor to a large extent

determined the stirred speed, which was a default setting during the experiments. The closed loop stirrer speed control was also implemented. The speed measurement was realized by a hall sensor positioned close to a permanent magnet bar used to couple the motor shaft and the internal stirrer in the MSBR. As the bar magnet has two poles (north and south), while rotating the frequency of the installed Hall sensor was used to directly evaluate the speed of the motor. To evaluate the frequency of the hall sensor, the internal counter of USB 6229 was employed. The output of the speed controller, regardless of the type, was the supply voltage of the permanent magnet DC motor, that was later used to generate appropriate Pulse Width Modulation (PWM), output on digital output of USB6229 and control the DC/DC Buck Drivers, shown in Figure 5.12.

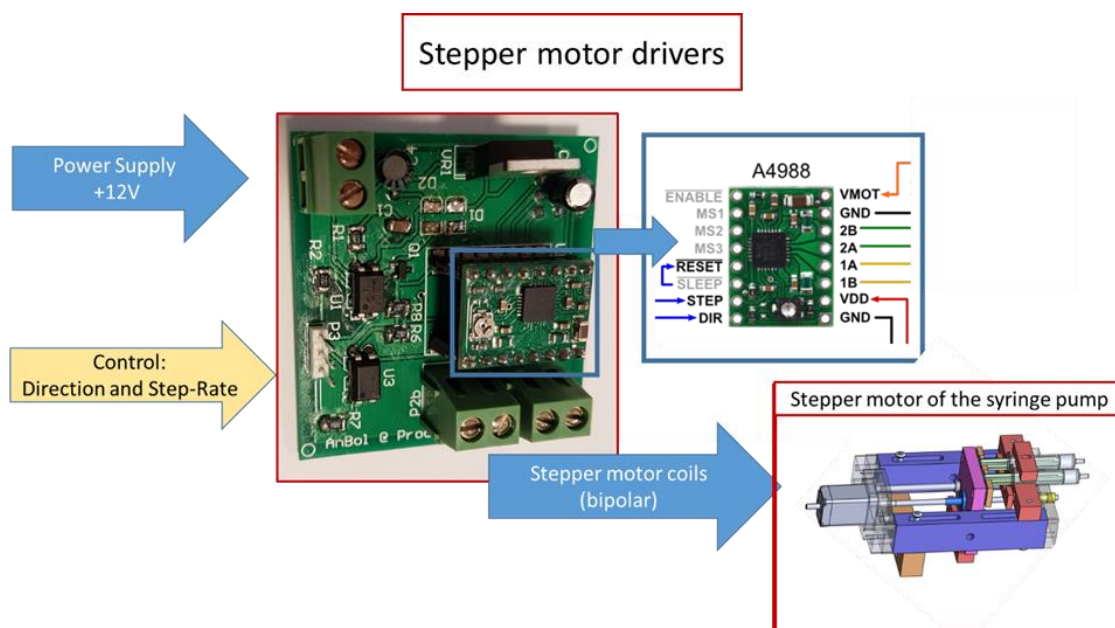


Figure 5.13. The stepper drive generates two phase output voltages with phase shift of 90 deg in order to drive the stepper motor. The input voltage is 12 V and the control inputs are the step rate input and the direction of the rotation input.

After stirrer speed, the control and setup of the syringe pumps for aeration and feed are still to be done. Both pumps were driven with a stepper motor supplied from the custom made PCB - "Stepper motor drives" shown in Figure 5.13 where the control signals were generated with USB6229 digital outputs. In order to control the stepper motors and thus the pumps, the "Stepper motor drives" PCB requires two TTL digital inputs, direction (where logical high stands for clockwise and low for contra clock wise rotation) and step rate (number of steps per second). The stepper motors used in pump assemblies are bipolar 12 V permanent magnet motors with 7.2 deg step resolution. The motor drivers were able to provide so called "micro-stepping" up to 16 steps gradation of each 7.2 deg step of the motor, effectively increasing the angular resolution of each step up to 0.45 deg.

Hence, accounting for the employed syringes volume, desired dilution rate/aeration and the parameters of the pump, the pump control task was to generate the toggle frequencies of two inputs in to “Stepper motor drives” PCB. Or more accurately, the step/rate input (in Hz) which controls dispensing/infusion speed, and the direction input (in Hz) which is responsible for reversal of the pump.

With all steps completed, the main sequence generates 50000 samples of calculated PWM modulation controllable outputs (used for Peltier, DC motor humidifier heater supplies) which are continually streamed on the digital port 0 of USB6229\_1 and are updated on each iteration if the modulation indexes have a new values.

The main control sequence concludes with updating of the GUI graphs for user visualization, logs the predefined data stream in to the log file and starts the sequence again for a new iteration.

## **5.3 Results and Discussion**

### **5.3.1 Temperature**

Temperature is an important process parameter for growth of microorganisms that needs to be closely monitored and controlled. Depending on the process requirements, temperature could be kept constant for a long period of time for optimal cell growth or it could be changed in a certain manner in order to study e.g. the impact of temperature on cell physiology (heat and cold shock responses) [145–147]. To provide the necessary temperature control in the MSBR that could support different bioprocess requirements with respect to temperature change, cascade regulation was applied with specifically designed heat exchangers. A detailed description of the cascade control and its hardware is provided in section 5.2.5.

Figure 5.14 shows the cascade regulation performance when the temperature set point is suddenly changed. It demonstrates how quickly the control system reacts and succeeds to keep the temperature at the desired level. First three set-point changes were applied for testing the heating capacity of the system, while the last three set-point changes showed how fast the MSBR could be cooled down based on 30% usage of the available cooling capacity, which was a limit imposed the by set-up. To have a closer look at the dynamic behavior and stability of the cascade regulation, a step change from 32 to 35°C was presented as inserted graph in figure 5.14. It took 2.7 min for the control system to reach the given set point at 35 °C. The slightly oscillatory response showed longer settling time which was the consequence of the fact that the controller parameters were set to higher values to achieve fast reaction of the system. Furthermore, all the responses had on average delay of 0.5 min, i.e. a dead time that was necessary for the process variables to

respond to the controller output. The main contributor to the delay is hardware inertia based on the configuration of the indirect contact heating.

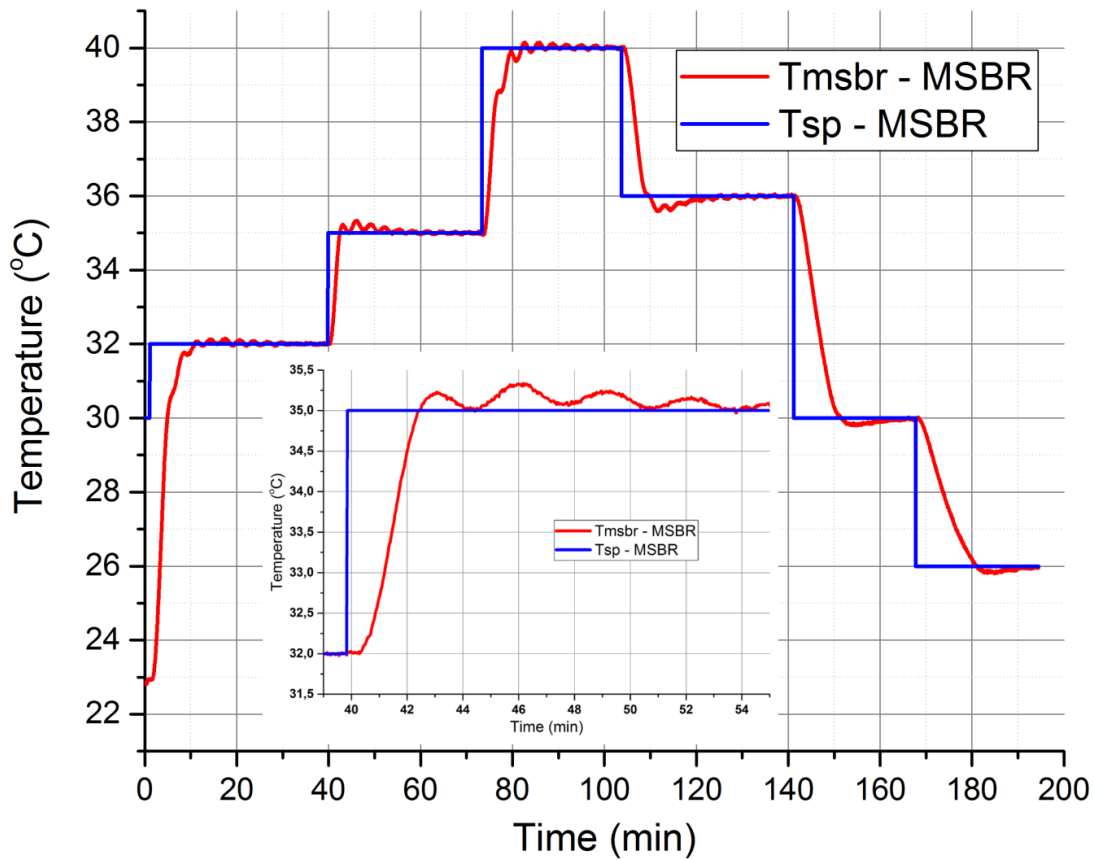


Figure 5.14. Temperature profile in the MSBR and control capabilities during multiple set point changes (heating and cooling).  $T_{sp}$  is the temperature set point;  $T_{msbr}$  is the temperature recorded in the MSBR. Temperature control was more effective during heating than during the cooling process. At temperatures closer to the room temperature, the cooling step was longer, which can be seen in the last  $T_{sp}$  set point change from 30°C to 26°C.

In Figure 5.15, the response and behavior of inner and outer control loop to a set point change is presented together to better understand the cause of the response delay. The orange curve presents input from the primary controller and it is a set point for heat exchanger 1 and 2. It is limited to a maximum temperature of 60° C, due to the risk of damaging plastic reactor parts at higher temperature. The green curve presents the response of heat exchanger 2 (Peltier + 2 aluminum plates) which has its own characteristic time necessary to reach the set point mainly due to the mass of the two aluminum plates that required a certain time to heat up (see Figure 5.16).

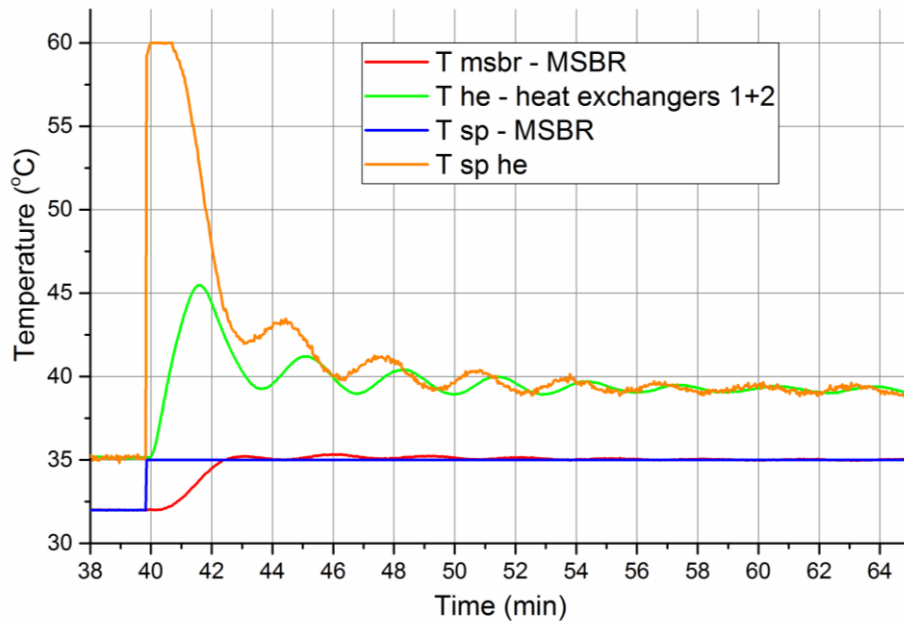


Figure 5.15. Temperature profile of heat exchangers and the MSBR during the set-point change from 32 to 35° C. When the set point for temperature in the MSBR was changed, also the set point for temperature of the heating element was changed due to the action of the cascade controller.  $T_{msbr}$  is the recorded temperature in the MSBR;  $T_{he}$  represents the recorded temperature of the heating element that is in direct contact with the heater in the MSBR;  $T_{sp}$  is the set point for the temperature in the MSBR;  $T_{sp\ he}$  is the set point for the temperature of the heating element.

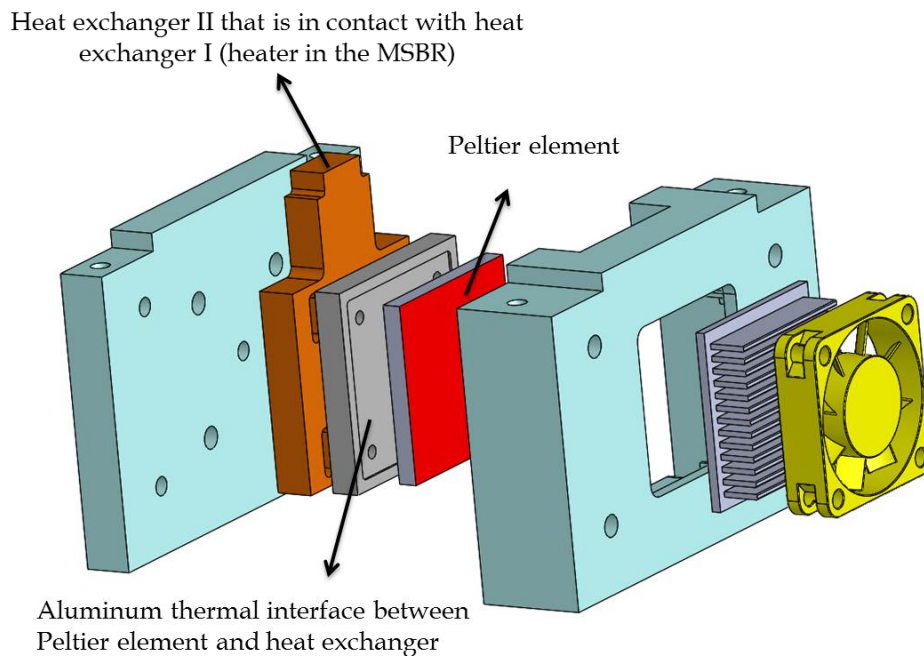


Figure 5.16. Heat exchanger II – 2 aluminium plates (orange and grey blocks) and Peltier element (red block) placed in plastic casing (two blue blocks) with heat sink (grey block with yellow fan)



In Figure 5.15, the reaction time of the heat exchanger 1 – heater in the MSBR is not visible and was obviously a major contributor to the dead time. When heat exchanger 2 changes temperature, it transfers that change to heat exchanger 1 that is in turn heating the MSBR chamber. Consequently, there is a certain time necessary to heat up the mass of aluminum elements in heat exchanger 1 and 2 which has an accumulating effect, and it is also the main reason for the dead time. For temperature control purposes in the MSBR, the effect of the dead time was not crucial since it didn't have a major influence on the stability of the cascade regulation. Moreover, process requirements didn't demand frequent changes of temperature. Also, the bioprocesses in the MSBR were not highly exothermic reactions where fast response would be necessary and crucial.

The robustness of cascade regulation was tested further by introduction of a disturbance in the temperature of the liquid in the MSBR. The result of this experiment presented in figure 5.17 where temperatures of the heat exchanger and the MSBR are showed with green and red curves, respectively.

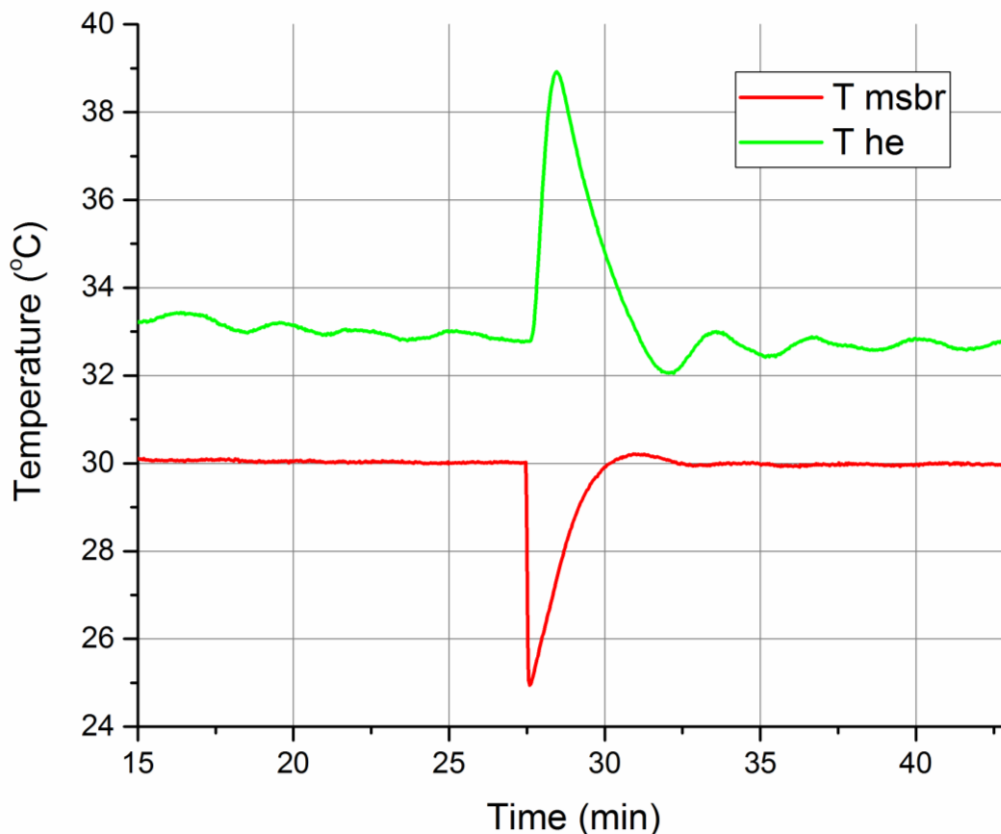


Figure 5.17. Cascade regulation response to introduction of a temperature disturbance in the MSBR. With introduction of the disturbance (cold water) in the MSBR, temperature of the liquid in the reactor dropped from 30 to 25°C. Consequently, the temperature of the heating element increased to compensate for the disturbance. T msbr is the recorded temperature in the MSBR; T he is the recorded temperature of the heating element that is in direct contact with the heater in the MSBR.

When cold liquid (4°C) was introduced in the MSBR (30°C), the temperature suddenly dropped and the perturbation peak was at 25°C. The recovery time was 2.8 min. The cascade regulation rejected the effect of the disturbance and returned the controlled variables back to the set point successfully.

### **5.3.2 Measurement of scattered light intensity (SLI) for biomass monitoring**

It is essential to obtain information about the most important process parameter, the biomass concentration, in real-time in order to follow cell growth and estimate the influence of different process conditions. The earlier described measurement principle for measurement of scattered light intensity (SLI) was tested, and first results showed that signal sensitivity and applicable measurement range depended on the strength of the LED light applied, which can be seen in Figure 5.18. The LED was powered by 10 mA, 30 mA and 50 mA current respectively. Measurements obtained at 50 mA showed low sensitivity at low cell densities, which appeared as a saturated signal, while measurements done at 10 mA indicated low sensitivity at higher cell density. Measurements performed at 30 mA had the broadest sensitivity, although 10 mA gave better sensitivity at very low cell concentrations. Consequently, in order to obtain the broadest range and increase the sensitivity at lower and higher biomass concentrations, it was decided to apply a 10 mA current at the beginning of the cultivation and later, after approximately 10h, the measurement was switched to 30 mA current to power the LED. At this point in the design, the switch between 10 and 30 mA was performed manually and the time point when the change happened was determined empirically from the experimental data obtained during active monitoring.

As can be seen in figure 5.18, the measured parameter that correlates with cell density is photodiode output voltage, expressed in volts and when this value is divided by the reference photodiode output voltage, also expressed in volts, the obtained dimensionless number represents the scattered light intensity characteristic for the MSBR. To avoid confusion, it is important to state that the scattered light intensity measured by the transfectance principle in the MSBR II called OD<sub>msbr</sub> doesn't follow the same measuring principle as the optical density (OD<sub>600</sub>) measured offline by a spectrophotometer. How OD<sub>msbr</sub> is obtained is presented in sections 5.2.12 and 4.2.5.

It is important to obtain a correlation between OD<sub>msbr</sub> and offline OD<sub>600</sub> and dry cell weight, such that in the near future OD<sub>600</sub> and dry cell weight can be used during the cultivation, calibration was necessary. Samples of different cell concentrations were measured in the MSBR and in the spectrophotometer at 600 nm and in addition cell dry weight was determined. Samples were diluted 20 or 40 times in order to be in the measurement range of the spectrophotometer, and the final OD<sub>600</sub> was obtained by multiplying the obtained number by the dilution factor. In this way the measurement of biomass concentration in the MSBR could be correlated with standard and typically performed offline methods for cell concentration determination.

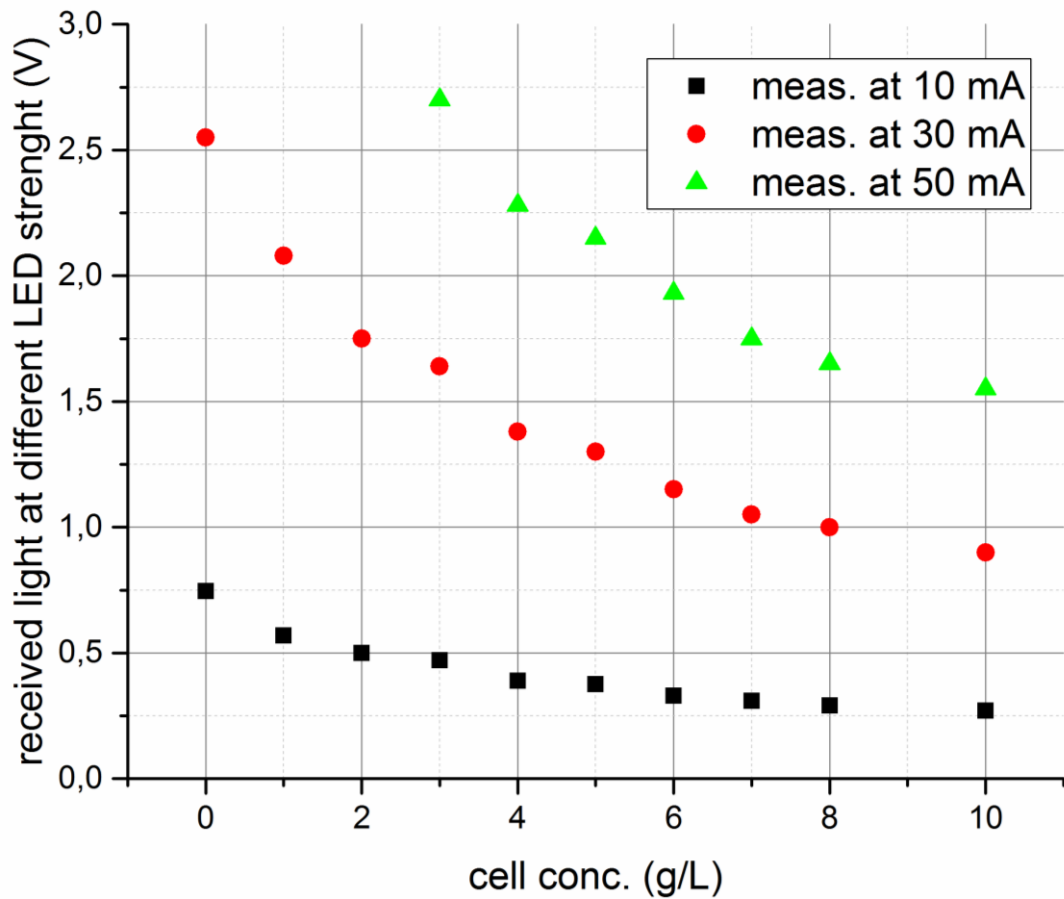


Figure 5.18. Influence of light intensity on measurement range and sensitivity of biomass concentration.

In the Figure 5.19, the correlation between optical density determined by the spectrophotometer at 600 nm (OD600) and the scattered light intensity determined in the MSBR (ODmsbr) is presented. An exponential function was used to fit the data and make a correlation between off-line and on-line measurements. Furthermore, a linear correlation with factor 2.8 was established for optical density measured by the spectrophotometer and cell dry weight, which is showed in Figure 5.20. Exponential function can be equally used to directly correlate the scattered light intensity determined in the MSBR (ODmsbr) and cell dry weight, which is depicted in Figure 5.21.

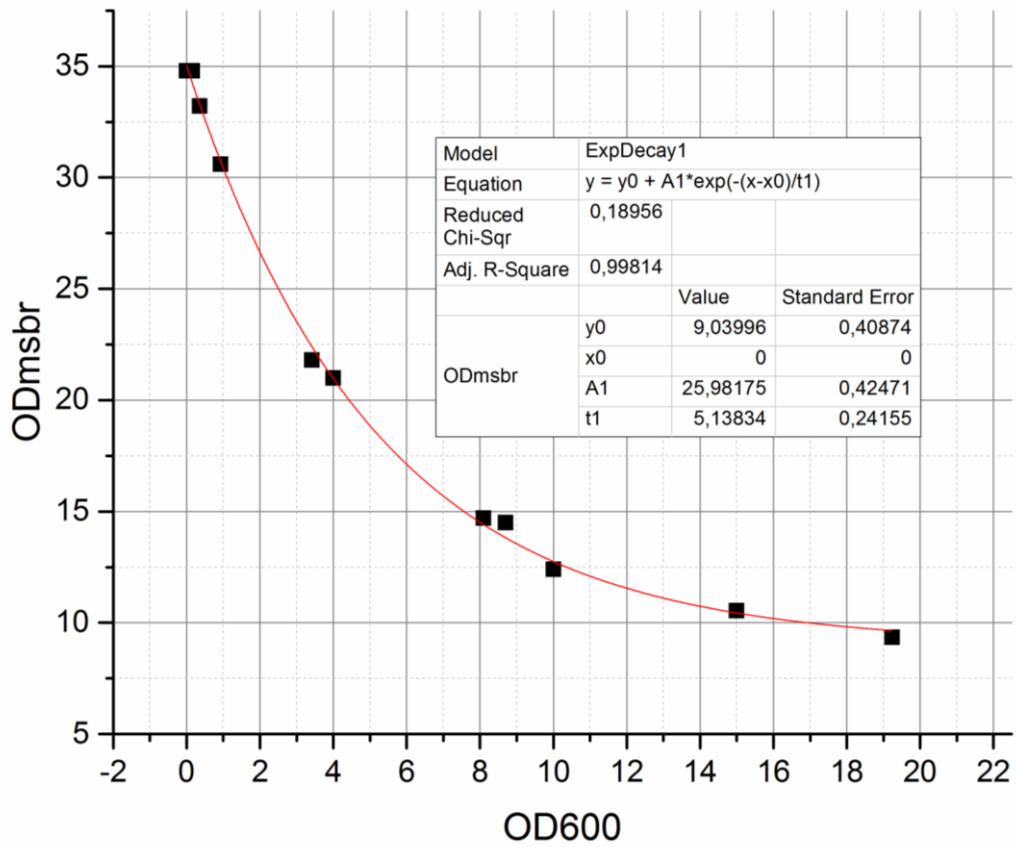


Figure 5.19. Exponential correlation between OD determined in the MSBR and by the spectrophotometer at 600 nm corrected for sample dilution.

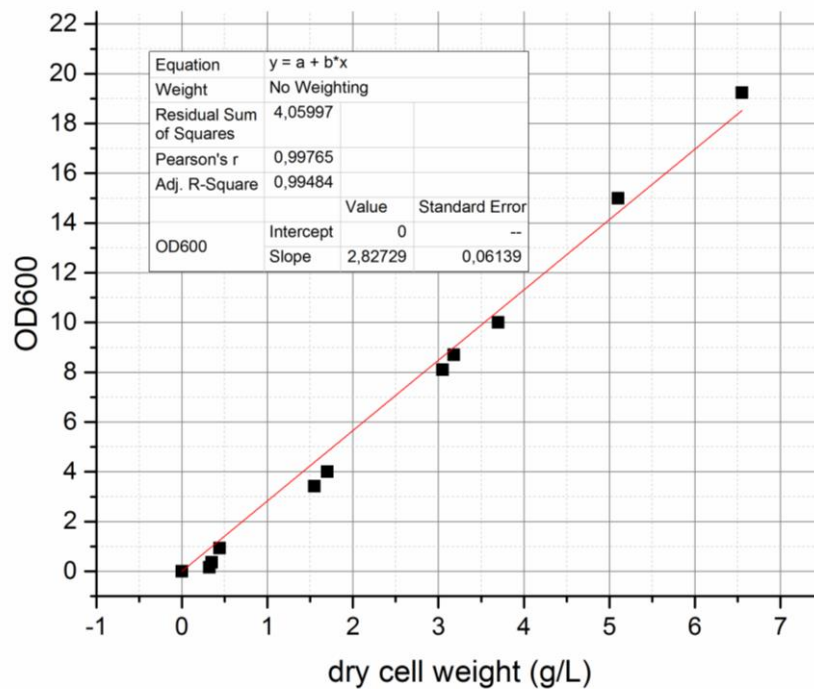


Figure 5.20. Linear correlation between OD determined by the spectrophotometer and cell dry weight.

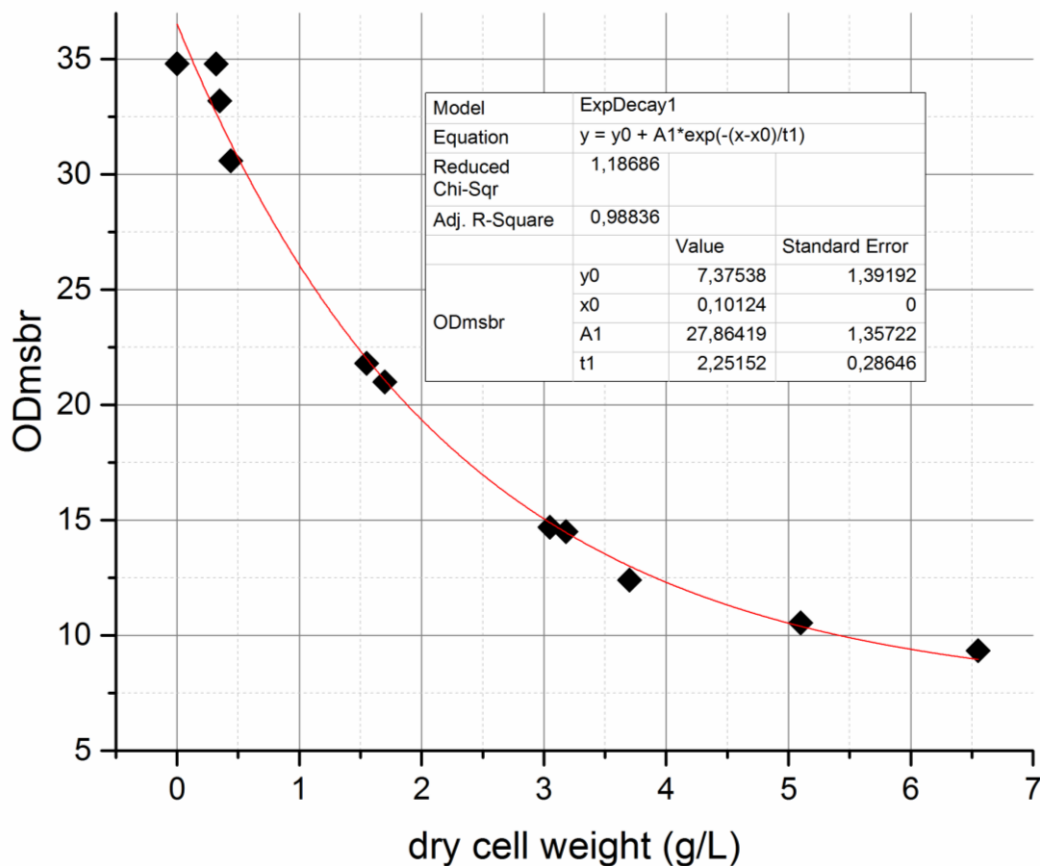


Figure 5.21. Exponential function used to establish a direct correlation between OD determined in the MSBR and dry cell weight.

The nature of the exponential dependence between OD measured in the MSBR and cell dry weight is not ideal since it shows that resolution and sensitivity of the measurement decline with the increase of the cell densities. Different light strengths didn't have impact on the exponential correlation and they displayed the same trend, which is depicted in Figures 5.18. There can be many reasons to explain why the OD calibration correlation is exponential in the MSBR II and linear in the MSBR I (figure 4.12). There are a few obvious differences between the two prototypes that can have a potential influence on the measurement principle. The optical fiber bundle and the mirror like surface are different in the two prototypes. In the first prototype aluminum tape was used as a reflector while here a highly polished stainless steel element had the role of a mirror, and thus the strength of the reflected light could be different. Furthermore, perhaps the most important difference between the two set-ups is in the distance, in other words, the light pathway length that includes different layers through which light has to pass in order to reach the sample. A comparison is presented in figure 5.22.

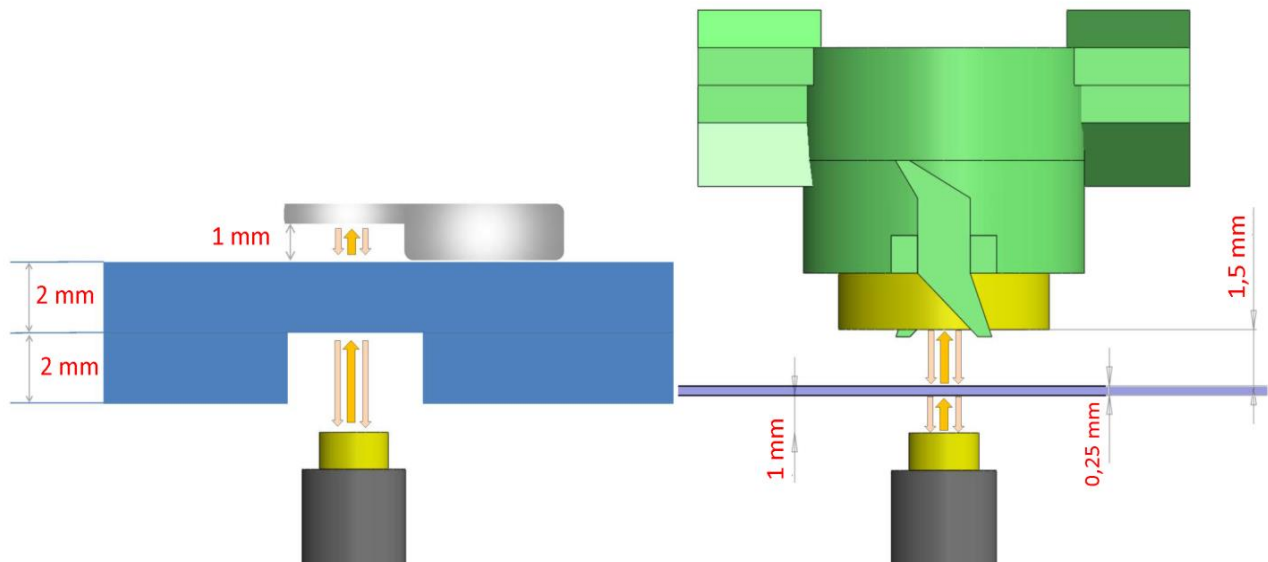


Figure 5.22. Light pathway in two prototypes: MSBR II (left) and MSBR I (right).

The overall distance for the light to travel in one direction, until the mirror like surface, is rather different: 2.75 mm (MSBR I) and 5 mm (MSBR II) respectively. Moreover, the light passes through a plastic plate that is substantially thicker in the prototype II (left picture in Figure 5.22). Finally, the light pathway throughout the sample is half a millimeter smaller in one direction for the MSBR II which in total gives 1 mm shorter path length for both directions.

In the original design of the second prototype the existence of another plate presented as the lower blue plate with an opening for light on the left-hand picture in Figure 5.22 was not planned. The optical fiber bundle was supposed to rest directly on the plastic plate; however the aluminum plate was added due to leakage problems and to give strength to the bottom part of the MSBR II. Consequently, shortening the length of the light pathway should be feasible with a slight modification in a future design by removing the aluminum plate and strengthening the plastic plate.

On-line monitoring of cell growth is convenient and gives an opportunity to follow the process in real time and to record each variation, which drastically reduces the labor intensity during cultivation e.g., taking samples every few hours. Likewise, it reduces the possibility that some important change during the cultivation would not be observed due to sampling intervals. Still, it should be kept in mind that optical density represents both live and dead cells, and initial effort has to be placed in establishing a calibration procedure for each cell type and strain since scattered light depends on the size and shape of cells. Shape may also change with growth conditions.

### 5.3.3 Mixing time

The second MSBR has a rather different configuration compared to the previous prototype featuring different stirrer geometry, and including a stainless steel element at the bioreactor bottom. Both elements have significant impact on the fluid behavior and mixing performance, so in order to evaluate these influences the mixing time was determined for different rotational speeds applied in the MSBR. The time necessary to observe a change of color from pink to transparent in the MSBR is established as the mixing time. This technique proved to be a good choice for small scale reactors where visual access is available, as it can display regions that are poorly mixed alongside expected information about mixing rate. Figure 5.23 demonstrates liquid behavior and disappearance of color as a function of time for a 200 rpm stirrer speed and using 2 mL working volume in the MSBR. Low stirring speed is chosen as an example, since the change of color is not instantaneous and it is easier to spot differently mixed zones in different parts of the MSBR. In Figure 5.23, addition of acid to the liquid surface can be observed in the upper left corner of the pink liquid at  $t = 0$  s where a slight change started to occur. Most of the liquid is rapidly mixed in the first few seconds. However, an area above the impeller blades along the shaft took a certain time to be properly mixed. Moreover, the main reason why mixing was not completed around 9 s was the small pink ring on the gas-liquid interface that was in contact with the bioreactor wall. It took more time for the ring to disappear than the time necessary for most of the bulk liquid to be mixed. One explanation for this behavior could maybe be found in the role of inlet/outlet channels that during cultivation would be actively used, but here they represented dead zones that could potentially increase overall mixing time. Another explanation could be related to surface tension on the wall being dominant over the shear forces produced by mixing.

To characterize overall mixing performance in the MBSR, other mixing speeds beside 200 rpm were tested as well. Results of extensive testing are presented in Figure 5.24. A working volume of 2 mL was chosen for this evaluation as a more challenging target than 1 mL volume, since the stirrer is relatively big and it would stir a small amount of liquid with ease, thereby yielding shorter mixing times than presented in Figure 5.24.

As expected, with an increase of mixing speed a decrease in mixing time resulted, from 17 s at 200 rpm to 1 s at 1000 rpm stirrer speed. At 600 rpm two experiments (marked with green and blue squares for 600 rpm in Figure 5.24) gave different values from the expected average time given by three other experiments. A longer mixing time (green square for 600 rpm in Figure 5.24) than average was assigned to effects of the inlet/outlet channels since color disappeared in the MSBR at the same time when it vanished in the channels. Another case of very short mixing time at 600 rpm (blue square for 600 rpm in Figure 5.24) is assigned to bubble formation around the shaft that acted as a gas-liquid interface at the impeller.

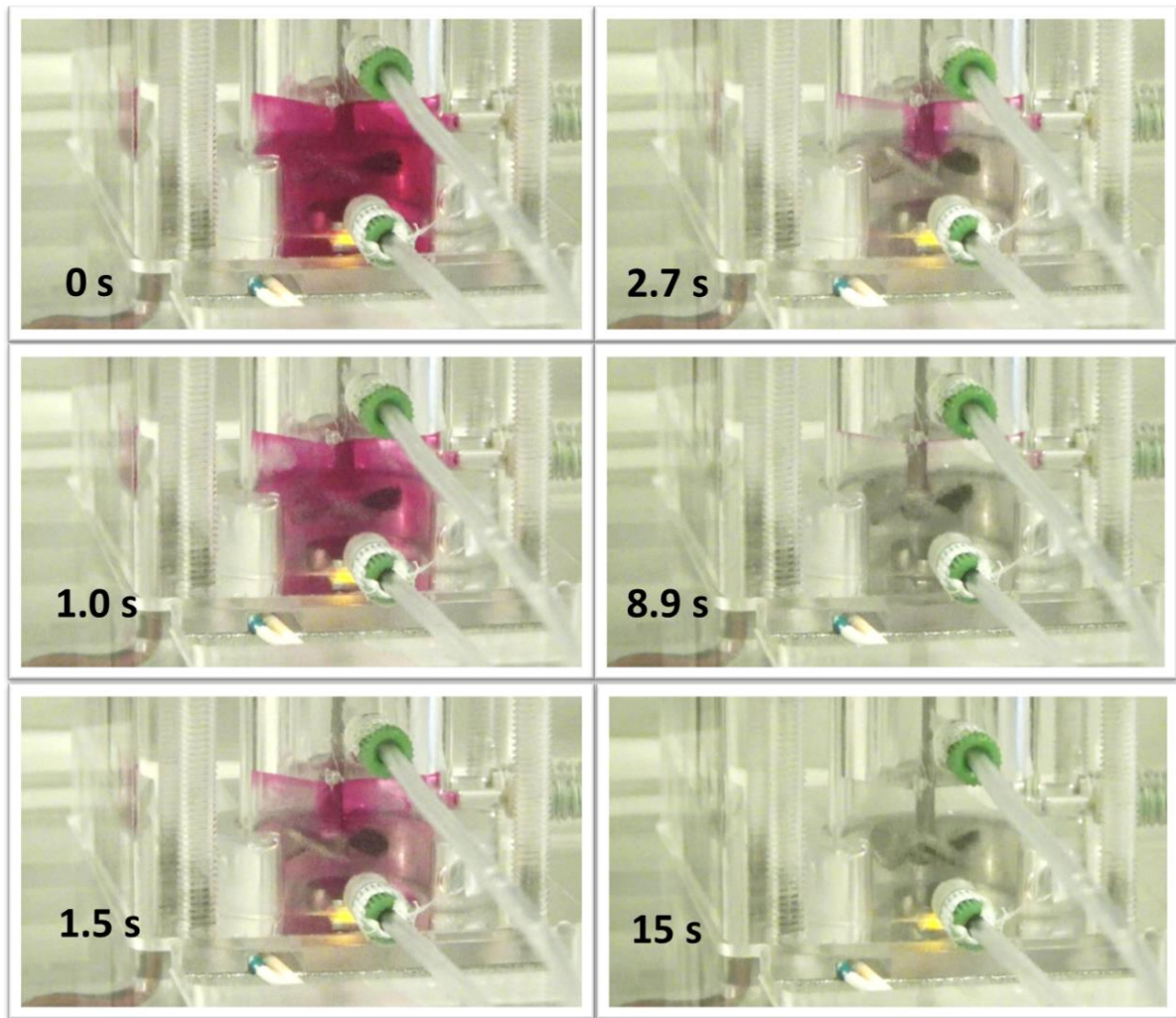


Figure 5.23. Determination of mixing time in the MSBR for an experiment with 200 rpm mixing speed.

This experiment demonstrated the effect of mixing the entire volume at two levels - in the upper and the lower part of the MSBR, which gave an idea to test two impellers and see how much the mixing time can be reduced by introduction of one more impeller on the shaft. A flat 3 - blade impeller was made by 3D printing and added to the shaft on a height that correspond to the gas-liquid interface at 2 mL working volume. It is assumed that the impeller position would also have a positive influence on the oxygen transfer rate by surface aeration besides improving the mixing time. The impeller position was adjustable and the impeller itself could be removed if needed. The effect of two impellers was tested at 200 rpm stirrer speed since this stirrer speed produced the longest mixing time. As expected, mixing time is reduced by more than 50% when an extra impeller is introduced; it went from 17 s to 7.5 s (presented in Figure 5.24 with the black arrow).



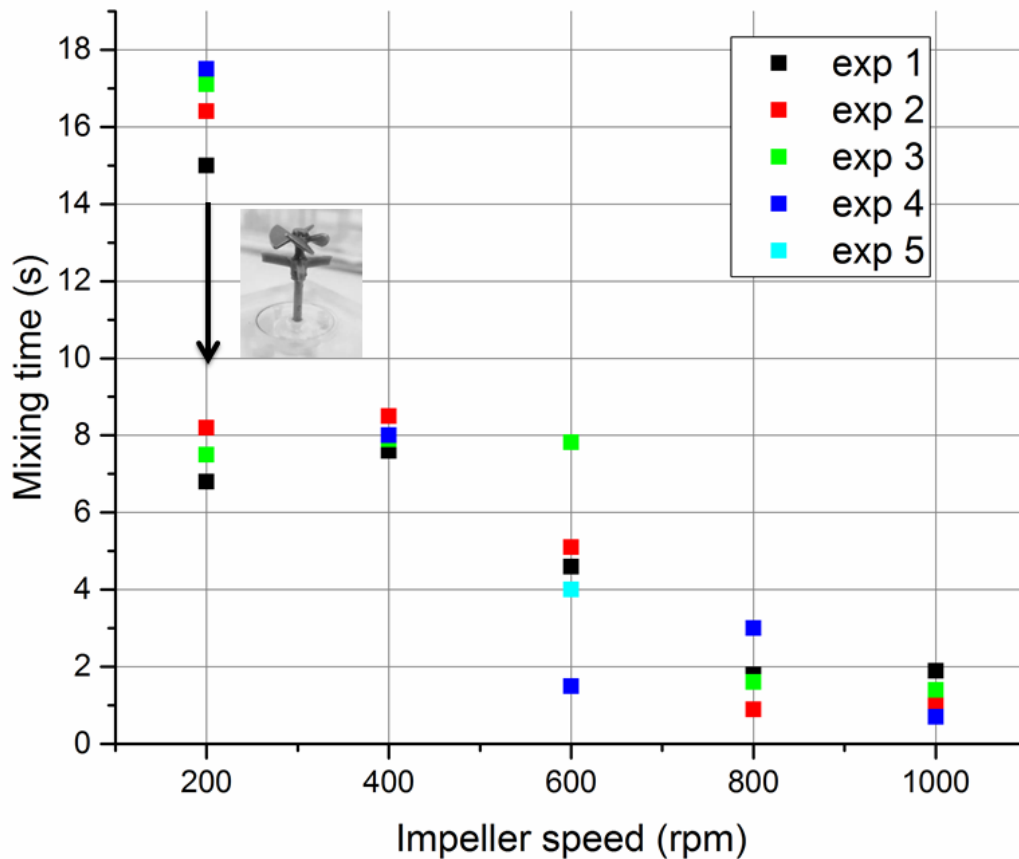


Figure 5.24. Mixing times at different mixing speeds in the MSBR (2 mL). For different stirring speeds 3 – 5 experiments were performed to determine mixing time in the MSBR. With increase of stirrer speed, mixing time decreased. Also, addition of another impeller to the existing one decreased the mixing time substantially which can for example be seen for the data obtained at 200 rpm stirring speed.

The above presented mixing times should not be taken as absolute values, but more as an indicator of the mixing efficiency and the mixing time range. Even though the color change method was good in many aspects, it is not the most exact testing method, since it depends on aspects related to how dispensing of acid is performed, and also how precise the analysis of the video is realized. Furthermore, the sensitivity of the method is reduced for increased rotational speed, which can be seen in Figure 5.24 where 800 and 1000 rpm have overlapping values for the achievable mixing time. With a further increase of the rotational speed, the accuracy of the results achieved by the method used here would probably be uncertain. Nevertheless, the mixing time range in the MSBR II is counted in seconds as it was the case with the prototype I (see Table 5.1) which is considered enough for an even distribution of nutrients, oxygen and heat, and for keeping cells in suspension for a longer time.

Mixing times are shorter in the MSBR I than in the MSBR II, which can be assigned to different volumes used during experiments and to a larger impeller in the MSBR I that had

impact on a larger portion of the liquid. Furthermore, inlet and outlet zones also had an impact on mixing time in the second prototype, while that was not the case with the first prototype.

Table 5.1. Mixing times for different stirrer speeds in prototype I and II.

	200 rpm	400 rpm	600rpm	800 rpm	1000 rpm
MSBR I (1 mL)	2.0 s	1.7 s	1.2 s	0.7 s	0.4 s
MSBR II (2 mL)	16.5 s (7.5 s)	8.0 s	4.6 s	1.8 s	1.2 s

It is difficult to compare two impellers and their mixing performance since geometries are very different in these two prototypes. Tip speed is often used as a parameter when impellers are compared over the different scales with the assumption that geometrical similarity exists between reactors. Tip speed is defined as  $\pi \cdot D \cdot N$  where D is impeller diameter (m) and N impeller speed (rps). This equation doesn't take impeller geometry into account so it has to be used with caution, only as approximation of a local condition within the impeller zone in case of the two impellers presented in this thesis. Tip speed for the impeller used in the MSBR I at 600 rpm is:

$$\text{Impeller tip speed (MSBR I)} = 3.14 \cdot 0.014 \text{ m} \cdot 10 \text{ (rps)} = 0.44 \text{ m/s}$$

and impeller speed of the prototype II, if it is based on the same tip speed 0.44 m/s, is:

$$0.44 \text{ m/s} = 3.14 \cdot 0.010 \text{ m} \cdot N; N = 0.44 / 0.0314 = 14 \text{ rps} = 840 \text{ rpm}$$

According to the tip speed calculation, an applied impeller speed of 600 rpm in the MSBR I corresponds to an impeller speed of 840 rpm in the MSBR II.

A much better way of comparing two different impeller designs would be based on fluid flow and power. However, these methods require experimental measurements which are often difficult to perform at milliliter scale [87] and were not performed in the frame of this thesis.

Similar mixing studies are performed in different microbioreactors where most of them have mixing times below 10 s. Schäpper et al. [57] tested chaotic mixing with a stirrer bar in 100  $\mu\text{L}$  microbioreactor at 500 rpm and obtained 1.2 s mixing time. Zhang et al. [33] presented experiments where it took 30 s to fully mix a 150  $\mu\text{L}$  microbioreactor with a 6 mm long magnetic bar at 180 rpm. Considering the calculated impeller tip speed for MSBR I at 600 rpm, it is interesting to see which impeller speed is needed in a 150  $\mu\text{L}$  microbioreactor to achieve the same tip speed:

$$0.44 \text{ m/s} = 3.14 \cdot 0.006 \text{ m} \cdot N; N = 0.44 / 0.019 = 23 \text{ rps} = 1401 \text{ rpm}$$

A mixing study in a 24-well plate miniature bioreactor with 3-4 mL working volume and orbital shaking showed that mixing below 500 rpm gave mixing times close to 100 s while at 500 rpm the mixing time was around 5 s and at 800 rpm around 1 s [48]. Nienow et al.

[87] did physical characterization of ambr bioreactors and they showed that mixing times for 13 and 15 mL volumes are below 10 s when the impeller speed was kept above 600 rpm. For 400 rpm and a fill volume of 15 mL it took 22 s to fully mix the liquid. The upper (air-liquid) interface of the bioreactor was defined as poorly mixed zone and the one that had a decisive effect on the mixing time [87].

### 5.3.4 The MSBR II platform hardware performance during continuous cultivations

To test and evaluate the MSBR performance and all the functions of the set-up, 12 continuous cultivations were performed. Simultaneously, the MSBR was also tested for its batch culture capability since the batch cultivations is an integral part of the continuous cultivation (the start up phase is a batch phase). Running cultivations in the new reactor involved troubleshooting, developing a standard operating procedure and fine-tuning the process parameters. From the 12 cultivations performed, one was without growth (due to presence of cleaning agent in the reactor), one was contaminated, one was stopped because the medium inlet tube protruded in the MSBR and prevented proper mixing and one was spilled after the batch part of the cultivation – when the pump needed to be connected. A summary of the problems and the potential solutions for the performed cultivations is presented in Table 5.2.

#### *Pump performance*

After performing the first two cultivations, it became clear that there was some problem with the pump, which eventually stopped working during cultivation number 5 (see appendix A, Figure 3). Therefore, the step motor used in the pump (described in section 5.2.3) was exchanged with a more powerful one and the issue was resolved.

As described earlier in section 5.2.3, the idea of continuous pumping can be established by introduction of one way valves in connection with the pump. This concept proved to be good, worked well and it was applicable in combination with the pump used for supplying gas. However, the use of one way valves for liquids containing medium and cells was somewhat problematic.

Table 5.2. Summary of problems that occurred and solutions that were implemented during cultivations in the MSBR

Number of Cultivation	Problem	Solution
Cultivation 1	Cultivation attempt failed.	N/A

<b>Cultivation 2</b>	In continuous mode the cultivation inlet flow rate was very low due to the strength of the motor in the pump and wrong settings in LabView.	Settings were changed but the problem with the pump was noticed in later cultivations.
<b>Cultivation 3</b>	The entire batch was spilled during attempt to connect pump to the MSBR.	Inlet and outlet tubes from the pump were attached to the MSBR before the inoculation step.
<b>Cultivation 4</b>	No growth, due to presence of cleaning agent residue (chlorhexidine gluconate) in the MSBR.	Change to 70 % ethanol from a commercial mixture of chlorhexidine gluconate and ethanol used in the lab.
<b>Cultivation 5</b>	Motor of the pump stopped working.	The step motor used in the pump was replaced with a stronger motor.
<b>Cultivation 6</b>	Cultivation attempt failed.	N/A
<b>Cultivation 7</b>	Water droplets were introduced to the MSBR from the humidifier because the gas inlet was too low and therefore allowing entering liquid directly in the MSBR. The volume of medium for continuous mode cultivation was limited by the pump syringe size and lack of possibility to continuously pump back and forth.	Inlet of gas was moved to the upper part of the MSBR entering the headspace, not the liquid phase. Syringe holders on the pump were slightly modified to accommodate bigger size syringes and allow longer cultivation time.
<b>Cultivation 8</b>	Temperature sensor was incorrectly attached (loose wire) to the power supply, so overall temperature during cultivation was 35°C.	Temperature sensor was fixed and verified that it is responsive and measuring correct values.
<b>Cultivation 9</b>	Cultivation was contaminated and SLI measurement displayed a lot of noise.	The MSBR was thoroughly cleaned. Furthermore, an eppendorf tube was introduced in the gas line between the humidifier and the MSBR as a condensate collector.
<b>Cultivation 10</b>	Steady state during cultivation was obtained at higher cell concentration than one would expect.	Inlet and outlet tubes were adjusted so to emphasize flows in the right direction from and toward pumps (by gravity), especially the outlet of the MSBR that was used for medium with cells.
<b>Cultivation 11</b>	Inlet tube for medium went in the MSBR and interrupted stirrer rotation.	When the MSBR was assembled for the next run, special attention was paid to the tubing position in the wall of the MSBR.
<b>Cultivation 12</b>	Not able to establish steady state in 55 h.	Inner diameter of the outlet tube from the MSBR and its branching to two syringes could be potential bottlenecks.

The valve was at some point not able to close properly due to buildup of cells and it created a bottleneck, thus the pump for liquid pumping was used in push/pull working mode with two syringes from each side.

The size of the syringes applied was 5 mL which gave 10 mL of medium in total for continuous cultivation. As a result, it was possible to exchange about 6 reactor volumes

during continuous cultivation since the working volume of the MSBR was 1.5 mL. In cultivation number 7 this was demonstrated, as well as a need for more medium that can then provide a longer cultivation time and an increased number of exchanged volumes (see appendix A, Figure 4). To be able to do that, the holders on the syringe pump were modified so they could accommodate bigger syringes. The latter made it possible to use 12 mL volume syringes.

### *Aeration performance*

As explained before in section 5.2.4, the gas inlet was positioned at the same level as the inlet of medium in the MSBR, and thus air was directly sparged in the broth and distributed by the stirrer. This raised the liquid up to the gas outlet, especially when foaming was occurring simultaneously. Consequently, a pressure would build up until the point when it was possible to push liquid further through the tube. This produced uneven flow, instability in the system and difficulty in maintaining a constant level of liquid. As a result, a slight modification of the MSBR was introduced where the gas inlet was closed and the gas outlet was used as inlet instead. The new gas outlet is made and located in the top plate of the reactor. In this way, air passed through the headspace instead of throughout the liquid phase enabling only surface aeration.

### *Mixing performance*

As a result of previously mentioned modifications from sparging to surface aeration, mixing had the most obvious impact on the amount of oxygen being dissolved in the liquid and made available to the cells. During cultivations when the dissolved oxygen dropped substantially, a change of the stirrer speed to higher values resulted in an increased dissolved oxygen level. On the other hand, introduction of a higher gas flow rate didn't have a noticeable effect on the dissolved oxygen concentration; it only increased the evaporation rate.

Mixing performance was steady and robust, yet flexible. It was effortless to switch from one- to bi-directional mixing, or to change stirrer speed according to the needs. Based on visual inspection and the SLI measurement results, it was concluded that the stirrer was able to keep cells in suspension and did not allow cell settling on the reactor bottom.

### *Humidifier performance*

Considering that a continuous cultivation lasts a long time, and that the applied dilution rate is dependent on the constant working volume in the MSBR, it was crucial to prevent

evaporation by passing air through a humidifier before entering to the MSBR. The humidifier was an effective solution in preventing evaporation, but then again it required fine-tuning. When the temperature of the water in the humidifier was 35°C and the applied tubing between the MSBR and the humidifier had a small inner diameter and was about 20 - 30 cm in length without thermal insulation, condensation occurred in the tube due to the surrounding, lower room temperature. Therefore, air would push the collected water in the tube to the MSBR and influence the working volume. This can be seen on the curves presenting dry cell weight results in the first seven cultivations where the line is not smooth but has small step changes. To solve this issue, the temperature of the humidifier was decreased to 33°C, and a tube with a larger diameter but shorter length was used to reduce the surface on which the condensation can occur and to provide more space inside the tube for condensate to slide back to the humidifier instead of being pushed forward by air. Furthermore, foam is used around the tube for thermal insulation. A final improvement was the introduction of a water collector – an eppendorf tube between the humidifier and the MSBR, which was a kind of a guarantee that if condensate is created and it is passed through the tube, there was a place where it would be collected before reaching the MSBR. Results of this improvement could be seen in the cultivations 10 and 12 (see appendix A, Figures 7 and 8) where the measurement of biomass concentration is smooth without step changes.

#### *Temperature sensing and control performance*

Temperature measurement and control worked fine during all cultivations except cultivation 8 (see appendix A, Figure 5), where the temperature sensor was connected incorrectly with the power supply, so the cultivation was performed at 35°C, which gave suboptimal cell growth as could be expected.

#### *The scattered light intensity (SLI) sensing performance*

On-line measurement of the scattered light intensity was stable and reproducible in most of the cultivations. During cultivation number 9, the on-line measured signal displayed considerable noise and the data were heavily influenced by this phenomenon. The cultivation was contaminated and that could be a partial reason for the considerable noise in the SLI measurement. Another reason for such a suboptimal measurement was due to the disrupted connection with the data acquisition card. Otherwise, the SLI measurement was quite robust towards the relatively aggressive environment in the MSBR II where the presence of bubbles and higher stirrer speeds produced considerable noise. At mixing speeds above 1000 rpm, the noise during the measurement is increased in such a way that

the curve for biomass concentration displays a certain band instead of a line (demonstrated in cultivation 10 and 12, appendix A, Figure 7 and 8). However, on the positive side, the data and the information level are still not compromised. In cultivation 12, the influence of bubble formation in the slit, where the scattered light intensity measurement occurs, was displayed during the continuous part of the cultivation with an interruption in the measurement for certain periods of time.

Eventually, each part of the MSBR II platform performed satisfactory without major issues, yet the results of the continuous cultivation were not as expected. A more detailed discussion of these cultivation results is presented in the next section.

### **5.3.5 Initial batch phase of the cultivations in the MSBR II (first part of the continuous cultivation)**

Each continuous cultivation started with a batch phase to allow the biomass concentration to build up to a certain concentration, before switching to continuous operation. Results of the batch phases are discussed separately in this section.

The glucose concentration in the continuous mode of cultivation was 5 g/L. A higher glucose concentration (20 g/L) was used during the initial batch phase to increase the biomass concentration and prevent washout as well as a delayed steady state upon switch to continuous mode. Apart from the first cultivation where the starting pH was 4.4, all the other cultivations were operated with a starting pH of 5.6. As pH sensing and control was not established, the end point pH (after continuous cultivation mode) was measured and it was around 3.2. Temperature was kept constant and stirrer speed was changed to keep the dissolved oxygen concentration above 15% (manually). The working volume was 1.5 mL for all cultivations.

The initial batch phase of the cultivations and the corresponding characteristic growth profile of *Saccharomyces cerevisiae* is presented in Figure 5.25 using data from cultivation 12, the one that was performed last. The initial optical density was 0.1 for all cultivations, and the lag phase ranged from 3 to 5 hours. Only the first two cultivations had a lag phase around 10 and 7h, respectively. Effort was placed on following the same procedure for inoculum preparation; however the age of the agar plate from where cells were taken from for inoculation as well as irregular mixing in culture tubes could influence the state of the cells in the preculture and consequently the inoculum. This could be a reason for the different lag phases observed during different cultivations.

As is expected, *S. cerevisiae* had two growth phases, first on glucose and then on the ethanol that was produced during the first growth phase. The growth rate on glucose was 0.46 h<sup>-1</sup> and as anticipated it was higher than the growth rate on ethanol, which was calculated to be 0.07 h<sup>-1</sup>. The diauxic shift occurred after 13 h of cultivation and the lag

period lasted around 3 hours, where cells were adapting to utilization of a different carbon source. During both growth stages biomass was produced and oxygen was consumed accordingly. Close to the end of the growth phase on glucose, the dissolved oxygen concentration dropped to around 35 % air saturation, while the mixing speed was kept constant at 500 rpm. The mixing speed was kept constant first 18 h with the purpose of observing oxygen consumption during growth on glucose and during the lag phase produced by the diauxic shift, and also to see if the mixing and aeration in the MSBR could support and satisfy the oxygen requirements of the cultivation. During the diauxic shift DO concentration increased to approximately 50 - 60 % air saturation. Around 18 h, mixing speed was increased up to 1000 rpm in the course of few hours and it was kept 1000 rpm until end of cultivation in order to keep DO concentration above 20%.

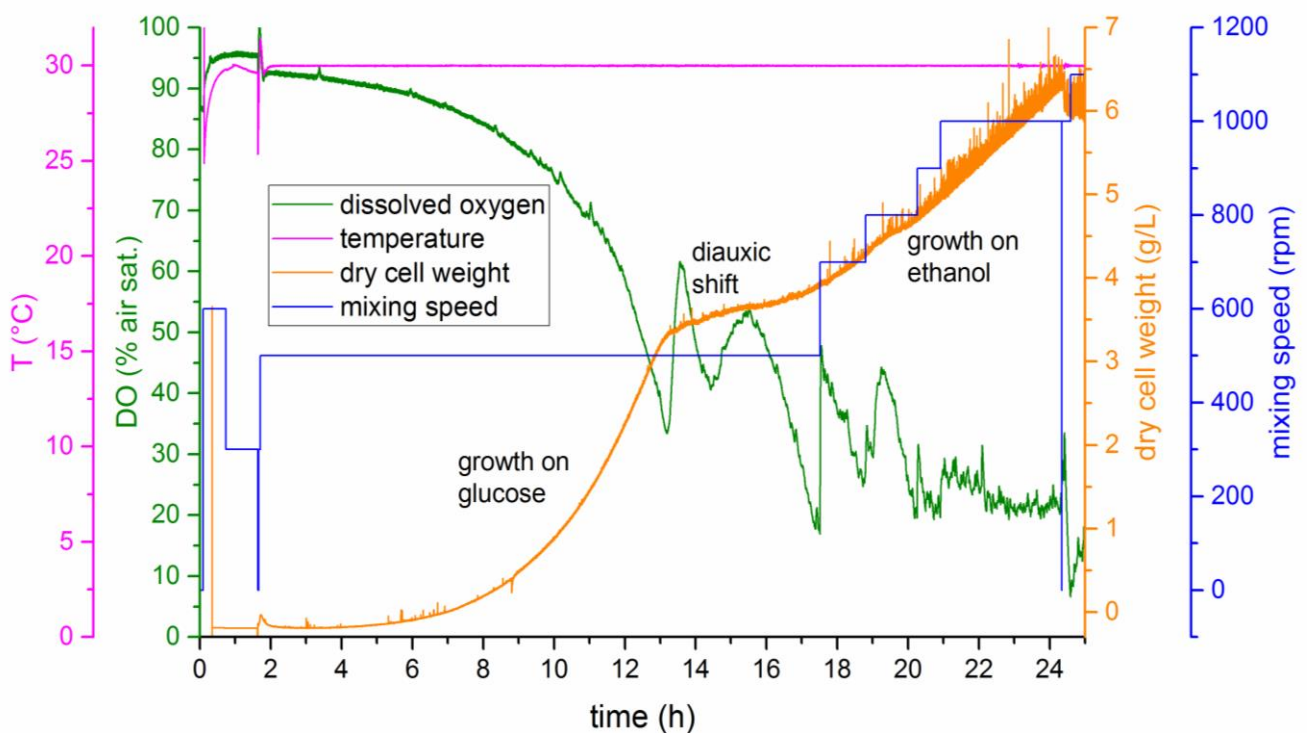


Figure 5.25. Batch phase of the last cultivation performed with *Saccharomyces cerevisiae*.

The change of mixing speed was performed manually, when drop in DO concentration was observed. Figure 5.25 also shows that the increase of the mixing speed increased the noise in the biomass density measurement. Mixing in the MSBR is limited to 1200 rpm with the notion that higher mixing speeds are not necessary. However, it would have been interesting to observe if the noise in the measuring signal of the biomass density would increase proportionally with a further increase of the stirrer speed, and also what would be the effect on the dissolved oxygen concentration of such a further increase.

One very important aspect of running cultivations in the MSBR is reproducibility, which creates trust in the performance of the entire MSBR platform. Figure 5.26 presents the



measurement of dry cell weight during batch mode in three different cultivations performed under similar conditions in the MSBR.

Three cultivations with *S. cerevisiae* displayed similar growth rates on glucose and ethanol, which is depicted graphically in Figure 5.26 and numerically in Table 5.3. Also, the length of the diauxic shift was about the same for each cultivation, and started after 13 h of cultivation in Figure 5.26. Considering that the small working volume is vigorously mixed in the MSBR II, there was an uncertainty regarding the repeatability of the growth rates on ethanol in different cultivations, due to potential evaporation. Ethanol evaporation, if present, is rather similar between batches according to similar slopes on cultivation curves in Figure 5.26 and similar growth rates on ethanol presented in Table 5.3. However, the relative standard deviation (see Table 5.3) shows that growth on glucose has less variation compared to growth on ethanol.

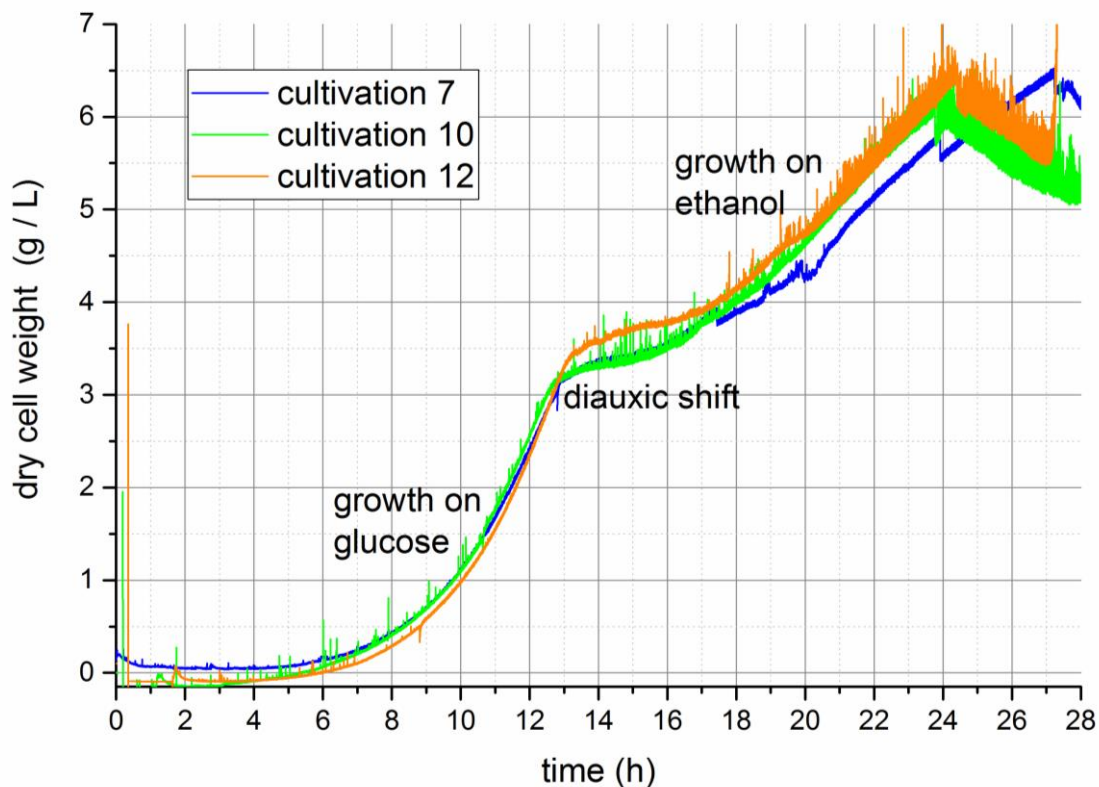


Figure 5.26. Initial batch phase of three different cultivations with *Saccharomyces cerevisiae*.

It is worth mentioning that in order to have reproducible cultivations, a rather complex system of wires, electronics, tubing, signals, optical fiber bundles on the one side and a reactor with mixing and sensors, a humidifier and pumps on the other side need to work in unity to produce and maintain the same conditions for a long time. It can be concluded from the batch phase results that the MSBR II platform can sustain reproducible growth of *S. cerevisiae* during batch cultivation with 0.56% variation in growth rate for glucose and

11% variation in growth rate for ethanol. The three presented cultivations were among the last performed cultivations where technical issues were reduced substantially, so with further improvements of the platform e.g., evaporation reduced by fine tuning of temperature in the humidifier and better tubing insulation, the relative standard deviation for ethanol growth rate could potentially be reduced.

Table 5.3. Growth rate comparison between three different cultivations.

	$\mu_{\text{glucose}} [\text{h}^{-1}]$	$\mu_{\text{ethanol}} [\text{h}^{-1}]$
<b>Cultivation 7</b>	0.471	0.061
<b>Cultivation 10</b>	0.470	0.071
<b>Cultivation 12</b>	0.466	0.076
<b>Relative standard deviation</b>	0.56 %	11.02%

### 5.3.6 Continuous mode of cultivation in the MSBR II

The final test for the MSBR II platform design was the evaluation of the performance of continuous cultivations. The continuous mode of operation started ca. after 25 h of batch mode, when substrate almost was used up, by activating the pump for the medium. After the first few experiments, it was clear that inlet and outlet tubes needed to be connected to the MSBR from the beginning of the cultivation to avoid spill of broth during connection. This introduced two potential issues:

- A concern existed that broth could come out through the outlet tube ( $D = 1 \text{ mm}$ ) during batch mode operation since the tube was not closed, but attached to the syringe pump.
  - ✓ This was prevented by slightly bending the tube upward close to the inlet connection in the MSBR. Also, the tube opening was not too large so liquid could not easily leave the reactor. A certain pressure was necessary for that to happen.
- The start-up behavior of the syringe pump could influence the amount of medium and the time when the medium is delivered to the MSBR if priming is not performed, which is normally required to start up the pump and flash the tube to displace air and fill it with medium. Usually, one line is open for priming, which increases the chance for contamination.

- ✓ Pump and tubing are primed just before continuous mode was employed by starting the pump at high flow rate and filling up the inlet tubing with medium until the entrance point to the MSBR. During that time, the other set of syringes attached to the outlet tube were kept unfastened, and thus liquid from the MSBR was not pumped out. Afterwards, the flow rate was changed to fit the required dilution rate and the pump was started again. In this way the beginning of the continuous mode was defined.

The continuous mode of cultivation in the MSBR II was tested at a dilution rate of  $0.15 \text{ h}^{-1}$ ,  $0.2 \text{ h}^{-1}$  and  $0.3 \text{ h}^{-1}$  with  $5 \text{ g/L}$  of glucose in the feed medium. The results of three different continuous cultivations are presented in Figure 5.27.

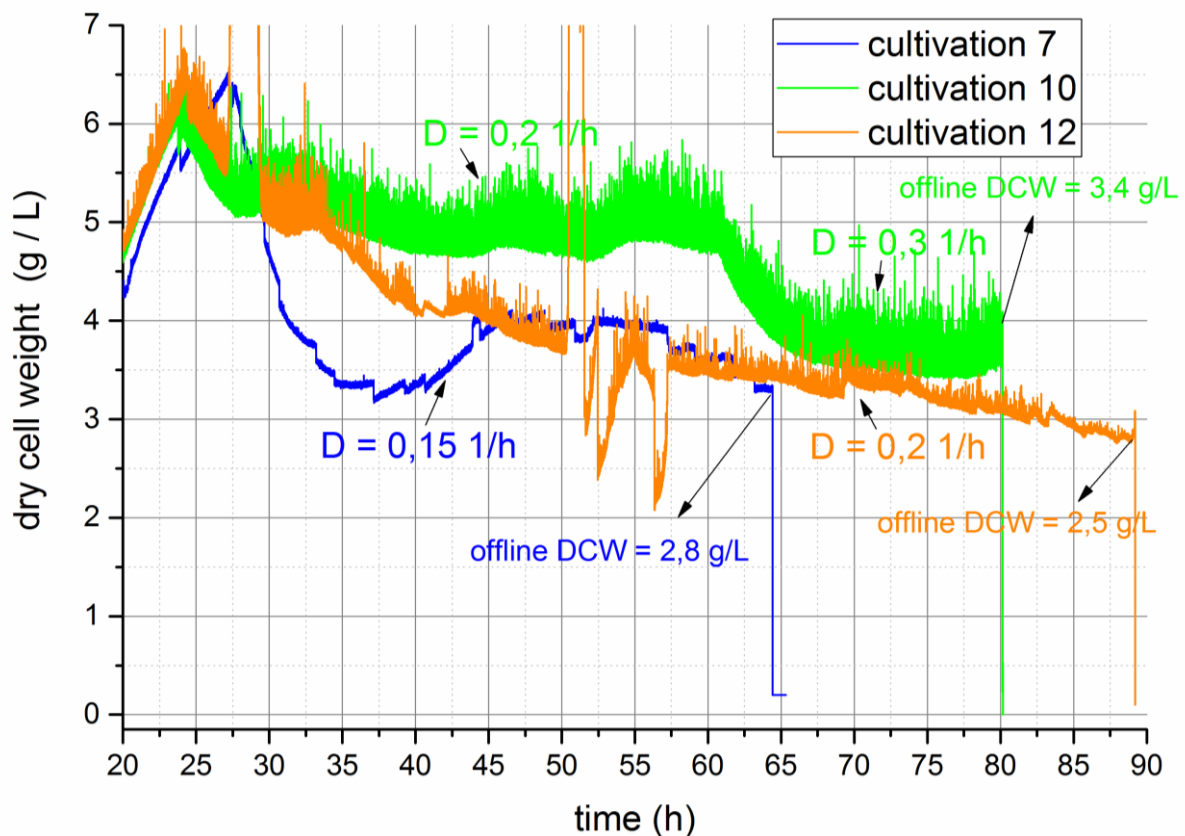


Figure 5.27. Continuous mode MSBR operation for three different cultivations with *Saccharomyces cerevisiae*.

A decrease of the cell concentration occurred after the feeding pump was started as was expected. However, the cell concentration did not reach the expected values in all three presented cultivations, even after 14 exchanged volumes. A quasi-steady state was established in cultivation 7 and 10, while a steady decline of the cell concentration was observed during cultivation 12.

In order to understand and predict which concentrations of biomass and substrate are expected in the reactor, a mass balance for the continuous mode of operation needs to be solved. A mass balance of a component can be written in a general way as:

$$\text{Change} = \text{Input} - \text{Output} + \text{Reaction} \quad [5.1]$$

If this expression is applied to the biomass concentration  $X$  in the reactor, the mass balance can be written as:

$$\frac{d(VX)}{dt} = F_i X_i - F_o X + V r_x \quad [5.2]$$

where  $V$  is volume [mL],  $F$  is flow [mL/min],  $X$  is biomass concentration [g/L] and  $r_x$  volumetric reaction rate [ $\text{kg m}^{-3} \text{h}^{-1}$ ]. For continuous cultivation at steady state:  $dX/dt = 0$ ;  $V = \text{const}$ ;  $F_i = F_o = F$ ;  $X_i = 0$ ;  $r_x = \mu X$  (volumetric reaction rate expressed as product of biomass concentration and specific reaction rate [ $\text{kg kg biomass}^{-1} \text{h}^{-1}$ ]) the previous equation is transformed in:

$$0 = \frac{F}{V}(0 - X) + \mu X$$

And if we consider  $F/V=D$ :

$$DX = \mu X \rightarrow D = \mu$$

When steady state is achieved during continuous cultivation, the dilution rate equals the specific growth rate.

If equation [5.1] is written for substrate instead of biomass we obtain:

$$\frac{d(VS)}{dt} = F_i S_i - F_o S - V r_s \quad [5.3]$$

where  $S$  is substrate concentration [g/L] and  $r_s$  is the volumetric reaction rate [ $\text{kg m}^{-3} \text{h}^{-1}$ ]. For continuous cultivation with 5 g/L glucose as substrate at steady state  $dS/dt = 0$ ;  $V = \text{const}$ ;  $F_i = F_o = F$ ;  $S_i = 5 \text{ g/L}$ ;  $r_s = q_s X$  and  $\mu = q_s Y_{x/s}$ ;  $Y_{x/s} = 0.5$ ; the previous equation is transformed in:

$$0 = D(S_i - 0) - \frac{D}{Y_{x/s}} X = 0.2 \cdot 5 - \frac{0.2}{0.5} \cdot X \rightarrow X = 2.5 \text{ g/L}$$

Based on the above calculation and assumptions, it is expected that 2.5 g/L of biomass is formed when 5 g/L of glucose is used as substrate during fully respiratory conditions of continuous cultivation. For cultivation 10 where the dilution was  $0.3 \text{ h}^{-1}$ , the biomass concentration was expected to be lower due to respiratory-fermentative condition. This is not the case for the cultivations presented in Figure 5.27.

Cultivation 7 was performed with 5 mL syringes (10 mL volume in total) which limited the length of the continuous cultivation to 65 h, while during the other two cultivations 12 mL syringes (22 mL feed in total) were used which increased the cultivation time to 90 h.

According to the data presented in Figure 5.27 there are two problems:

- Reaching steady state at much higher cell concentrations (around 5 g/L) than expected (max 2.5 g/L according to the calculation) based on the glucose concentration in the medium (5 g/L) that is continuously pumped in the reactor at a dilution rate of 0.2 h<sup>-1</sup> for cultivation 7 and 10.
- Not reaching steady state – cultivation 12.

The first bullet point immediately raises a question of calibration accuracy. On the other hand, off-line dry cell weight also confirmed that there were more cells in the MSBR than there were supposed to be. HPLC analysis of the medium for batch and continuous mode was performed and it was confirmed that there was 21 g/L in medium for batch mode and 5 g/L of glucose in the medium for continuous mode. Furthermore, when cultivation 10 was finished, the broth was centrifuged and the supernatant was analyzed by HPLC to determine the concentration of glucose and ethanol. As expected, there was hardly any presence of glucose in the supernatant. However, there was approximately 100 mmol (4.6 g/L) of ethanol measured by HPLC. With a dilution rate of 0.3 h<sup>-1</sup> (see Figure 5.27, cultivation 10), it was expected to find ethanol at the end of cultivation, but not in such a high concentration. Considering that the end of the outlet tube for the gas was submerged in a beaker with ethanol to prevent possible contamination, it could be that somehow ethanol came to the MSBR through the gas outlet. Another possibility could be that ethanol was present in the humidifier since it was used in the cleaning procedure of the equipment.

Beside calibration accuracy, a concentration gradient in the feed medium due to lack of mixing was also considered as a potential cause for the observations, since the medium was stored for up to 60 h in the syringes during the continuous cultivation. Precipitation in the medium was not observed by visual inspection at any point and if there was a glucose concentration gradient it should be reflected in the biomass measurement as well, which is not the case.

Achieving a constant dilution rate is very much dependent on the ability to keep a constant volume in the MSBR, so the evaporation could be an important issue that is interfering with the objective of providing constant conditions during continuous cultivation. During 90 h of cultivation, the working volume in the MSBR decreased from 1.5 mL to 1.3 mL resulting in about 13 % liquid loss due to evaporation, and consequently the dilution rate could slowly change from 0.20 h<sup>-1</sup> to 0.23 h<sup>-1</sup> if the evaporation rate was the same over the cultivation time.

Another possibility is that cells are retained in the MSBR due to the small inner diameter of the opening on the wall of the MSBR and its position. Furthermore, it could be that the presence of cells influences the flow in the outlet stream by partially clogging the way to the syringes due to the existence of a Y connector.

In cultivation 12 it seems that the expected cell concentration is only reached after 90 h and if the cultivation lasted longer perhaps a steady state would be established at a certain

point. Still, the question is why it took so much time for cells to be properly influenced by the applied dilution rate. Normally, as a rule of thumb, one assumes that steady state is reached after about 5 residence times have passed, i.e. after 25 hours for  $D = 0.2 \text{ h}^{-1}$ . Further work with continuous cultivations in the MSBR with additional improvements regarding tubing, connections and choice of syringe size can probably provide an answer and solve this issue.

To sum up, a number of continuous cultivations with *Saccharomyces cerevisiae* were performed in the MSBR II with limited success. Compared to Prototype I, the evaporation issue was considerably reduced; still there is space for further improvement. Moreover, addition of DO control as well as pH sensing and control can contribute to maintaining of reproducible and stable process conditions.

Based on the results from batch mode cultivations, it is possible to conclude that one can perform consistent batch cultivations in the MSBR II. Furthermore, fed-batch cultivation should be feasible as well since there is a medium feed pump in place. The starting working volume could be 0.5 mL and it could increase up to 2 mL, for example. The dissolved oxygen concentration would be the limiting factor at a certain point, determining the highest biomass concentration possible in the MSBR II. Establishing steady state in continuous cultivations proved to be rather problematic and challenging. It requires further investigation in defining the bottlenecks and making further improvements on the current MSBR II platform.

## 5.4 Conclusion

The second prototype of the milliliter scale bioreactor together with a pump and humidifier presents a compact yet flexible design providing:

- More standardized performance due to better design solutions.
- Robust temperature sensing and control.
- On-line measurement of the scattered light intensity is more consistent and repeatable since the distance between the optical fiber bundle and the mirror is constant. However the correlation between the scattered light intensity measured in the reactor and the cell dry weight has a more complex correlation than the one obtained in the previous prototype.
- Good one- and bi- directional mixing, no need for baffles. A smaller stirrer with flexible design is used - including the possibility for add-ons, closer to standard performing mixers.
- Adjustable working volume (1 - 2 mL).

- Ability to control gas supply to the MSBR by low flow rates due to the specifically designed pump.
- Continuous cultivation possible due to the existence of pumps and humidifier.

Considering that continuous cultivations are performed with problems related to achieving steady state, there are certain parts of the platform that didn't show satisfactory performance:

- Due to low flow applied during continuous cultivation, cell accumulation occurred at the outlet of the MSBR and at certain points along tubes and connectors where gravity didn't have major influence.
- Evaporation and condensation still occurred during cultivations although they were less pronounced than in the first prototype. They influenced air flow, OD measurement and liquid level.
- Scattered light intensity measurement was performed with a new bifurcated optical fiber bundle which has 61 fibers, while the optical fiber used for reference measurement was the same as in the previous set-up. This setting produces uneven signal strength.
- Increased distance between optical probes and sensors due to addition of an aluminum plate decreased measurement sensitivity for DO.
- One-way valves didn't work with medium and cells, which prevented continuous pumping without volume limitation, which therefore determined cultivation duration based on the available syringe volume.

#### 6.1 Conclusion

The need for small scale devices in many different applications is strongly present today, and it is propelling innovation, research and development. Already established micro-devices are changing the field work of doctors where DNA sequencing or different small analyzer kits find a valuable role in saving lives in remote areas without access to sophisticated lab size equipment. In biotechnology and pharma, the request for a small scale platform that can provide valuable information about strains or bioprocesses, faster and cheaper than bench scale equipment, has been present for a long time. It is a challenging task, and a fine balance is needed between functionality, complexity and price. Growth of different microorganisms in a controlled manner is a complex task which is not always clear and completely understood. Usually simple solutions are the best solutions. However with the currently available tools and technologies, and considering the inherent bioprocess and bioreactor complexity, it is a challenge to develop simple solutions aiming at achieving a fermentation process at miniaturized scale. For that to happen, supporting technologies need to advance and, who knows, with the innovative leaps and scientific breakthroughs occurring in many research areas today, certain postulates could be reshaped by questioning and revolutionizing already established standards in chemical and biochemical engineering as well. It is only a matter of time when a paradigm shift will occur from bulk production to personalized medicines with dedicated custom manufacturing that would probably have different requirements than the standard solutions of today have.

The aim of this thesis was to develop the small scale bioreactor for batch and continuous cultivations with an opportunity for parallelization and high throughput applications. As discussed in chapter 3, different micro and milliliter scale bioreactors have been created by diverse techniques to overcome design obstacles and provide cultivation results. In most of the cases, these new design solutions end their application lifetime with the completion of a research project and follow-up studies do not happen further in the future. Although, there are a few commercial solutions available today that started at research institutes and universities, many potentially promising products are still in their infancy, trying to establish the golden standard for high throughput miniaturized bioreactor platforms. The obvious trend for commercial platforms was to adapt and modify already used and established equipment e.g. microtiter plates and robotic handling systems, or mimicking the existing bench scale bioreactors for scale up purposes. Both approaches are fueled with the mindset that is entrenched in the established rules of chemical engineering, and the idea that solutions should fit to already existing infrastructure for ease of integration.



Two design case studies of the milliliter scale bioreactor were described and presented in this thesis. Both prototypes were made of inexpensive materials to provide cost effective single-use bioreactors. The chosen working volumes for bioreactor design were between 0.5 and 2.0 mL, since a majority of already established small scale bioreactors with impellers in academy and industry have working volumes below 0.5 mL or above 2 mL. The intention was to fill this research gap by providing a bioreactor design that can ensure adequate mixing and oxygen transfer rates at milliliter scale with inexpensive custom made supporting equipment that is not adapted from standard laboratory equipment, but is specifically designed to support bioreactor performance at milliliter scale at low cost.

The first prototype of the milliliter scale bioreactor platform was designed with an idea to provide a cost-effective versatile functionality on a small footprint. One- and bi-directional mixing with a special stirrer design ensured good mixing capabilities, which was confirmed with extensive mixing characterization. Sparging and/or surface aeration coupled with different mixing modes provided an adequate oxygen transfer rate. Scattered light intensity and temperature measurement had satisfactory performance as well as temperature control. The MSBR showed potential for anaerobic and aerobic batch cultivations, although with one major bottleneck – the effect of evaporation was rather explicit in aerobic cultivations. Lack of an adequate pH sensor and control capabilities were also issues since buffer capacity had only limited applicability.

Further development of the bioreactor platform, with the objective to run a continuous cultivation, produced a second prototype of the milliliter scale bioreactor which included two new units – a humidifier and push/pull pumps. Overall, the second prototype showed greater capability in providing more robust and consistent performance during cultivations. Addition of the humidifier and the two custom-made pumps increased somewhat the complexity of the whole platform. On the other hand, it also provided controllable low flows of gas and the possibility to run fed-batch and continuous cultivations due to existence of a pump for supplying medium. Evaporation has been reduced to approximately 13 % of the working volume per cultivation, which can be further optimized by fine-tuning the conditions in the humidifier. Temperature and mixing control were satisfactory. Mixing proved to be good in maintaining cells in suspension and supplying them with enough oxygen. On-line measurement of the scattered light intensity was reliable and reproducible, but the sensitivity and resolution were somewhat lower than expected with a more complex correlation with offline measurement methods of optical density. Each part of the platform eventually performed satisfactory, however with all parts together – the whole platform was not able to deliver suitable conditions for continuous cultivation as they would exist at larger scale, whereas the cultivation in batch mode went fine. With a few more improvements in the MSBR II platform design, the goal of performing continuous cultivations at milliliter scale is just around the corner.

A chemostat is considered a valuable tool when researching cell physiology and application of chemostat at small scale is considered beneficial due to reduced medium consumption during cultivation. However, creating a small-scale chemostat seems to be a challenging task since there are only handful of milliliter scale chemostats developed in the last decade. One of the first milliliter scale chemostats (3 mL) was reported by Walther et al. (1994) for application in space with focus on the effects of microgravity on cell growth. Klein et al. [67] and Schmieder et al. [69] reported continuous cultivation at 10 mL scale with  $k_{La}$  up to  $50 \text{ h}^{-1}$  (mixing by stirrer bar) and  $1440 \text{ h}^{-1}$  (mixing by gas inducing impeller) respectively, showing the relevance of good mixing. Furthermore, different chemostat designs at microliter scale ( $< 1 \text{ mL}$ ) are reported in the literature [25,32,53,59] with working volumes ranging from 16 nL to 150  $\mu\text{L}$  where introduction of a proper stirrer is not possible and the oxygen transfer rate is on the lower side which limits the applicable range of dilution rates during continuous cultivations [21]. Both, MSBR I and II had better performance with respect to mixing and oxygen transfer rate than the above mentioned microbioreactors ( $< 1 \text{ mL}$ ) equipped with PDMS membrane for aeration and mixing achieved by diffusion or stirrer bars. Although  $k_{La}$  was not determined for the MSBR II, the previous statement is based on the comparison of achieved biomass concentrations and dissolved oxygen profiles between different platforms. Furthermore, both MSBRs do not exhibit cell growth on the wall as it is often the case with very small working volume bioreactors. The oxygen transfer rate achieved in the MSBR I ( $70 - 2000 \text{ h}^{-1}$ ) is comparable to the oxygen transfer rate obtained in a 10 mL reactor ( $180 - 1440 \text{ h}^{-1}$ ) [21] with gas inducing impeller, despite the fact that the maximum stirring speed in the MSBR I was much lower (1100 rpm vs 2300 rpm). On-line measurement of optical density was applied in few micro-chemostats where small working volume and low biomass concentration allowed exploiting a linear range, while in the 10 mL chemostat at-line measurement was performed. In the current work, an attempt was made to measure scattered light intensity and correlate it with off-line standards, so an on-line measurement of the biomass concentration is present.

## 6.2 Future work

This thesis demonstrated the prospective of batch and continuous cultivations at milliliter scale with *Saccharomyces cerevisiae* as a model organism. There are opportunities for further utilization of the MSBR platform as well as for further improvement of the existing performance. In this final section of the thesis follow some suggestions for further enhancement of the whole platform:

- Further characterization of mixing and aeration performance by determining  $k_{La}$  values at different mixing speeds, gas flow rates and different oxygen concentrations in the inlet gas stream.

- Control of dissolved oxygen should be implemented based on the acquired  $k_{LA}$  results, such that the dissolved oxygen concentration could be kept constant and above 30 % air saturation.
- One sensing position in the MSBR is coupled with an optical fiber bundle based in the platform and it is not used in the existing design. Consequently an additional measurement could be implemented. Most obvious would be the implementation of a pH sensor spot in order to establish pH control. However, disposable sensor spots for pH measurement between 3 and 5 are not yet established on the market, thus only the pH sensor with a range 5.5 – 8.5 could be used. Instead, CO<sub>2</sub> sensor spots or Near-infrared spectroscopy could be introduced as well in order to expand the information level per experiment.
- The measurement range of the scattered light intensity measurement could be expanded by changing the distance between the optical fiber bundle and a mirror like surface. The characteristics of that mirror like surface could be improved as well, by further polishing the existing element or by introduction of an actual mirror.
- One important improvement is related to tubing, connectors and potential cell clogging on the way to syringes, since it is crucial for realizing steady state during continuous cultivation. Increasing the tube inner diameter or applying small volume syringes with the presence of valves that allow rapid refill, could be potential solutions.
- Certain limitations in communication between hardware and software in the current design were determined by the available data acquisition cards. Today there are new more capable and compact products on the market e.g., the CompactRIO Platform that can simplify the design of the control and the monitoring system and replace the functionality of a computer which adds to the mobility of the MSBR platform.

After expanding the physical functionality of the MSBR platform, different applications should be further explored in order to see how resourceful the MSBR system really is:

- Batch (until stationary phase) and fed-batch cultivations with *Saccharomyces cerevisiae* as model organism should be performed, to observe the maximal biomass concentration defined by the process parameters.
- Continuous cultivations with *Saccharomyces cerevisiae* should be repeated after remaining issues in the experimental set up are fixed.
- Anaerobic cultivations with *Lactobacillus paracasei* were performed within the first prototype of the MSBR. It would be interesting to perform the same type of experiments in the second prototype where gas flow control is present and

the reactor is properly sealed. Although, a slight modification in the pump section would be necessary in that case in order for the pump to deliver nitrogen instead of air.

- A modular approach in the MSBR design provides adaptable functionality. For example, by changing the stirrer design, the mixing conditions could be altered so they fit more to applications with mammalian cells.
- In general, different microorganisms could be grown under aerobic or anaerobic conditions in the MSBR. And comparison of such cultivation results could be made with larger scale cultivations.

Many practical problems and limitations occurred during the design and experimental work due to lack of access to proper tools and professional solutions supported by different experts e.g., software, mechanical, electrical engineers as well as engineers specialized in light sources and optical microsensors. Consequently, the presented design of a small scale reactor in this thesis could be further simplified by different production methods with more functional composition which could give more space for smart and simple solutions, which are a necessity if parallelization and high throughput is considered as the final goal. Another aspect worth considering and investigating is the cost of such a system and what would be the minimal cost per data point.

In general, solutions applied in microbioreactor design are heavily dependent on the development of other research areas and industries e.g., non-invasive sensing, wireless communication and availability of new materials with unique properties. The pillars (production method, material choice, connectivity and communication, sensing) on which microbioreactor design and fabrication rest need to advance in order to see major future breakthroughs in this research field.



## References

- [1] D. Mark, S. Haeberle, G. Roth, F. Von Stetten, R. Zengerle, Microfluidic Lab-on-a-Chip Platforms: Requirements, Characteristics and Applications, in: S. Kakaç, B. Kosoy, D. Li, A. Pramuanjaroenkij (Eds.), *Microfluid. Based Microsystems Fundam. Appl.*, Springer Netherlands, Dordrecht, 2010: pp. 305–376.
- [2] X. Yao, Y. Zhang, L. Du, J. Liu, J. Yao, Review of the applications of microreactors, *Renew. Sustain. Energy Rev.* 47 (2015) 519–539.
- [3] P.K. Seelam, M. Huuhtanen, R.L. Keiski, 5 - Microreactors and membrane microreactors: fabrication and applications, in: *Handb. Membr. React.*, 2013: pp. 188–235.
- [4] Y. Kostov, P. Harms, L. Randers-Eichhorn, G. Rao, Low-cost microbioreactor for high-throughput bioprocessing, *Biotechnol. Bioeng.* 72 (2001) 346–352.
- [5] D. Weuster-Botz, D. Hekmat, R. Puskeiler, E. Franco-Lara, Enabling Technologies: Fermentation and Downstream Processing, in: *White Biotechnol.*, Springer Berlin Heidelberg, Berlin, Heidelberg, 2007: pp. 205–247.
- [6] J. Büchs, Introduction to advantages and problems of shaken cultures, *Biochem. Eng. J.* 7 (2001) 91–98.
- [7] C. Blesken, T. Olfers, A. Grimm, N. Frische, The microfluidic bioreactor for a new era of bioprocess development, *Eng. Life Sci.* 16 (2016) 190–193.
- [8] D. Schapper, M.N.H.Z. Alam, N. Szita, A.E. Lantz, K. V Gernaey, Application of microbioreactors in fermentation process development: a review, *Anal. Bioanal. Chem.* 395 (2009) 679–695.
- [9] C. Musmann, K. Joeris, S. Markert, D. Solle, T. Scheper, Spectroscopic methods and their applicability for high-throughput characterization of mammalian cell cultures in automated cell culture systems, *Eng. Life Sci.* 16 (2016) 405–416.
- [10] S. Kumar, C. Wittmann, E. Heinzle, Minibioreactors, *Biotechnol. Lett.* 26 (2004) 1–10.
- [11] J.I. Betts, F. Baganz, Miniature bioreactors: current practices and future opportunities, *Microb. Cell Fact.* 5 (2006) 21.
- [12] M. Micheletti, G.J. Lye, Microscale bioprocess optimisation, *Curr. Opin. Biotechnol.* 17 (2006) 611–618.
- [13] P. Fernandes, J.M.S. Cabral, Microlitre/millilitre shaken bioreactors in fermentative and biotransformation processes - a review, *Biocatal. Biotransformation.* 24 (2006) 237–252.
- [14] W.A. Duetz, Microtiter plates as mini-bioreactors: miniaturization of fermentation methods, *Trends Microbiol.* 15 (2007) 469–475.
- [15] M.P.C. Marques, P. Fernandes, Microfluidic devices: useful tools for bioprocess intensification, *Molecules.* 16 (2011) 8368–8401.
- [16] R. Hortsch, D. Weuster-Botz, Milliliter-Scale Stirred Tank Reactors for the Cultivation of Microorganisms, *Adv. Appl. Microbiol.* 73 (2010) 61–82.
- [17] R. Bareither, D. Pollard, A Review of Advanced Small-Scale Parallel Bioreactor Technology for Accelerated Process Development: Current State and Future Need, *Biotechnol. Prog.* 27 (2011) 2–14.
- [18] G. Pasirayi, V. Auger, S.M. Scott, P.K.S.M. Rahman, M. Islam, L. O'Hare, et al., Microfluidic bioreactors for cell culturing: A review, *Micro Nanosyst.* 3 (2011) 137–160.

- [19] B.J. Kim, J. Diao, M.L. Shuler, Mini-scale bioprocessing systems for highly parallel animal cell cultures, *Biotechnol. Prog.* 28 (2012) 595–607.
- [20] K. V. Gernaey, F. Baganz, E. Franco-Lara, F. Kensy, U. Krühne, M. Luebberstedt, et al., Monitoring and control of microbioreactors: An expert opinion on development needs, *Biotechnol. J.* 7 (2012) 1308–1314.
- [21] T. V Kirk, N. Szita, Oxygen transfer characteristics of miniaturized bioreactor systems, *Biotechnol. Bioeng.* 110 (2013) 1005–1019.
- [22] P. Neubauer, N. Cruz, F. Glauche, S. Junne, A. Knepper, M. Raven, Consistent development of bioprocesses from microliter cultures to the industrial scale, *Eng. Life Sci.* 13 (2013) 224–238.
- [23] C. Lattermann, J. Büchs, Microscale and miniscale fermentation and screening, *Curr. Opin. Biotechnol.* 35 (2015) 1–6.
- [24] Q. Long, X. Liu, Y. Yang, L. Li, L. Harvey, B. McNeil, et al., The development and application of high throughput cultivation technology in bioprocess development, *J. Biotechnol.* 192 (2014) 323–338.
- [25] F.K. Balagaddé, L. You, C.L. Hansen, F.H. Arnold, S.R. Quake, Long-term monitoring of bacteria undergoing programmed population control in a microchemostat, *Science* (80-. ). 309 (2005) 137–140.
- [26] I. Walther, B.H. van der Schoot, S. Jeanneret, P. Arquint, N.F. de Rooij, V. Gass, et al., Development of a miniature bioreactor for continuous culture in a space laboratory, *J. Biotechnol.* 38 (1994) 21–32.
- [27] P. Girard, M. Jordan, M. Tsao, F.M. Wurm, Small-scale bioreactor system for process development and optimization, *Biochem. Eng. J.* 7 (2001) 117–119.
- [28] S.R. Lamping, H. Zhang, B. Allen, P. Ayazi Shamlou, Design of a prototype miniature bioreactor for high throughput automated bioprocessing, *Chem. Eng. Sci.* 58 (2003) 747–758.
- [29] A. Zanzotto, N. Szita, P. Boccazzi, P. Lessard, A.J. Sinskey, K.F. Jensen, Membrane-aerated microbioreactor for high-throughput bioprocessing, *Biotechnol. Bioeng.* 87 (2004) 243–254.
- [30] M.M. Maharbiz, W.J. Holtz, R.T. Howe, J.D. Keasling, Microbioreactor Arrays with Parametric Control for High-Throughput Experimentation, *Biotechnol. Bioeng.* 85 (2004) 376–381.
- [31] N. Szita, P. Boccazzi, Z. Zhang, P. Boyle, A.J. Sinskey, K.F. Jensen, Development of a multiplexed microbioreactor system for high-throughput bioprocessing, *Lab Chip.* 5 (2005) 819–826.
- [32] Z. Zhang, P. Boccazzi, H.-G. Choi, G. Perozziello, A.J. Sinskey, K.F. Jensen, Microchemostat – microbial continuous culture in a polymer-based, instrumented microbioreactor, *Lab Chip.* 6 (2006) 906–913.
- [33] Z. Zhang, N. Szita, P. Boccazzi, A.J. Sinskey, K.F. Jensen, A well-mixed, polymer-based microbioreactor with integrated optical measurements, *Biotechnol. Bioeng.* 93 (2006) 286–296.
- [34] P. Boccazzi, Z. Zhang, K. Kurosawa, N. Szita, S. Bhattacharya, K.F. Jensen, et al., Differential gene expression profiles and real-time measurements of growth parameters in *Saccharomyces cerevisiae* grown in microliter-scale bioreactors equipped with internal stirring, *Biotechnol. Prog.* 22 (2006) 710–717.
- [35] R. Puskeiler, K. Kaufmann, D. Weuster-Botz, Development, parallelization, and automation of a gas-inducing milliliter-scale bioreactor for high-throughput

- bioprocess design (HTBD), *Biotechnol. Bioeng.* 89 (2005) 512–523.
- [36] G. Gebhardt, R. Hortsch, K. Kaufmann, M. Arnold, D. Weuster-Botz, A new microfluidic concept for parallel operated milliliter-scale stirred tank bioreactors, *Biotechnol. Prog.* 27 (2011) 684–690.
- [37] D. Weuster-Botz, R. Puskeiler, A. Kusterer, K. Kaufmann, G.T. John, M. Arnold, Methods and milliliter scale devices for high-throughput bioprocess design, *Bioprocess Biosyst. Eng.* 28 (2005) 109–119.
- [38] M. Funke, A. Buchenauer, U. Schnakenberg, W. Mokwa, S. Diederichs, A. Mertens, et al., Microfluidic biolector-microfluidic bioprocess control in microtiter plates., *Biotechnol. Bioeng.* 107 (2010) 497–505.
- [39] F. Kensy, E. Zang, C. Faulhammer, R.-K. Tan, J. Büchs, Validation of a high-throughput fermentation system based on online monitoring of biomass and fluorescence in continuously shaken microtiter plates, *Microb. Cell Fact.* 8 (2009) 31.
- [40] M. Samorski, G. Müller-Newen, J. Büchs, Quasi-continuous combined scattered light and fluorescence measurements: A novel measurement technique for shaken microtiter plates, *Biotechnol. Bioeng.* 92 (2005) 61–68.
- [41] R. Huber, D. Ritter, T. Hering, A.-K. Hillmer, F. Kensy, C. Müller, et al., Robo-Lector—a novel platform for automated high-throughput cultivations in microtiter plates with high information content, *Microb. Cell Fact.* 8 (2009) 42.
- [42] P.J. Lee, P.J. Hung, V.M. Rao, L.P. Lee, Nanoliter scale microbioreactor array for quantitative cell biology, *Biotechnol. Bioeng.* 94 (2006) 5–14.
- [43] P. Harms, Y. Kostov, J.A. French, M. Soliman, M. Anjanappa, A. Ram, et al., Design and performance of a 24-station high throughput microbioreactor, *Biotechnol. Bioeng.* 93 (2006) 6–13.
- [44] X. Ge, M. Hanson, H. Shen, Y. Kostov, K.A. Brorson, D.D. Frey, et al., Validation of an optical sensor-based high-throughput bioreactor system for mammalian cell culture, *J. Biotechnol.* 122 (2006) 293–306.
- [45] J. Diao, L. Young, P. Zhou, M.L. Shuler, An actively mixed mini-bioreactor for protein production from suspended animal cells, *Biotechnol. Bioeng.* 100 (2008) 72–81.
- [46] B.J. Kim, T. Zhao, L. Young, P. Zhou, M.L. Shuler, Batch, fed-batch, and microcarrier cultures with CHO cell lines in a pressure-cycle driven miniaturized bioreactor, *Biotechnol. Bioeng.* 109 (2012) 137–145.
- [47] A. Chen, R. Chitta, D. Chang, A. Amanullah, Twenty-four well plate miniature bioreactor system as a scale-down model for cell culture process development., *Biotechnol. Bioeng.* 102 (2009) 148–60.
- [48] K. Isett, H. George, W. Herber, A. Amanullah, Twenty-four-well plate miniature Bioreactor high-throughput system: Assessment for microbial cultivations, *Biotechnol. Bioeng.* 98 (2007) 1017–1028.
- [49] L. Villain, L. Meyer, S. Kroll, S. Beutel, T. Scheper, Development of a Novel Membrane Aerated Hollow-Fiber Microbioreactor, *Biotechnol. Prog.* 24 (2008) 367–371.
- [50] N.K. Gill, M. Appleton, F. Baganz, G.J. Lye, Design and characterisation of a miniature stirred bioreactor system for parallel microbial fermentations, *Biochem. Eng. J.* 39 (2008) 164–176.
- [51] A. Buchenauer, M.C. Hofmann, M. Funke, J. Büchs, W. Mokwa, U. Schnakenberg, Micro-bioreactors for fed-batch fermentations with integrated online monitoring and



- microfluidic devices, *Biosens. Bioelectron.* 24 (2009) 1411–1416.
- [52] P.K.S.M. Rahman, G. Pasirayi, V. Auger, Z. Ali, Development of a simple and low cost microbioreactor for high-throughput bioprocessing, *Biotechnol. Lett.* 31 (2009) 209–214.
- [53] A. Edlich, V. Magdanz, D. Rasch, S. Demming, S. Aliasghar Zadeh, R. Segura, et al., Microfluidic reactor for continuous cultivation of *Saccharomyces cerevisiae*, *Biotechnol. Prog.* 26 (2010) 1259–1270.
- [54] R. Hortsch, A. Stratmann, D. Weuster-Botz, New milliliter-scale stirred tank bioreactors for the cultivation of mycelium forming microorganisms, *Biotechnol. Bioeng.* 106 (2010) 443–451.
- [55] A. Amanullah, J.M. Otero, M. Mikola, A. Hsu, J. Zhang, J. Aunins, et al., Novel micro-bioreactor high throughput technology for cell culture process development: Reproducibility and scalability assessment of fed-batch CHO cultures, *Biotechnol. Bioeng.* 106 (2010) 57–67.
- [56] R. Legmann, H.B. Schreyer, R.G. Combs, E.L. McCormick, A.P. Russo, S.T. Rodgers, A predictive high-throughput scale-down model of monoclonal antibody production in CHO cells, *Biotechnol. Bioeng.* 104 (2009) 1107–1120.
- [57] D. Schäpper, S.M. Stocks, N. Szita, A.E. Lantz, K. V Gernaey, Development of a single-use microbioreactor for cultivation of microorganisms, *Chem. Eng. J.* 160 (2010) 891–898.
- [58] B.S. Demming, B. Sommer, A. Llobera, D. Rasch, R. Krull, Disposable parallel poly(dimethylsiloxane) microbioreactor with integrated readout grid for germination screening of *Aspergillus ochraceus*, *Biomicrofluidics.* 5 (2011) 14104.
- [59] K.S. Lee, P. Boccazzi, A.J. Sinskey, R.J. Ram, Microfluidic chemostat and turbidostat with flow rate, oxygen, and temperature control for dynamic continuous culture, *Lab Chip.* 11 (2011) 1730–1739.
- [60] S.H. Au, S.C.C. Shih, A.R. Wheeler, Integrated microbioreactor for culture and analysis of bacteria, algae and yeast, *Biomed. Microdevices.* 13 (2011) 41–50.
- [61] S. Moses, M. Manahan, A. Ambrogelly, W.L.W. Ling, Assessment of AMBR™ as a model for high-throughput cell culture process development strategy, *Adv. Biosci. Biotechnol.* 3 (2012) 918–927.
- [62] F. Delouvroy, G. Le Reverend, B. Fessler, G. Mathy, M. Harmsen, N. Kochanowski, et al., Evaluation of the advanced micro-scale bioreactor (ambr™) as a highthroughput tool for cell culture process development, *BMC Proc.* 7 (2013) P73.
- [63] S. Rameez, S.S. Mostafa, C. Miller, A.A. Shukla, High-throughput miniaturized bioreactors for cell culture process development: Reproducibility, scalability, and control, *Biotechnol. Prog.* 30 (2014) 718–727.
- [64] D.M. Bower, K.S. Lee, R.J. Ram, K.L.J. Prather, Fed-batch microbioreactor platform for scale down and analysis of a plasmid DNA production process, *Biotechnol. Bioeng.* 109 (2012) 1976–1986.
- [65] J.Z. Baboo, J.L. Galman, G.J. Lye, J.M. Ward, H.C. Hailes, M. Micheletti, An automated microscale platform for evaluation and optimization of oxidative bioconversion processes, *Biotechnol. Prog.* 28 (2012) 392–405.
- [66] S. Demming, G. Peterat, A. Llobera, H. Schmolke, A. Bruns, M. Kohlstedt, et al., Vertical microbubble column—A photonic lab-on-chip for cultivation and online analysis of yeast cell cultures, *Biomicrofluidics.* 6 (2012) 34106.
- [67] T. Klein, K. Schneider, E. Heinzle, A system of miniaturized stirred bioreactors for

- parallel continuous cultivation of yeast with online measurement of dissolved oxygen and off-gas, *Biotechnol. Bioeng.* 110 (2013) 535–542.
- [68] U.M. Tillich, N. Wolter, K. Schulze, D. Kramer, O. Brödel, M. Frohme, High-throughput cultivation and screening platform for unicellular phototrophs, *BMC Microbiol.* 14 (2014) 239.
- [69] A. Schmideder, T.S. Severin, J.H. Cremer, D. Weuster-Botz, A novel milliliter-scale chemostat system for parallel cultivation of microorganisms in stirred-tank bioreactors, *J. Biotechnol.* 210 (2015) 19–24.
- [70] S. Kheradmandnia, S. Hashemi-Najafabadi, S.A. Shojaosadati, S.M. Mousavi, K. Malek Khosravi, Development of parallel miniature bubble column bioreactors for fermentation process, *J. Chem. Technol. Biotechnol.* 90 (2015) 1051–1061.
- [71] J. Marles-Wright, R.J. Lewis, Stress responses of bacteria, *Curr. Opin. Struct. Biol.* 17 (2007) 755–760.
- [72] A. Grünberger, W. Wiechert, D. Kohlheyer, Single-cell microfluidics: opportunity for bioprocess development, *Curr. Opin. Biotechnol.* 29 (2014) 15–23.
- [73] M. Mehling, S. Tay, Microfluidic cell culture., *Curr. Opin. Biotechnol.* 25 (2014).
- [74] A.H.C. Ng, B.B. Li, M.D. Chamberlain, A.R. Wheeler, Digital microfluidic cell culture, *Annu. Rev. Biomed. Eng.* 17 (2015).
- [75] N.J. Mozdierz, K.R. Love, K.S. Lee, H.L.T. Lee, K.A. Shah, R.J. Ram, et al., A perfusion-capable microfluidic bioreactor for assessing microbial heterologous protein production, *Lab Chip.* 15 (2015) 2918–2922.
- [76] G. Faust, N.H. Janzen, C. Bendig, L. Römer, K. Kaufmann, D. Weuster-Botz, Feeding strategies enhance high cell density cultivation and protein expression in milliliter scale bioreactors, *Biotechnol. J.* 9 (2014) 1293–1303.
- [77] G. Gebhardt, R. Hortsch, K. Kaufmann, M. Arnold, D. Weuster-Botz, A new microfluidic concept for parallel operated milliliter-scale stirred tank bioreactors, *Biotechnol. Prog.* 27 (2011) 684–690.
- [78] C. Toeroek, M. Cserjan-Puschmann, K. Bayer, G. Striedner, Fed-batch like cultivation in a micro-bioreactor: screening conditions relevant for *Escherichia coli* based production processes, *Springerplus.* 4 (2015) 490.
- [79] C. Demuth, J. Varonier, V. Jossen, R. Eibl, D. Eibl, Novel probes for pH and dissolved oxygen measurements in cultivations from millilitre to benchtop scale, *Appl. Microbiol. Biotechnol.* 100 (2016) 3853–3863.
- [80] N.H. Janzen, M. Schmidt, C. Krause, D. Weuster-Botz, Evaluation of fluorimetric pH sensors for bioprocess monitoring at low pH, *Bioprocess Biosyst. Eng.* 38 (2015) 1685–1692.
- [81] M. Funke, A. Buchenauer, W. Mokwa, S. Kluge, L. Hein, C. Mueller, et al., Bioprocess Control in Microscale: Scalable Fermentations in Disposable and User-Friendly Microfluidic Systems, *Microb. Cell Fact.* 9 (2010) 86.
- [82] P. Rohe, D. Venkanna, B. Kleine, R. Freudl, M. Oldiges, An automated workflow for enhancing microbial bioprocess optimization on a novel microbioreactor platform, *Microb. Cell Fact.* 11 (2012) 144.
- [83] C. Bendig, D. Weuster-Botz, Reaction engineering analysis of cellulase production with *Trichoderma reesei* RUT-C30 with intermittent substrate supply, *Bioprocess Biosyst. Eng.* 36 (2013) 893–900.
- [84] T. Hoefel, G. Faust, L. Reinecke, N. Rudinger, D. Weuster-Botz, Comparative reaction engineering studies for succinic acid production from sucrose by

- metabolically engineered *Escherichia coli* in fed-batch-operated stirred tank bioreactors, *Biotechnol. J.* 7 (2012) 1277–1287.
- [85] R.H.J. Das, G.J.V.M. van Osch, M. Kreukniet, J. Oostra, H. Weinans, H. Jahr, Effects of individual control of pH and hypoxia in chondrocyte culture, *J. Orthop. Res.* 28 (2009) 537–545.
- [86] W.T. Hsu, R.P.S. Aulakh, D.L. Traul, I.H. Yuk, Advanced microscale bioreactor system: a representative scale-down model for bench-top bioreactors, *Cytotechnology.* 64 (2012) 667–678.
- [87] A.W. Nienow, The physical characterisation of a microscale parallel bioreactor platform with an industrial CHO cell line expressing an IgG4, *Biochem. Eng. J.* 76 (2013).
- [88] R. Bareither, N. Bargh, R. Oakeshott, K. Watts, D. Pollard, Automated disposable small scale reactor for high throughput bioprocess development: A proof of concept study, *Biotechnol. Bioeng.* 110 (2013) 3126–3138.
- [89] P.F. Stanbury, A. Whitaker, S.J. Hall, *Principles of Fermentation Technology*, Elsevier, 1995.
- [90] N. Ziv, N.J. Brandt, D. Gresham, The Use of Chemostats in Microbial Systems Biology, *J. Vis. Exp.* (2013).
- [91] A.E. Cervera, N. Petersen, A.E. Lantz, A. Larsen, K. V Gernaey, Application of near-infrared spectroscopy for monitoring and control of cell culture and fermentation, *Biotechnol. Prog.* 25 (2009) 1561–1581.
- [92] F. Zamora, *Biochemistry of Alcoholic Fermentation*, in: M.V. Moreno-Arribas, M.C. Polo (Eds.), *Wine Chem. Biochem.*, Springer New York, New York, NY, 2009: pp. 3–26.
- [93] A. Hagman, J. Piškur, A Study on the Fundamental Mechanism and the Evolutionary Driving Forces behind Aerobic Fermentation in Yeast, *PLoS One.* 10 (2015) e0116942.
- [94] L. Galdieri, S. Mehrotra, S. Yu, A. Vancura, Transcriptional Regulation in Yeast during Diauxic Shift and Stationary Phase, *Omi. A J. Integr. Biol.* 14 (2010) 629–638.
- [95] A. Ertas, J.C. Jones, *The Engineering Design Process*, second ed., John Wiley & Sons, Inc, 1996.
- [96] G.E. Dieter, L.C. Schmidt, *Engineering design*, Vol. 3. New York: McGraw-Hill, 2013.
- [97] C.L. Dym, P. Little, E. Orwin, *Engineering Design: A Project-Based Introduction*, Fourth Edition, Wiley Global Education, 2013.
- [98] B.I. Hyman, *Fundamentals of Engineering Design*, Prentice Hall/Pearson Education, 2002.
- [99] S. George, G. Larsson, K. Olsson, S.-O. Enfors, Comparison of the Baker's yeast process performance in laboratory and production scale, *Bioprocess Eng.* 18 (1998) 135.
- [100] D. Schäpper, *Continuous Culture Microbioreactors*, PhD Thesis, Tech. Univ. Denmark. (2010).
- [101] P.H. King, R.C. Fries, *Design of biomedical devices and systems*, Marcel Dekker, 2003.
- [102] W.H. Yang, Oxygen permeability coefficients of polymers for hard and soft contact lens applications, *J. Memb. Sci.* 9 (1981). (accessed September 9, 2017).
- [103] T.C. Merkel, V.I. Bondar, K. Nagai, B.D. Freeman, I. Pinnau, Gas sorption, diffusion, and permeation in poly(dimethylsiloxane), *J. Polym. Sci. Part B Polym. Phys.* 38

(2000) 415–434.

- [104] K.N. Otto, K.L. Wood, Product Evolution: A Reverse Engineering and Redesign Methodology, *Res. Eng. Des.* 10 (1998) 226–243.
- [105] L. Capretto, W. Cheng, M. Hill, X. Zhang, Micromixing Within Microfluidic Devices, in: B. Lin (Ed.), *Microfluid. SE - 150*, Springer Berlin Heidelberg, 2011: pp. 27–68.
- [106] C.Y. Lee, C.L. Chang, Y.N. Wang, L.M. Fu, Microfluidic Mixing: A Review, *Int. J. Mol. Sci.* 12 (2011) 3263–3287.
- [107] H.L.T. Lee, P. Boccazzi, R.J. Ram, A.J. Sinskey, Microbioreactor arrays with integrated mixers and fluid injectors for high-throughput experimentation with pH and dissolved oxygen control., *Lab Chip.* 6 (2006) 1229–1235.
- [108] R. Lencastre Fernandes, M. Nierychlo, L. Lundin, A.E. Pedersen, P.E. Puentes Tellez, A. Dutta, et al., Experimental methods and modeling techniques for description of cell population heterogeneity, *Biotechnol. Adv.* 29 (2011) 575–599.
- [109] R. Bailey, F. Jones, B. Fisher, B. Elmore, Enhancing Design of Immobilized Enzymatic Microbioreactors Using Computational Simulation, *Appl. Biochem. Biotechnol.* 122 (2005) 0639–0652.
- [110] R.L. Fernandes, U. Krühne, I. Nopens, A.D. Jensen, K. V. Gernaey, Multi-scale modeling for prediction of distributed cellular properties in response to substrate spatial gradients in a continuously run microreactor, in: *Comput. Aided Chem. Eng.*, 2012: pp. 545–549.
- [111] I. Landa, M.M. Anthony, G.E. Toth, Probe for transmitting and receiving light from a sample, (1991). <https://www.google.com/patents/US5044755>.
- [112] K.P. VonBargen, Transflectance probe having adjustable window gap adapted to measure viscous substances for spectrometric analysis and method of use, (1998). <https://www.google.com/patents/US5708273>.
- [113] D.A.R. Brown, P.N. Jones, J.C. Middleton, G. Papadopoulos, E.B. Arik, Experimental Methods, in: *Handb. Ind. Mix.*, John Wiley & Sons, Inc., 2004: pp. 145–256.
- [114] J.C. Van. Suijdam, N.W.F. Kossen, A.C. Joha, Model for Oxygen Transfer in a Shake Flask, *Biotechnol. Bioeng.* 20 (1978) 1695–1709.
- [115] F. Garcia-Ochoa, E. Gomez, Bioreactor scale-up and oxygen transfer rate in microbial processes: An overview, *Biotechnol. Adv.* 27 (2009) 153–176.
- [116] W. A. Brown, Developing the best correlation for estimating the transfer of oxygen from air to water, *Chem. Eng. Educ.* 35 (2001) 134–139+147.
- [117] S. Hugelier, Mass transfer in stirred microbioreactors, *Massetransport i omrørte mikrobioreaktorer - DTU Findit*, DTU, 2012. (accessed September 25, 2017).
- [118] H. Lambrecht, Comparison between yeast cultivation in a miniature stirred bioreactor and a bench-scale reactor, 2013. <http://bib.howest.be/catalog/hws01:002006993>.
- [119] J.C. Lamont, D.S. Scott, An eddy cell model of mass transfer into the surface of a turbulent liquid, *AIChE J.* 16 (1970) 513–519.
- [120] S. Brüning, D. Weuster-Botz, CFD analysis of interphase mass transfer and energy dissipation in a milliliter-scale stirred-tank reactor for filamentous microorganisms, *Chem. Eng. Res. Des.* 92 (2014) 240–248.
- [121] S.C. Kaiser, Characterization and optimization of single-use bioreactors and biopharmaceutical production processes using Computational Fluid Dynamics, (n.d.).
- [122] P. Moilanen, M. Laakkonen, O. Visuri, V. Alopaeus, J. Aittamaa, Modelling mass

- transfer in an aerated 0.2m<sup>3</sup> vessel agitated by Rushton, Phasejet and Combijet impellers, *Chem. Eng. J.* 142 (2008) 95–108.
- [123] K.D. Entian, *Yeast Gene Analysis - Second Edition, Methods in Microbiology* 36 (2007) 629-666, n.d.
- [124] S.S. Chiang, T.M. Pan, Beneficial effects of *Lactobacillus paracasei* subsp. *paracasei* NTU 101 and its fermented products, *Appl. Microbiol. Biotechnol.* 93 (2012) 903–916.
- [125] M.D. Collins, B.A. Phillips, P. Zanoni, Deoxyribonucleic Acid Homology Studies of *Lactobacillus casei*, *Lactobacillus paracasei* sp. nov., subsp. *paracasei* and subsp. *tolerans*, and *Lactobacillus rhamnosus* sp. nov., comb. nov., *Int. J. Syst. Bacteriol.* 39 (1989) 105–108.
- [126] G. Waites, M. J., Morgan, N. L., Rockey, J. S., Higton, *Industrial Microbiology : An Introduction*, 2009.
- [127] A. Goffeau, B.G. Barrell, H. Bussey, R.W. Davis, B. Dujon, H. Feldmann, et al., Life with 6000 Genes, *Science* (80-. ). 274 (1996) 546–567.
- [128] C. Verduyn, E. Postma, W. a. Scheffers, J.P. Van Dijken, Effect of benzoic acid on metabolic fluxes in yeasts: A continuous-culture study on the regulation of respiration and alcoholic fermentation, *Yeast.* 8 (1992) 501–517.
- [129] J.T. Alander, V. Bochko, B. Martinkauppi, S. Saranwong, T. Mantere, *A Review of Optical Nondestructive Visual and Near-Infrared Methods for Food Quality and Safety*, (2013).
- [130] O. Levenspiel, *Chemical reaction engineering*, Wiley, 1999.
- [131] E.B. Nauman, Residence Time Distributions, in: *Handb. Ind. Mix.*, John Wiley & Sons, Inc., 2004: pp. 1–17.
- [132] D. Quintanilla, T. Hagemann, K. Hansen, K. V Gernaey, Fungal Morphology in Industrial Enzyme Production-Modelling and Monitoring., *Adv. Biochem. Eng. Biotechnol.* 149 (2015) 29–54.
- [133] R.A. Prior, T. Vilby, Validation of 2 mL microbioreactors and near-infrared spectroscopy monitoring , Validering af 2 mL mikrobioreaktorer og nær-infrarød spektroskopi monitorering - DTU Findit, Technical University of Denmark, 2012. (accessed September 4, 2017).
- [134] J.P. van Dijken, R.A. Weusthuis, J.T. Pronk, Kinetics of growth and sugar consumption in yeasts, *Antonie Van Leeuwenhoek.* 63 (1993) 343–352.
- [135] N.J. Silk, S. Denby, G. Lewis, M. Kuiper, D. Hatton, R. Field, et al., Fed-batch operation of an industrial cell culture process in shaken microwells, *Biotechnol. Lett.* 32 (2010) 73–78.
- [136] W.A. Duetz, L. Ruedi, R. Hermann, K. O'Connor, J. Buchs, B. Witholt, Methods for Intense Aeration, Growth, Storage, and Replication of Bacterial Strains in Microtiter Plates, *Appl. Environ. Microbiol.* 66 (2000) 2641–2646.
- [137] A.B. Chambers, A psychrometric chart for physiological research, *J. Appl. Physiol.* 29 (1970). (accessed October 2, 2017).
- [138] S. de Kock, Anomalies in the growth kinetics of *Saccharomyces cerevisiae* strains in aerobic chemostat cultures, *J. Ind. Microbiol. Biotechnol.* 24 (2000) 231–236.
- [139] D. Pejin, Continuous cultivation of the yeast *Saccharomyces cerevisiae* at different dilution rates and glucose concentrations in nutrient media, *Folia Microbiol. (Praha).* 38 (1993) 141–146.
- [140] O. Frick, C. Wittmann, Characterization of the metabolic shift between oxidative and fermentative growth in *Saccharomyces cerevisiae* by comparative C-13 flux analysis,

Microb. Cell Fact. 4 (2005) 30.

- [141] S.J. Parulekar, G.B. Semones, M.J. Rolf, J.C. Lievens, H.C. Lim, Induction and elimination of oscillations in continuous cultures of *Saccharomyces cerevisiae*., *Biotechnol. Bioeng.* 28 (1986) 700–10.
- [142] M. Carlquist, R. Fernandes, S. Helmark, A.-L. Heins, L. Lundin, S.J. Sørensen, et al., Physiological heterogeneities in microbial populations and implications for physical stress tolerance, *Microb. Cell Fact.* 11 (2012) 94.
- [143] P. Van Hoek, Effect of specific growth rate on fermentative capacity of baker's yeast, *Appl. Environ. Microbiol.* 64 (1998) 4226–4233.
- [144] C. Abel, F. Linz, T. Scheper, K. Schügerl, Transient behaviour of continuously cultivated Baker's yeast during enforced variations of dissolved oxygen and glucose concentrations, *J. Biotechnol.* 33 (1994) 183–193.
- [145] M.B. Al-Fageeh, C.M. Smales, Control and regulation of the cellular responses to cold shock: the responses in yeast and mammalian systems, *Biochem. J.* 397 (2006) 247 LP-259.
- [146] B. Klinkert, F. Narberhaus, Microbial thermosensors, *Cell. Mol. Life Sci.* 66 (2009) 2661–2676.
- [147] M. Hebly, D. de Ridder, E.A.F. de Hulster, P. de la Torre Cortes, J.T. Pronk, P. Daran-Lapujade, Physiological and Transcriptional Responses of Anaerobic Chemostat Cultures of *Saccharomyces cerevisiae* Subjected to Diurnal Temperature Cycles, *Appl. Environ. Microbiol.* 80 (2014) 4433–4449.



## Appendix A

### Continuous cultivations with *Saccharomyces cerevisiae* CEN.PK-113-7D performed in the MSBR II

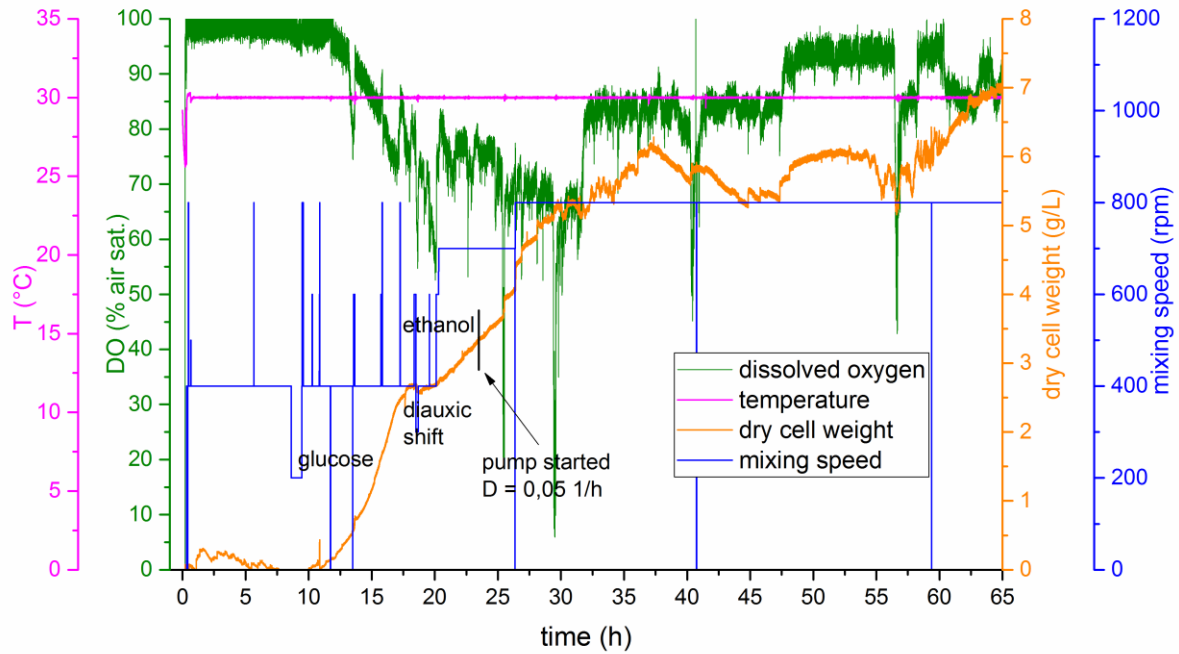


Figure 1. Aerobic cultivation with *Saccharomyces cerevisiae* CEN.PK-113-7D - number 2.

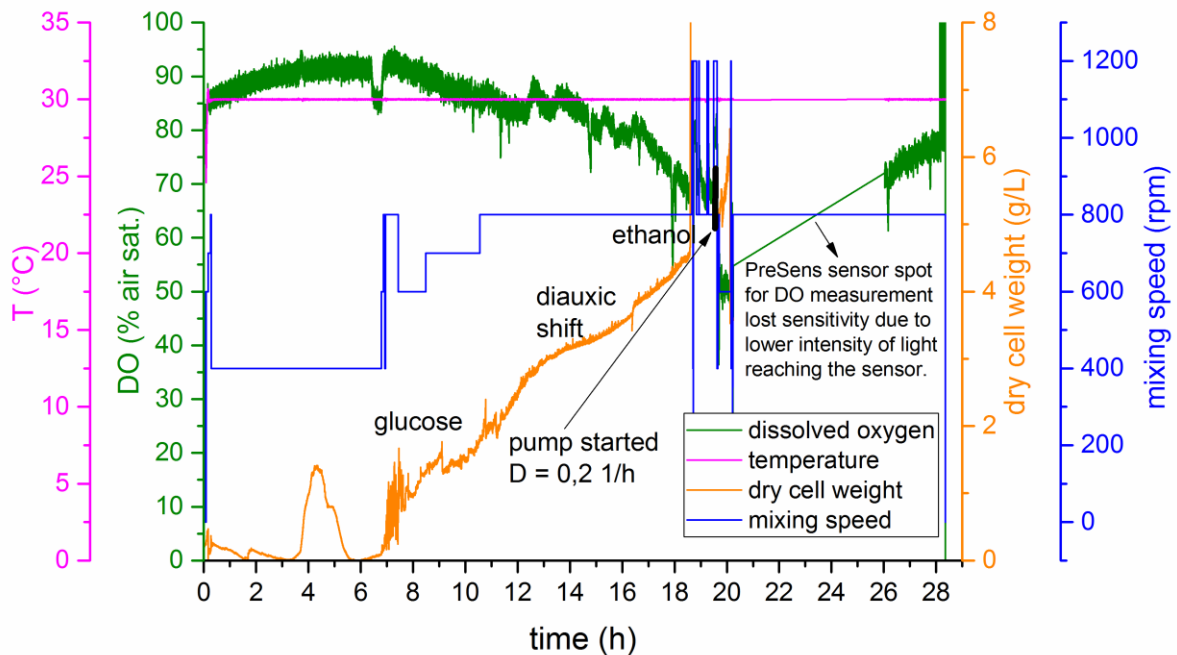


Figure 2. Aerobic cultivation with *Saccharomyces cerevisiae* CEN.PK-113-7D - number 3.



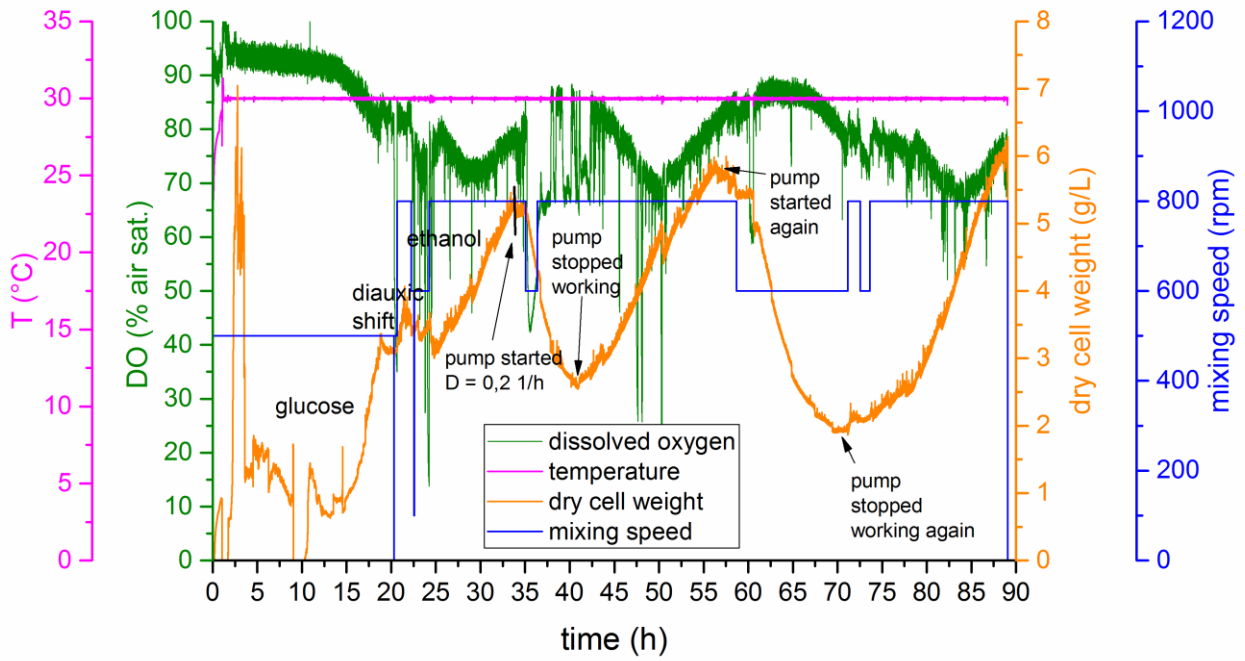


Figure 3. Aerobic cultivation with *Saccharomyces cerevisiae* CEN.PK-113-7D – number 5.

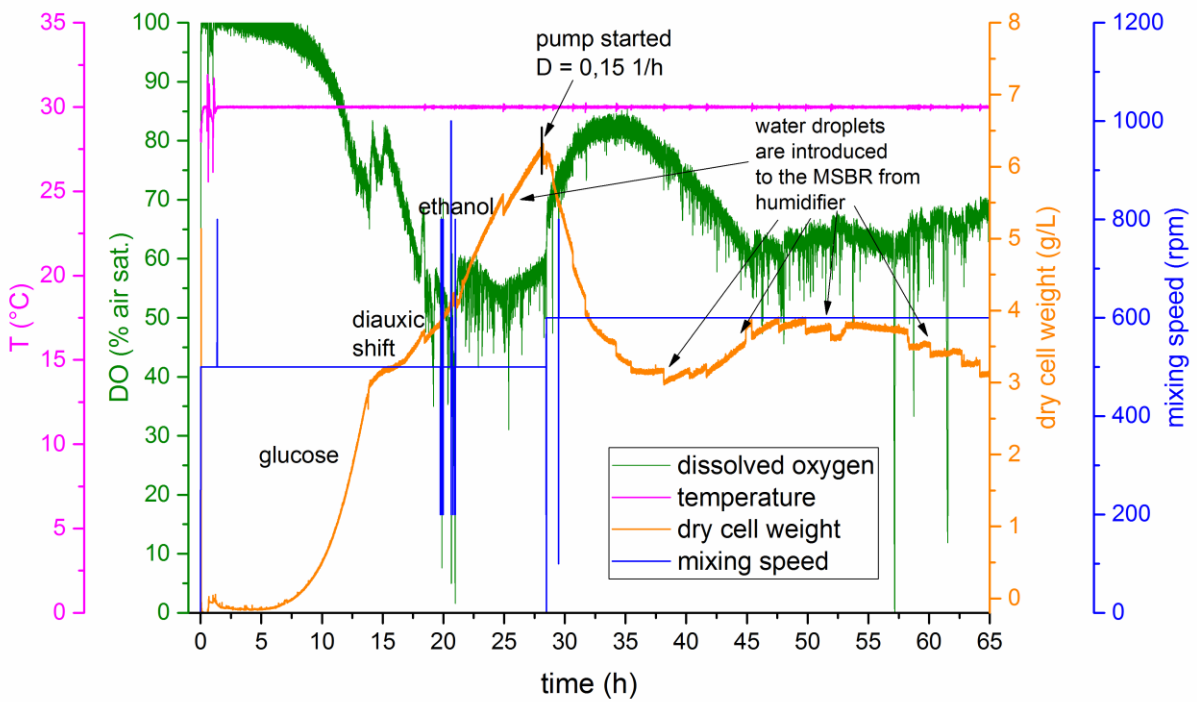


Figure 4. Aerobic cultivation with *Saccharomyces cerevisiae* CEN.PK-113-7D – number 7.

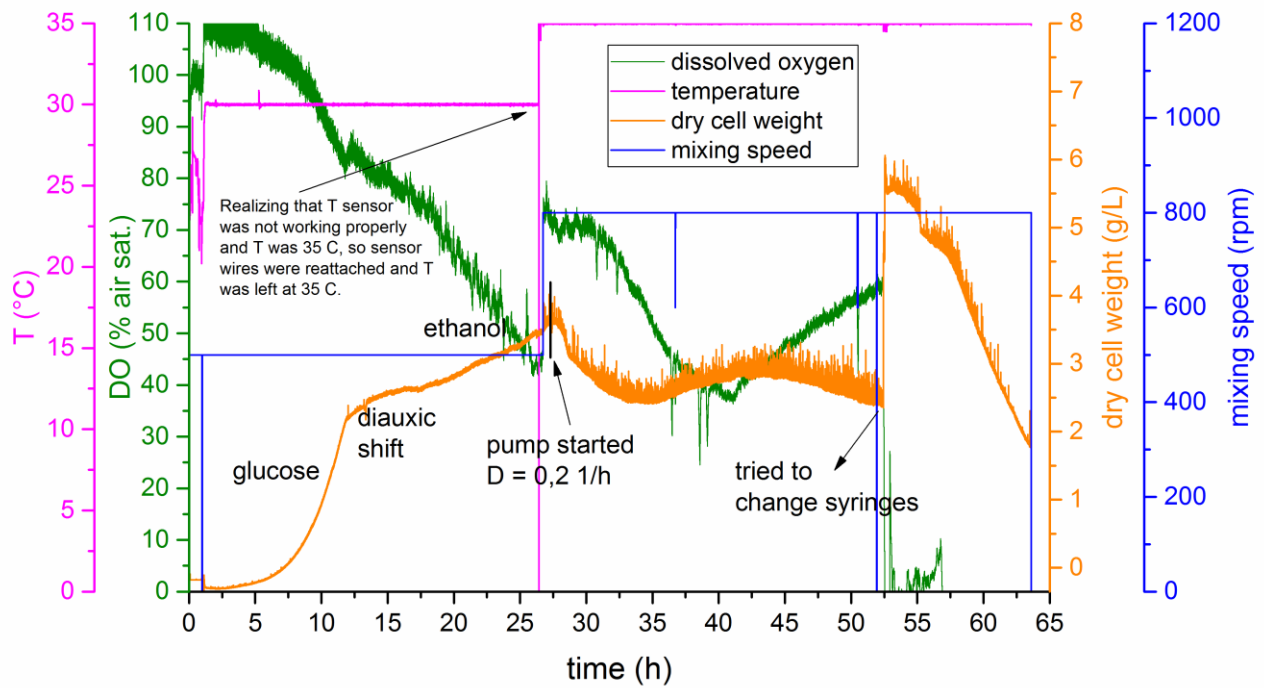


Figure 5. Aerobic cultivation with *Saccharomyces cerevisiae* CEN.PK-113-7D - number 8.

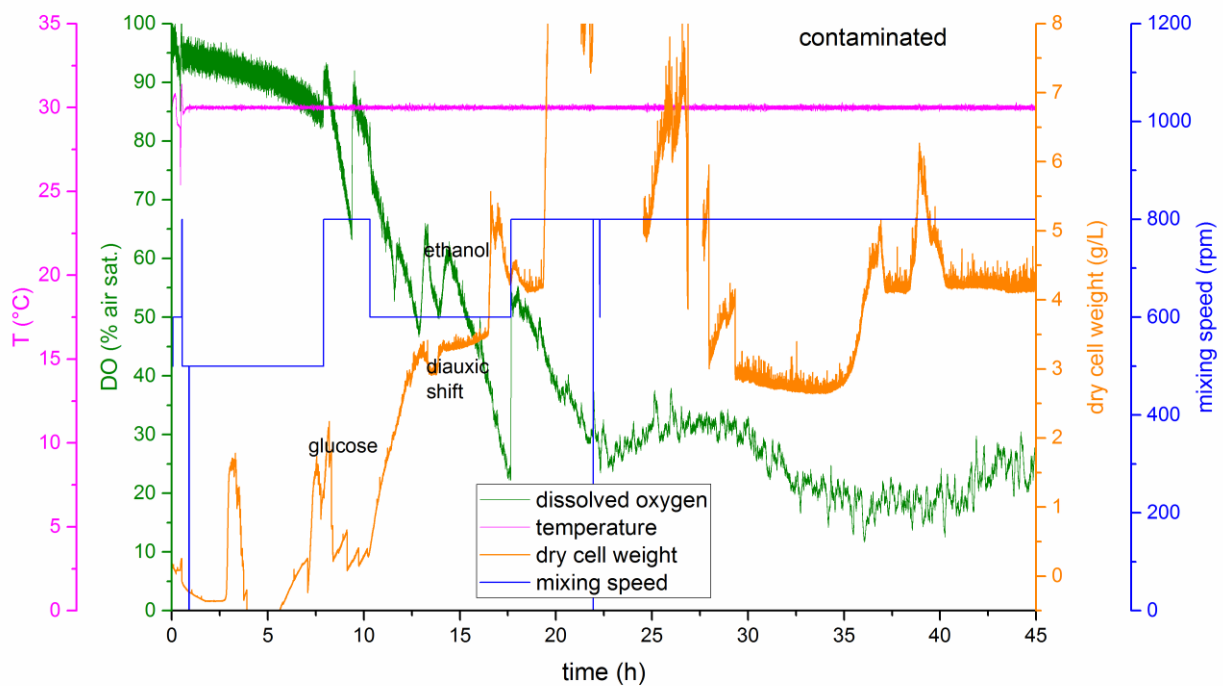


Figure 6. Aerobic cultivation with *Saccharomyces cerevisiae* CEN.PK-113-7D - number 9.

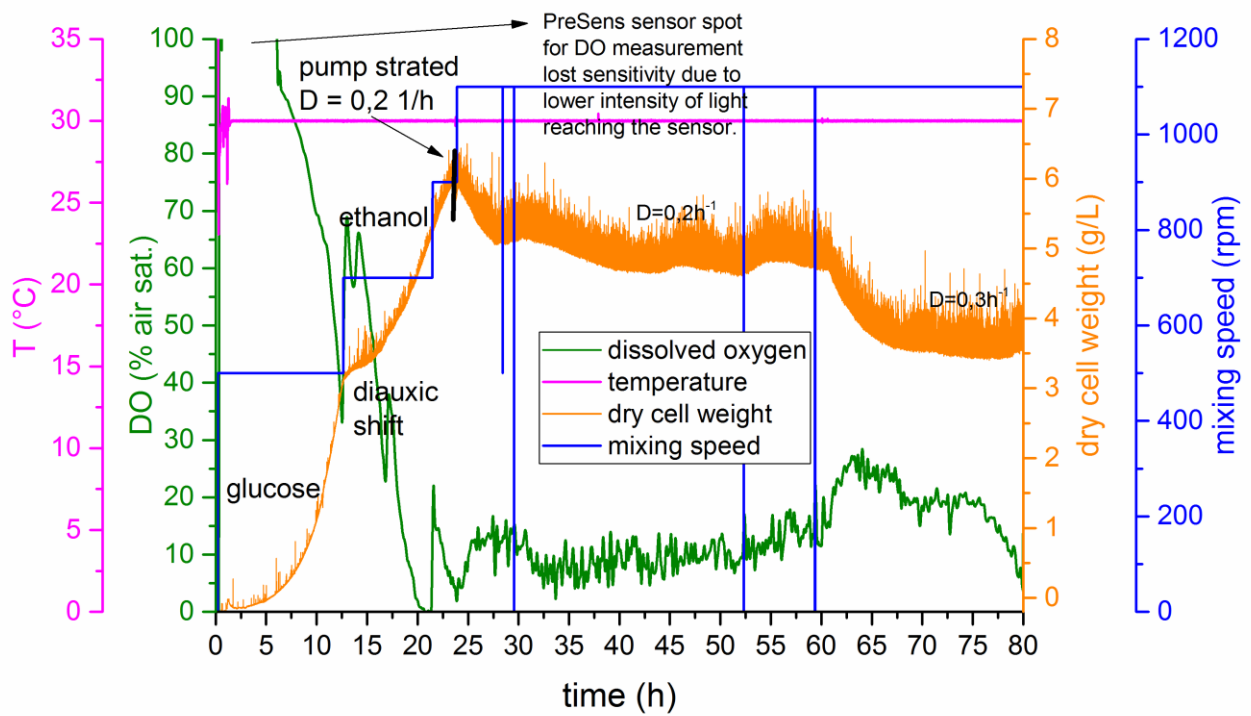


Figure 7. Aerobic cultivation with *Saccharomyces cerevisiae* CEN.PK-113-7D – number 10.

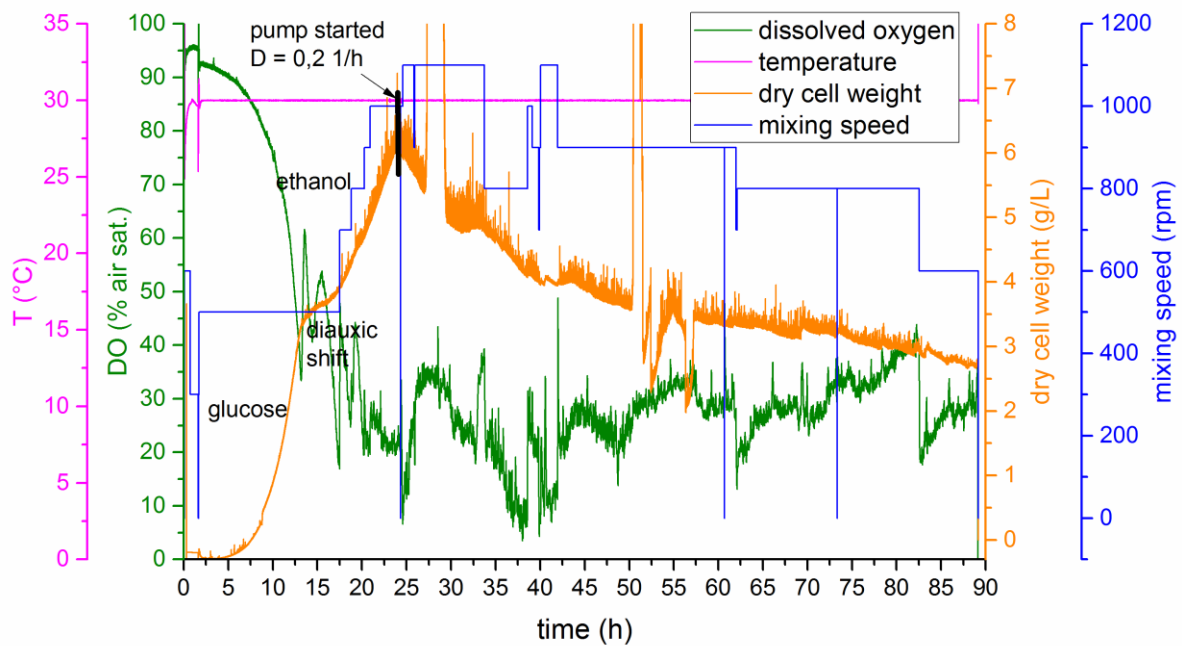
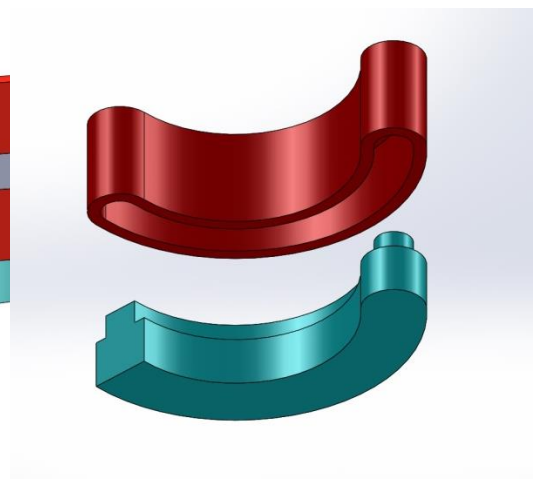
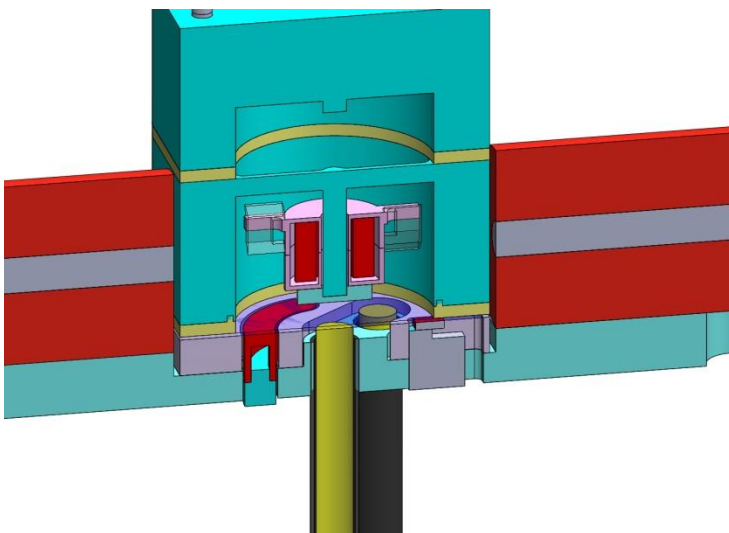
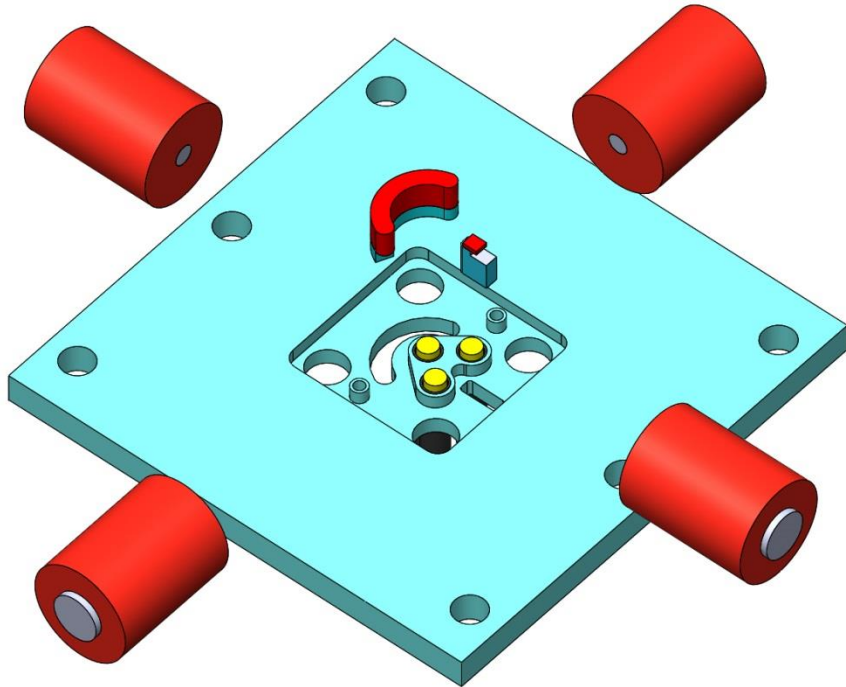


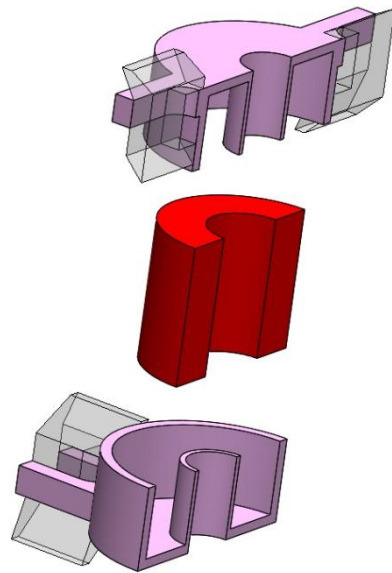
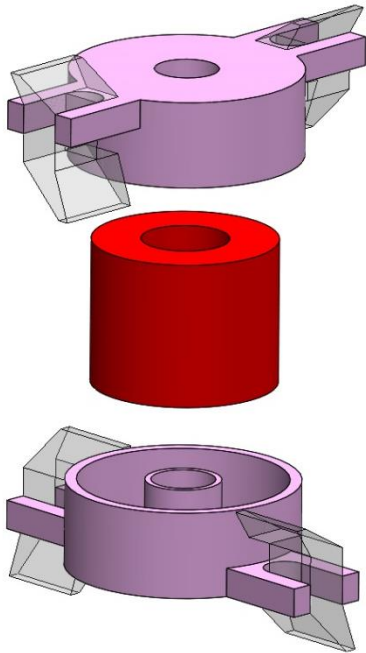
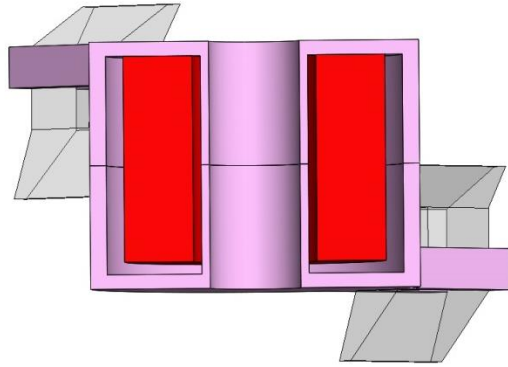
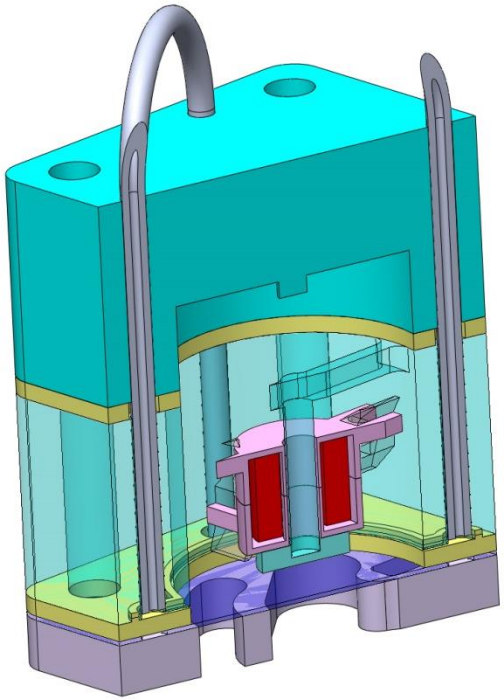
Figure 8. Aerobic cultivation with *Saccharomyces cerevisiae* CEN.PK-113-7D – number 12.

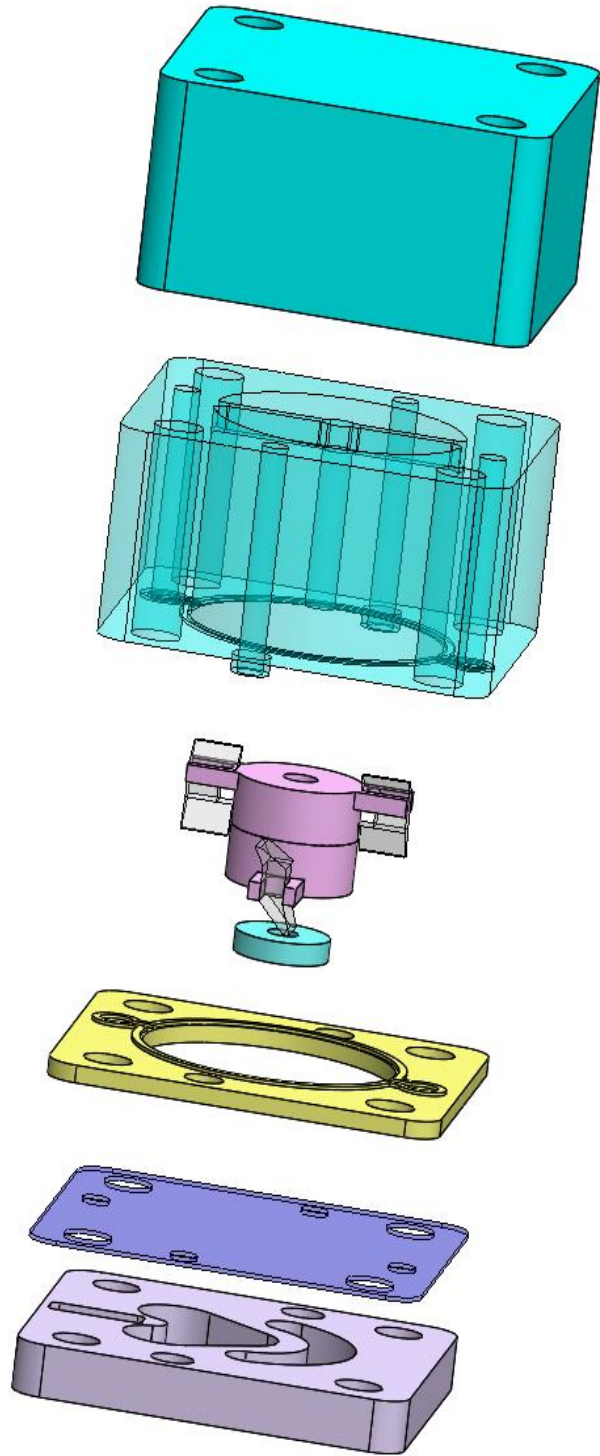
## Appendix B

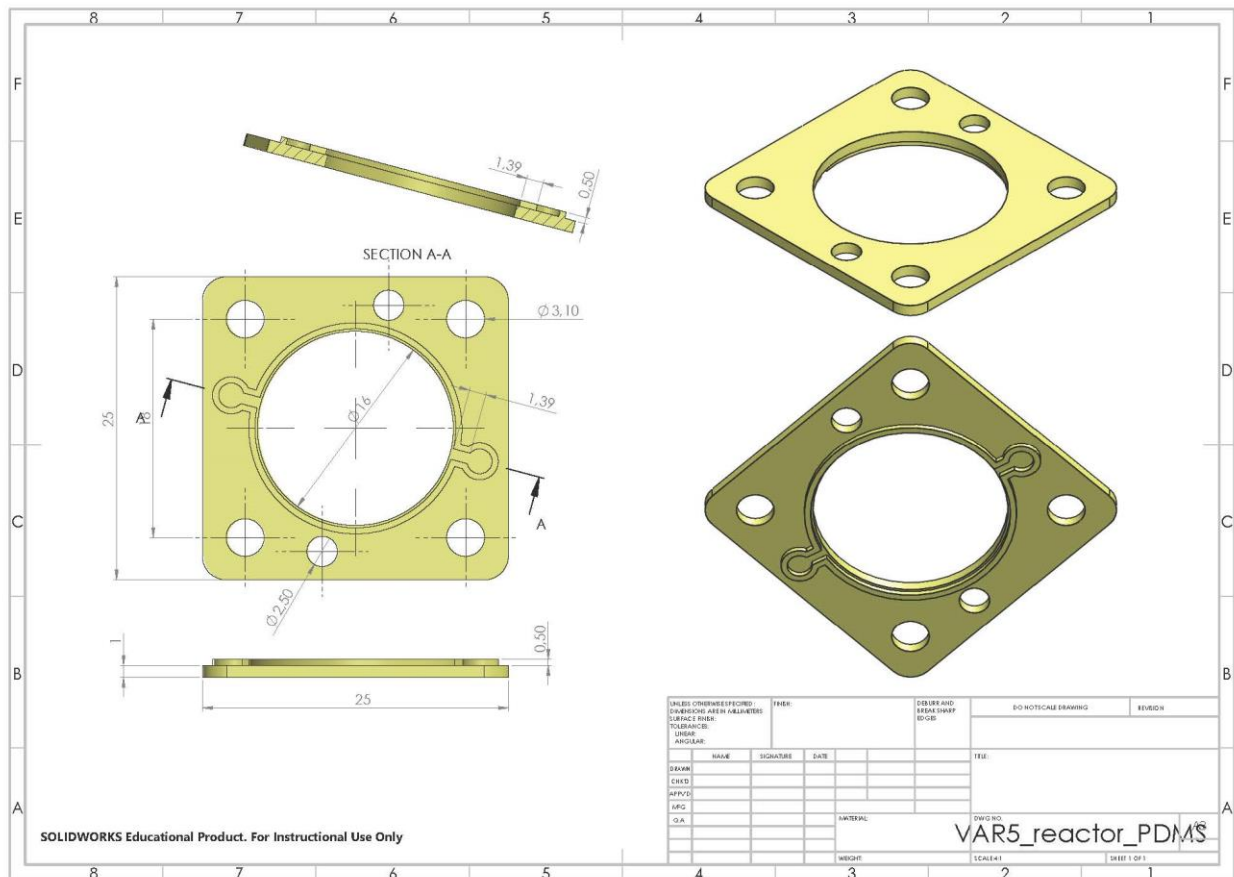
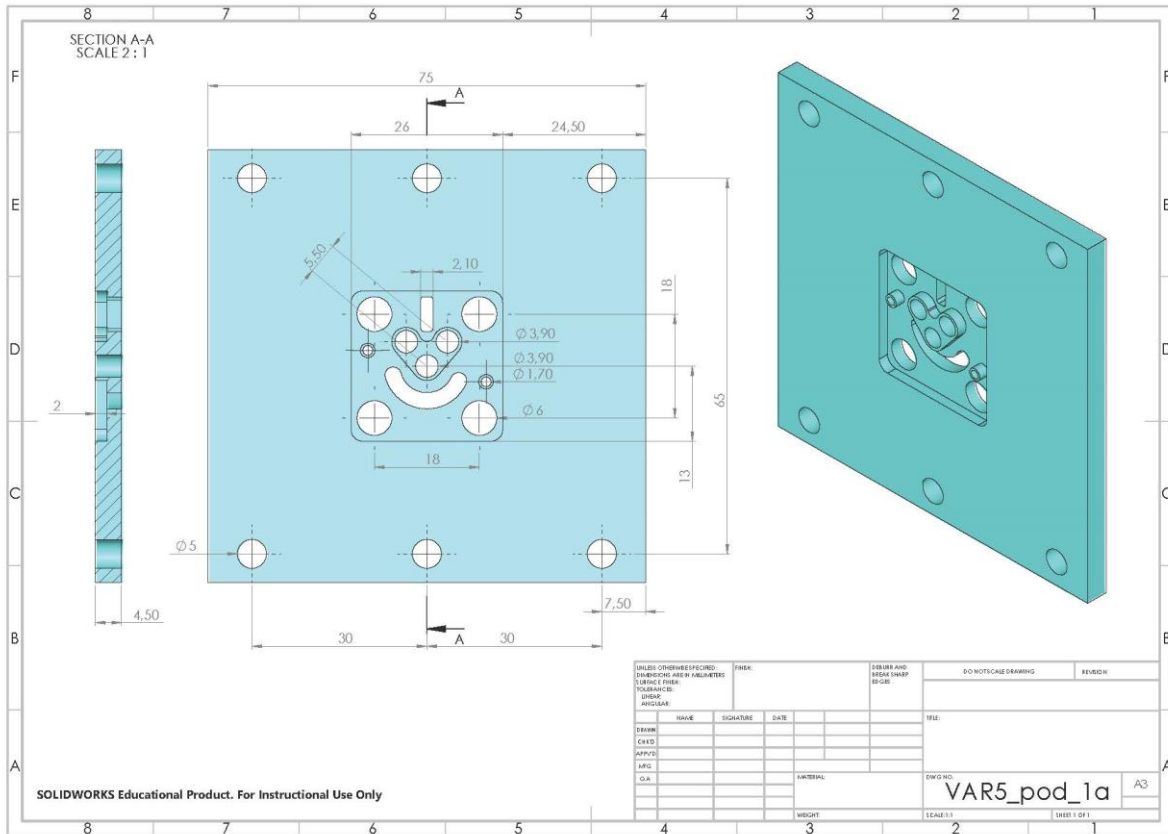
---

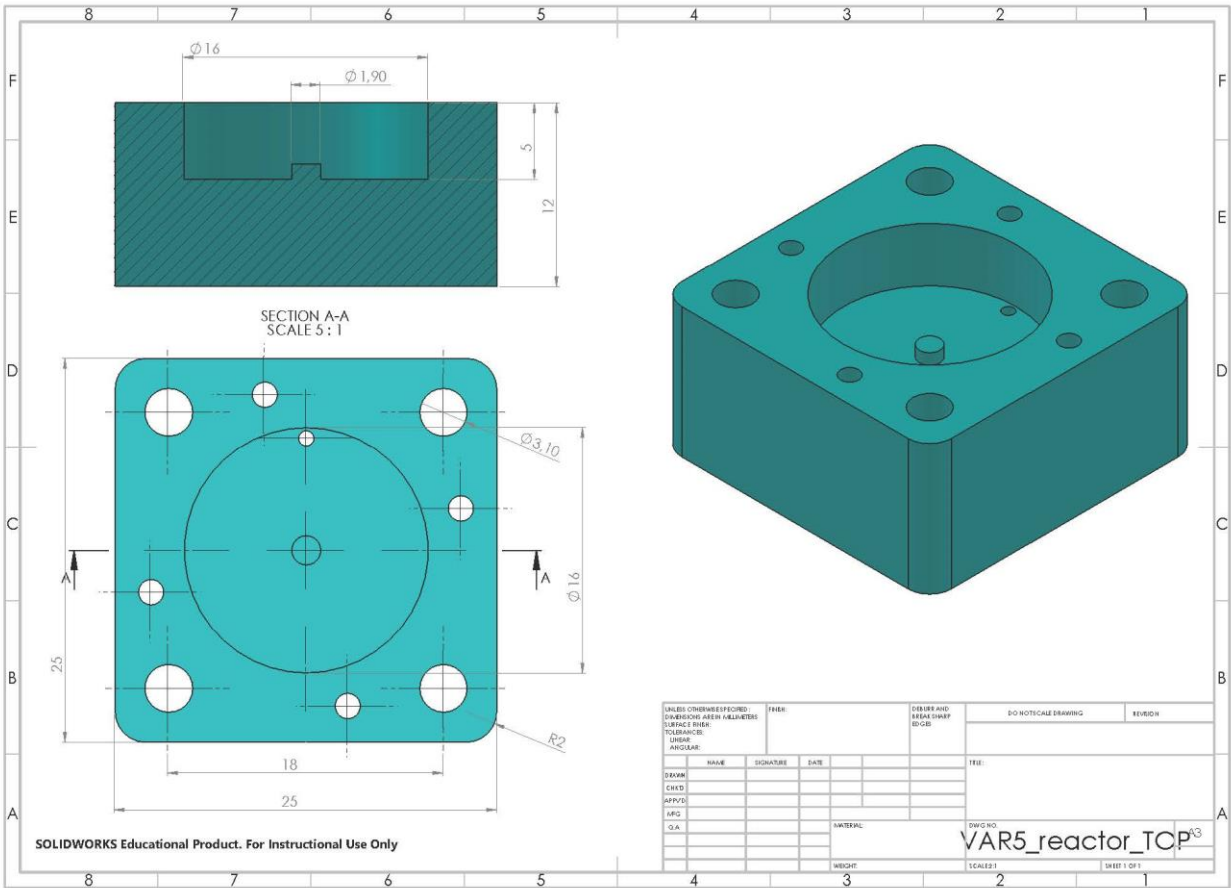
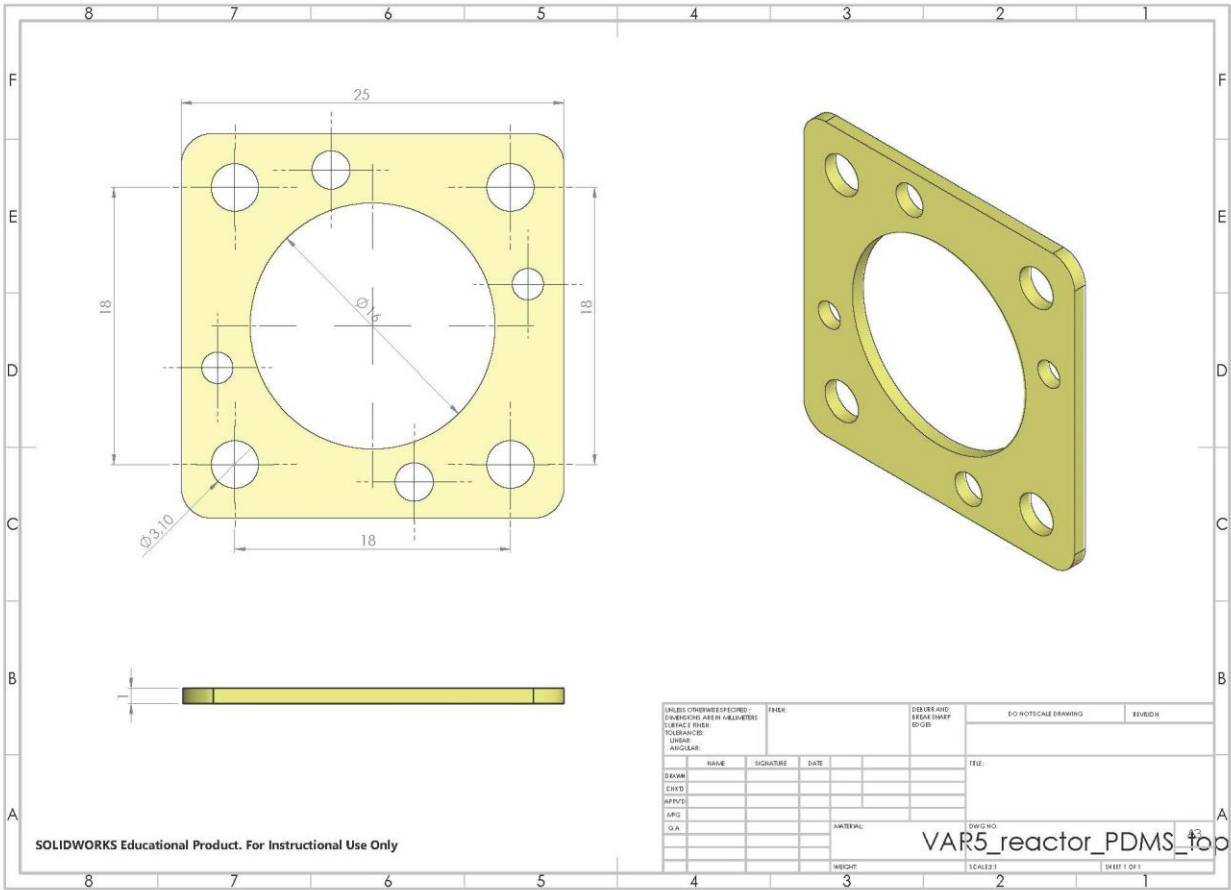
### Milliliter scale bioreactor prototype I



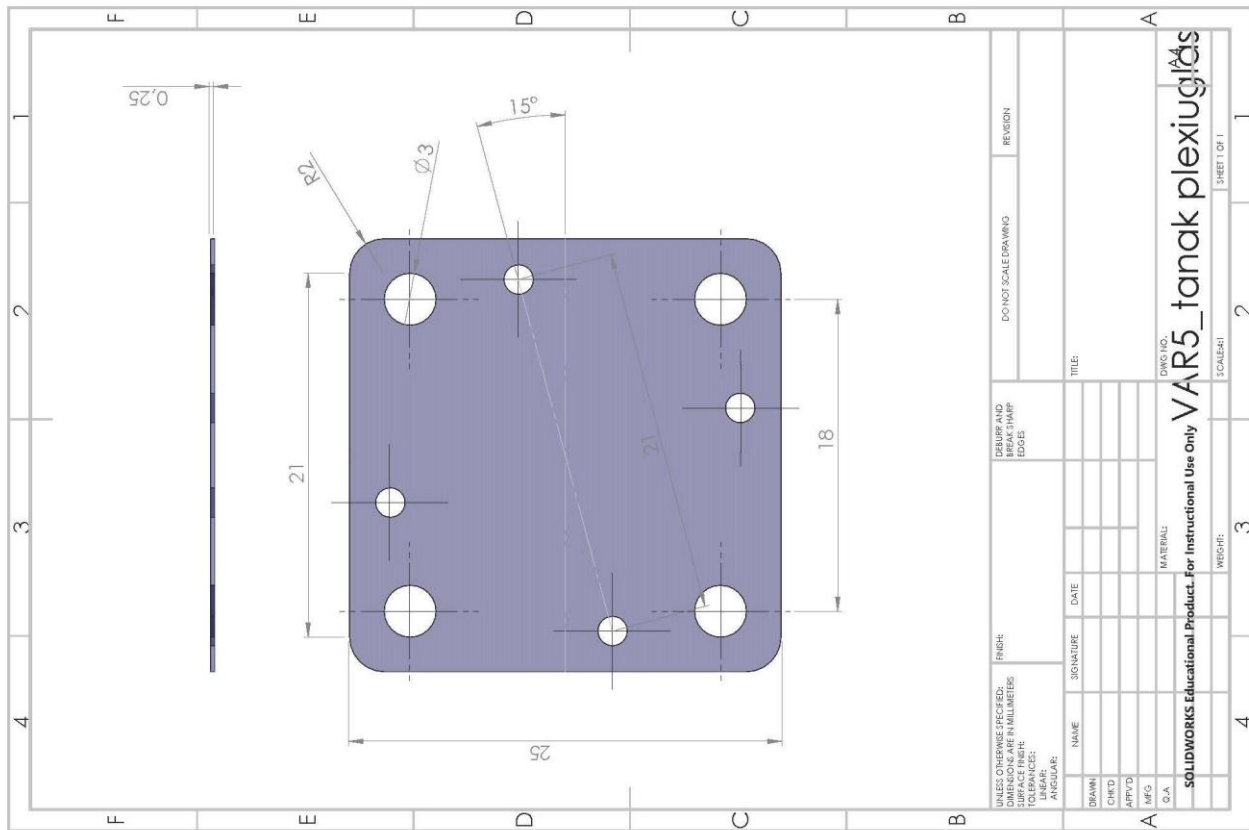
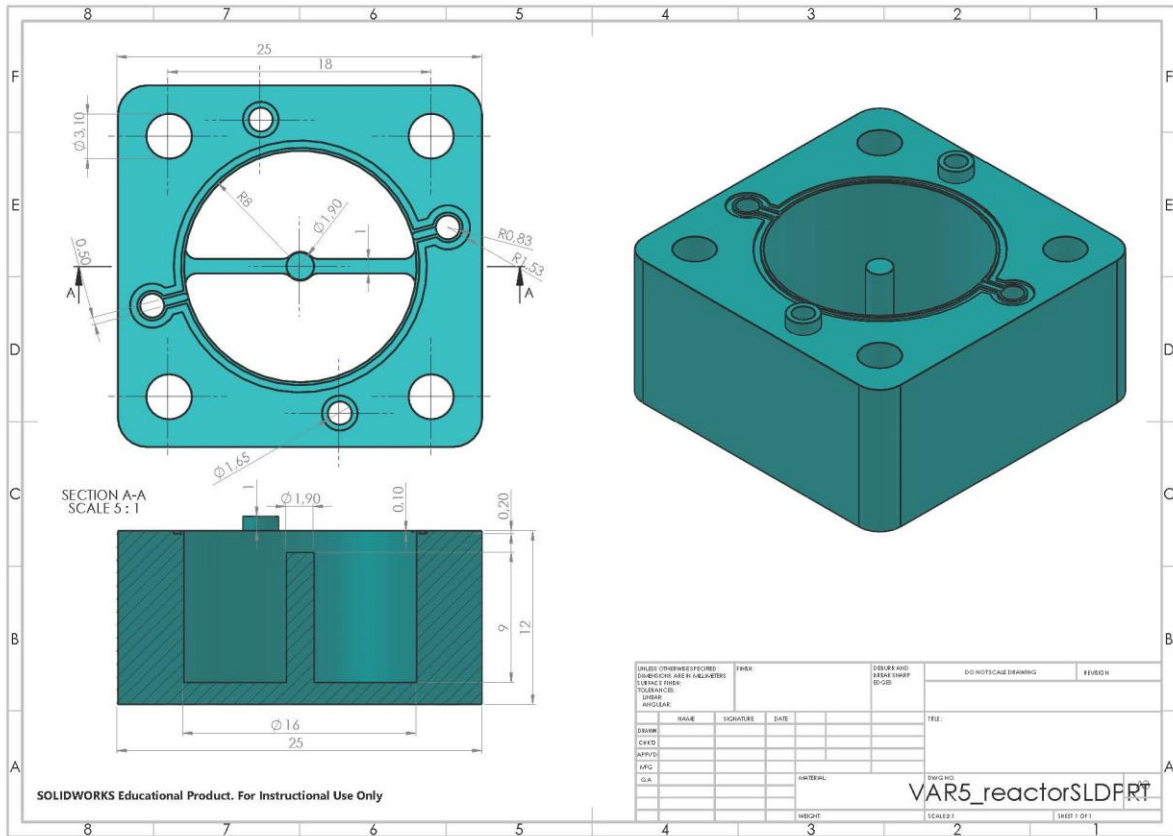




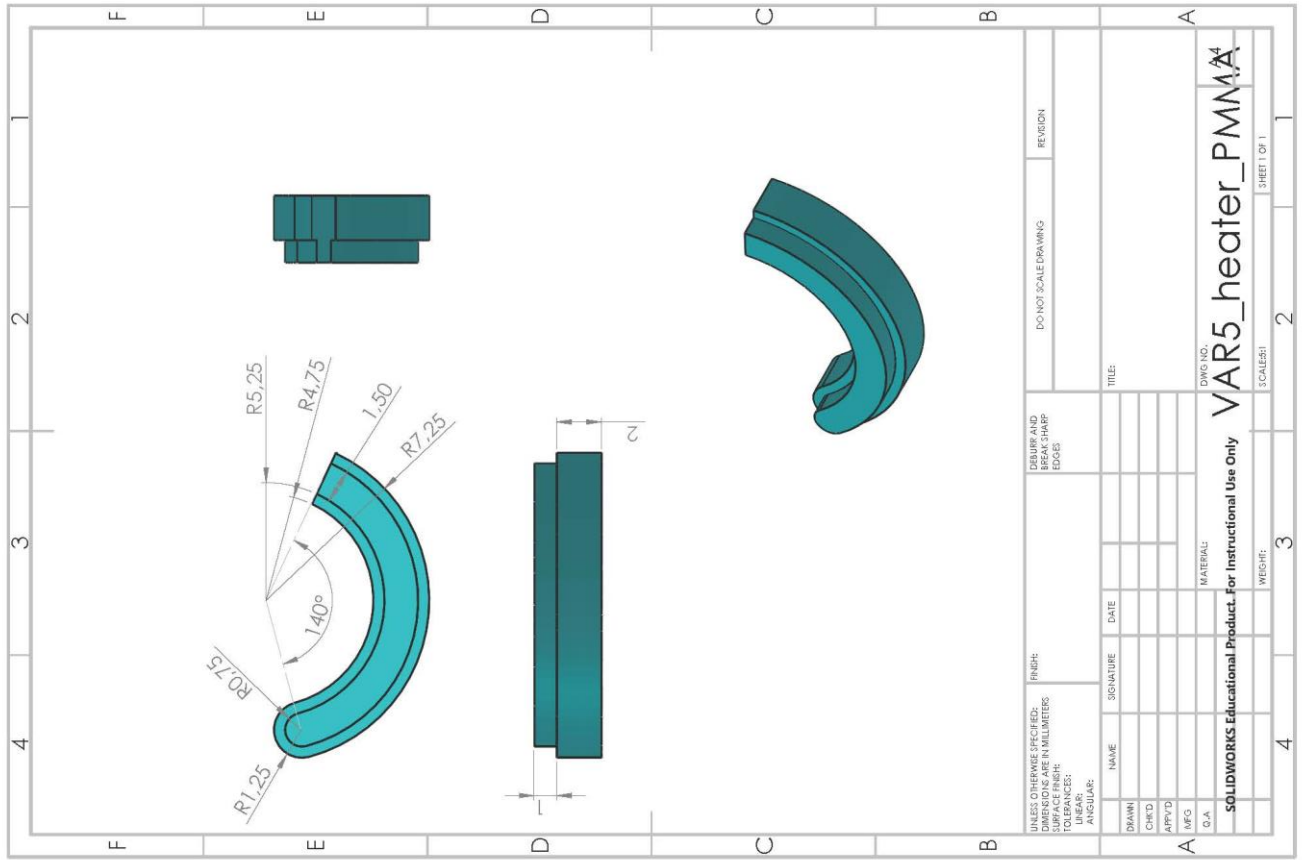








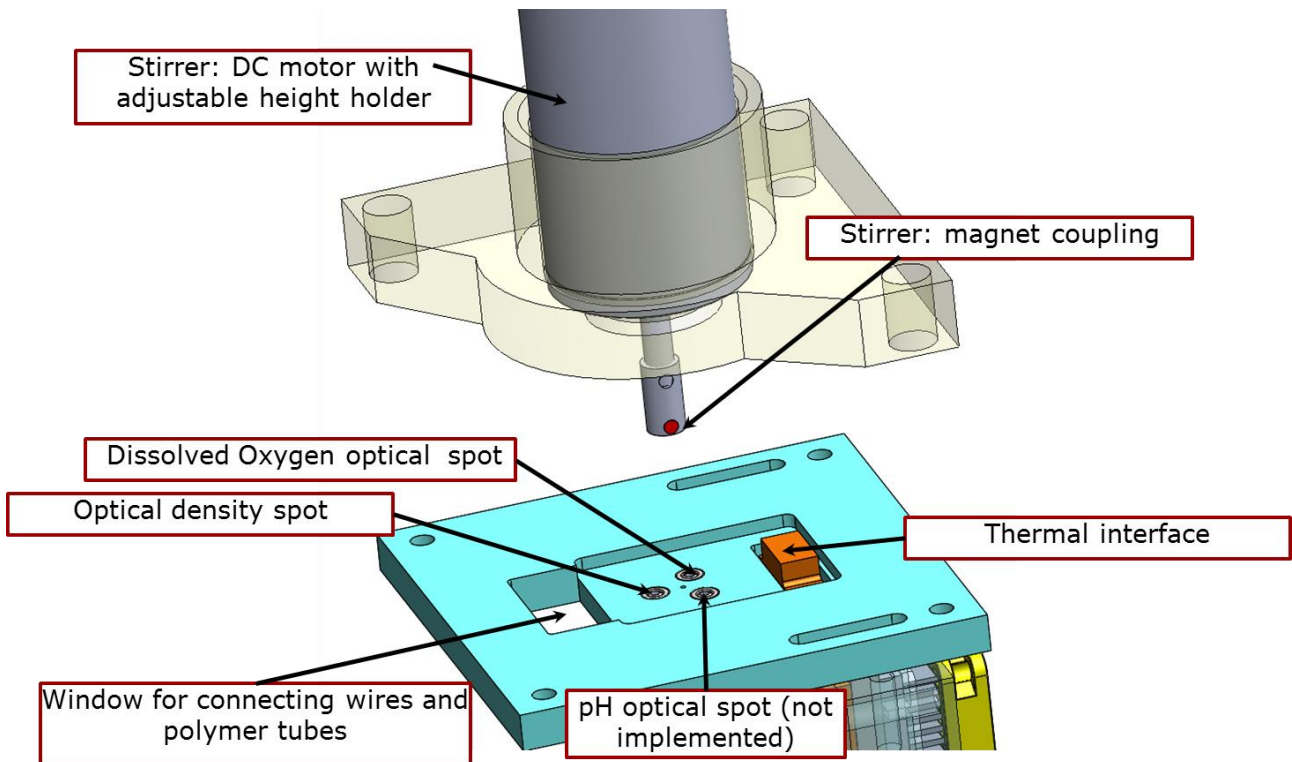
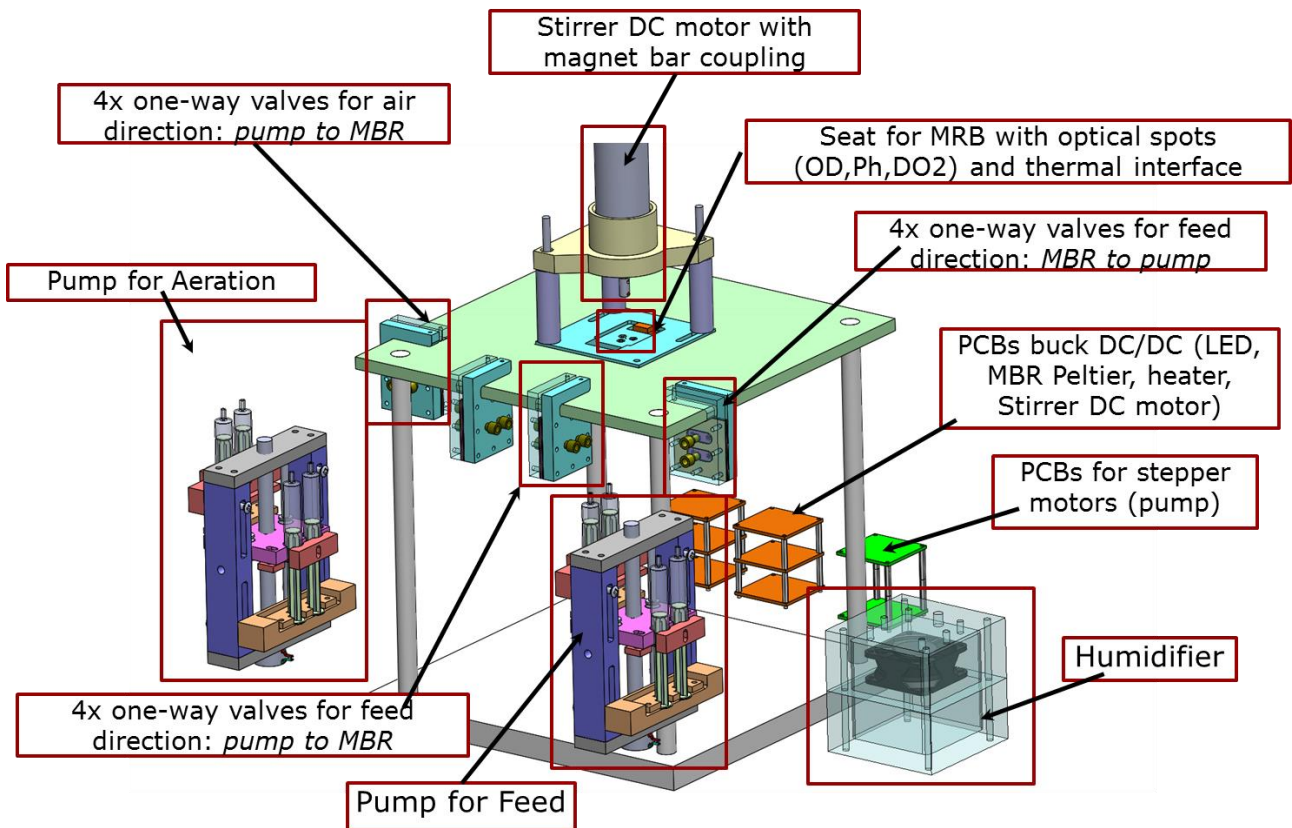


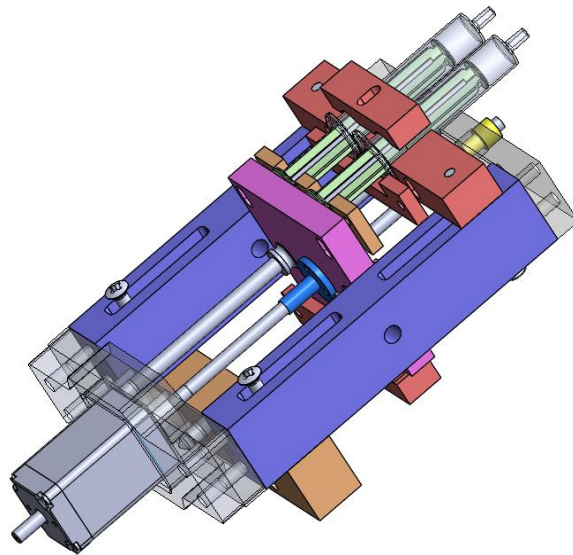
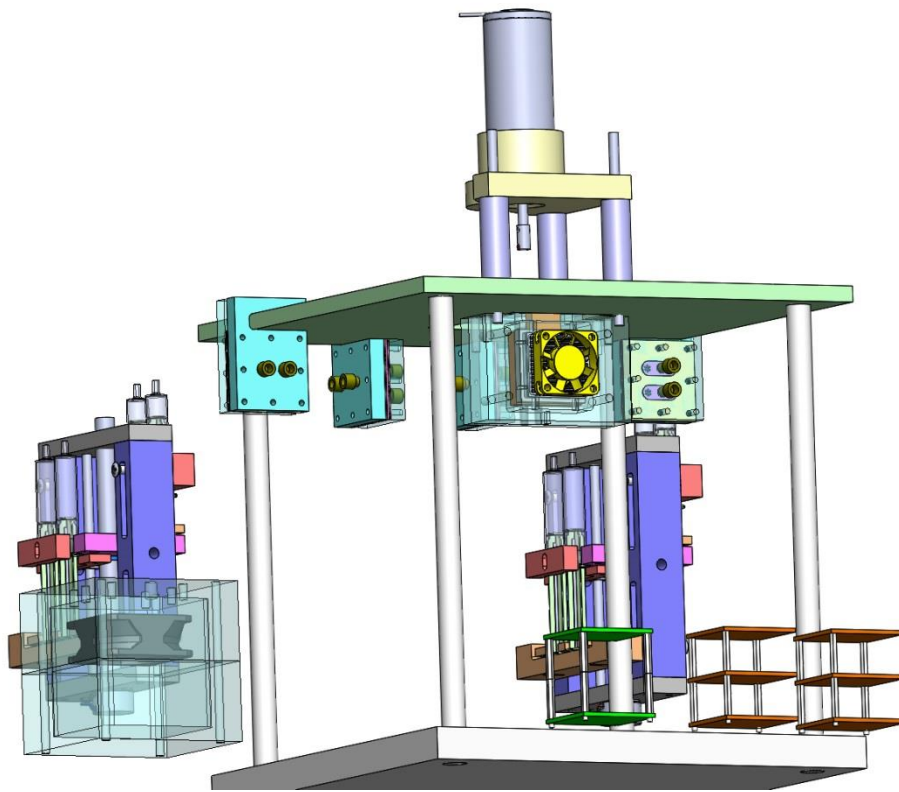


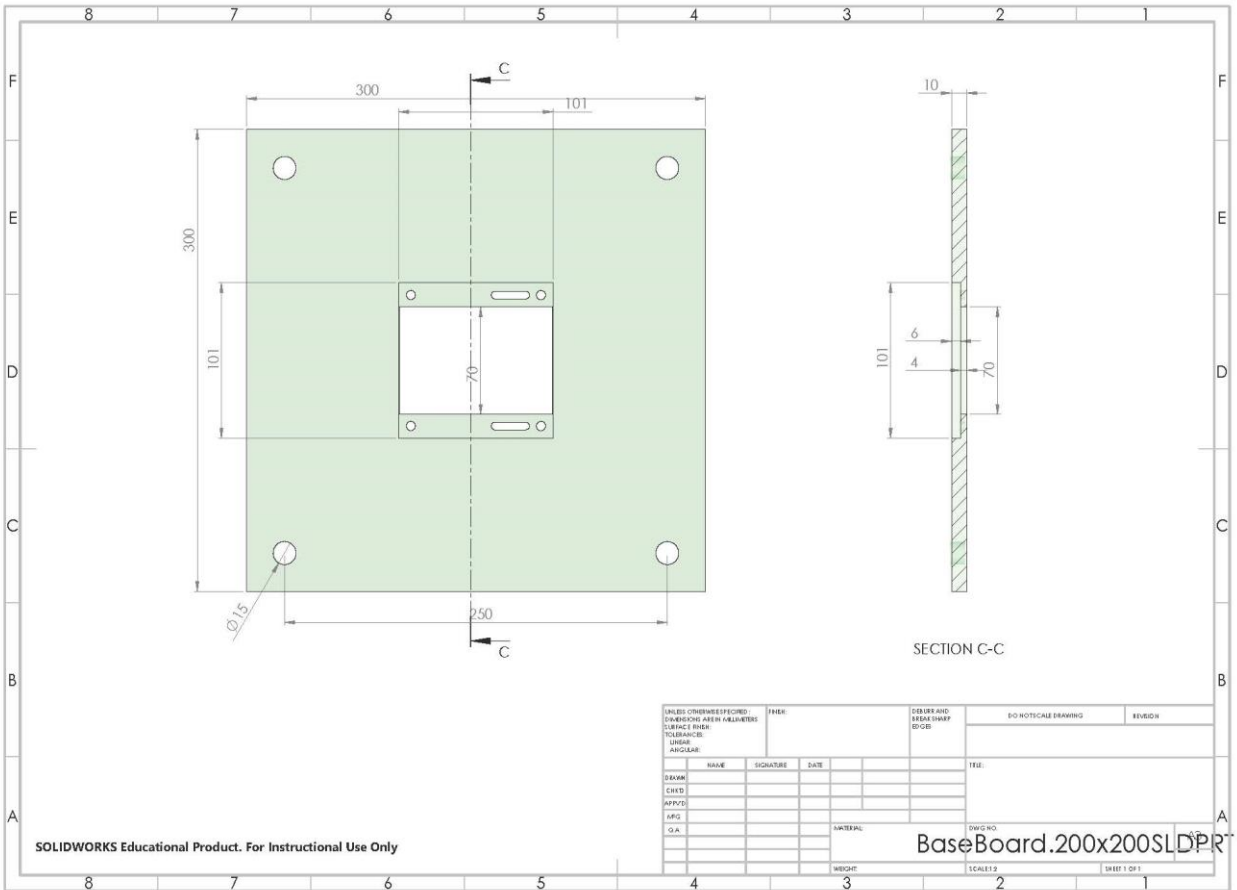
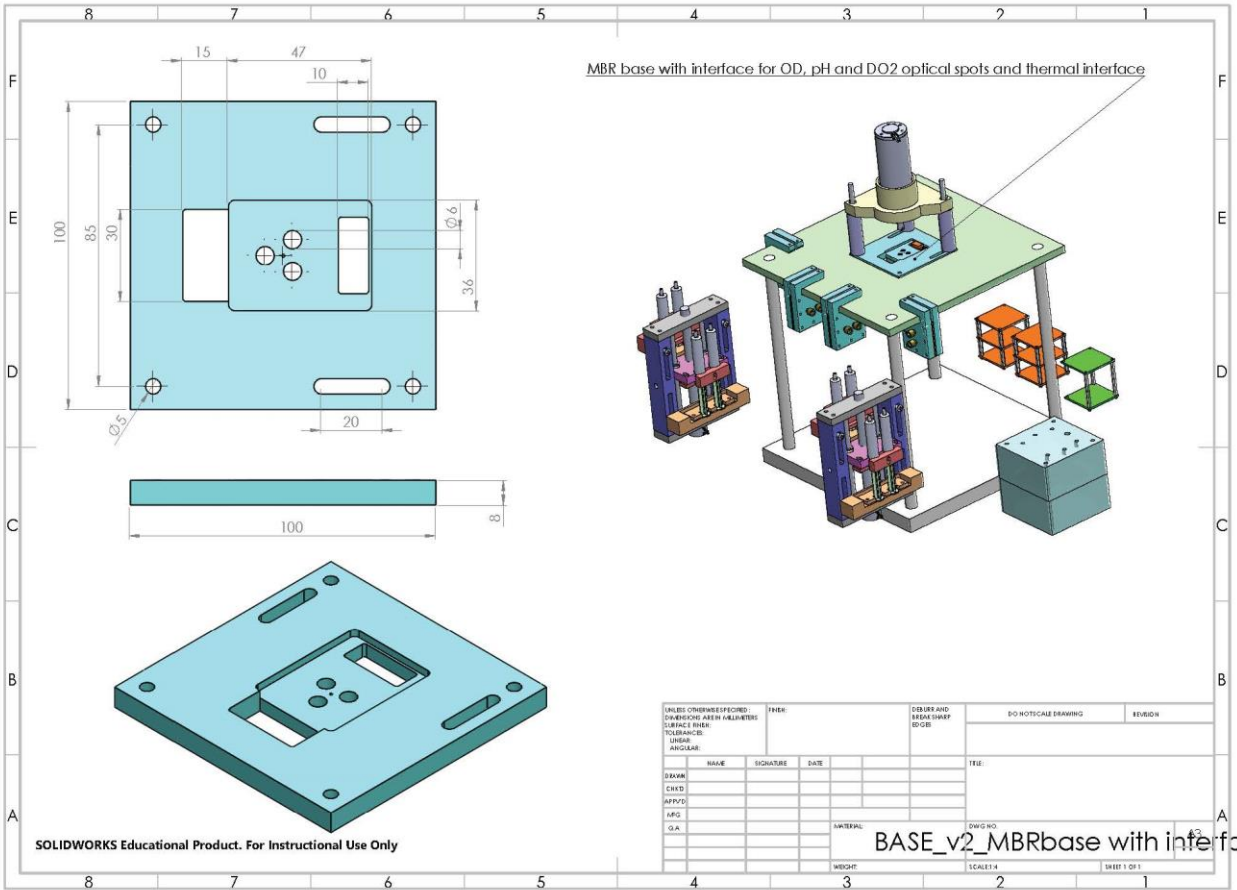
UNLESS OTHERWISE SPECIFIED: DIMENSIONS ARE IN MILLIMETERS		FINISH:	DEBURR AND BREAK SHARP EDGES	DO NOT SCALE DRAWING	REVISION
TOLERANCES:					
LINEAR:					
ANGULAR:					
DRWN	NAME	SIGNATURE	DATE	TITLE:	
CHKD					
APP'D					
MFG					
D.A.					
MATERIAL:			DWG. NO.:		
			VAR5_heater_PMM.A		
SOLIDWORKS Educational Product. For Instructional Use Only			SCALE(S):		
			SHEET 1 OF 1		

# Appendix C

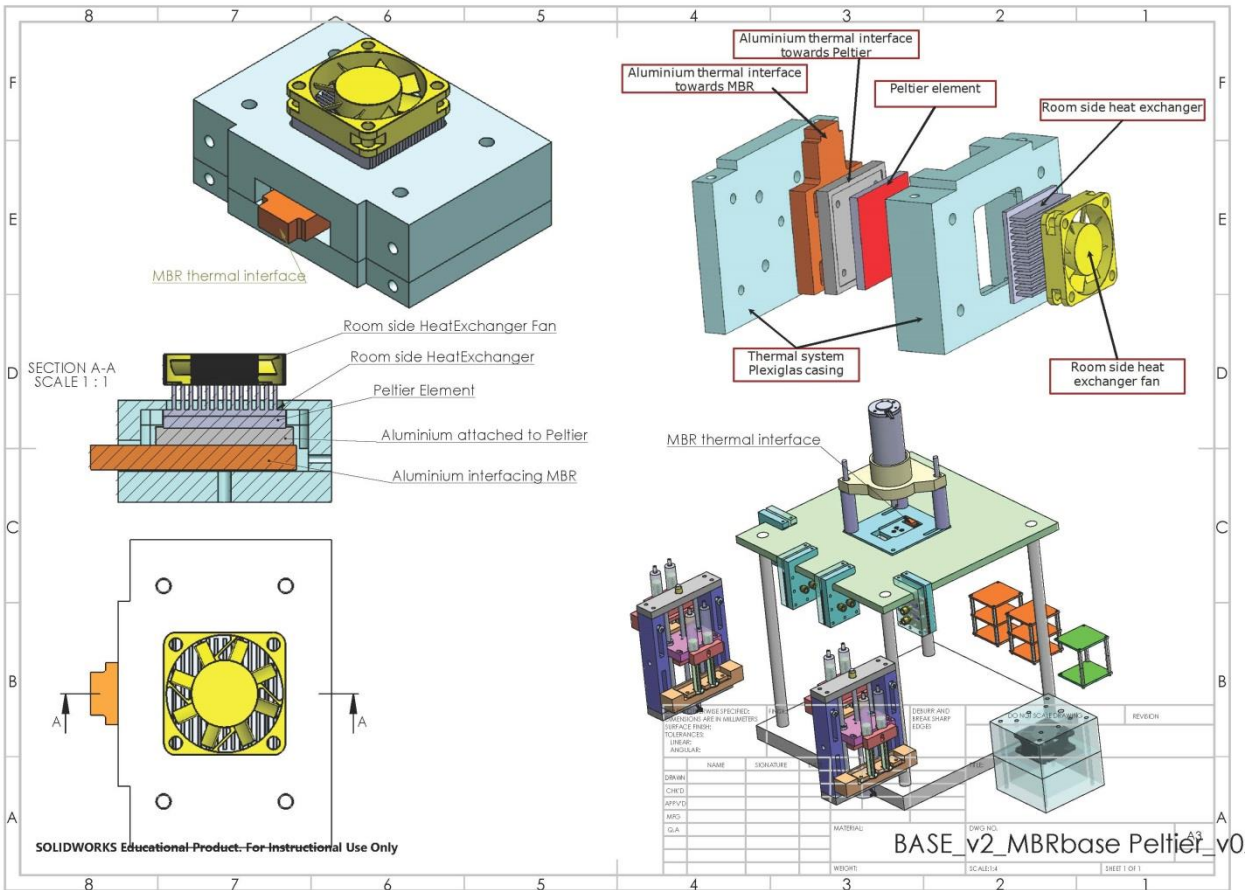
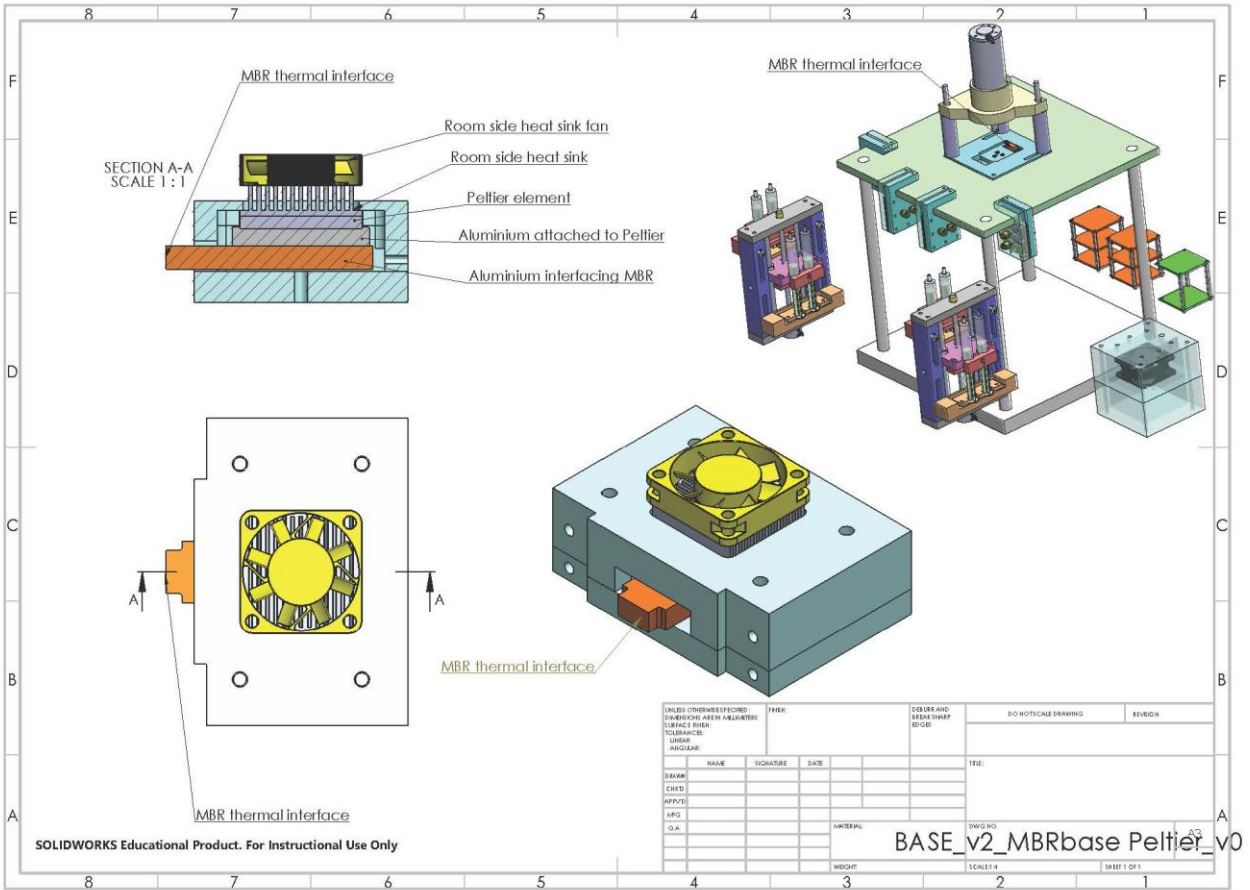
## Milliliter scale bioreactor prototype II



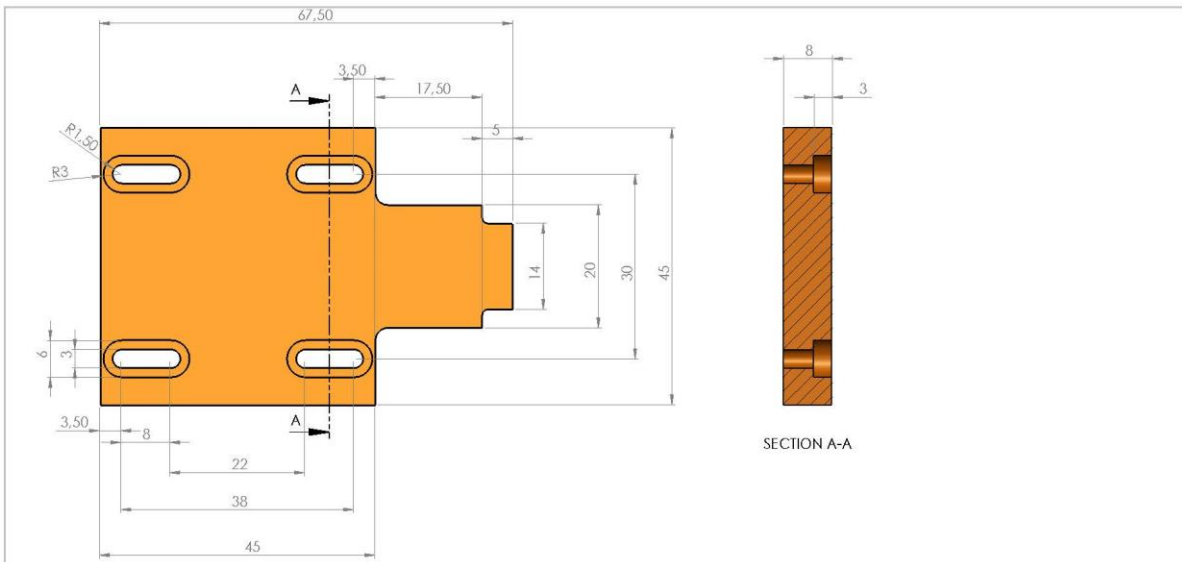








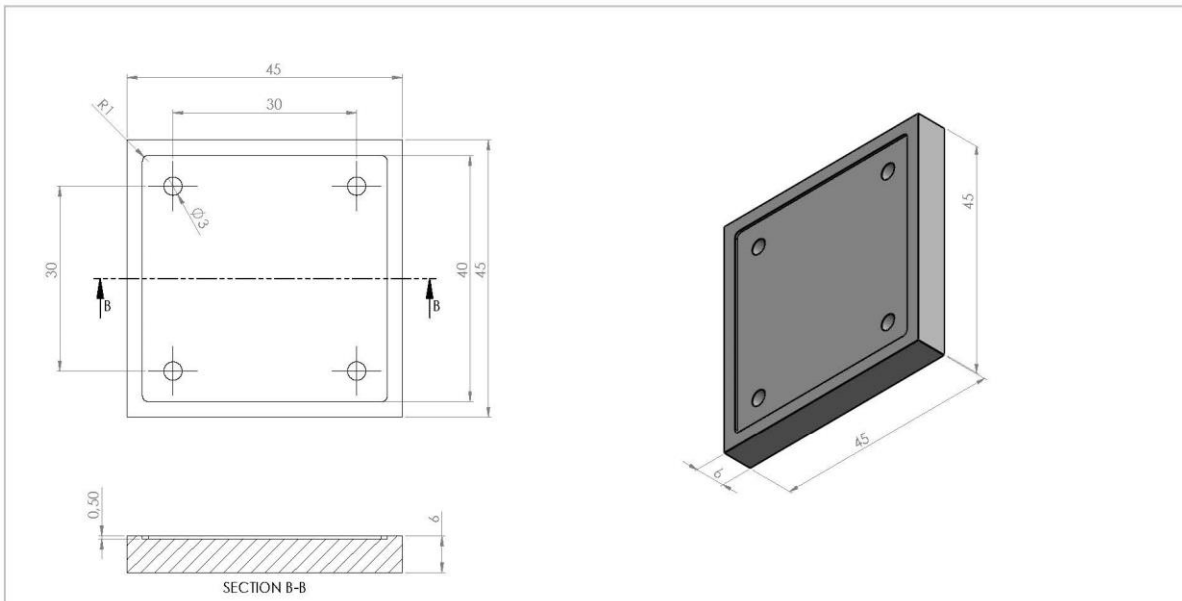




SECTION A-A

SolidWorks Student Edition.  
For Academic Use Only.

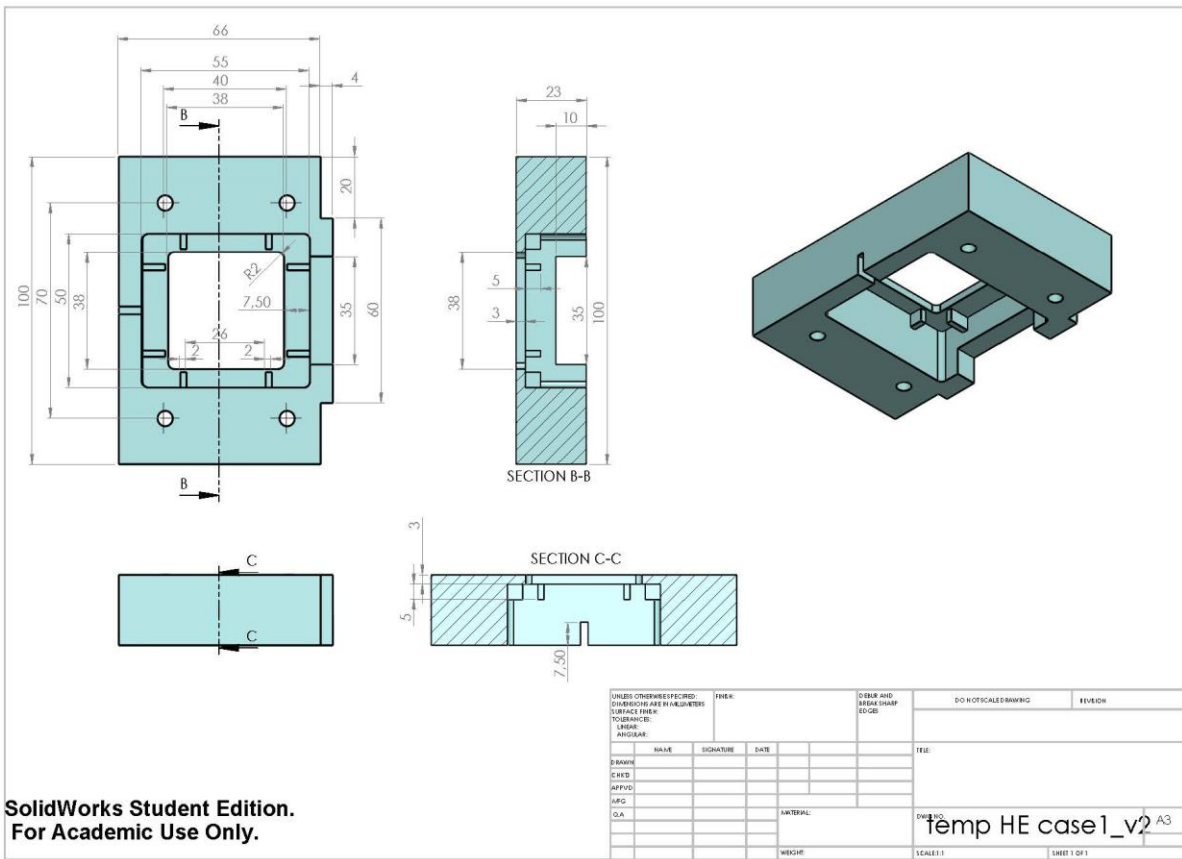
UNLESS OTHERWISE SPECIFIED: DIMENSIONS ARE IN MILLIMETERS SURFACE FINISH: TOLERANCES: LINEAR ANGULAR				FINISH:	DIMENSIONS AND BREAKS: SHARP EDGES	DO NOT SCALE DRAWING	REVISION
NAME	SIGNATURE	DATE				TITLE	
DRAWN							
CHECKED							
APPROVED							
DATE							
QA				MATERIAL:		DWG NO. Aluminum_sheet1	A3
				WEIGHT:		SCALE: 1:1	SHEET 1 OF 1



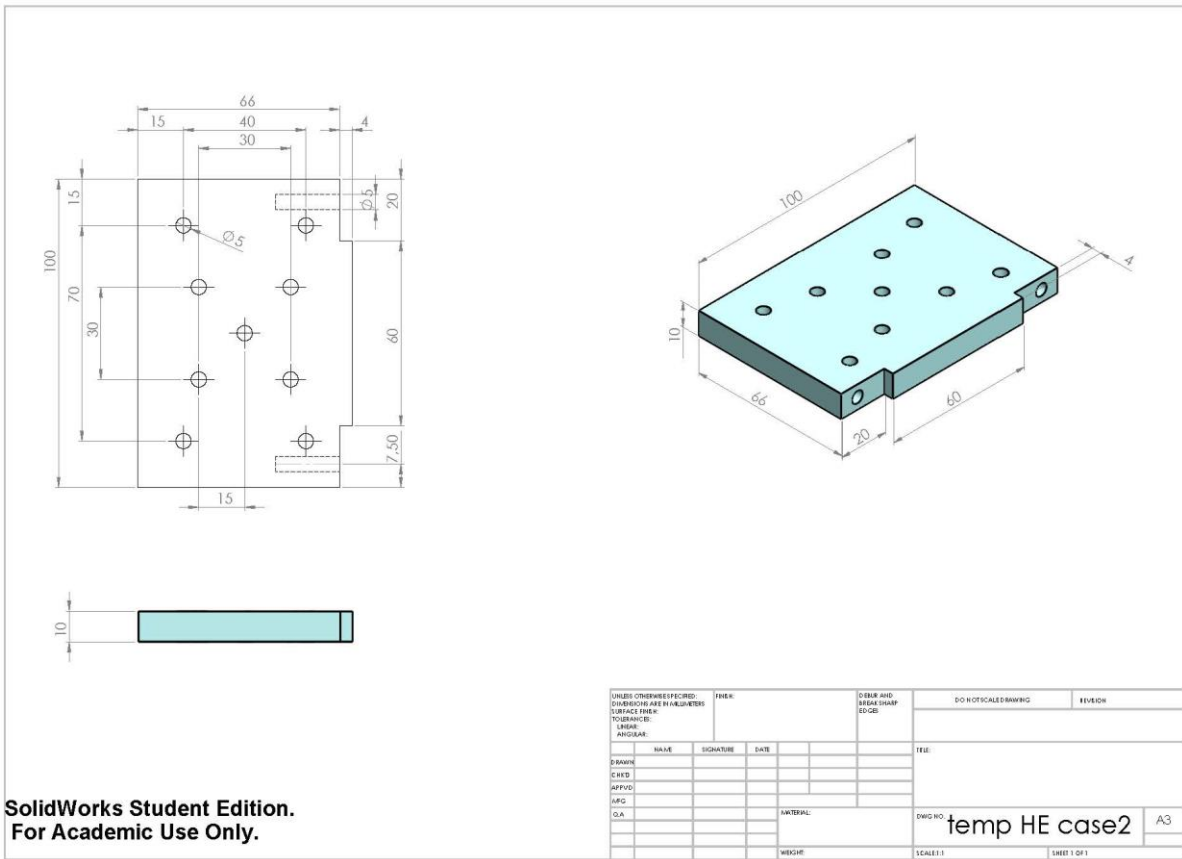
SECTION B-B

SolidWorks Student Edition.  
For Academic Use Only.

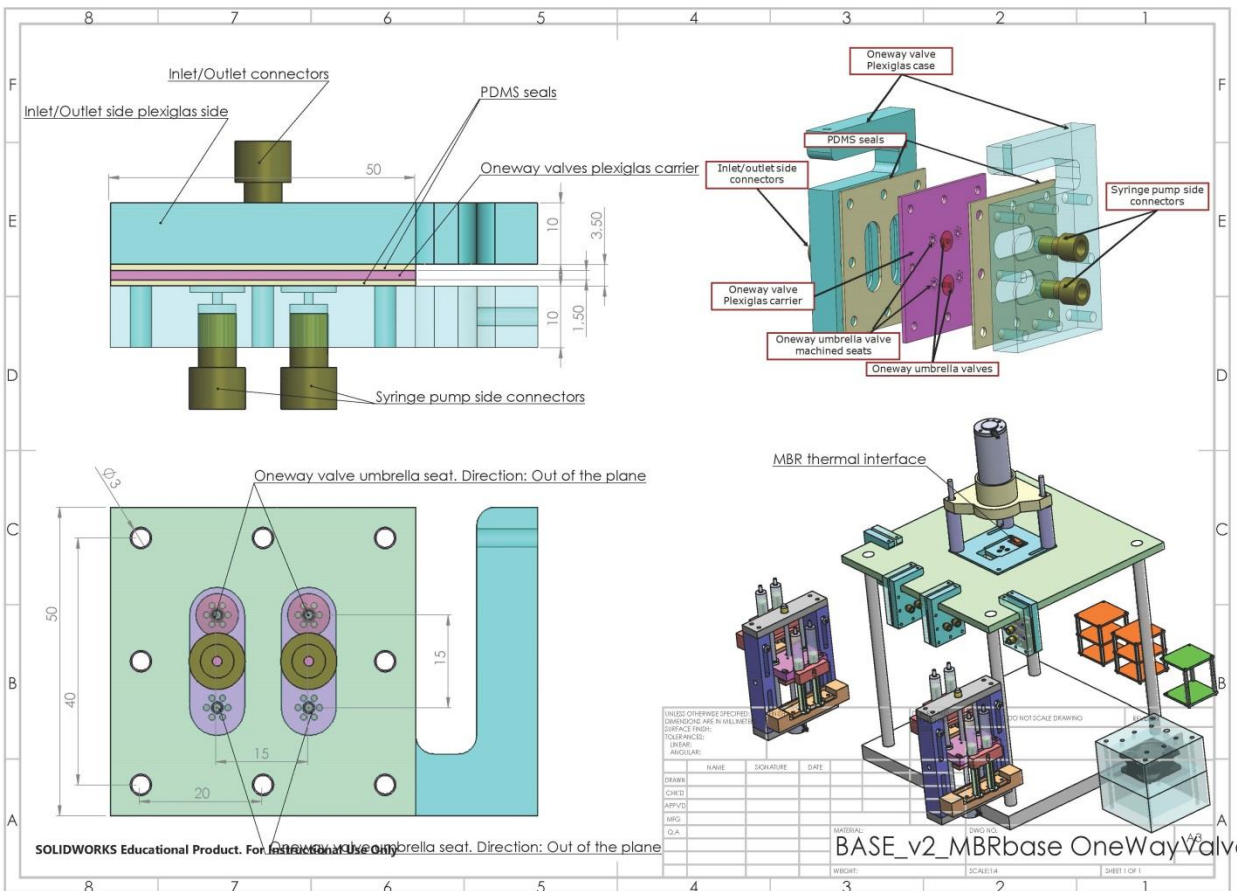
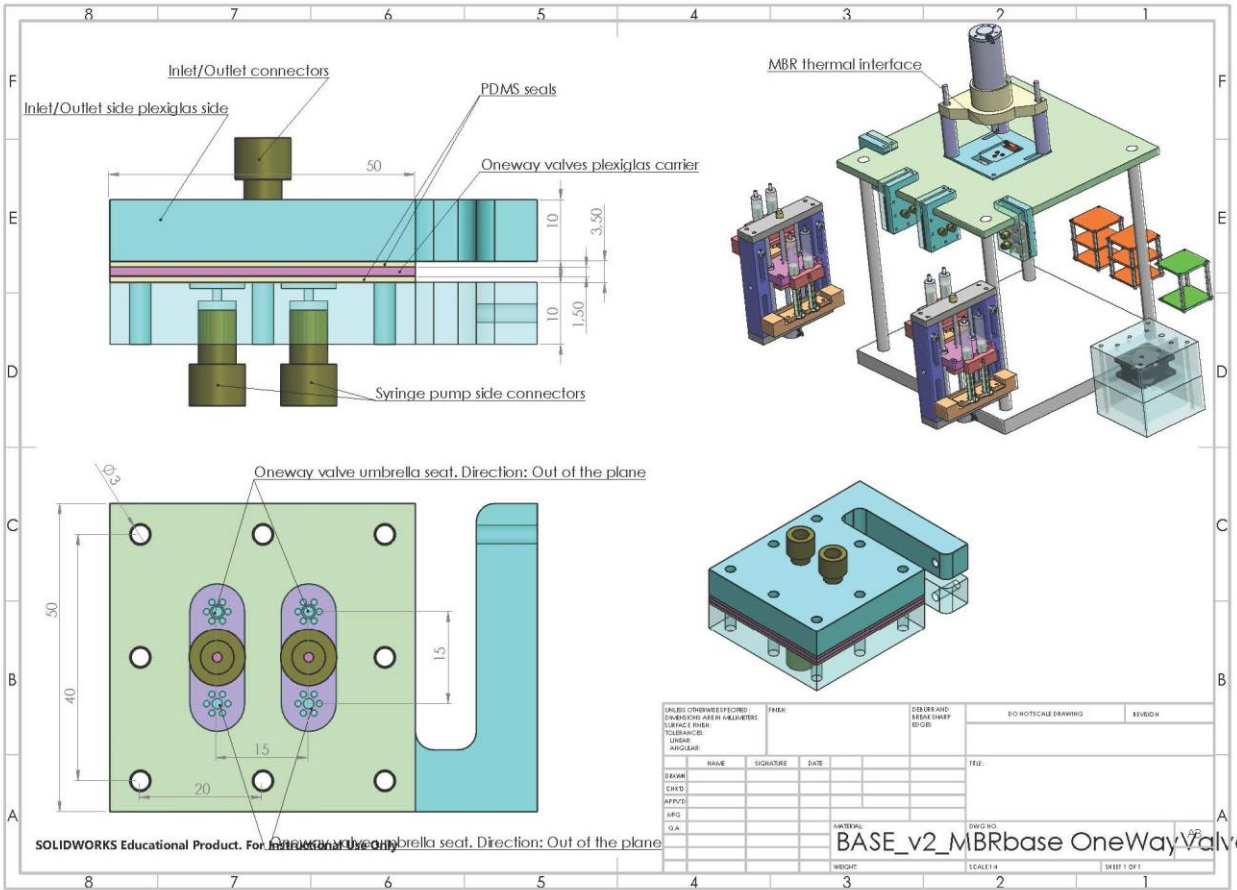
UNLESS OTHERWISE SPECIFIED: DIMENSIONS ARE IN MILLIMETERS SURFACE FINISH: TOLERANCES: LINEAR ANGULAR				FINISH:	DIMENSIONS AND BREAKS: SHARP EDGES	DO NOT SCALE DRAWING	REVISION
NAME	SIGNATURE	DATE				TITLE	
DRAWN							
CHECKED							
APPROVED							
DATE							
QA				MATERIAL:		DWG NO. Aluminum_sheet2	A3
				WEIGHT:		SCALE: 1:1	SHEET 1 OF 1

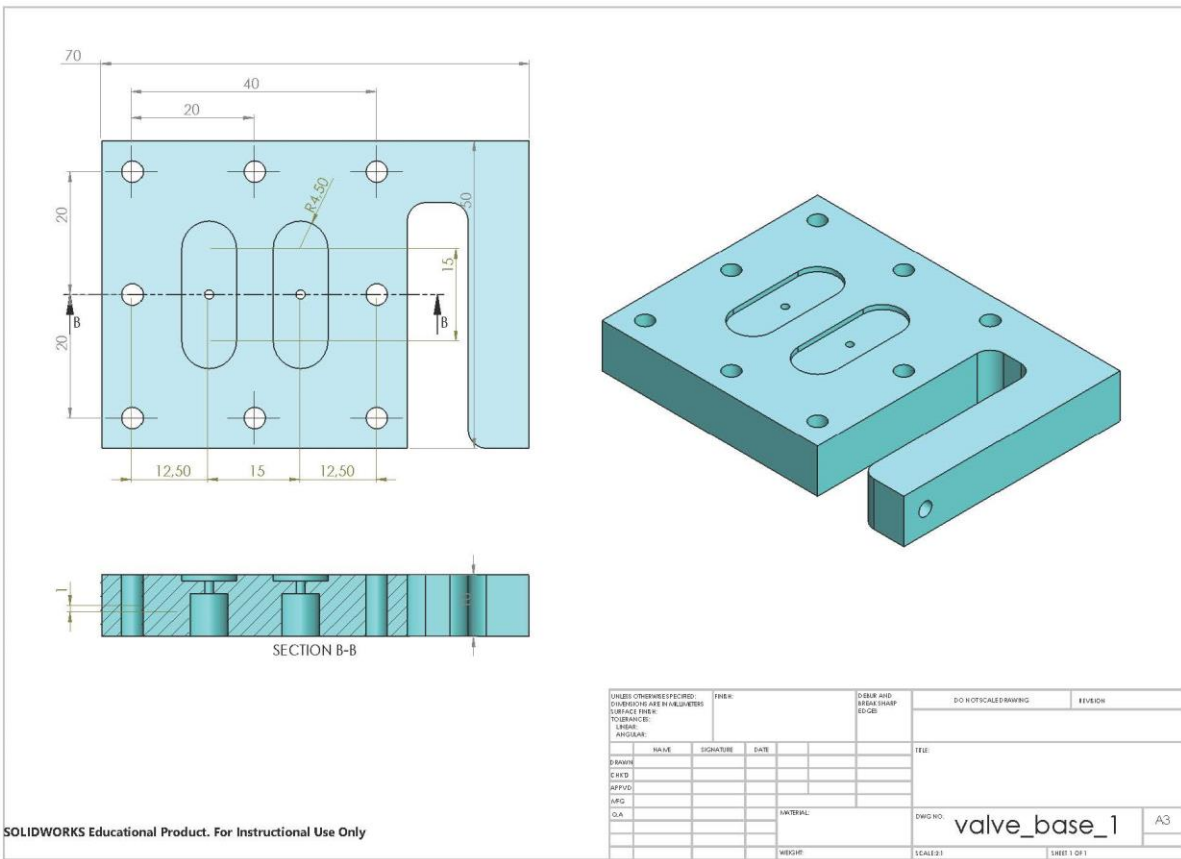


SolidWorks Student Edition.  
For Academic Use Only.

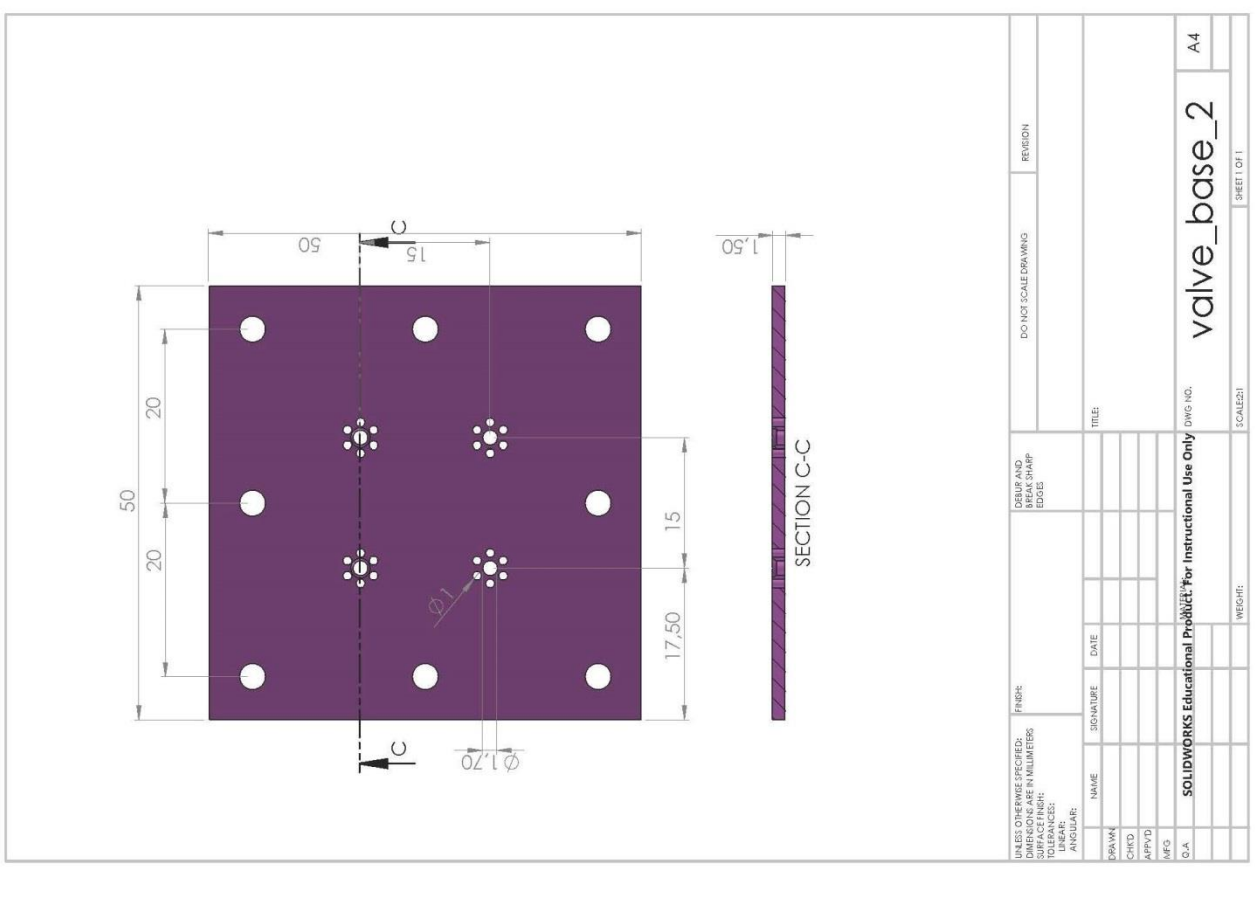


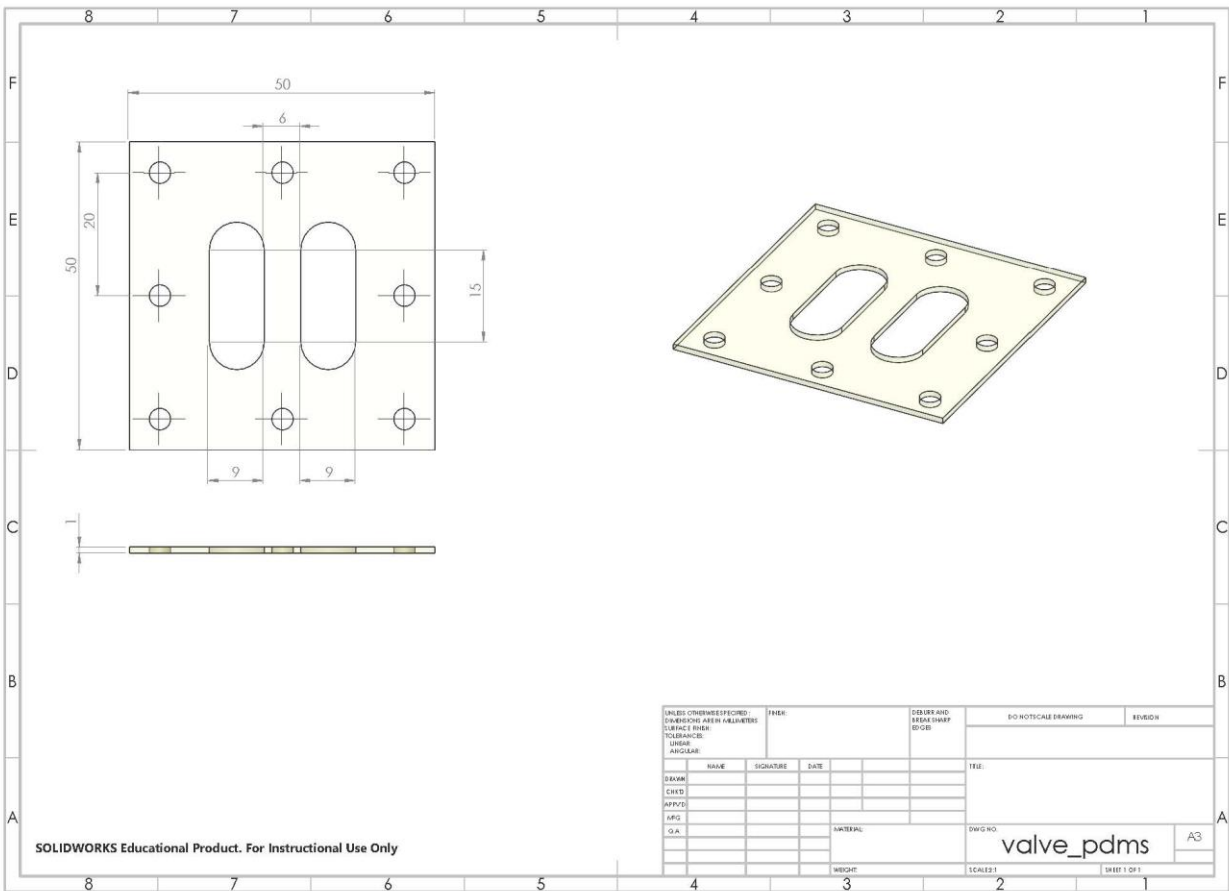
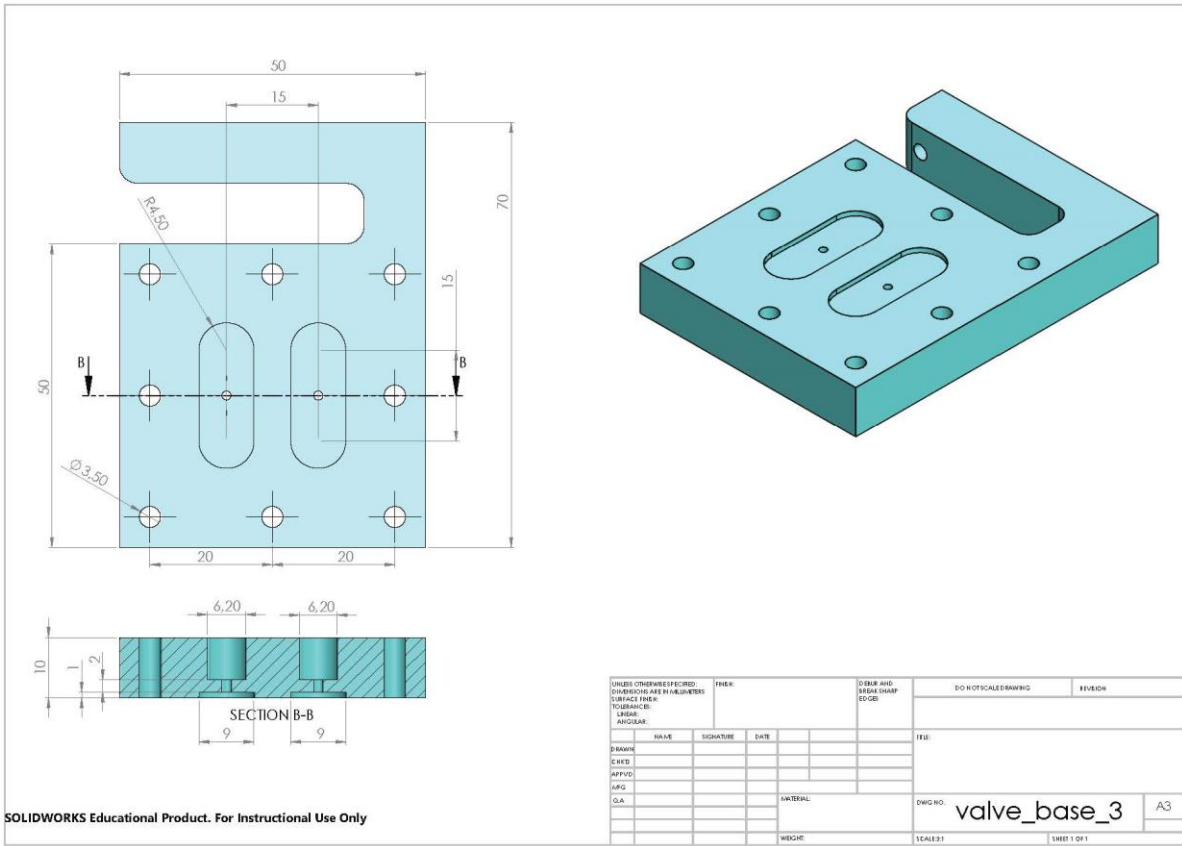
SolidWorks Student Edition.  
For Academic Use Only.

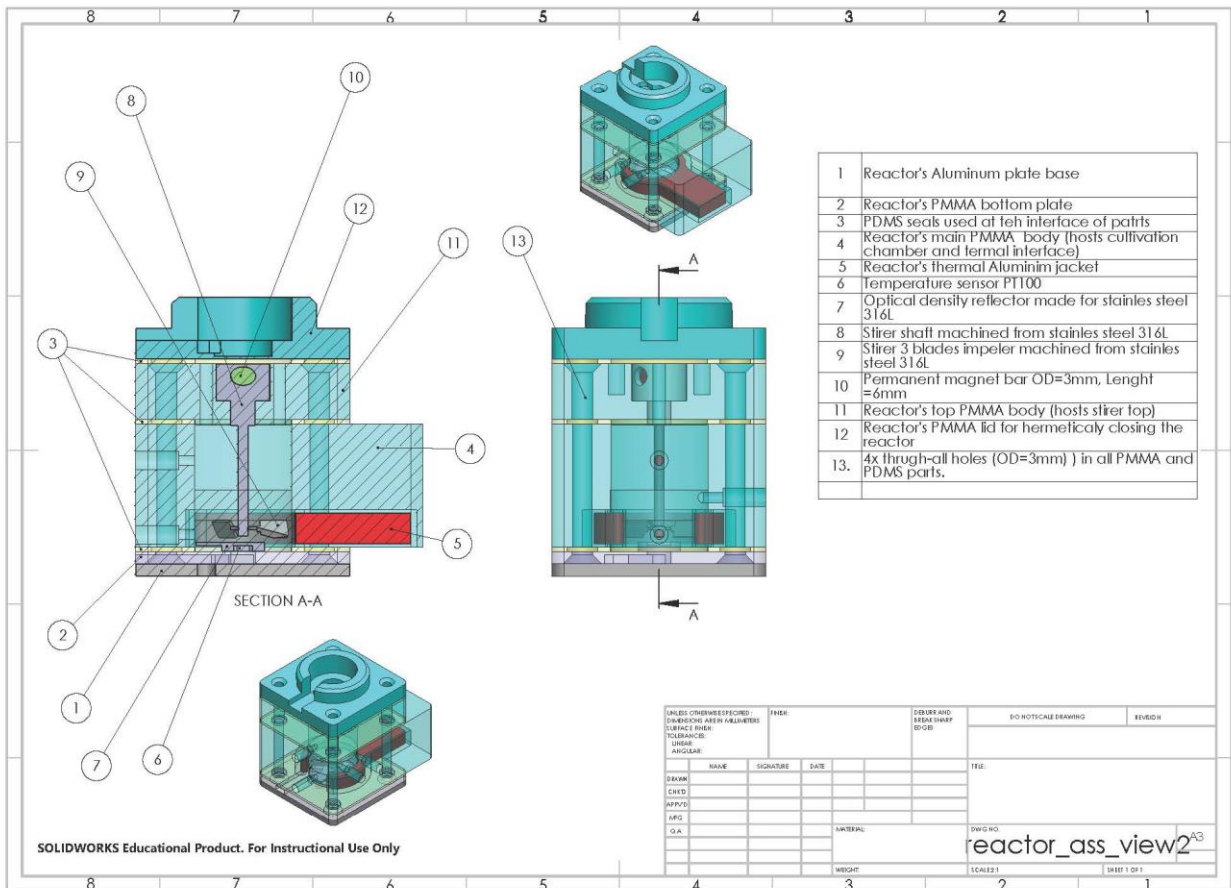
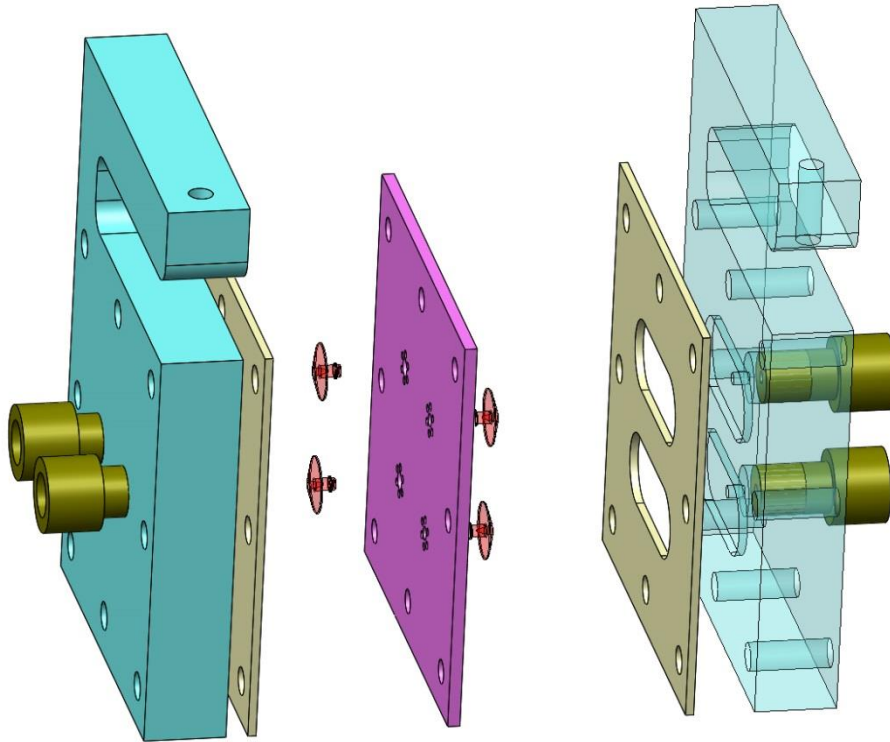


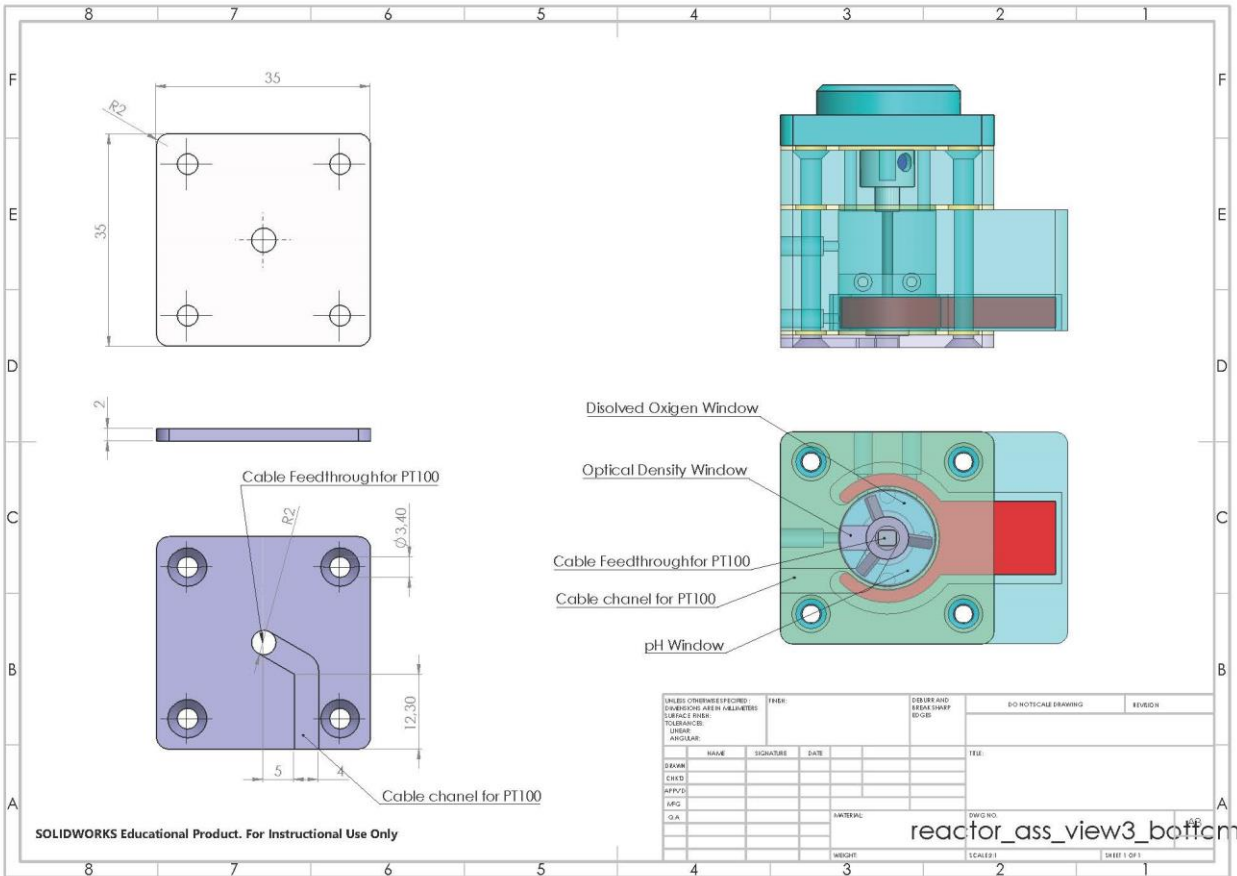
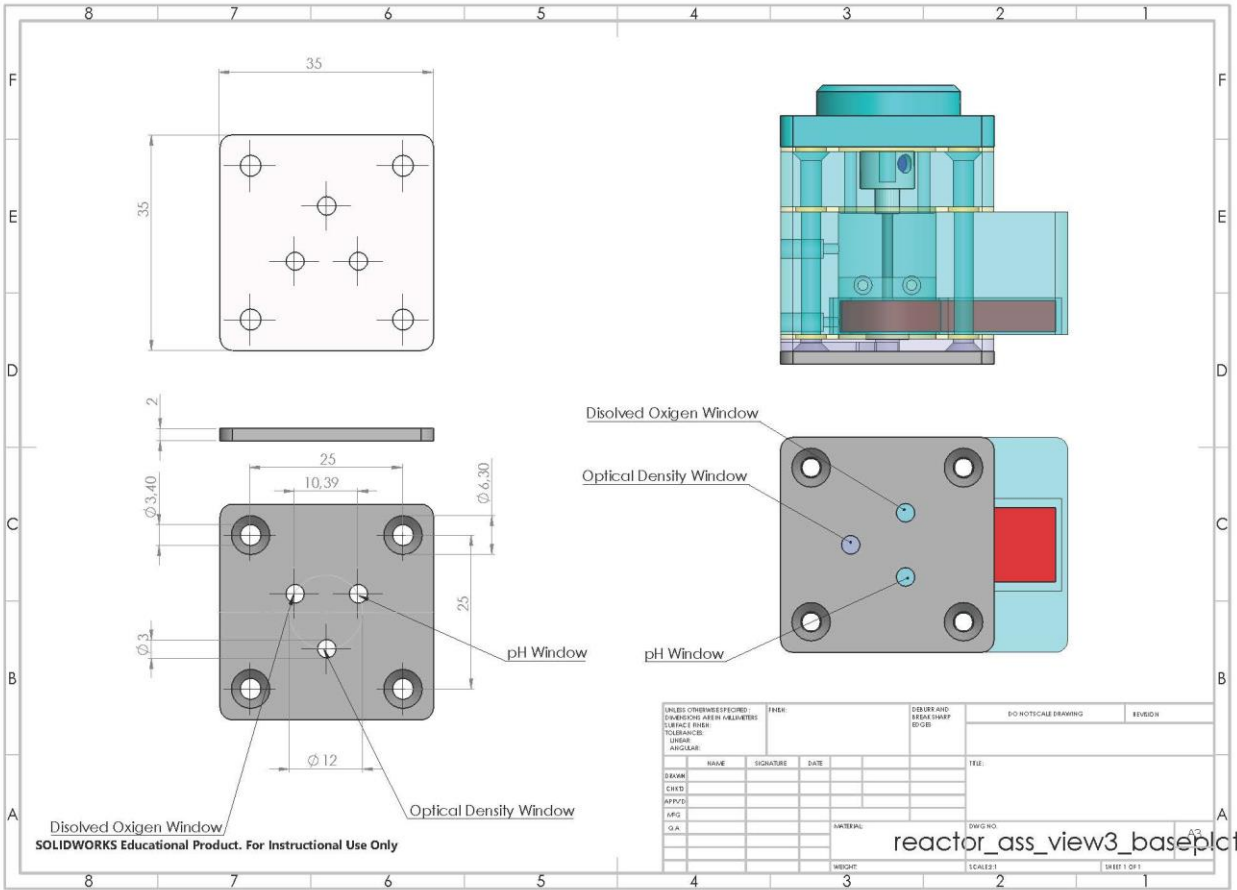


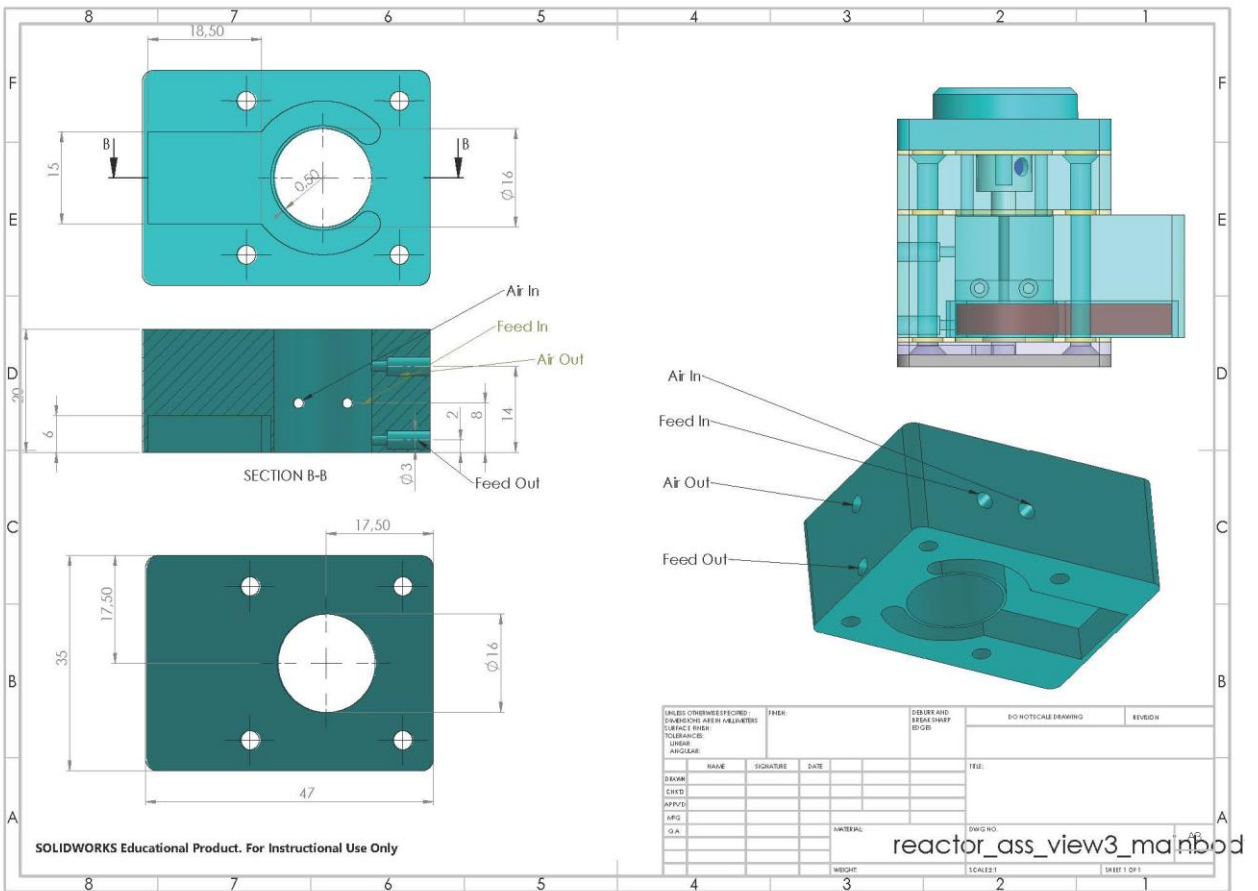
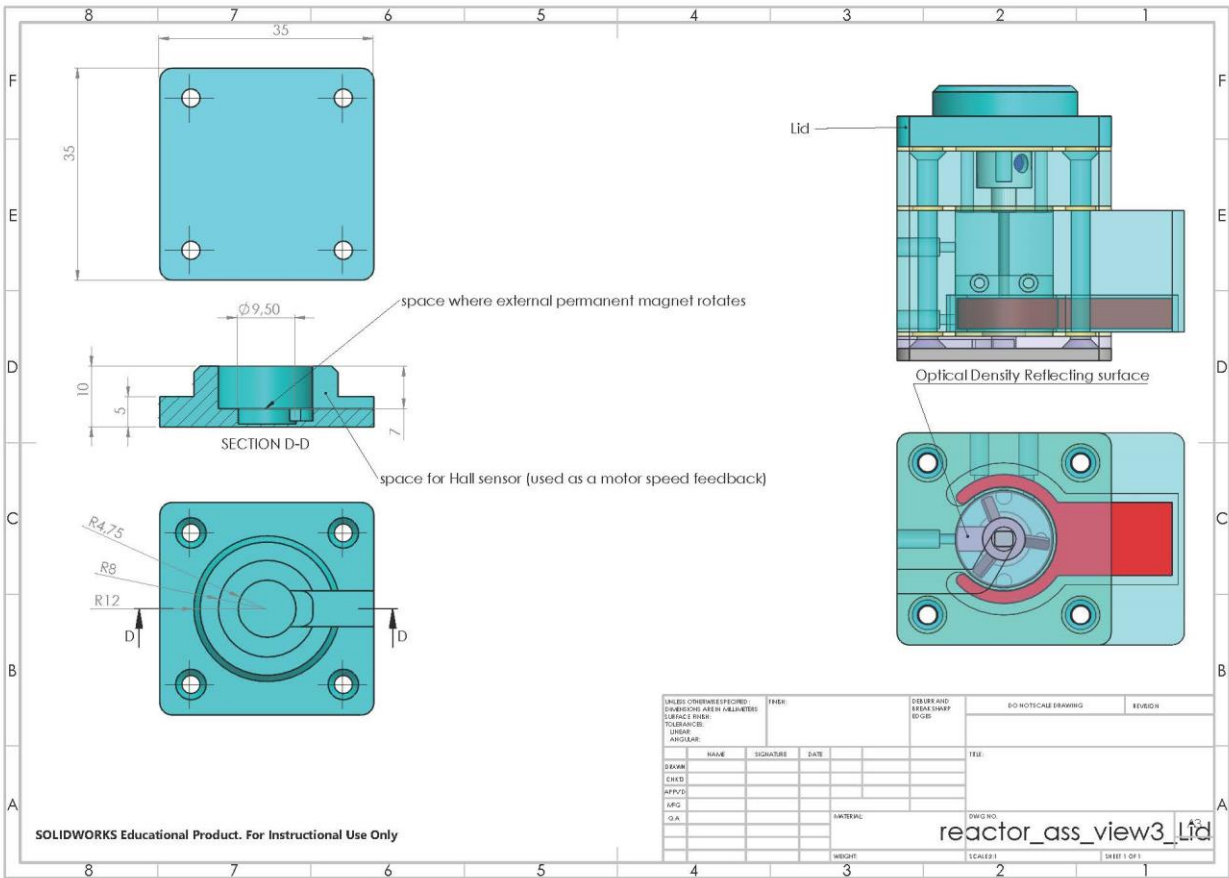
SOLIDWORKS Educational Product. For Instructional Use Only





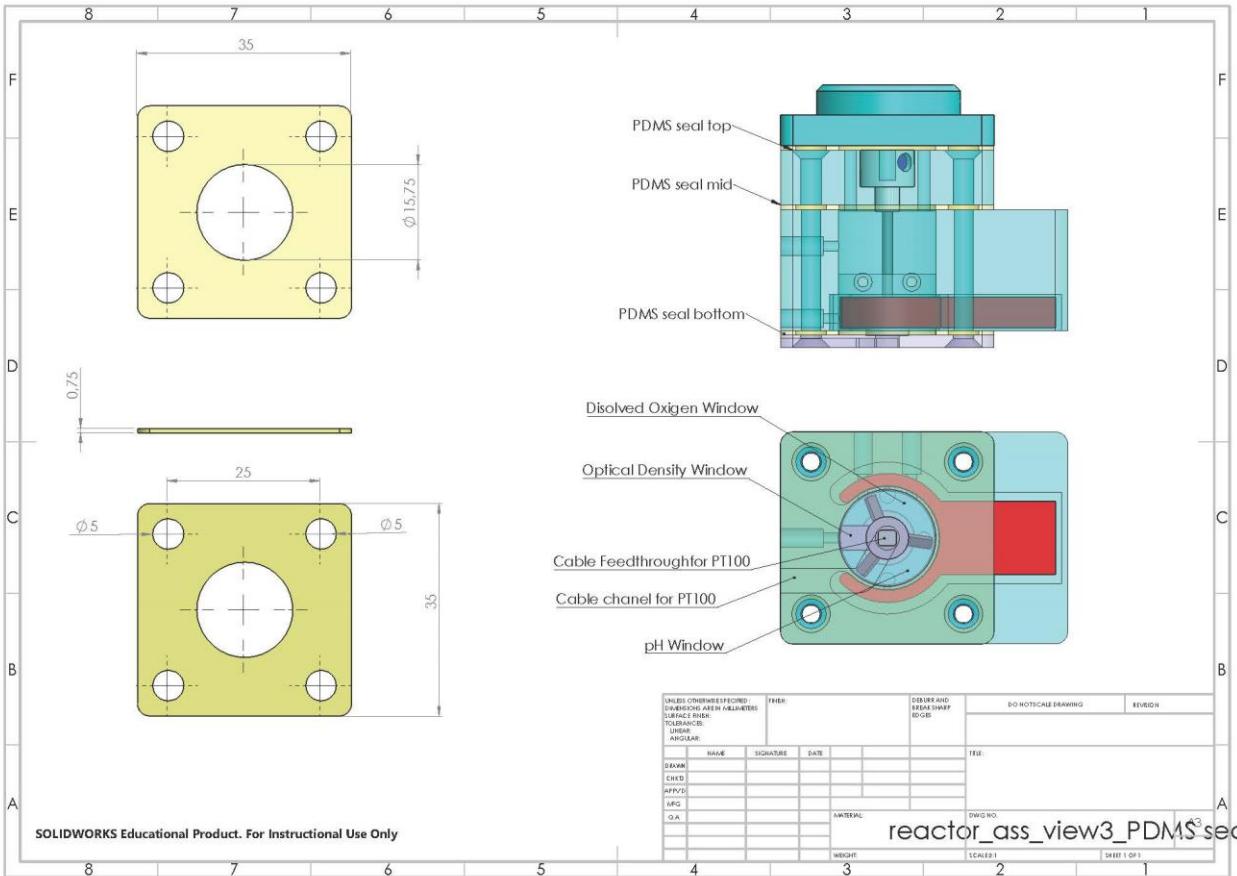
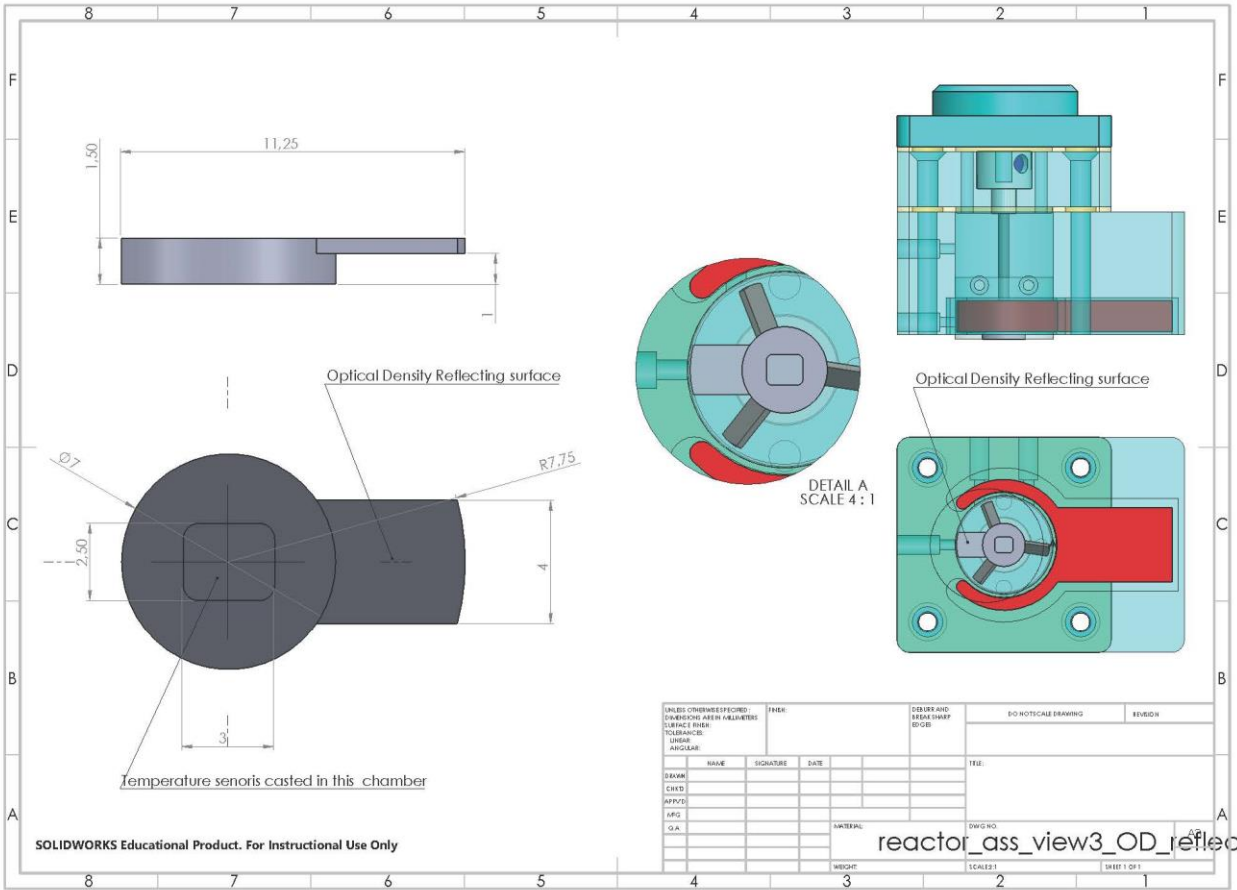


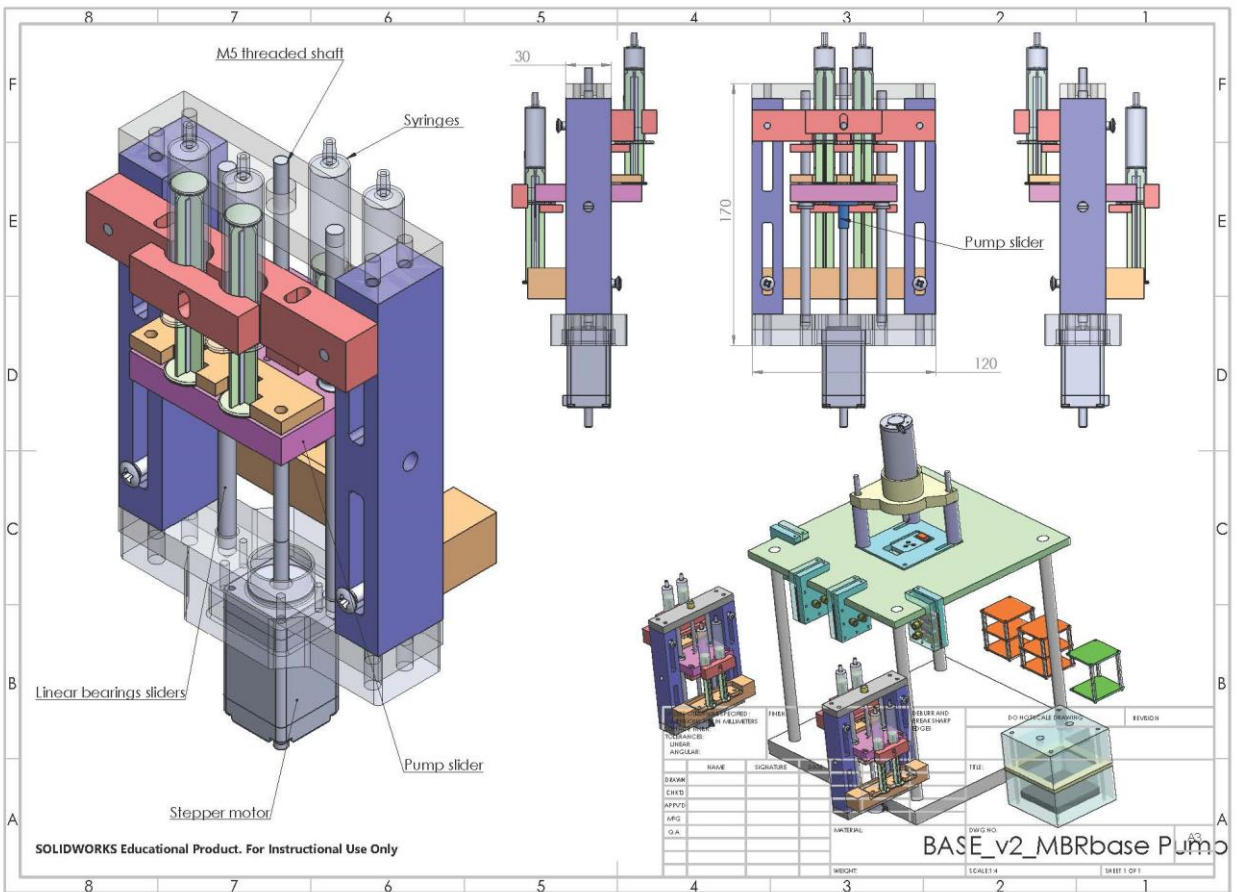
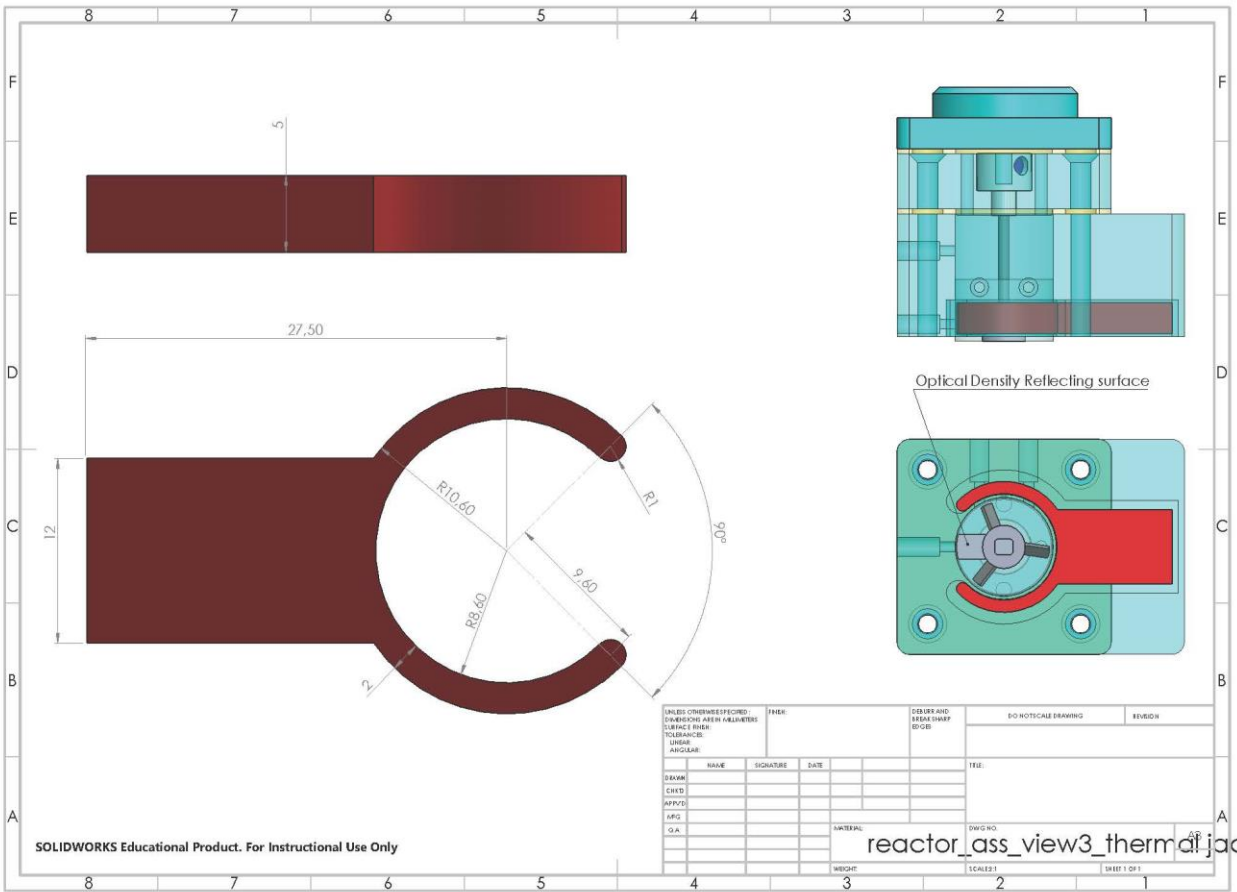


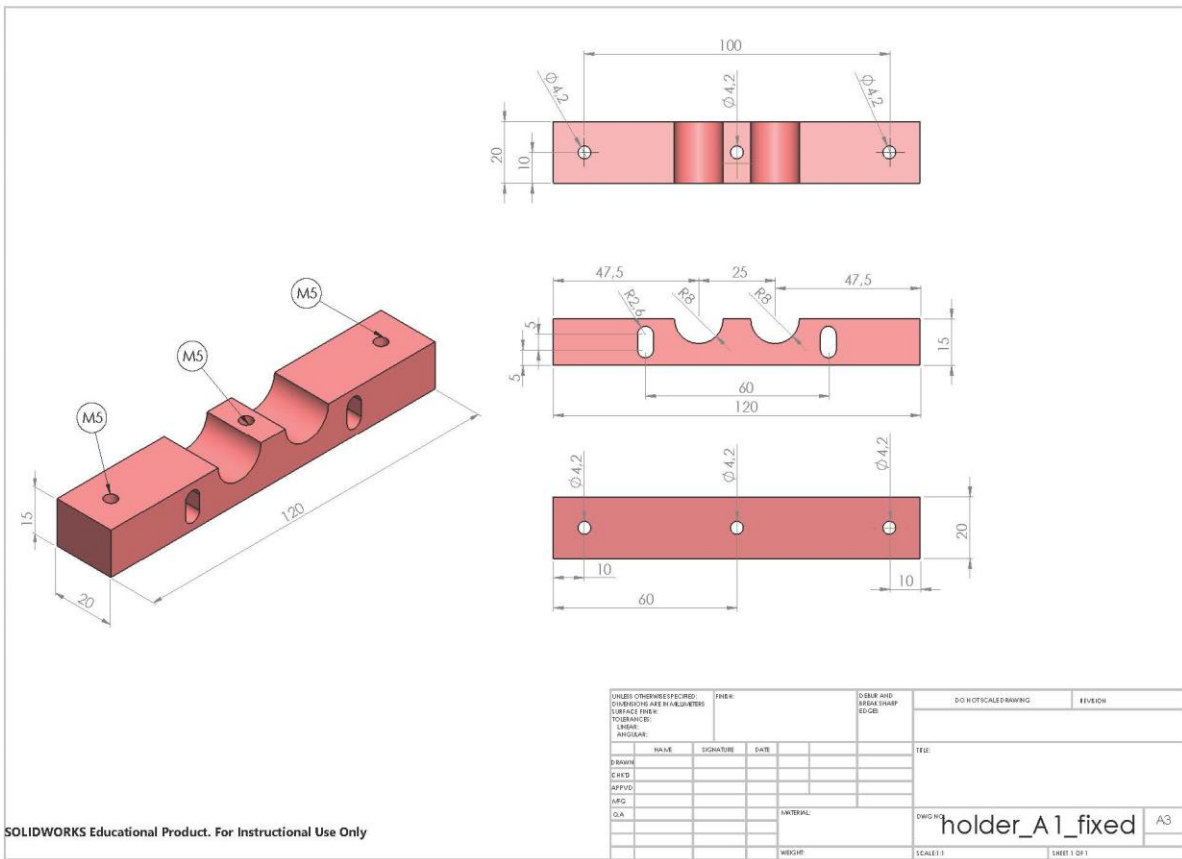




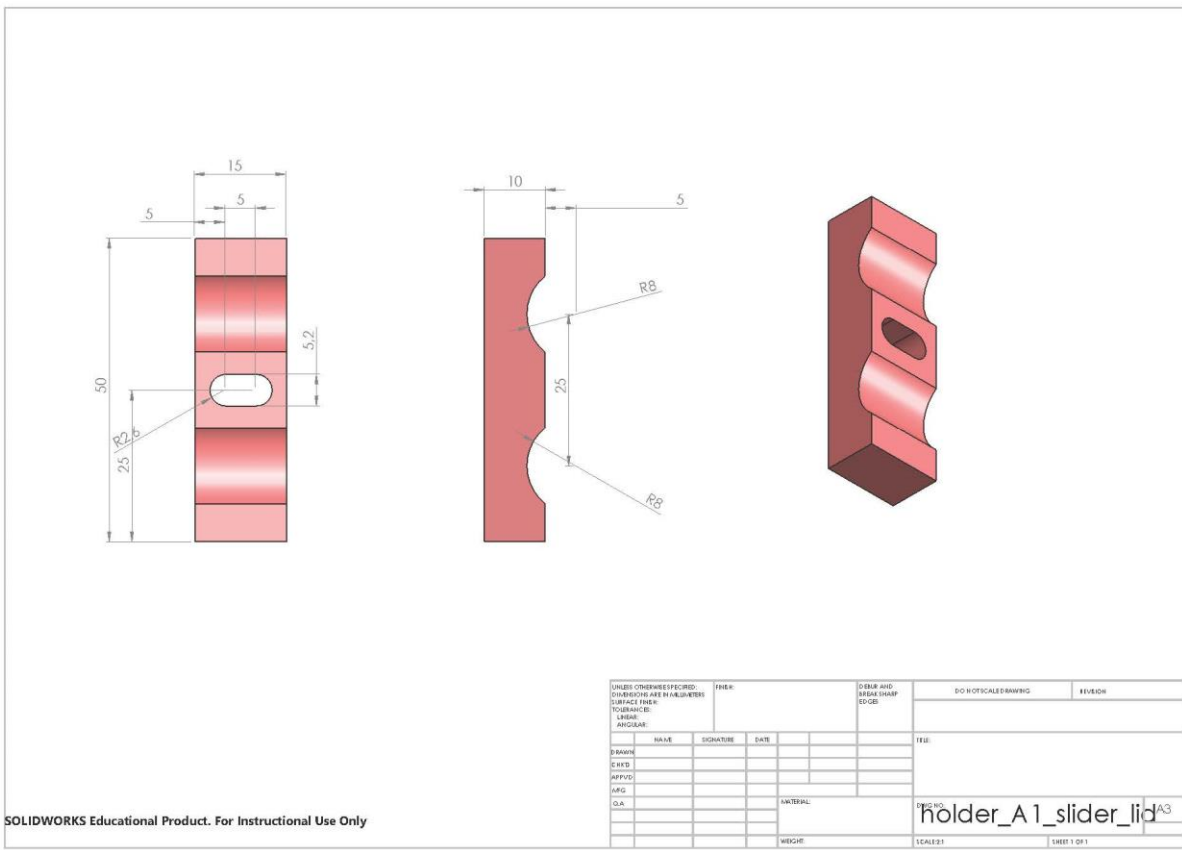




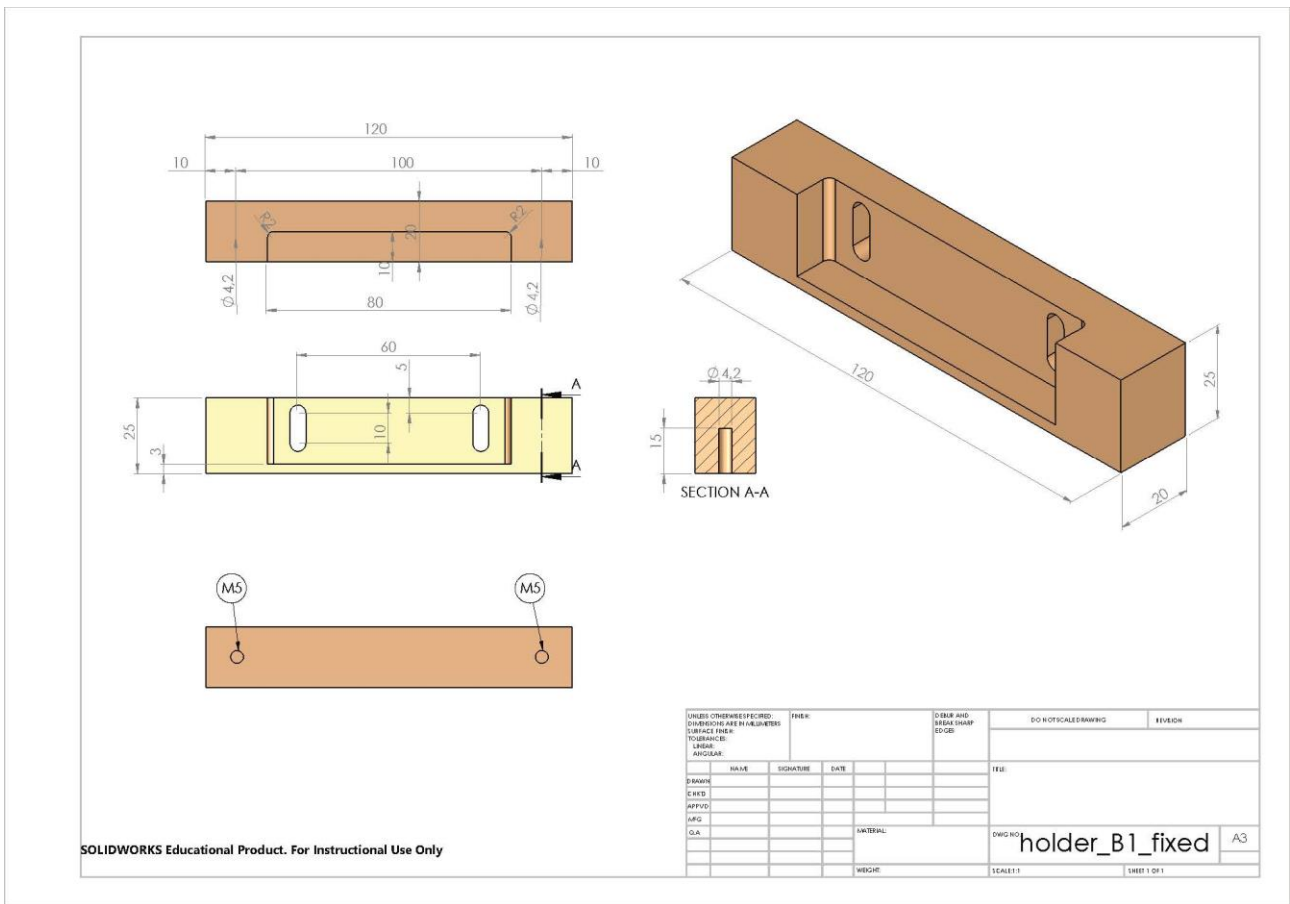
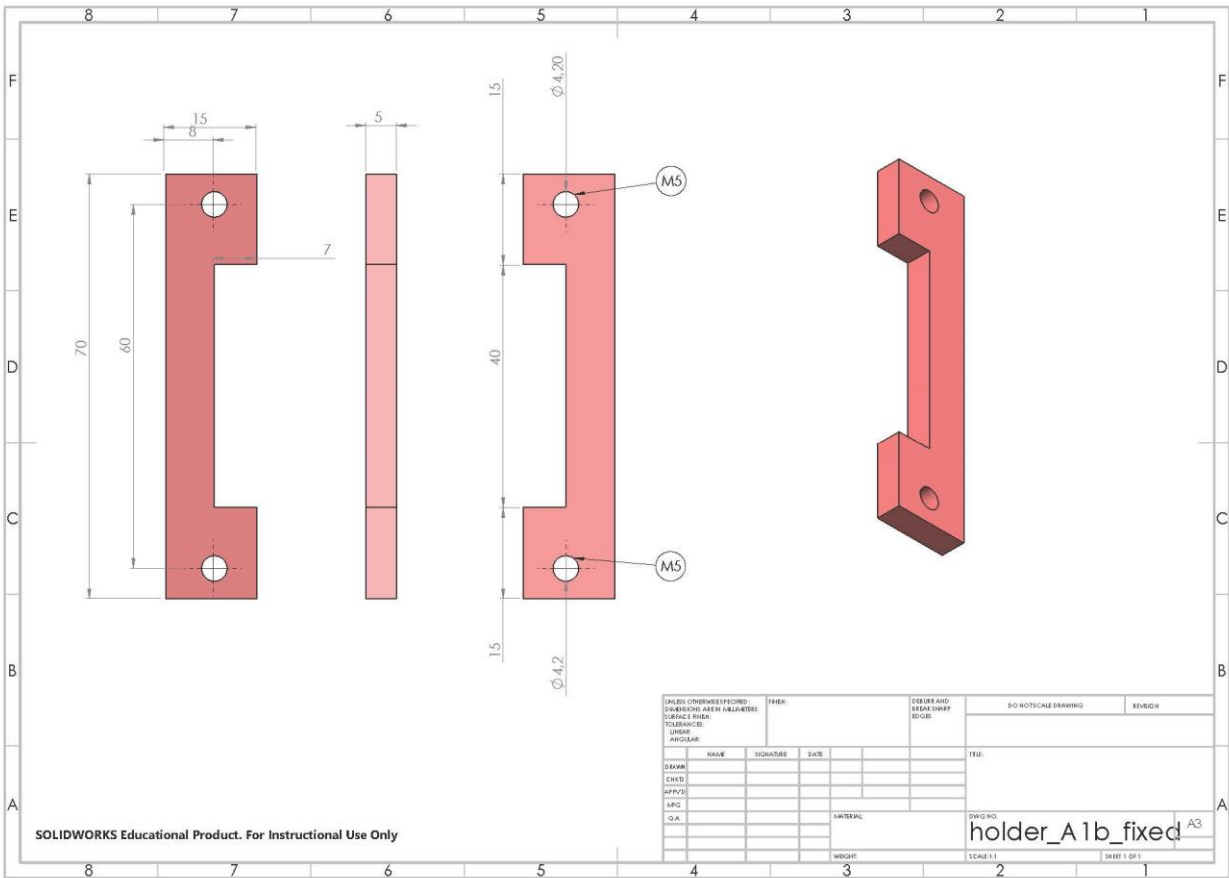


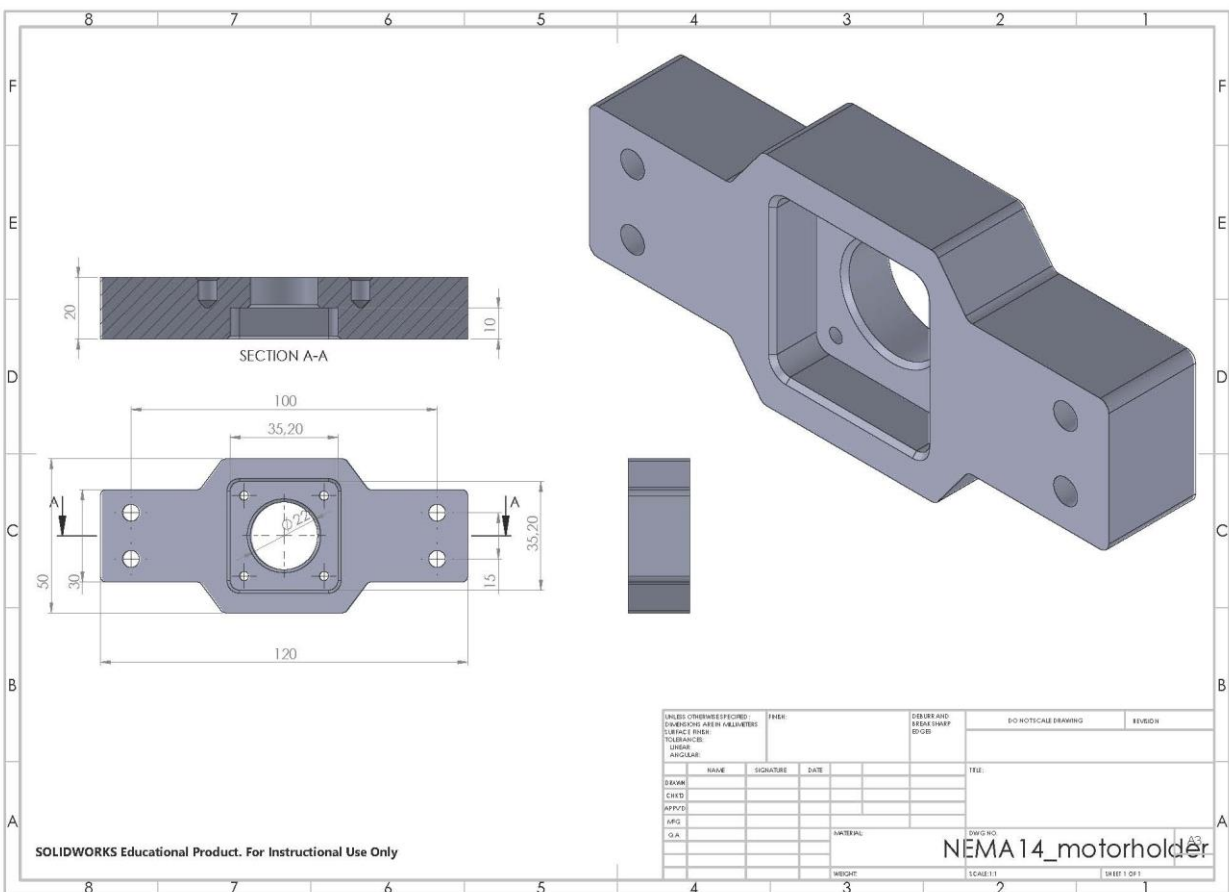
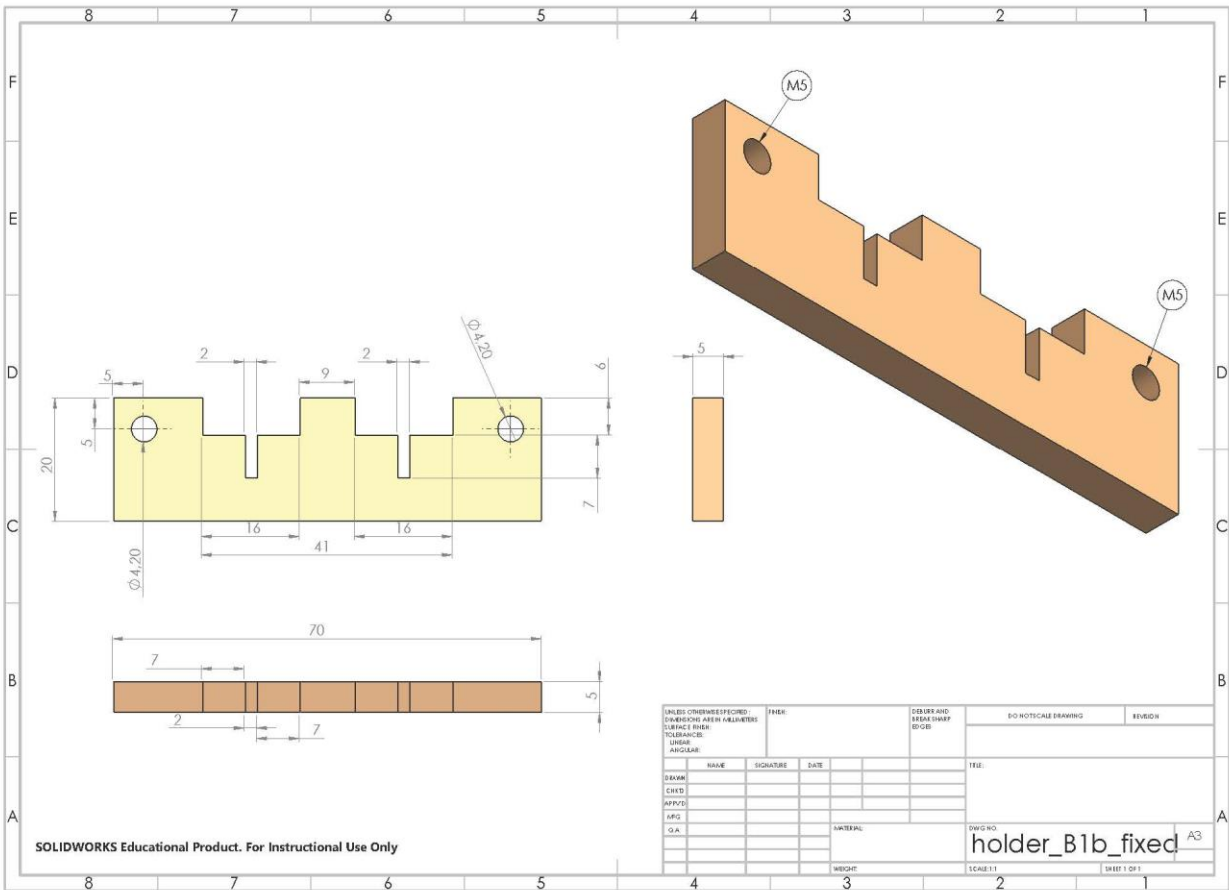


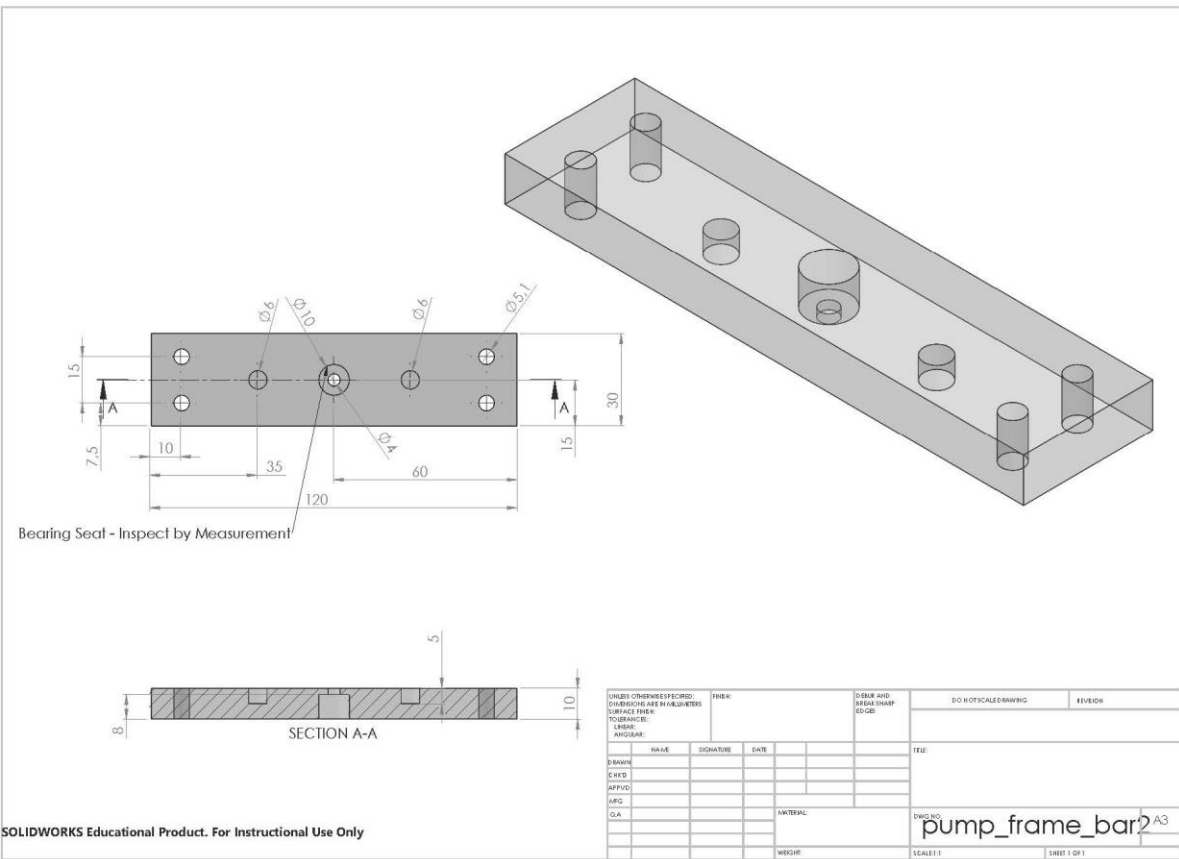
SOLIDWORKS Educational Product. For Instructional Use Only



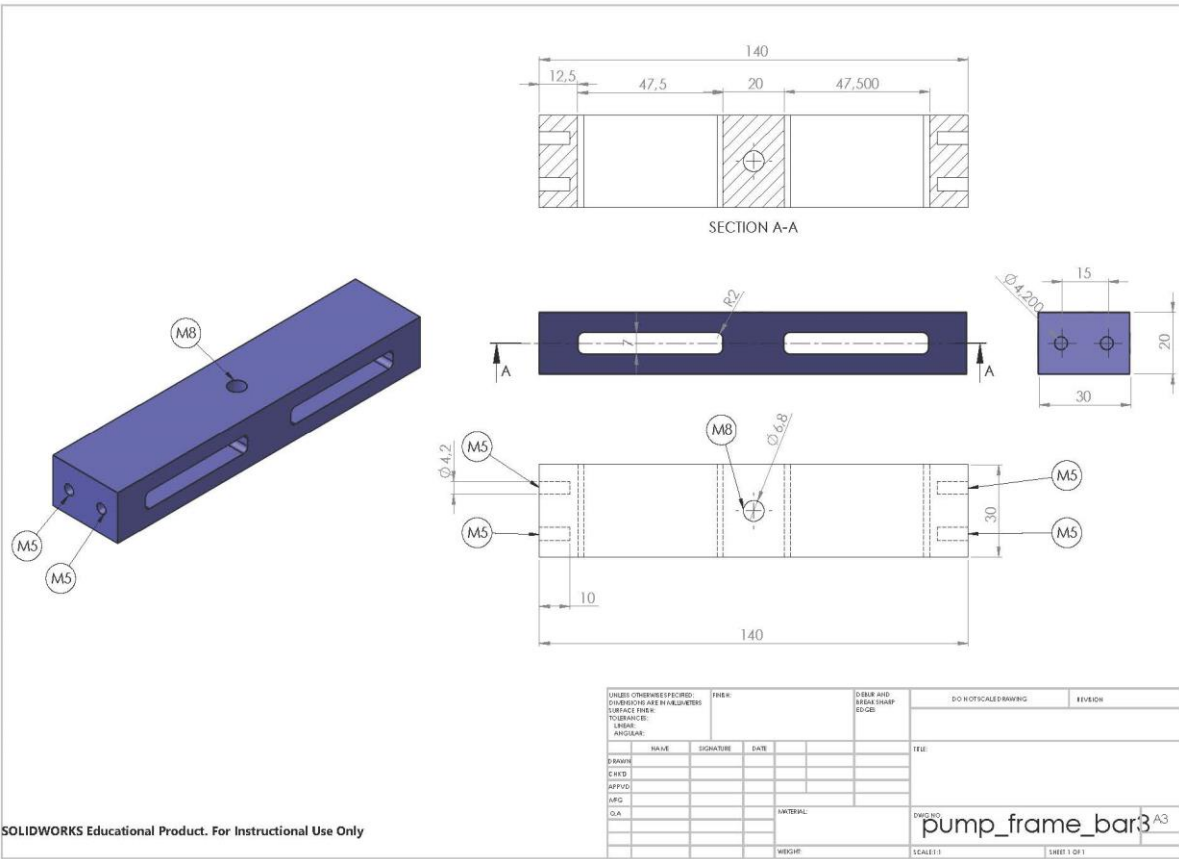
SOLIDWORKS Educational Product. For Instructional Use Only



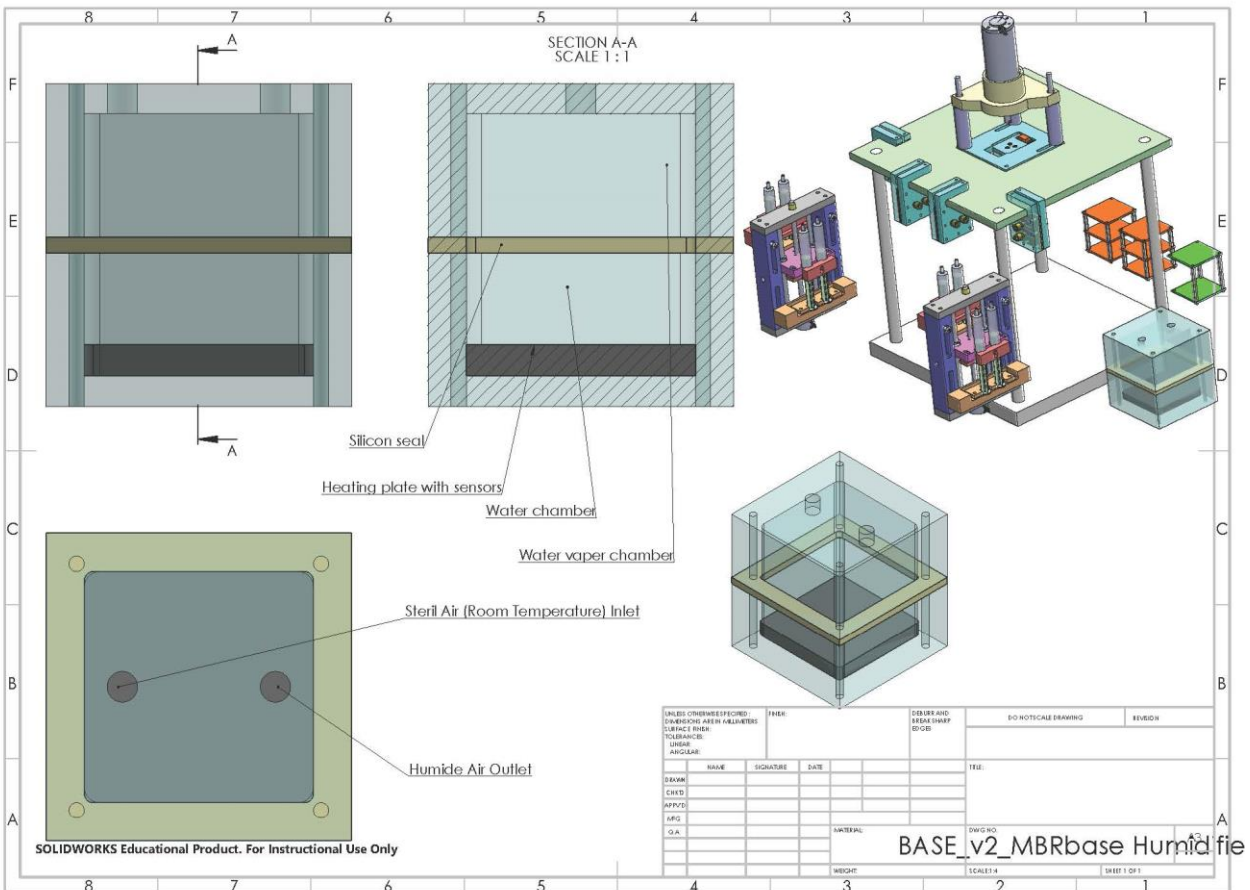
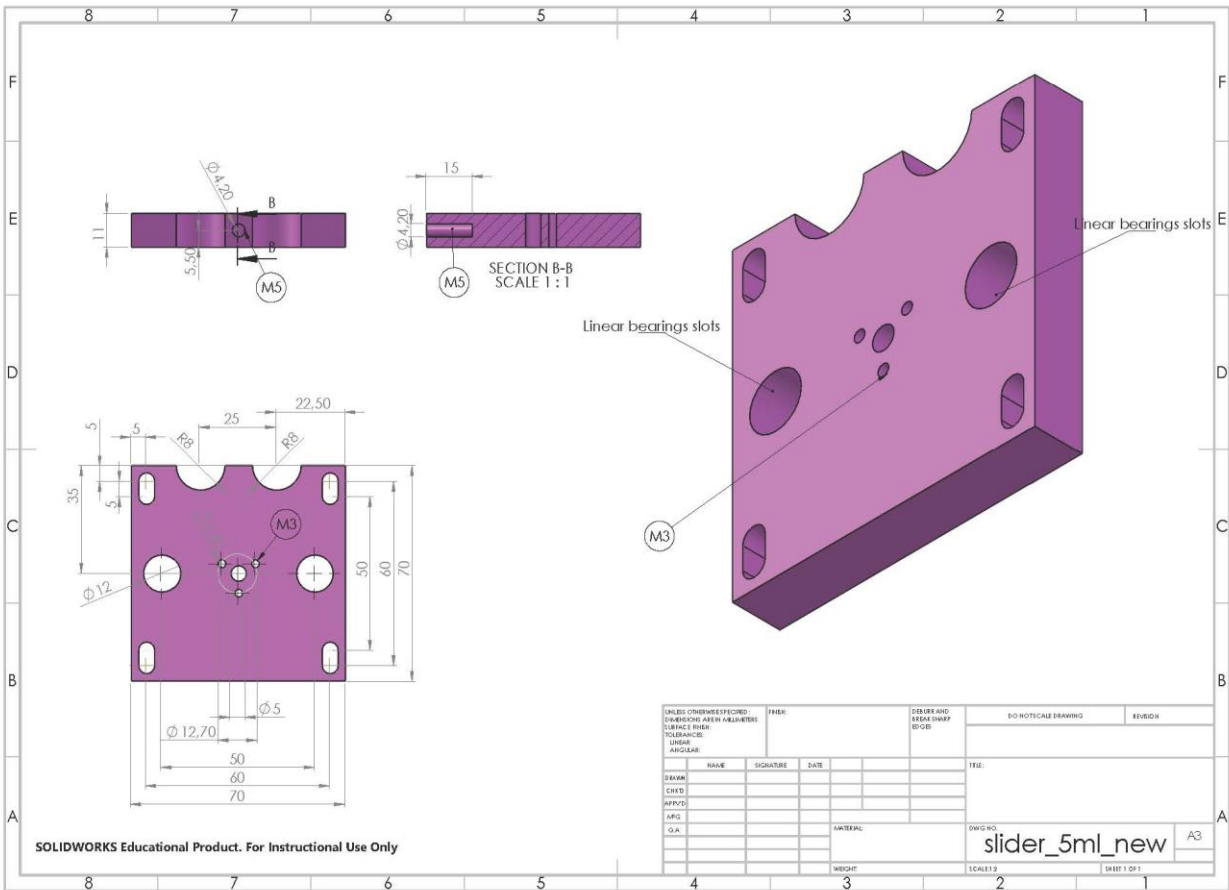




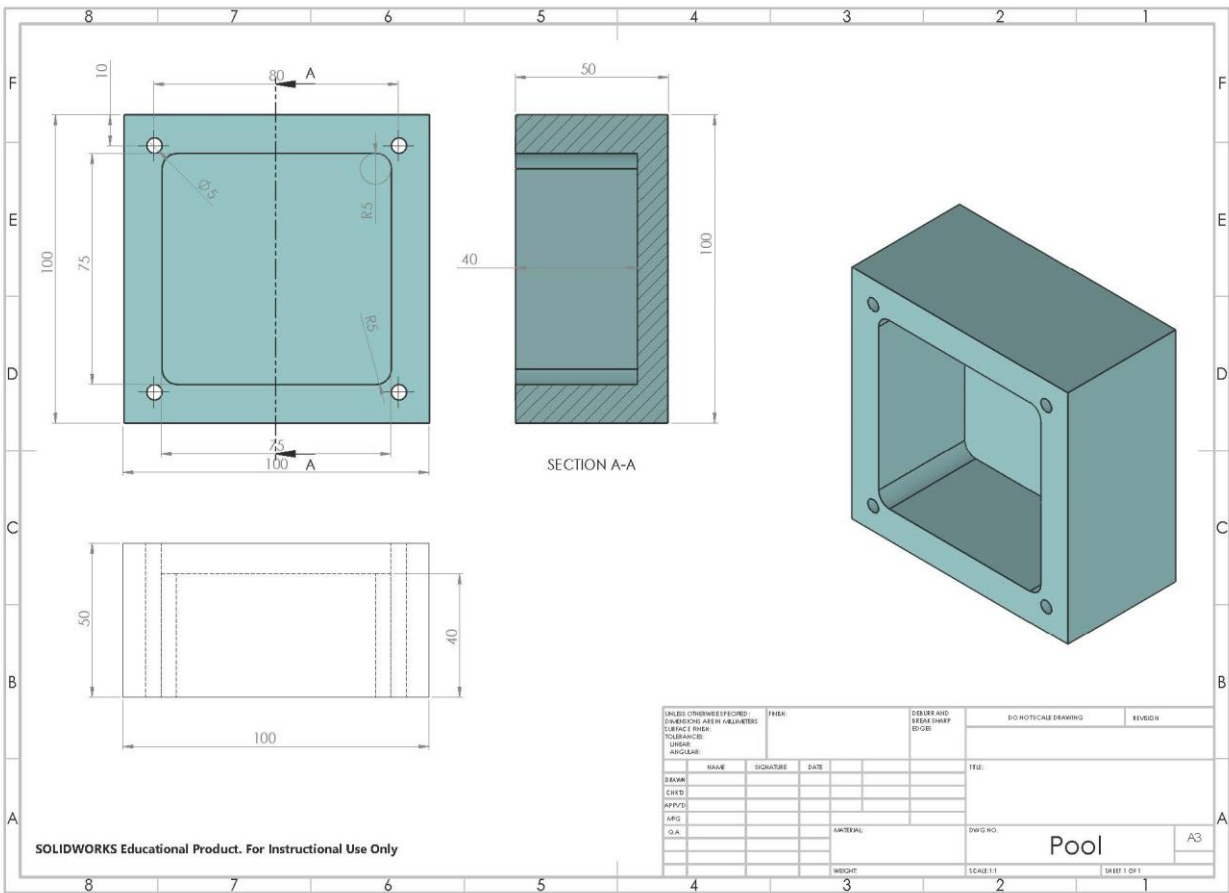
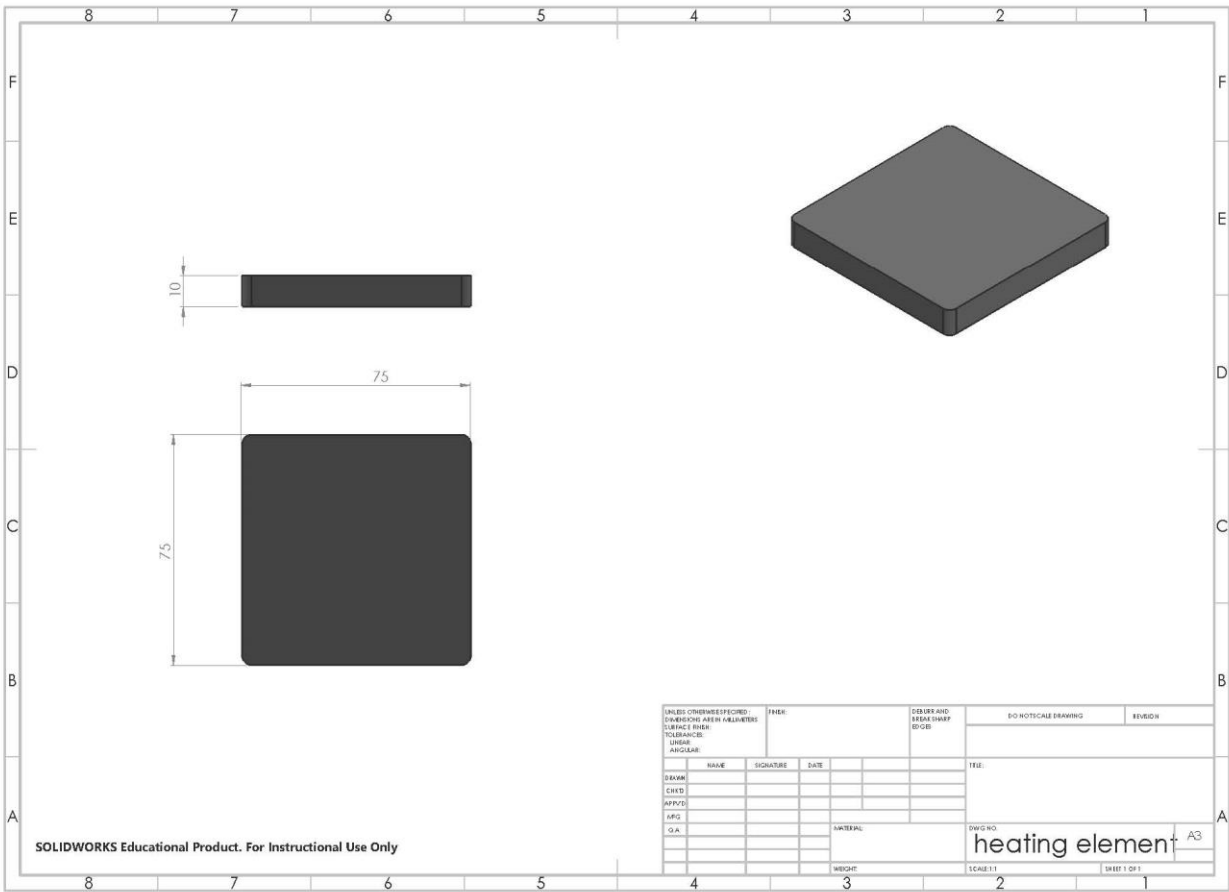
SOLIDWORKS Educational Product. For Instructional Use Only

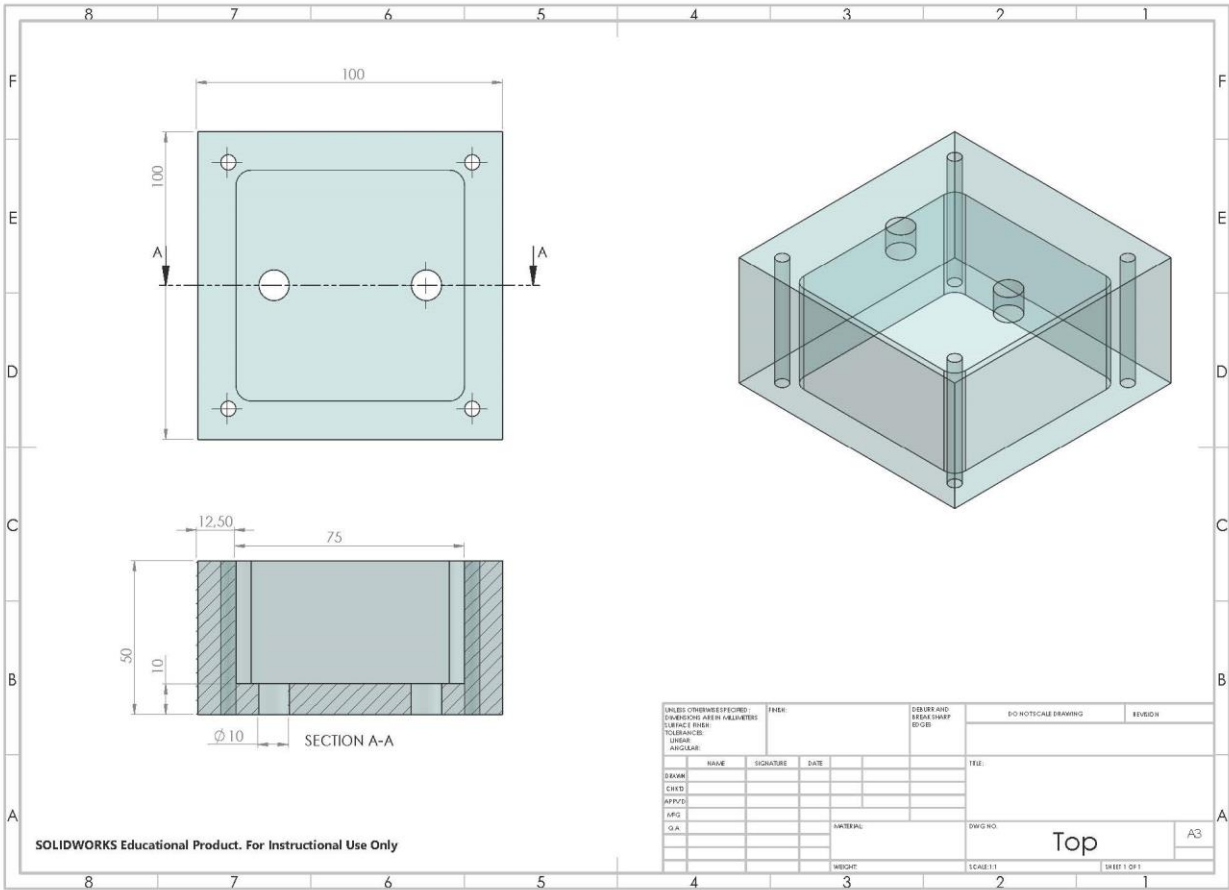


SOLIDWORKS Educational Product. For Instructional Use Only



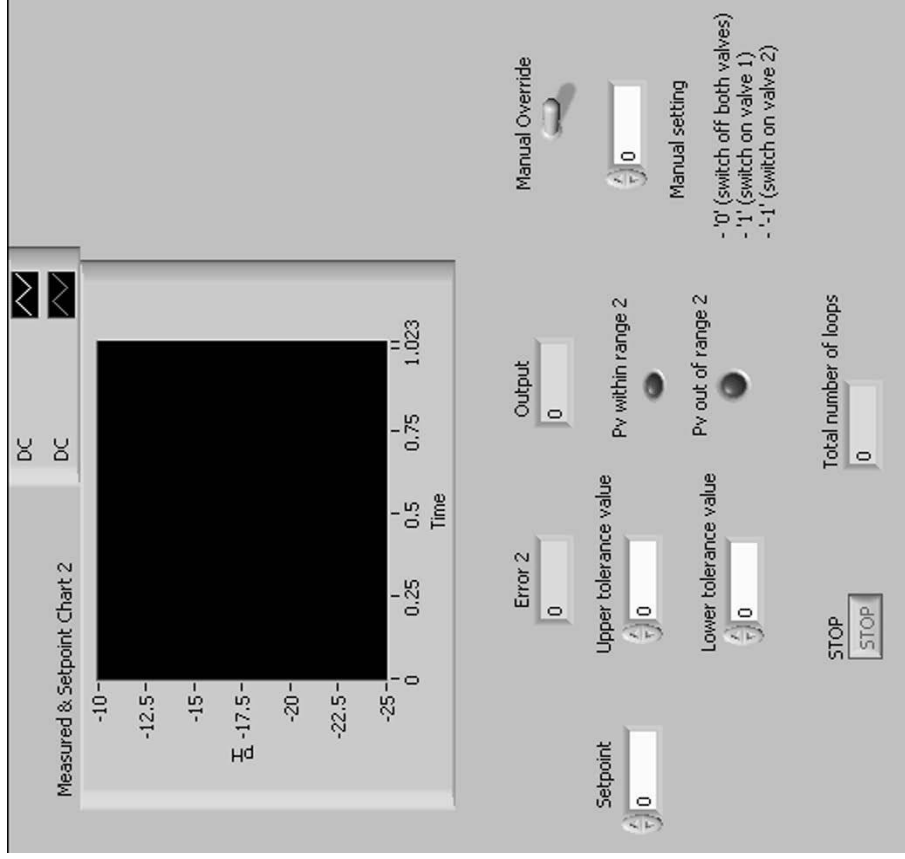
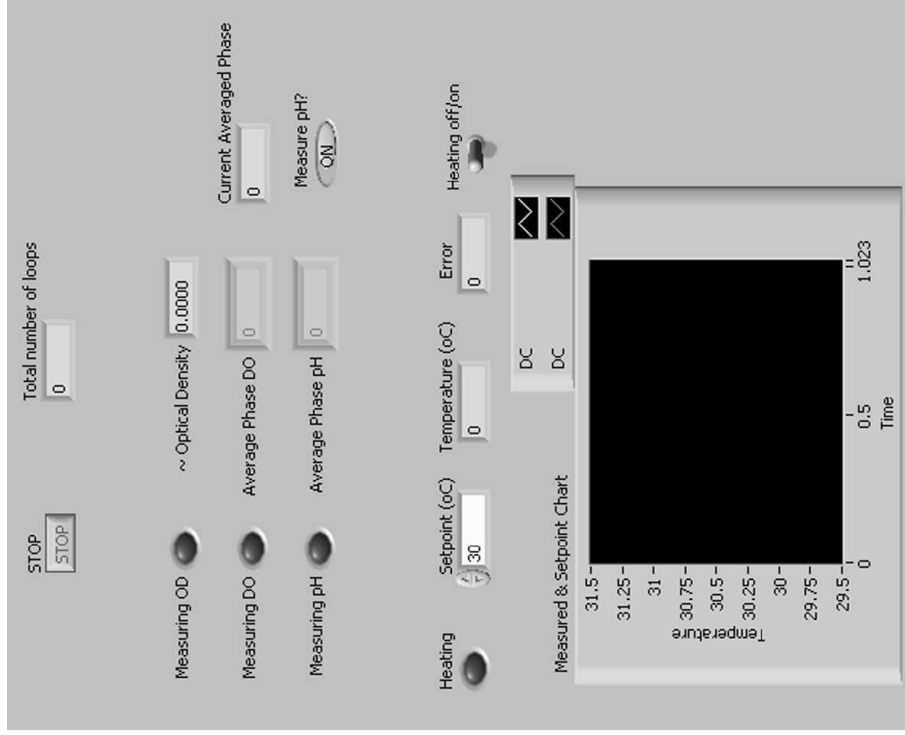




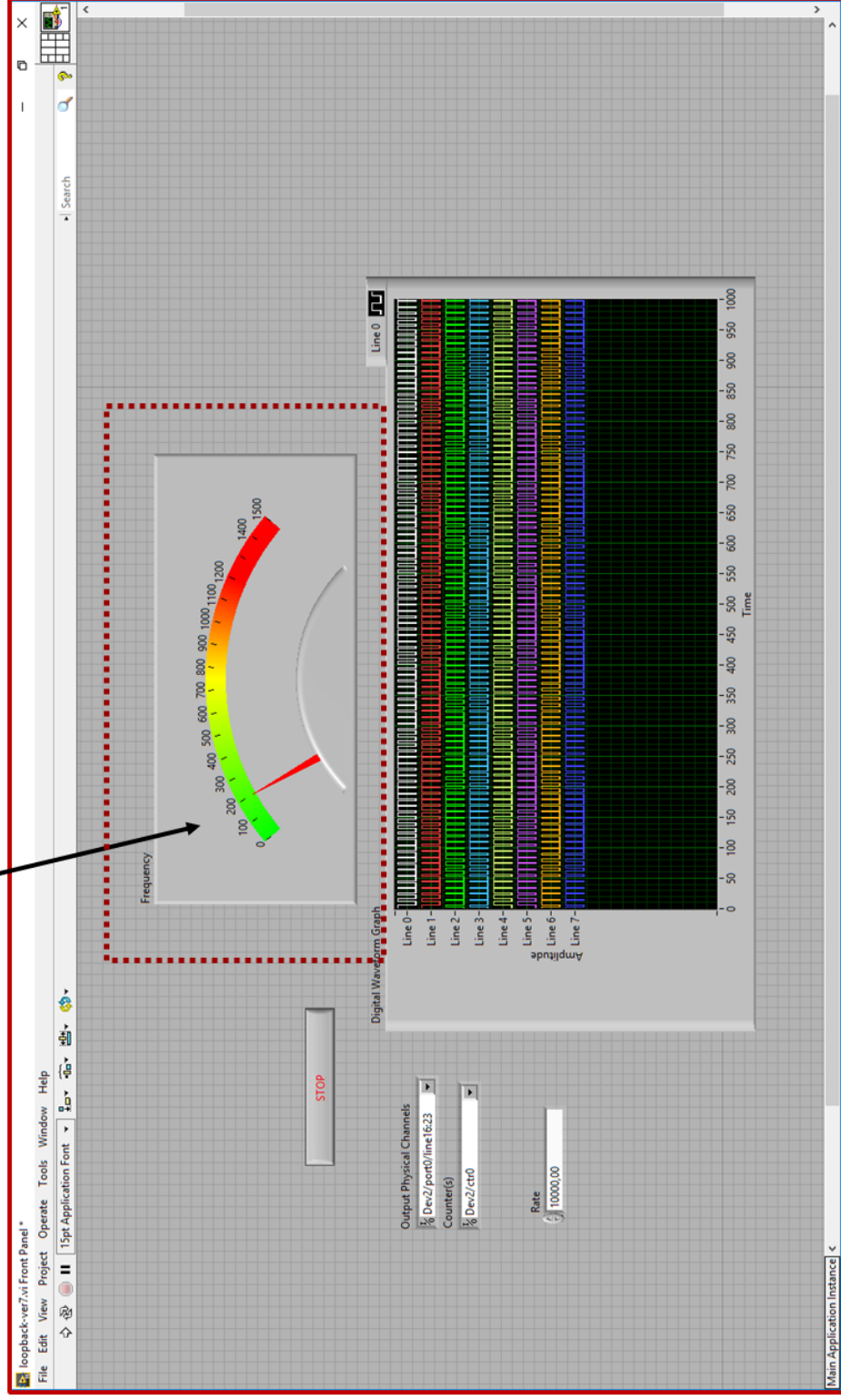


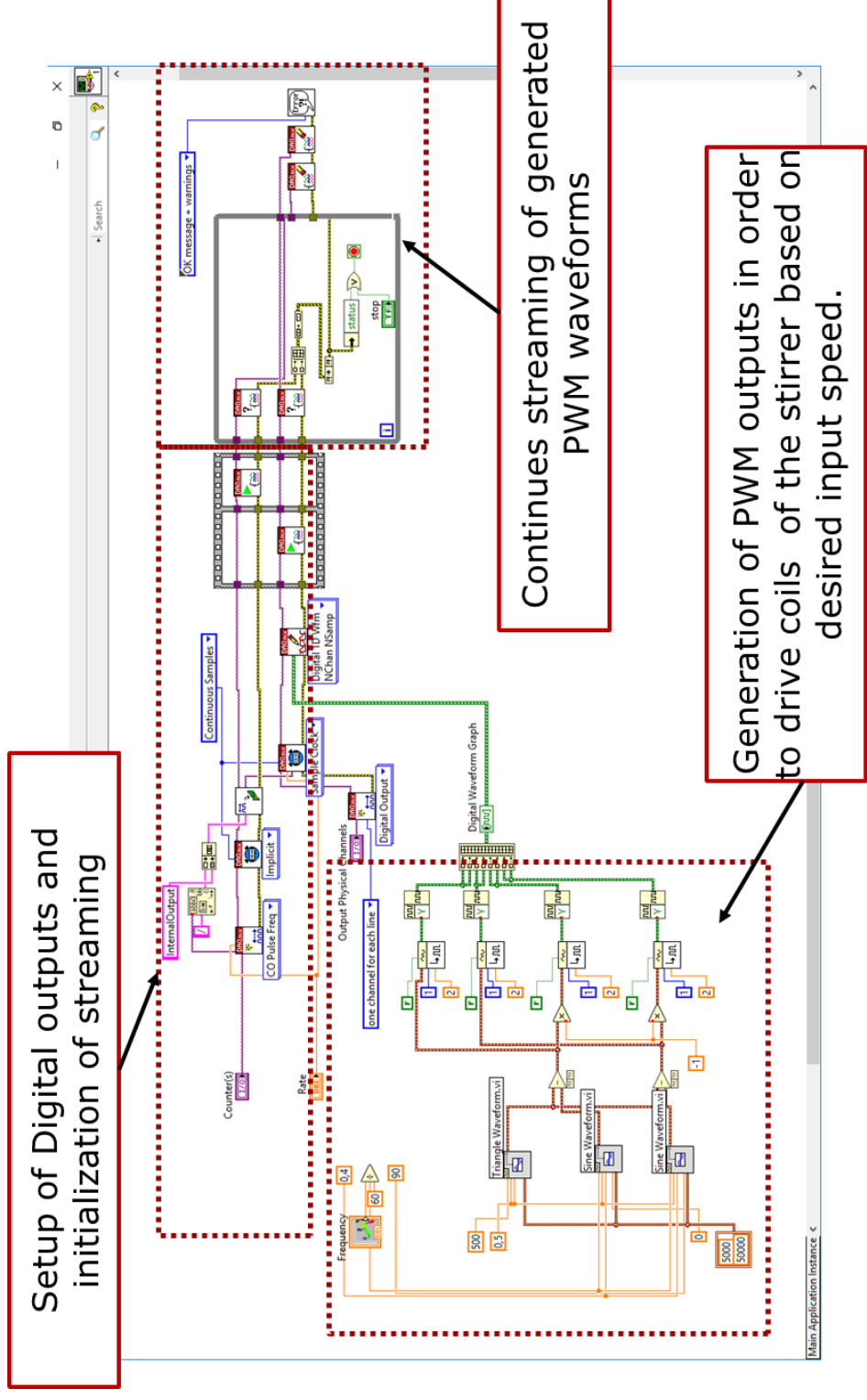
# Appendix D

## LabView program - user interface and block diagram for the MSBR prototype I



User input for stirrer speed





Setup of Digital outputs and initialization of streaming

Continues streaming of generated PWM waveforms

Generation of PWM outputs in order to drive coils of the stirrer based on desired input speed.

The block diagram where DO, pH, OD and T measurements are presented in the PhD thesis of Daniel Schapper. [1]  
 [1] D. Schapper, Continuous Culture Microbioreactors, PhD Thesis, Tech. Univ. Denmark. (2010).

# Appendix E

## LabView program - user interface and block diagram for the MSBR prototype II

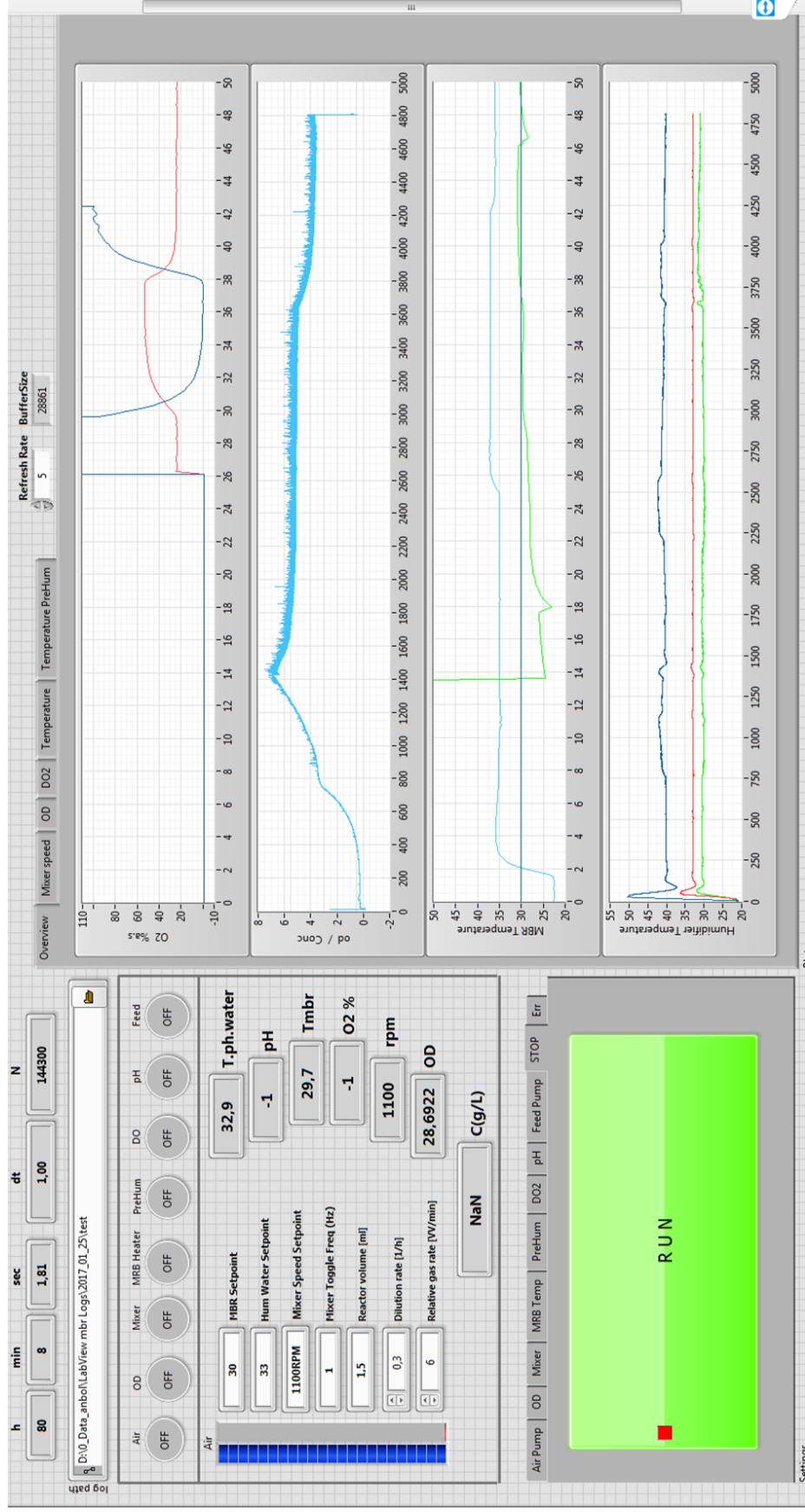
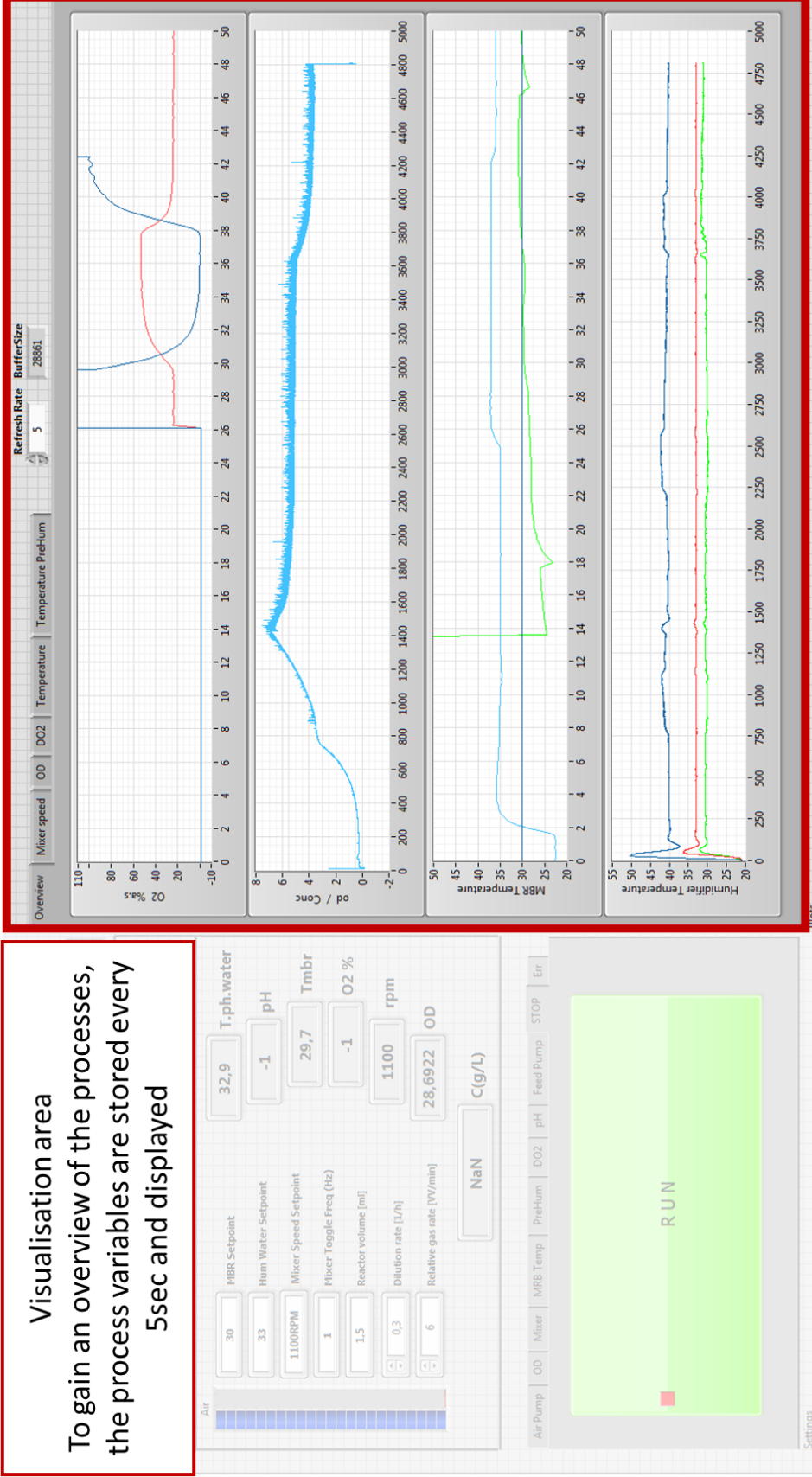


Figure 1. User graphical interface of the MSBR cultivation platform developed in LabView – Overview.



**Visualisation area**

To gain an overview of the processes, the process variables are stored every 5sec and displayed

Figure 2. User graphical interface of the MSBR cultivation platform developed in LabView – Cultivation process monitoring.

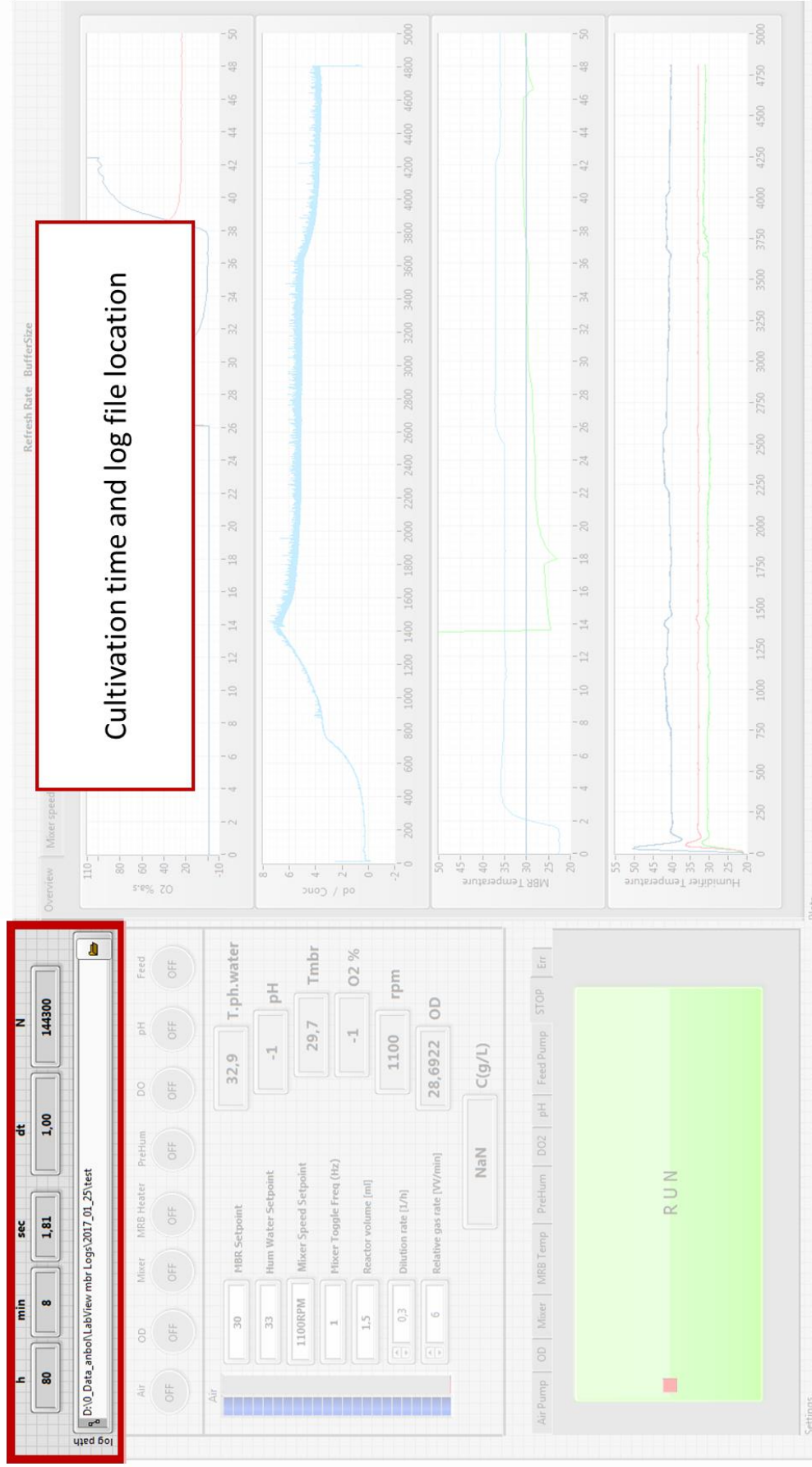


Figure 3. User graphical interface of the MSBR cultivation platform developed in LabView – Log file settings and run time.



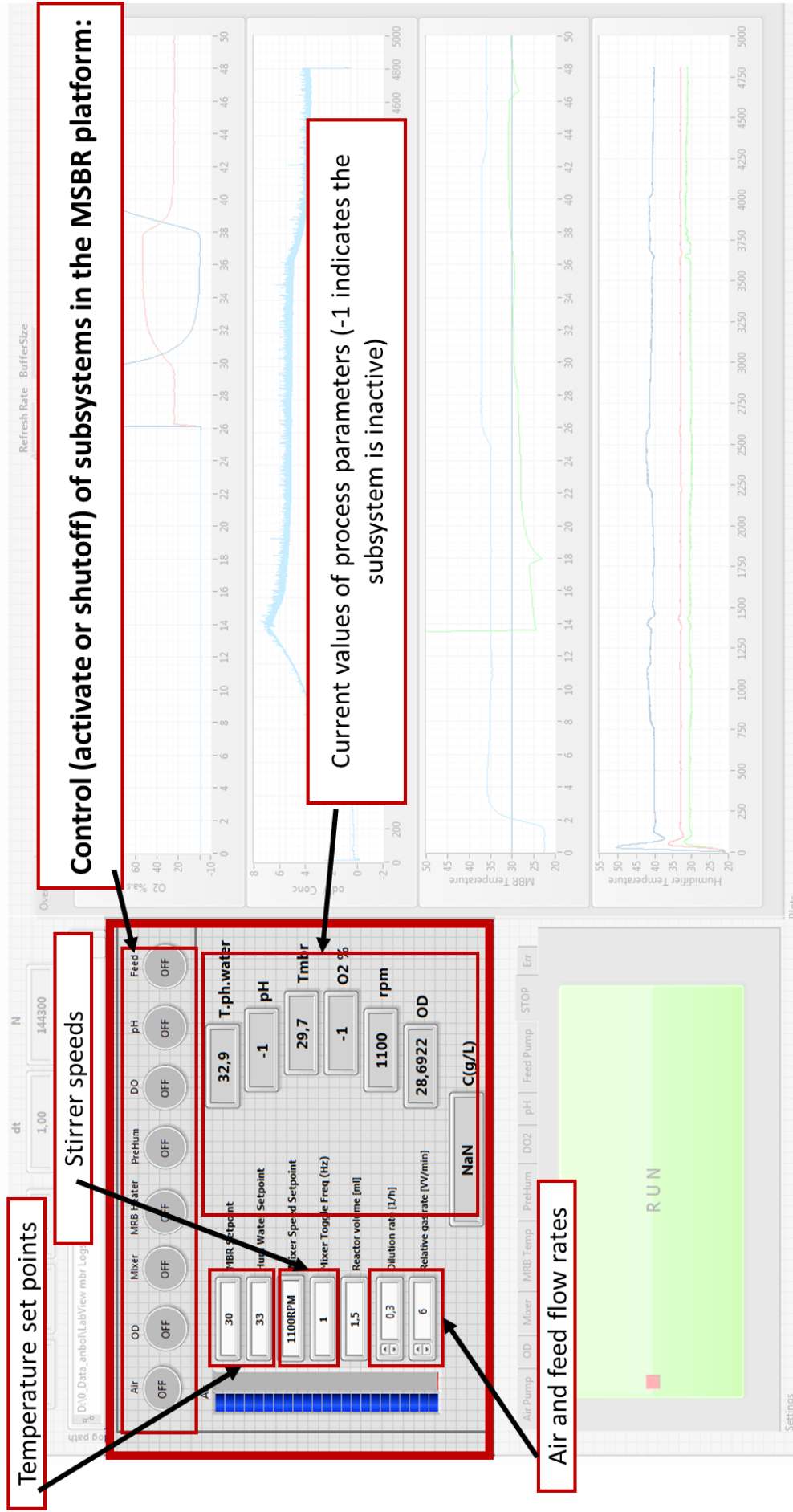


Figure 4. User graphical interface of the MSBR cultivation platform developed in LabView – Process parameter settings and subsystem control.

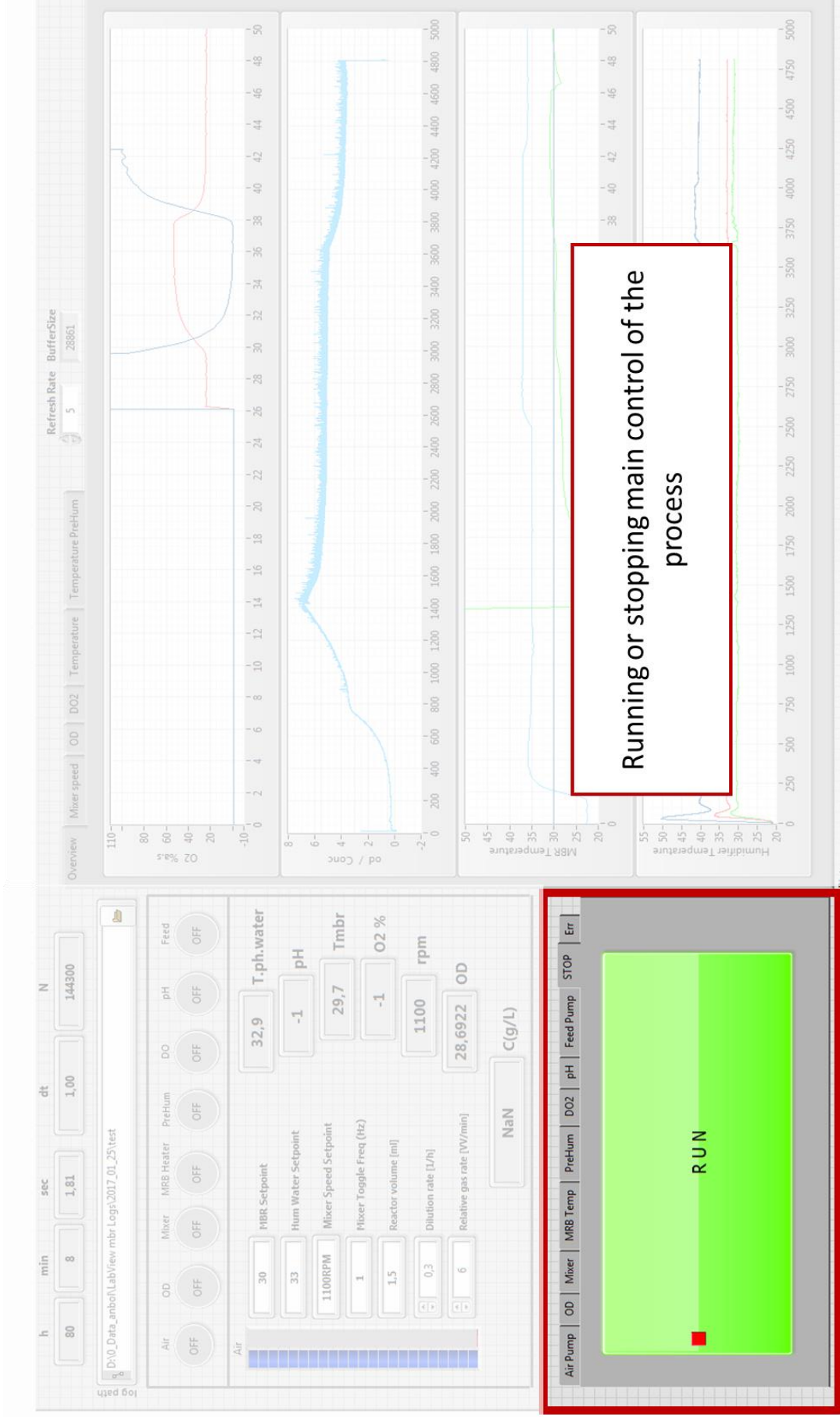


Figure 5. User graphical interface of the MSBR cultivation platform developed in LabView – Start/Stop of the main control.

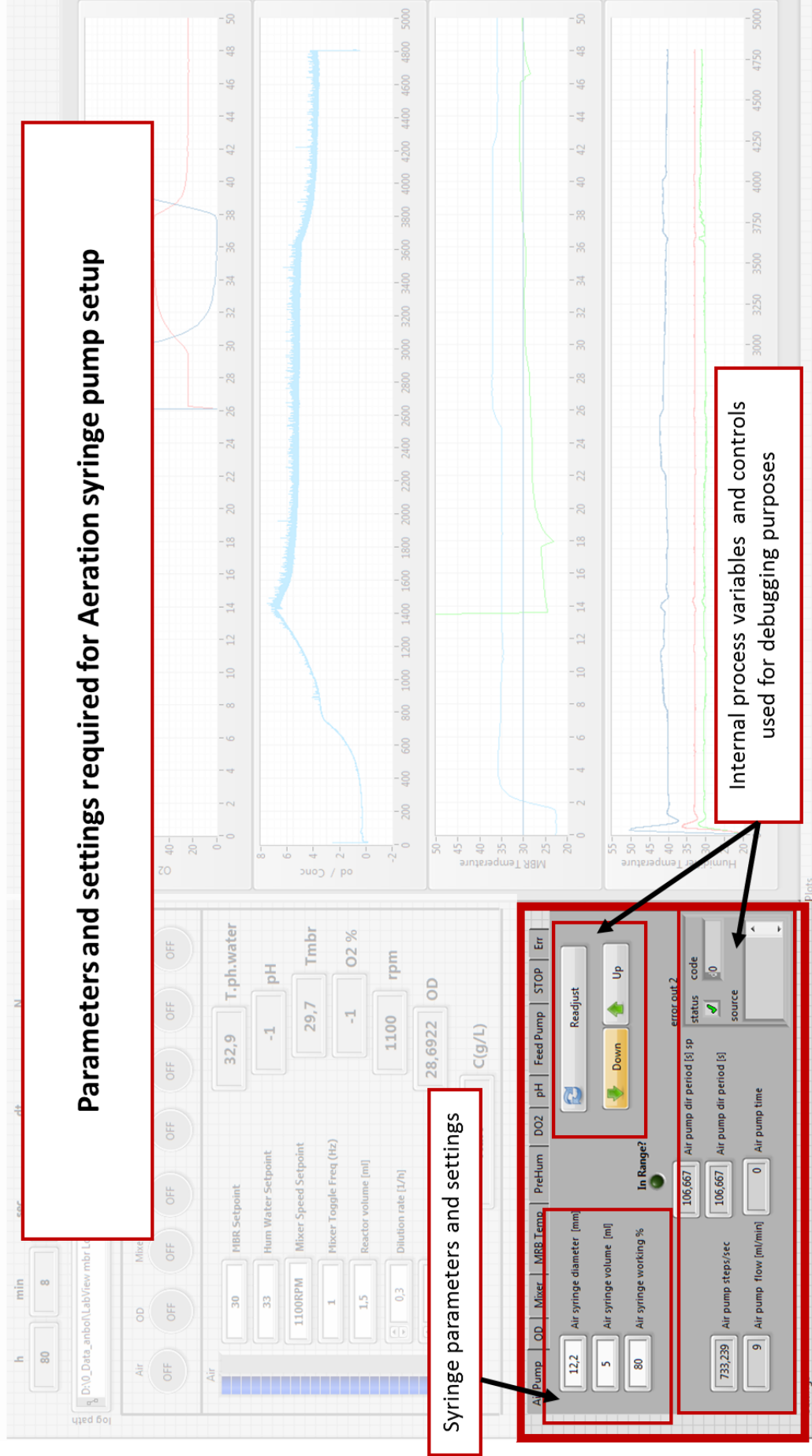


Figure 6. User graphical interface of the MSBR cultivation platform developed in LabView – Settings of the syringe pump used for aeration.

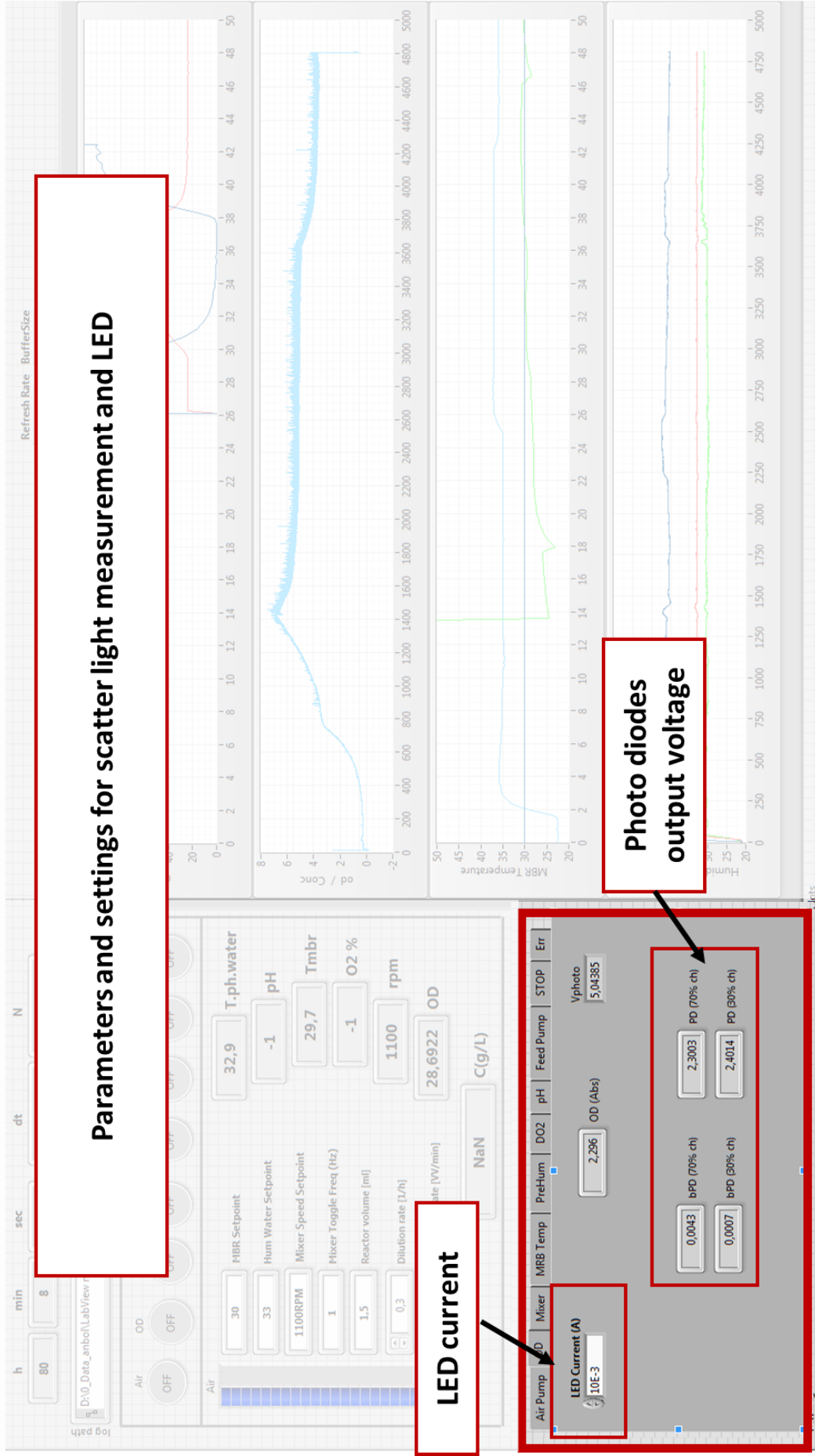


Figure 7. User graphical interface of the MSBR cultivation platform developed in LabView - Settings for LED scatter light calculation.

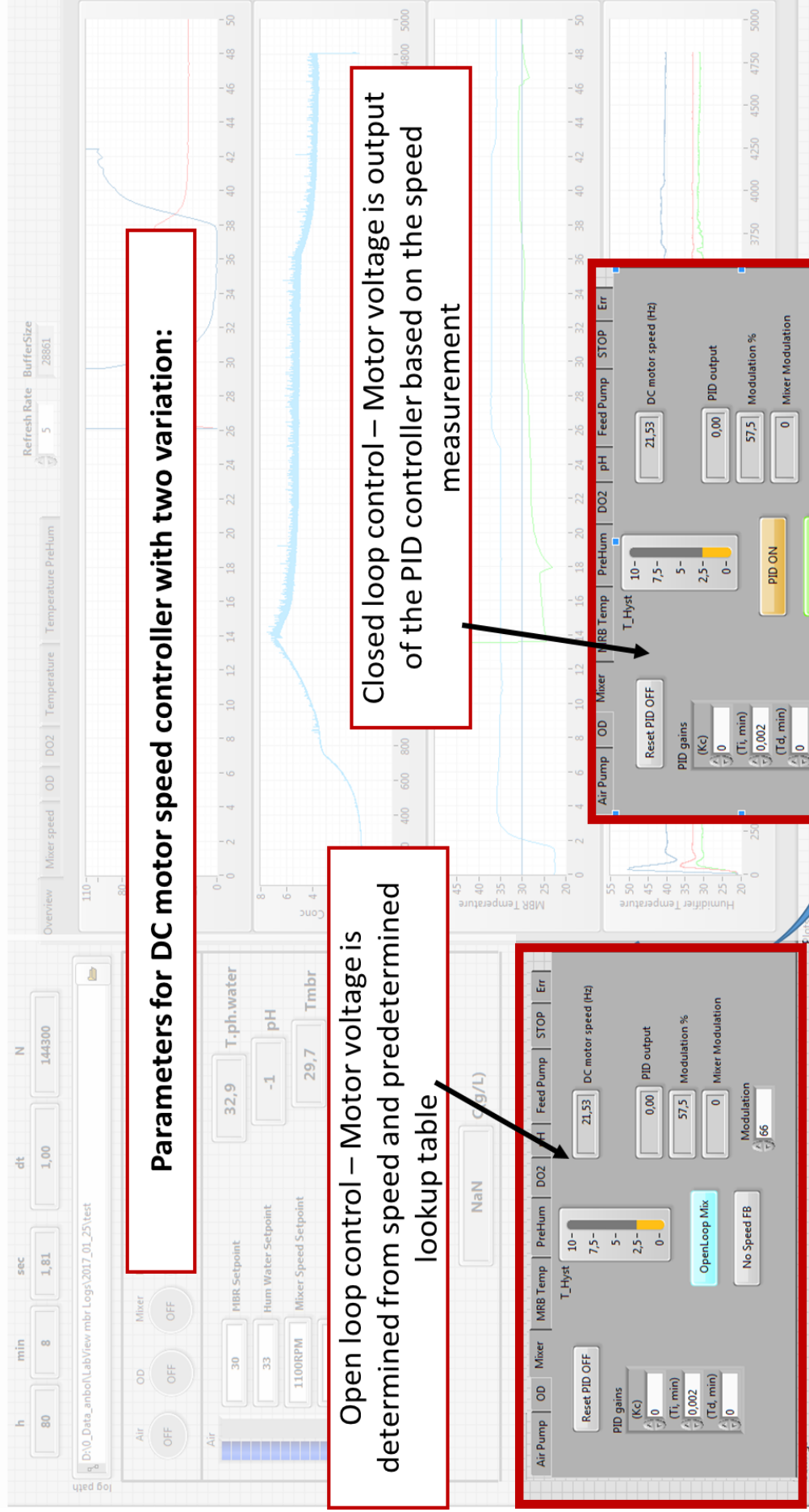


Figure 8. User graphical interface of the MSBR cultivation platform developed in LabView – Settings for Stirrer speed control.

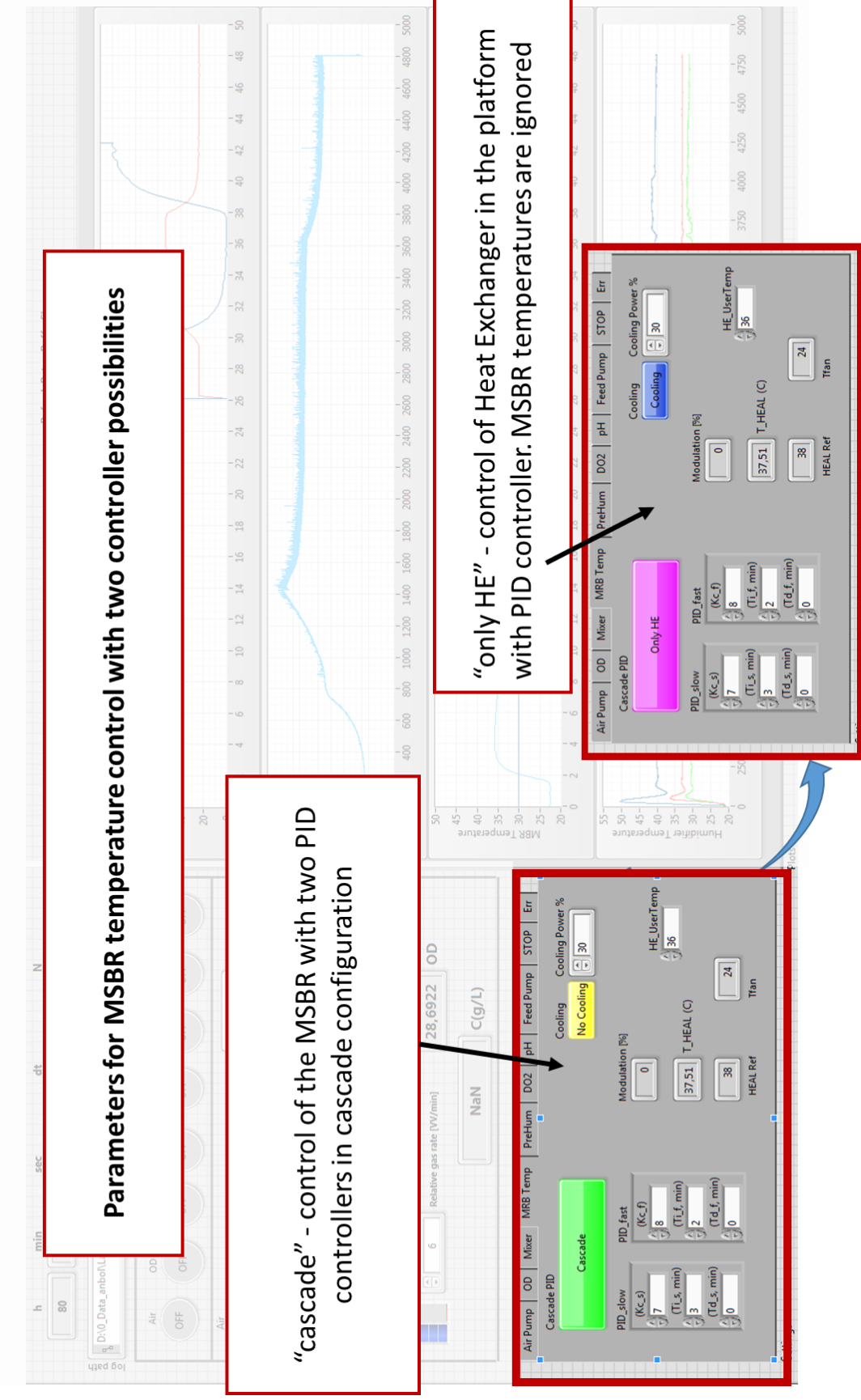


Figure 9. User graphical interface of the MSBR cultivation platform developed in LabView – Settings for MSBR temperature control.

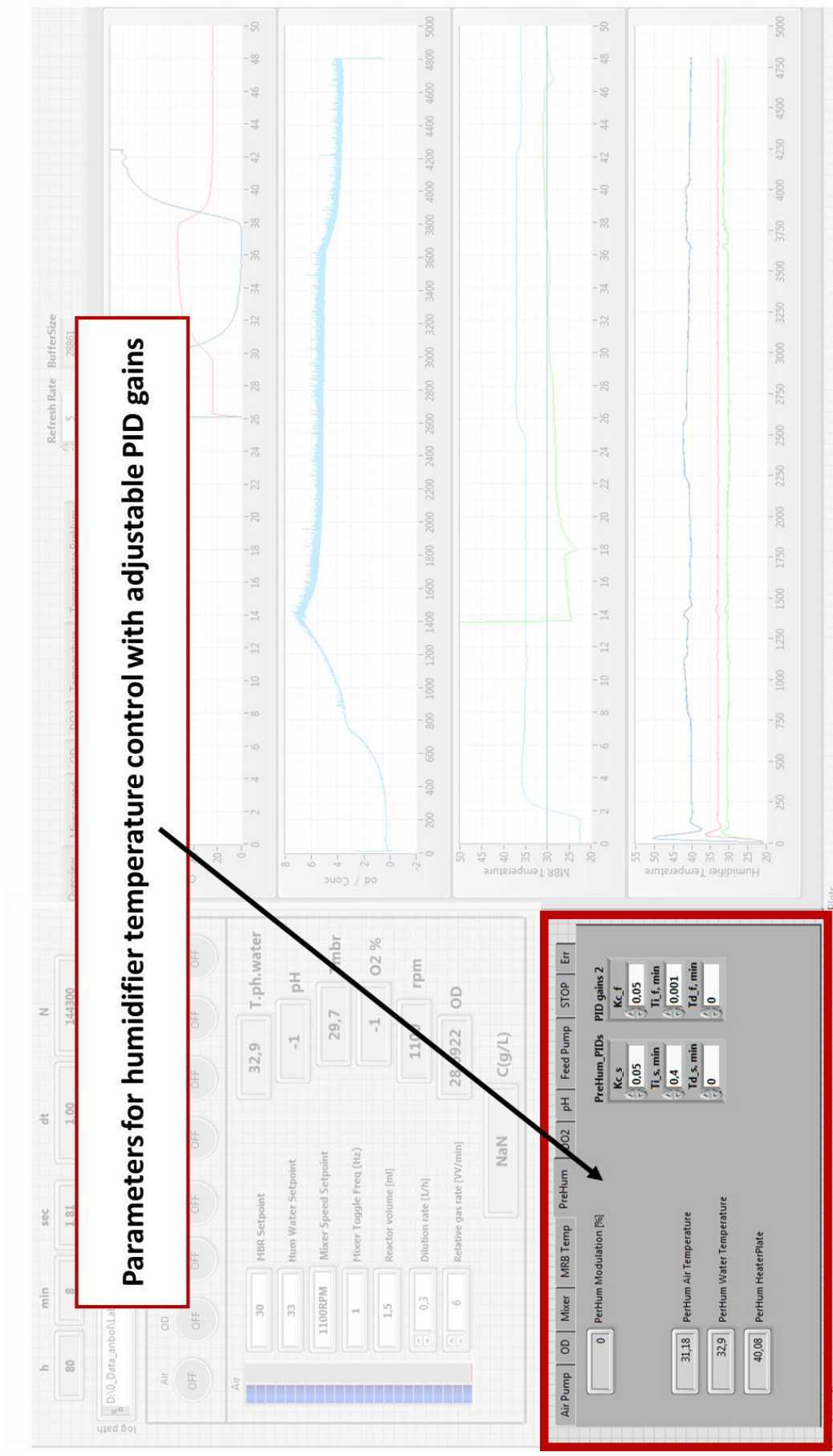


Figure 10. User graphical of the MSBR cultivation platform interface developed in LabView – Settings for humidifier temperature control.

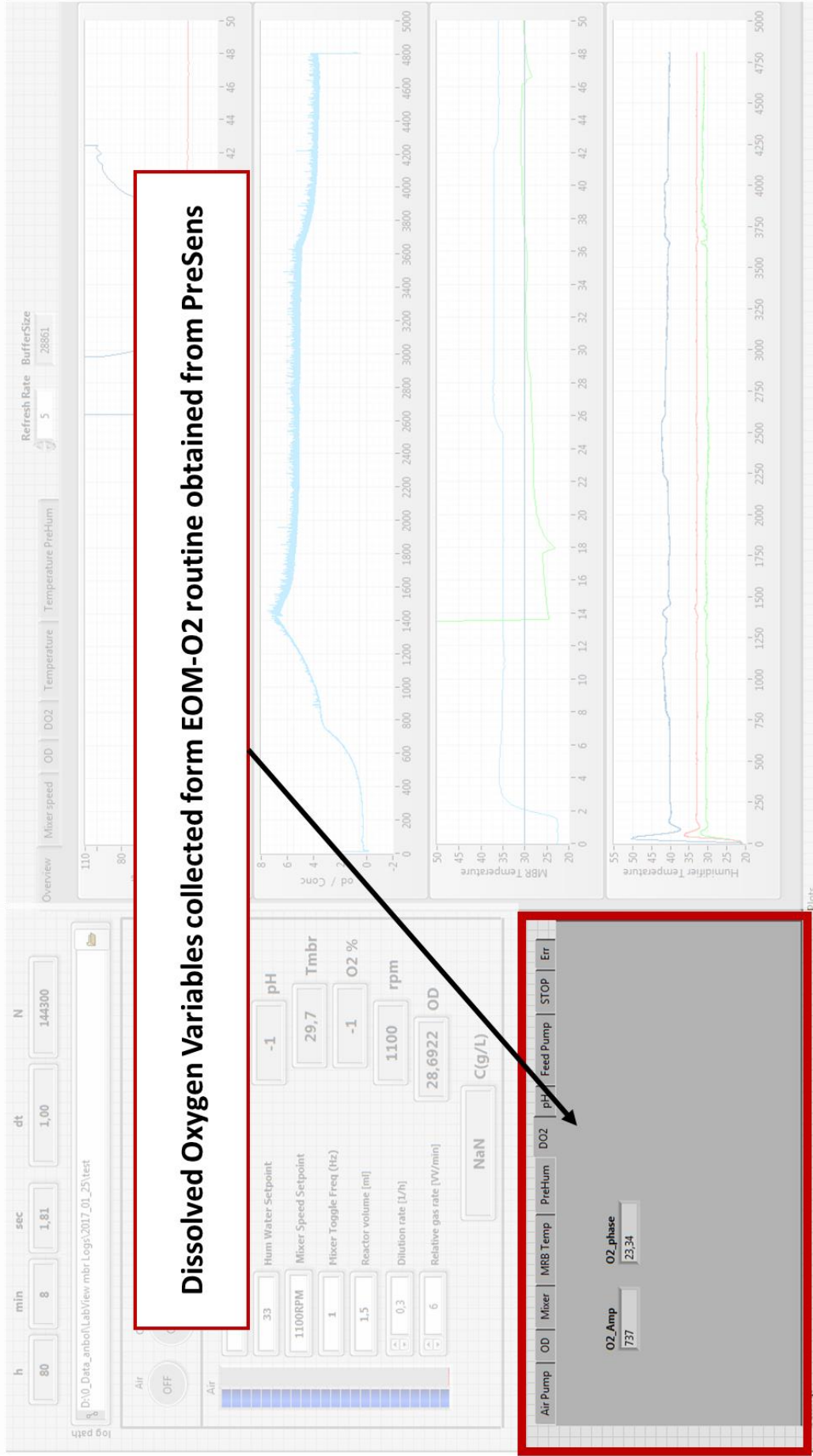


Figure 11. User graphical interface of the MSBR cultivation platform developed in LabView – Dissolved Oxygen internal variables.



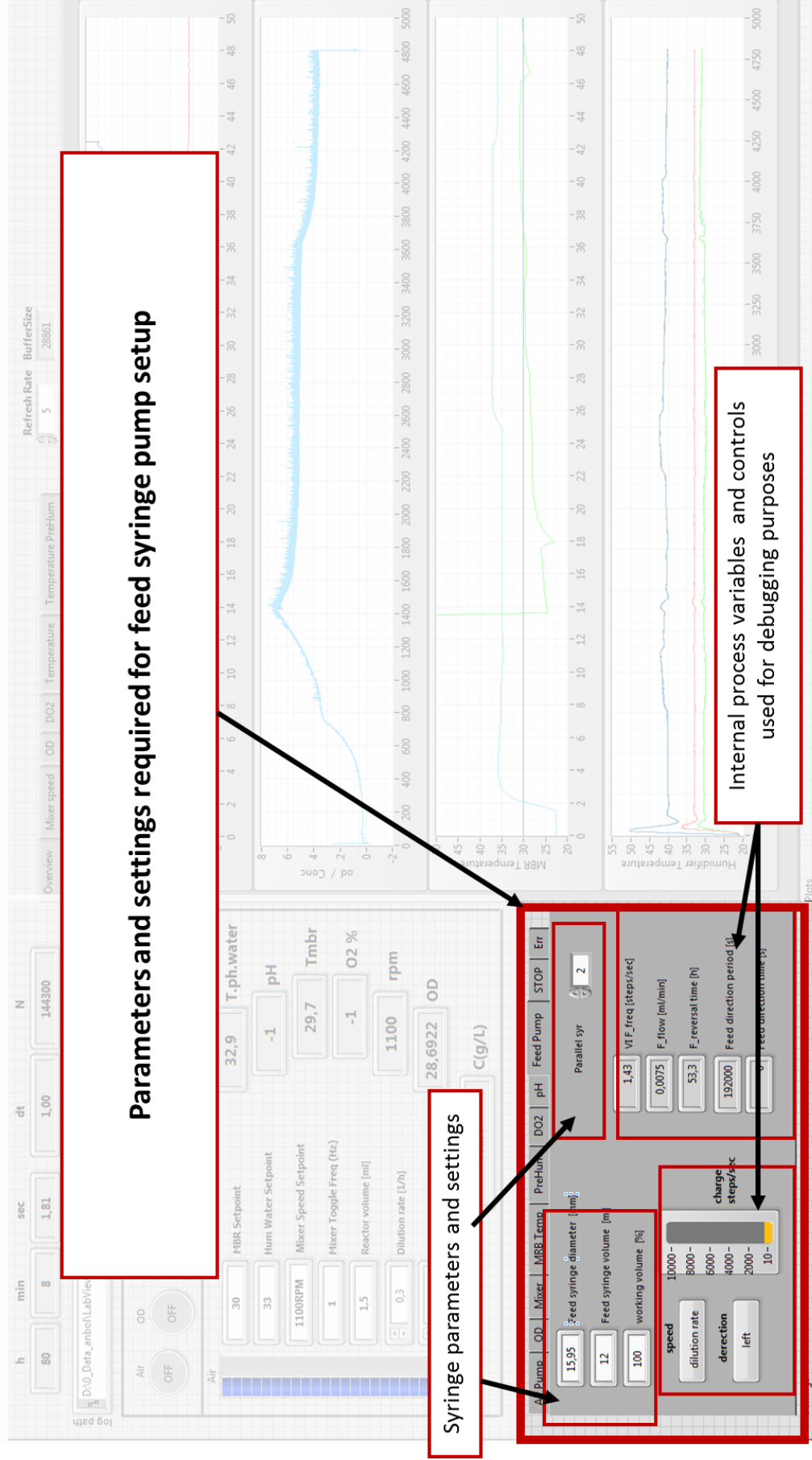


Figure 12. User graphical interface of the MSBR cultivation platform developed in LabView – Settings of the syringe pump used for feed inflow and outflow.

Shutdown measurement and  
put hardware in safe state

Main measurement and control loop (~1sec)

Initialize the hardware and data logging

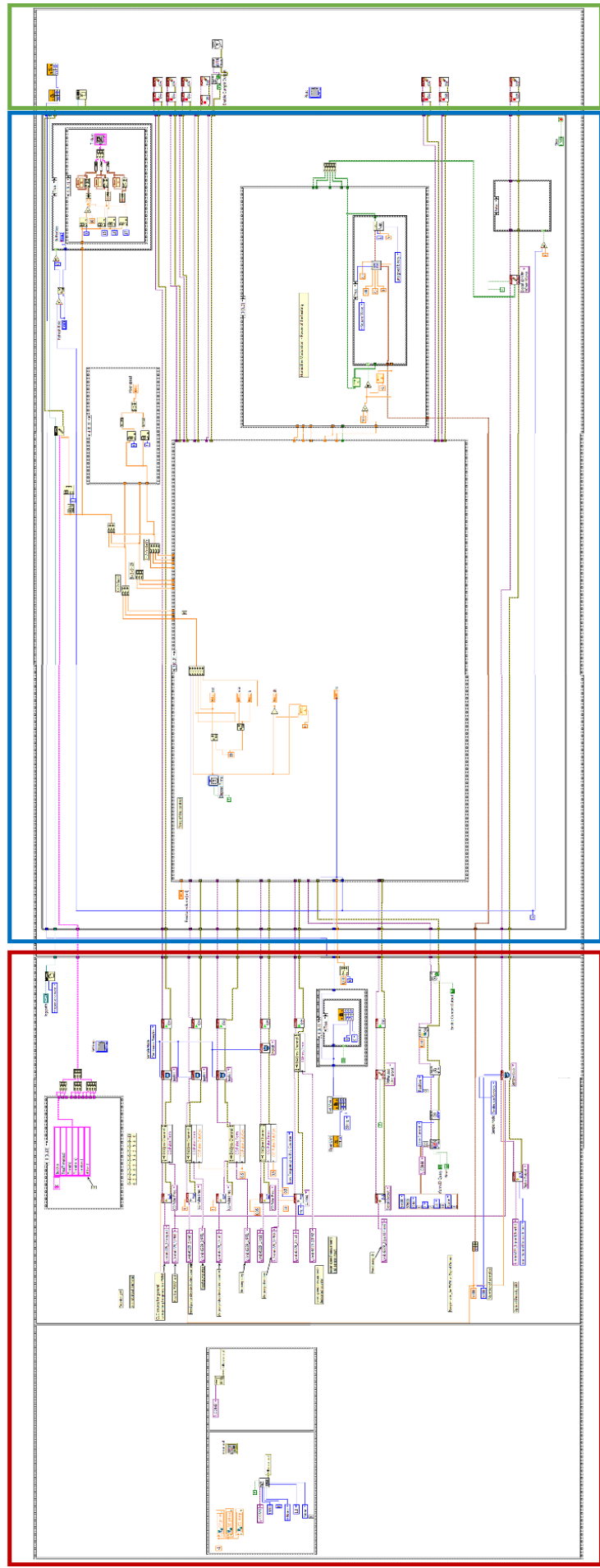


Figure 13. User graphical interface of the MSBR cultivation platform developed in LabView – Block diagram of the whole LabView routine

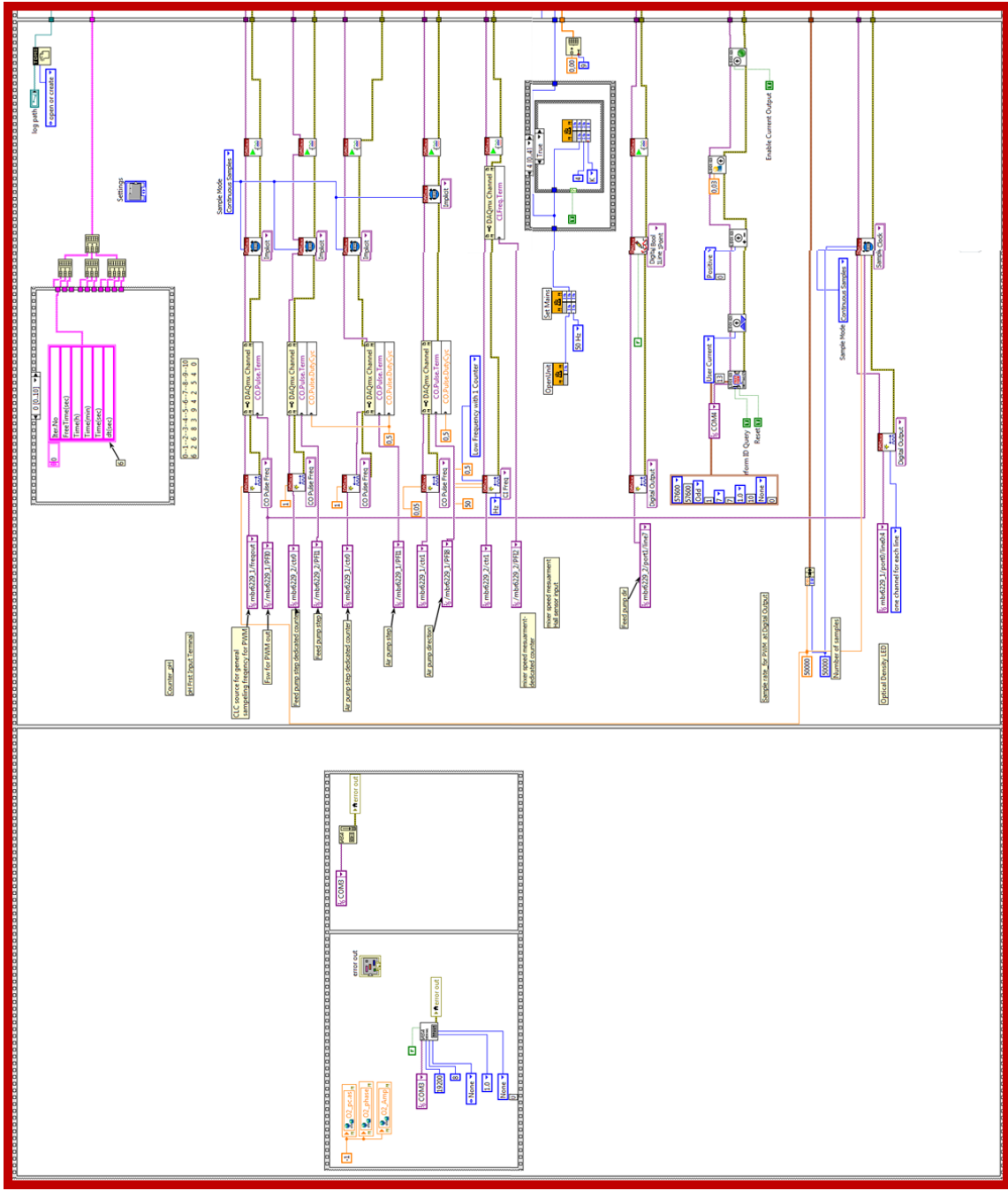


Figure 14. User graphical interface of the MSBR cultivation platform developed in LabView – Block diagram of the initialization routine – overview

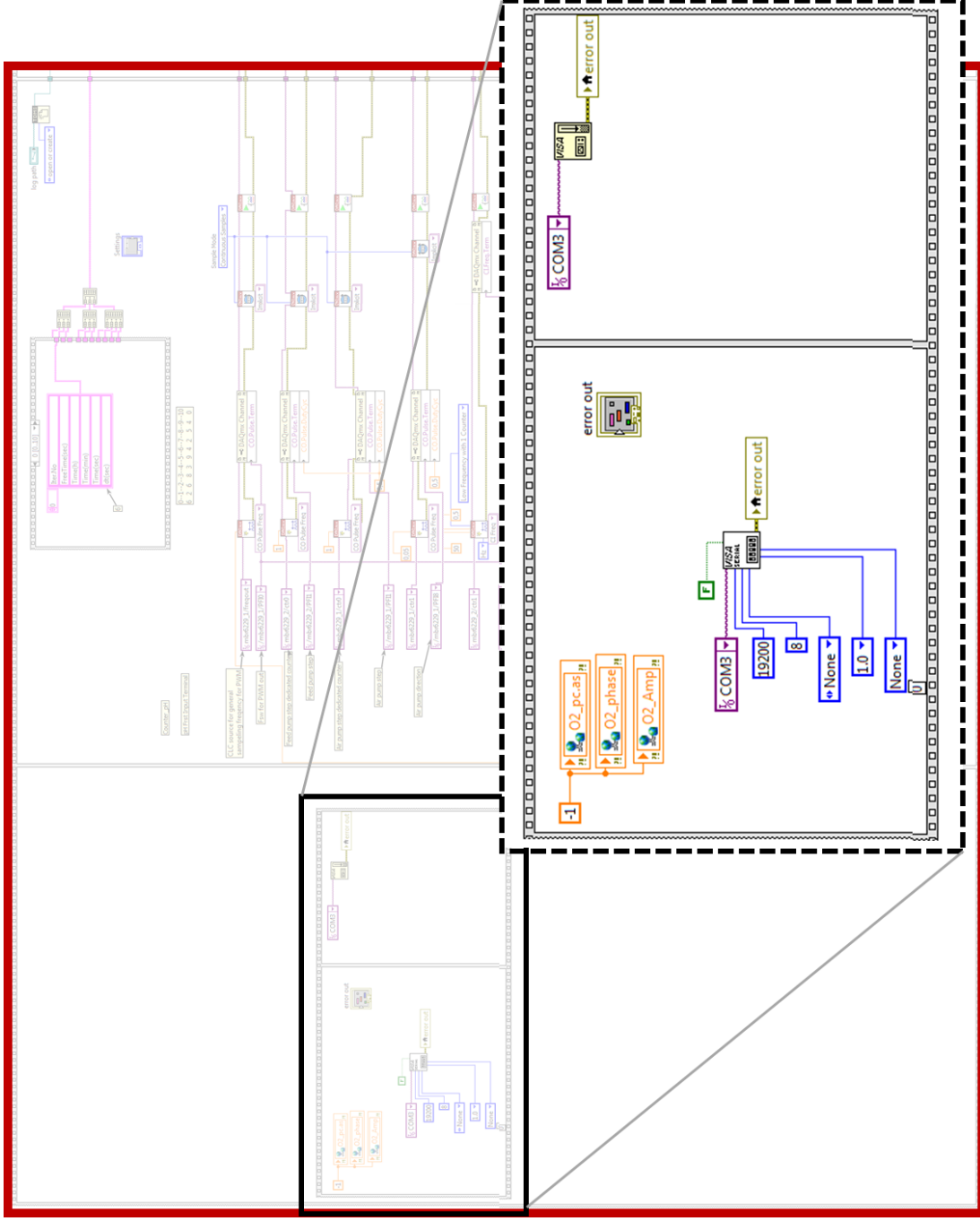


Figure 15. User graphical interface of the MSBR cultivation platform developed in LabView – Block diagram of the initialization routine – Setting up the communication with DC121 current supply and initializing the internal variables for EOM-O2 module.

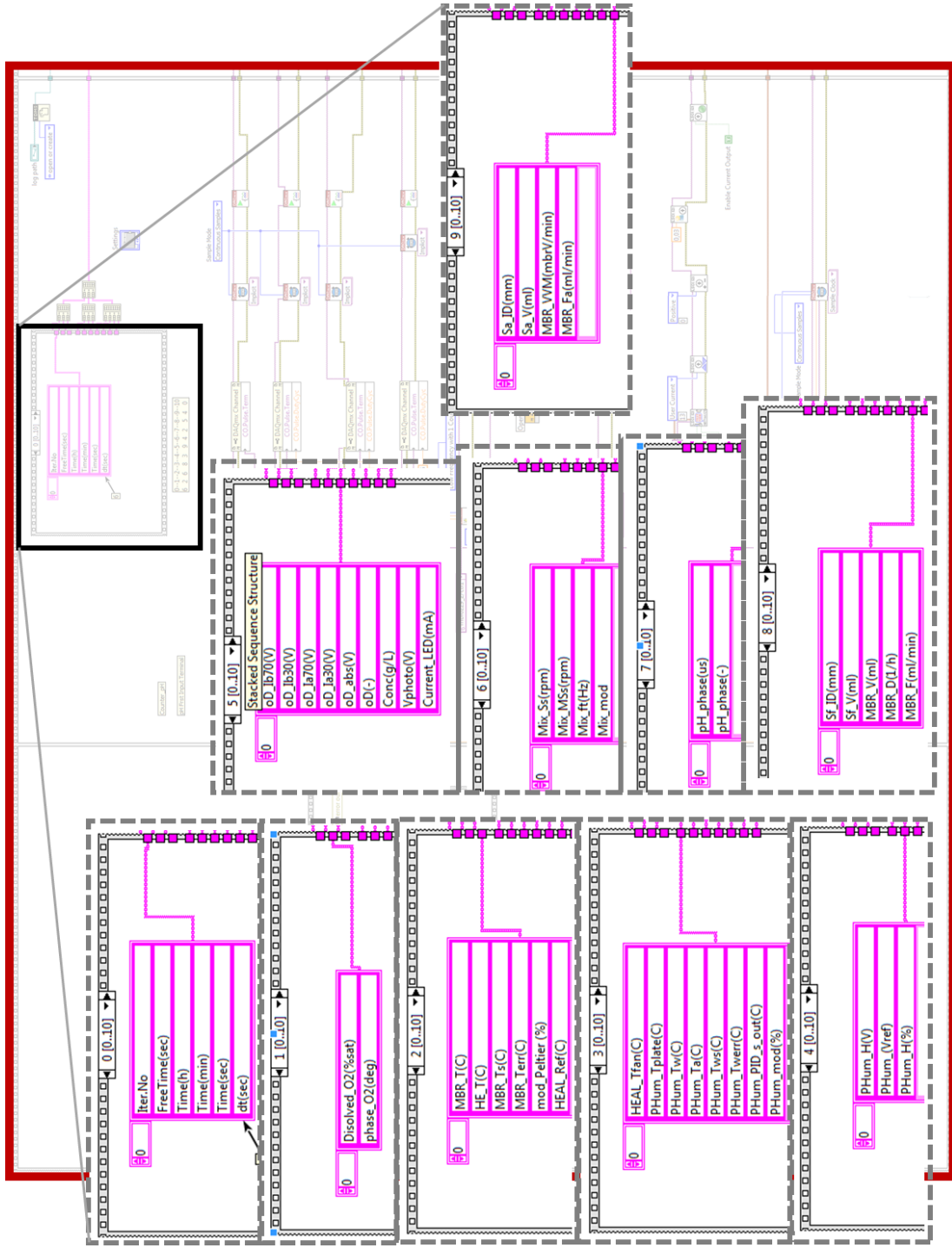


Figure 16. User graphical interface of the MSBR cultivation platform developed in LabView – Block diagram of the initialization routine – Creating the header names for log file.





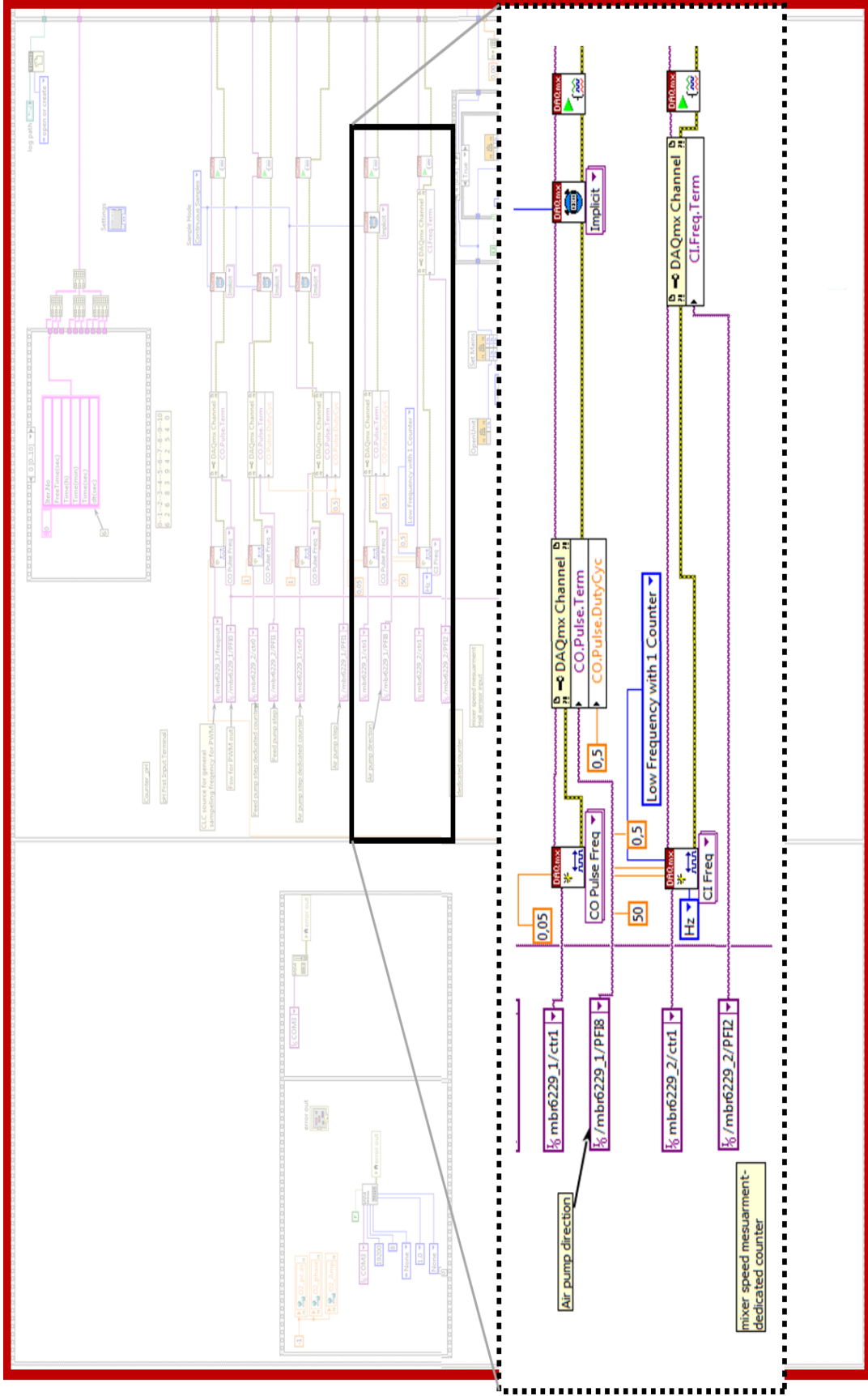


Figure 19. User graphical interface of the MSBR cultivation platform developed in LabView – Block diagram of the initialization routine – Creating the channel for outputting the frequency of the pump used in aeration and the frequency measurement of the Hall sensors used in connection with a DC motor which drives the stirrer to achieve the speed measurement.







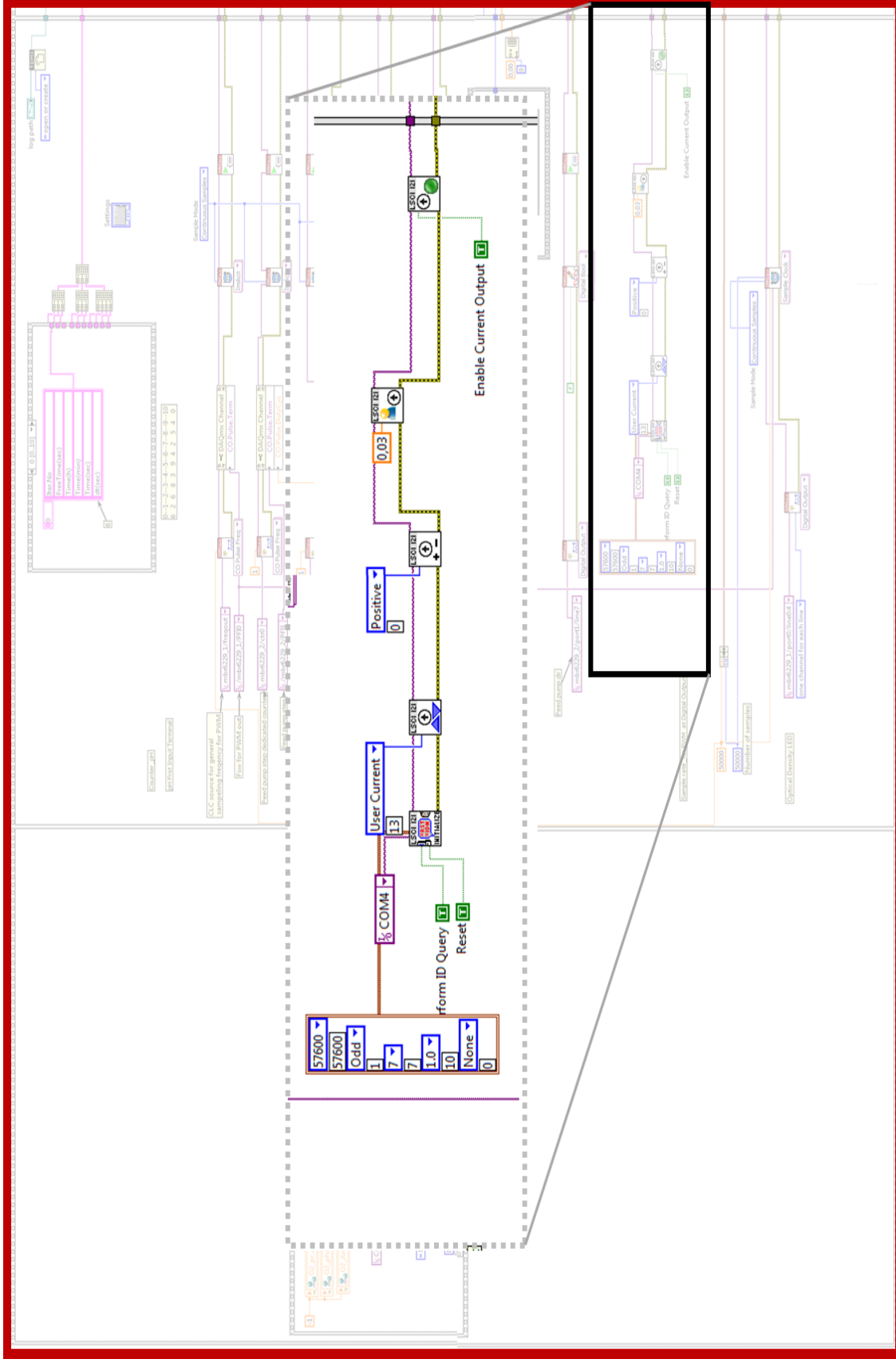


Figure 22. User graphical interface of the MSBR cultivation platform developed in LabView – Block diagram of the initialization routine – Setting up the communication with DC121 current supply and initializing the current value to 30 mA.

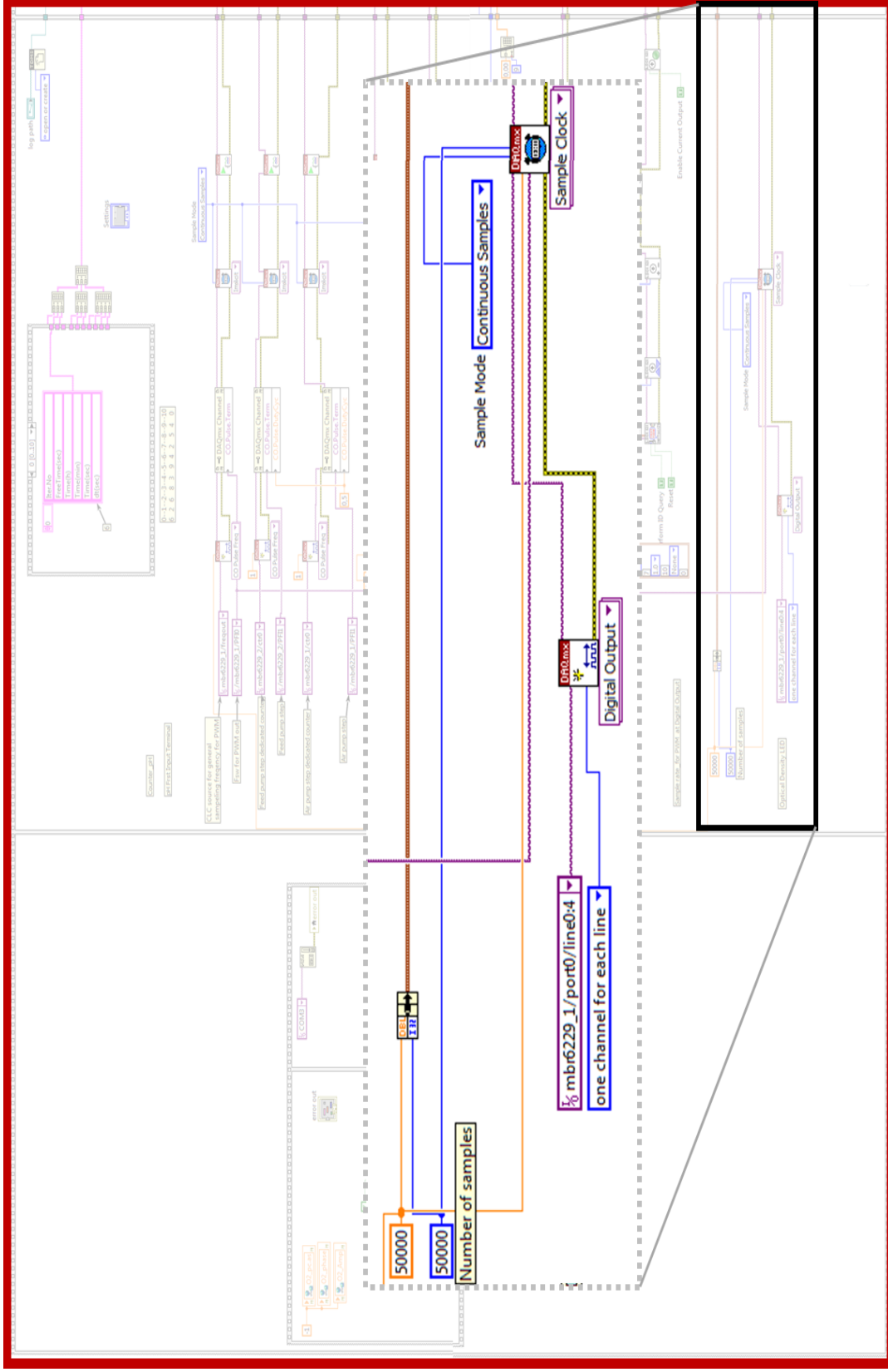


Figure 23. User graphical interface of the MSBR cultivation platform developed in LabView – Block diagram of the initialization routine – Reserving digital output line of 5 for all PWM channels and initializing its waveform memory buffer for 50000 samples, resulting in 1 sec of PWM waveform which is looped continuously.

Main measurement and control loop (~1sec)

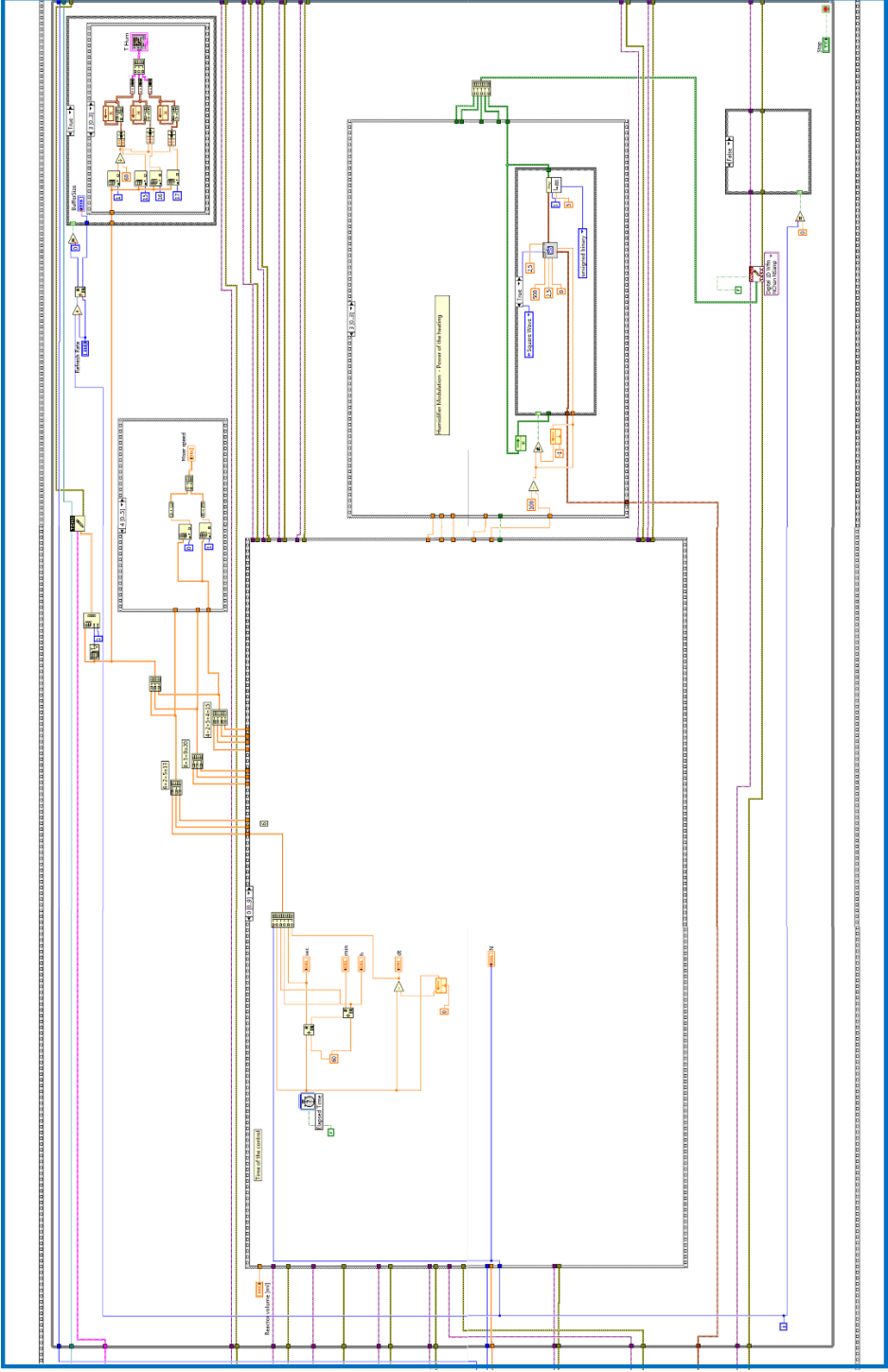


Figure 24. User graphical interface of the MSBR cultivation platform developed in LabView – Block diagram of the main control routine.

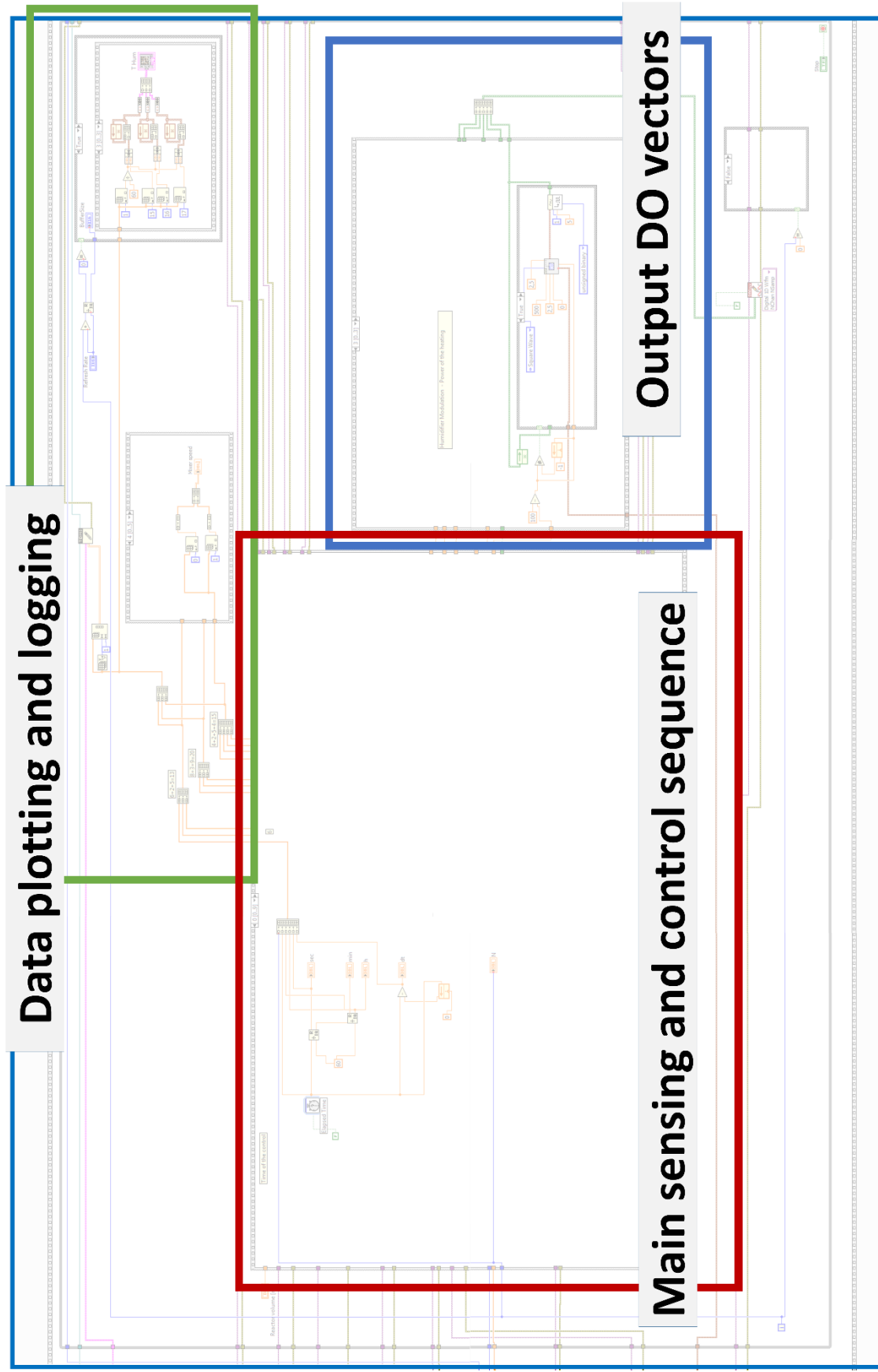


Figure 25. User graphical interface of the MSBR cultivation platform developed in LabView – Block diagram of the main control routine with overview of blocks with different functionality.

# Frame 1: Time update and calculation

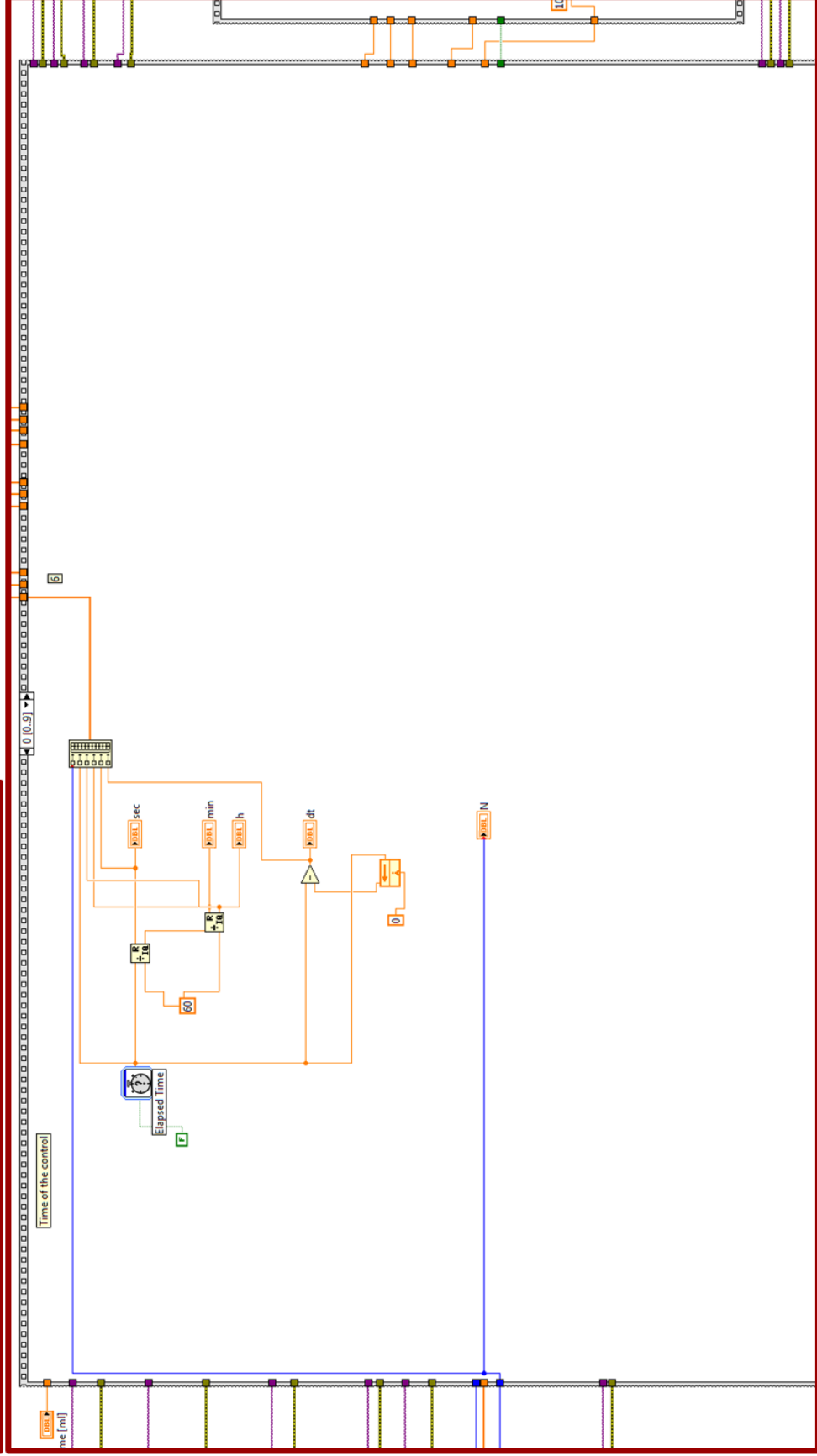


Figure 26. User graphical interface of the MSBR cultivation platform developed in LabView – Block diagram of the main control routine – 1<sup>st</sup> in the sequence of tasks is the time calculation.

## Frame 2: MSBR Temperature Measurement and Control

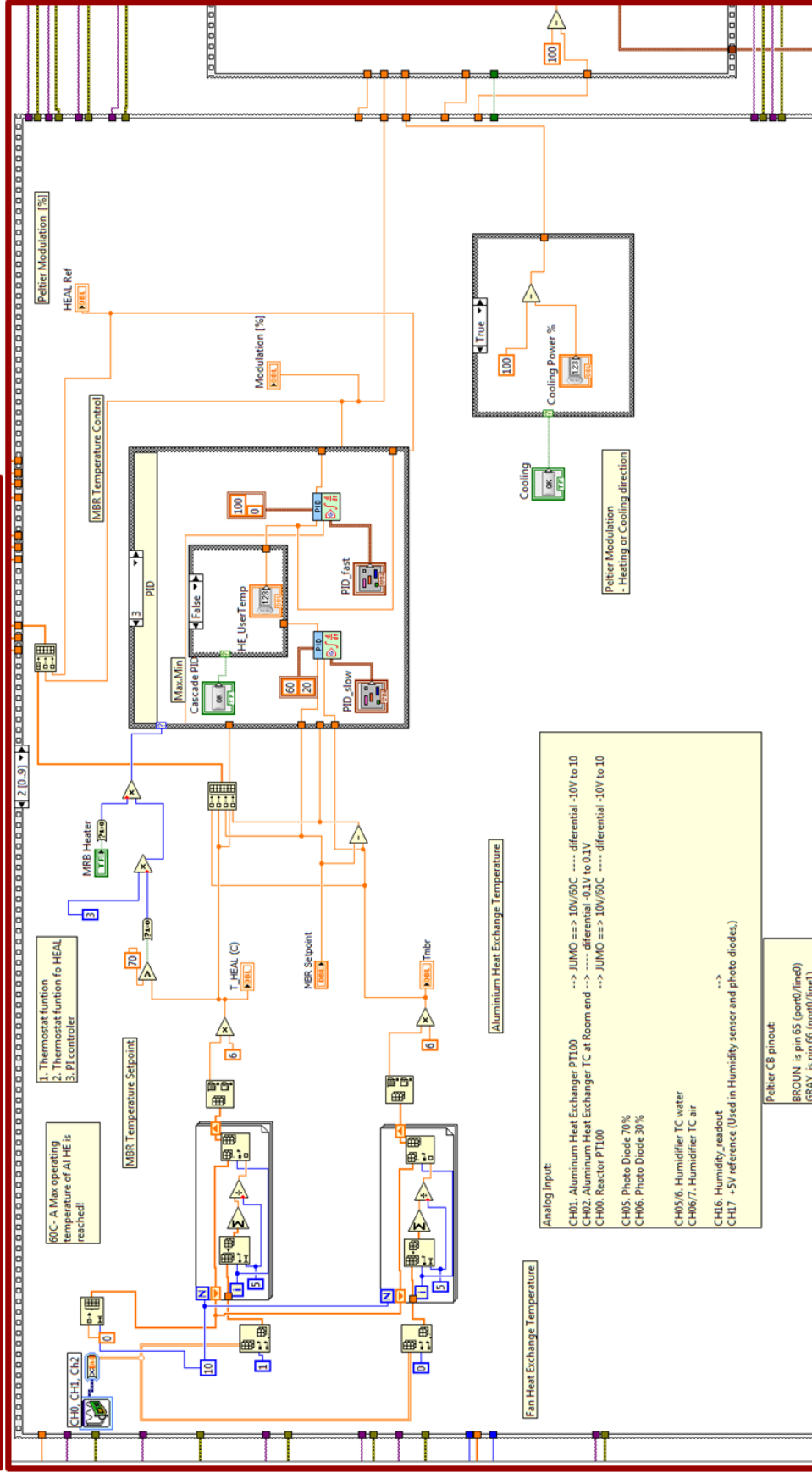


Figure 27. User graphical interface of the MSBR cultivation platform developed in LabView – Block diagram of the main control routine – 2nd frame in the sequence of tasks is the MSBR temperature control





# Frame 5: Optical Density Measurement

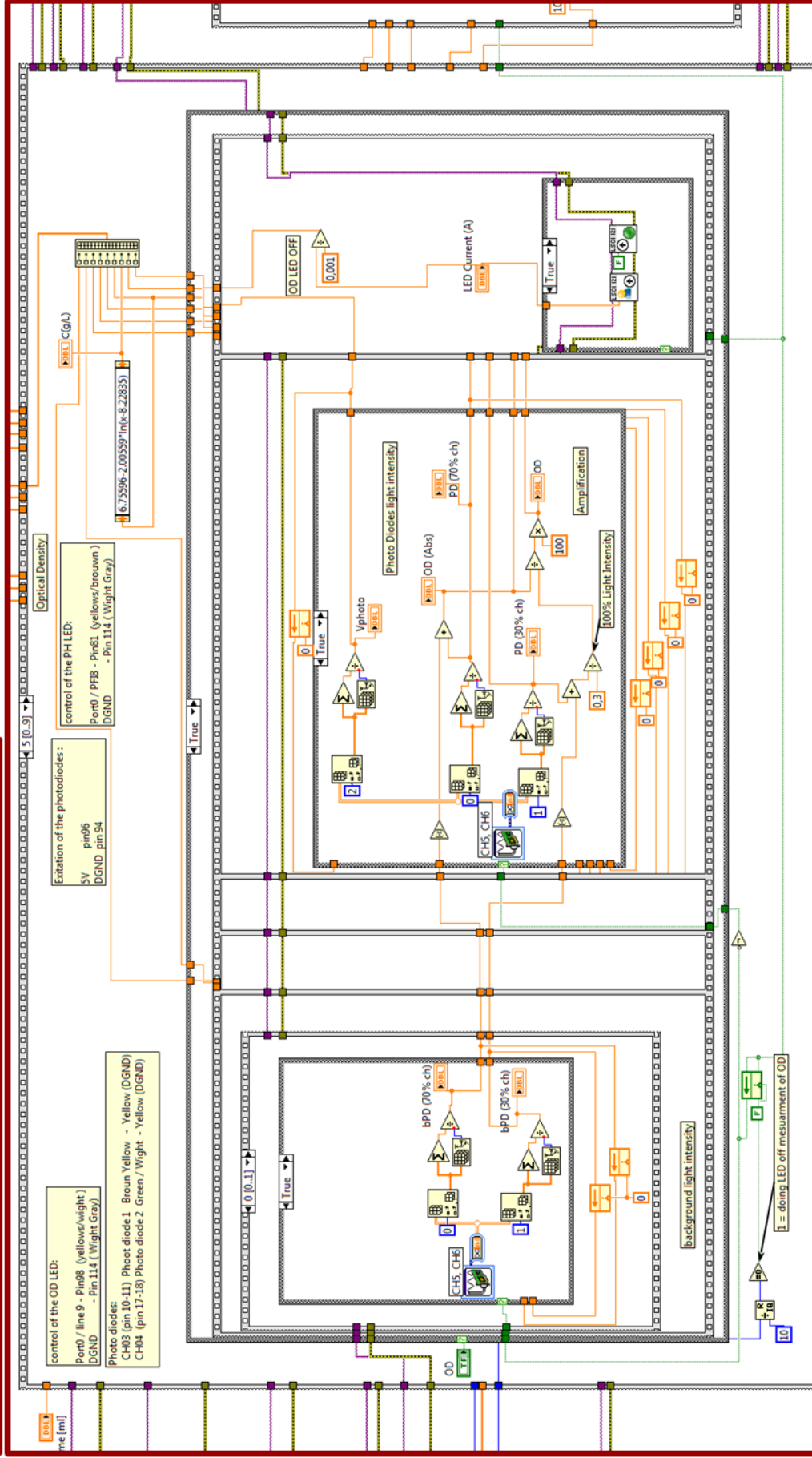


Figure 29. User graphical interface of the MSBR cultivation platform developed in LabView – Block diagram of the main control routine – 5<sup>th</sup> frame in the sequence of tasks is the scatter light measurement.

## Frame 6: Mixer Speed Measurement and Control

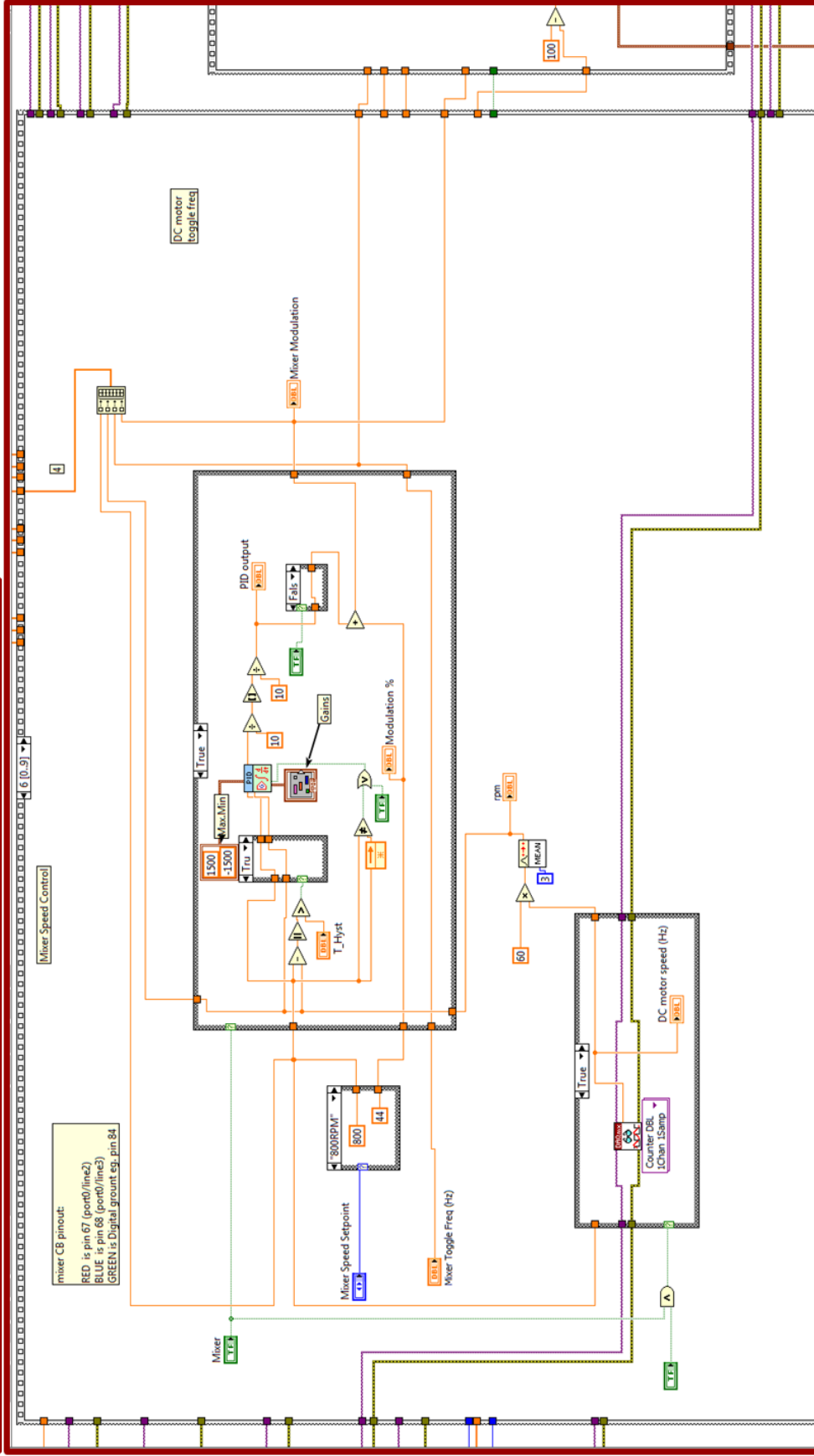


Figure 30. User graphical interface of the MSBR cultivation platform developed in LabView – Block diagram of the main control routine – 6<sup>th</sup> frame in the sequence of tasks is the scatter light measurement.

Frame number 7 in the sequence of tasks was allocated for pH measurement and control.

**Frame 8: Feed syringe pump control of direction and speed**

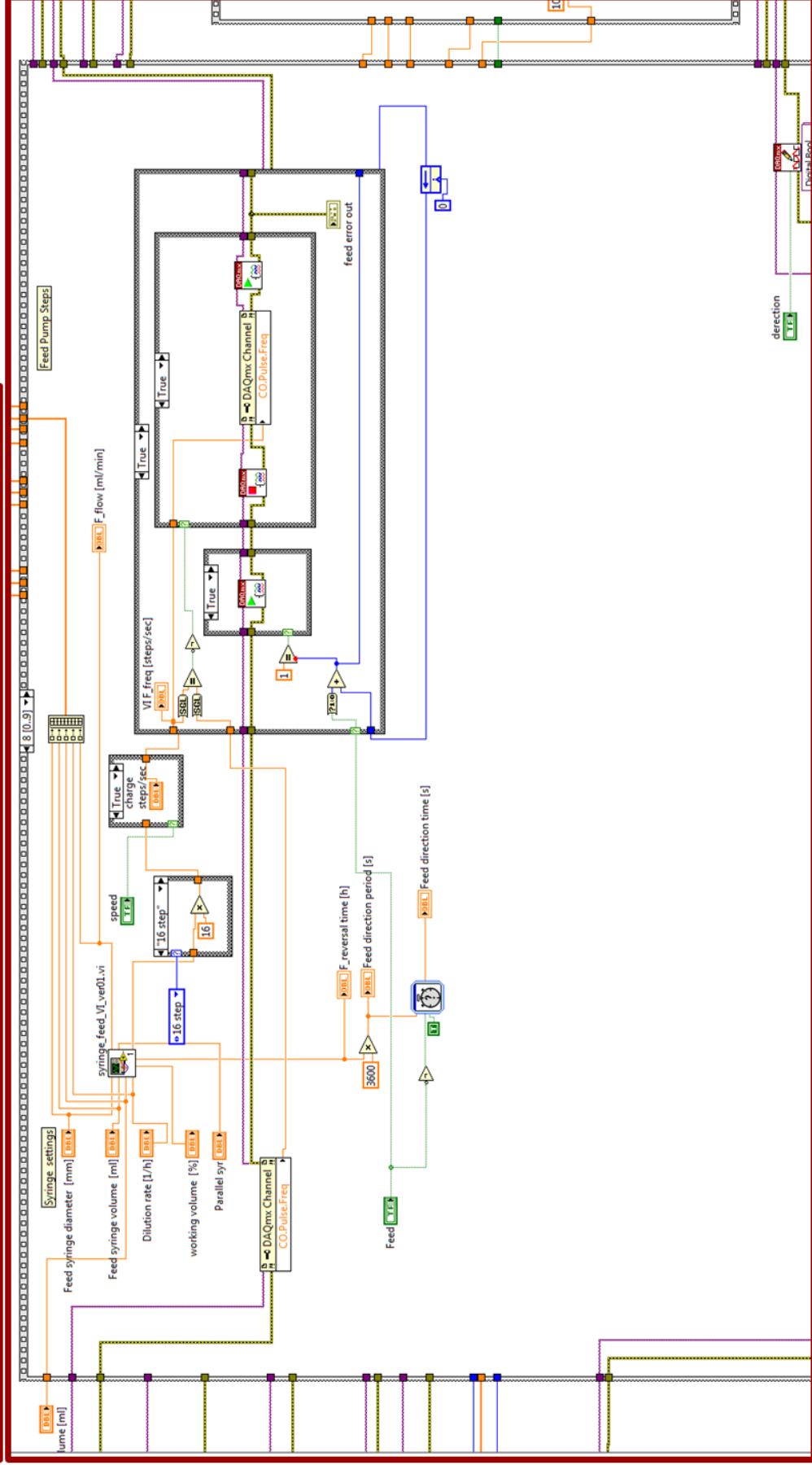


Figure 31. User graphical interface of the MSBR cultivation platform developed in LabView – Block diagram of the main control routine – 8<sup>th</sup> frame in the sequence of tasks is the control of the syringe pump used for feed inflow and outflow.

# Frame 9: Aeration syringe pump control of direction and speed

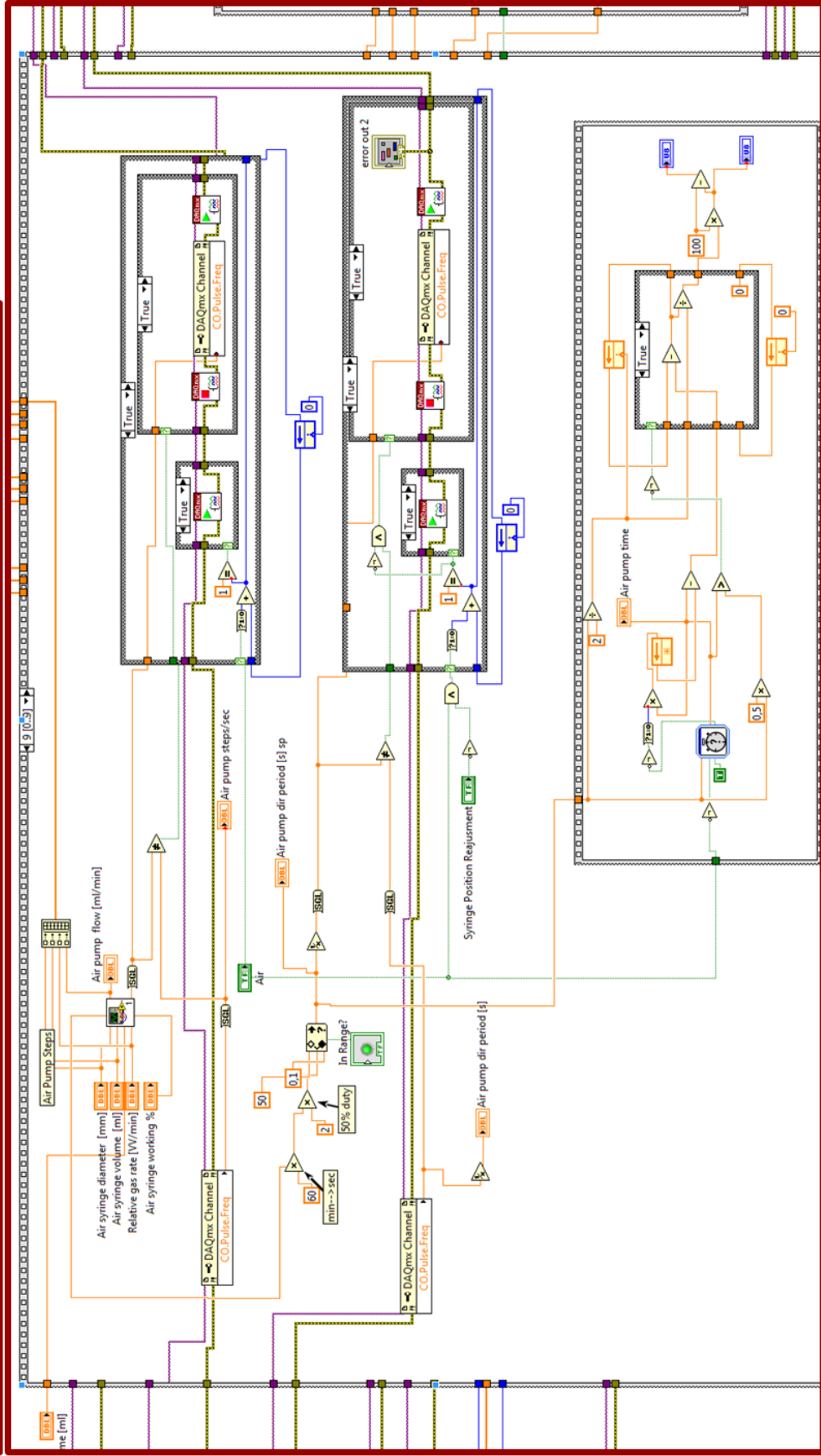


Figure 32. User graphical interface of the MSBR cultivation platform developed in LabView – Block diagram of the main control routine – 8<sup>th</sup> frame in the sequence of tasks is the control of the syringe pump used for aeration.

## DO Frame 0: MSBR temperature control – Peltier PWM modulation

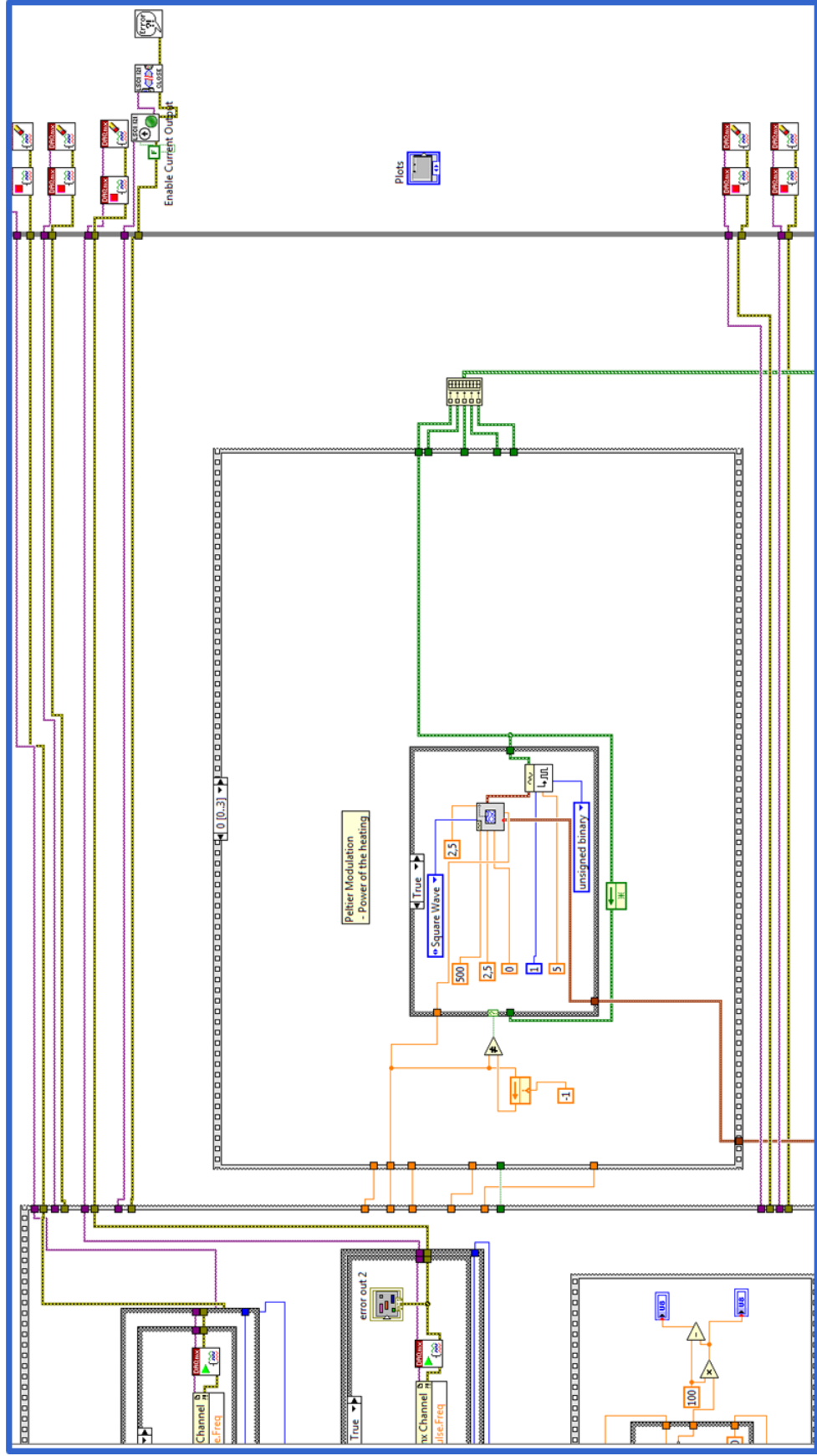


Figure 33. User graphical interface of the MSBR cultivation platform developed in LabView – Block diagram of the main control routine – the PWM digital output waveform update. Frame 0 outputs the voltage to the Peltier element (MSBR heater).

## DO Frame 1: MBR temperature control – Peltier heating or cooling

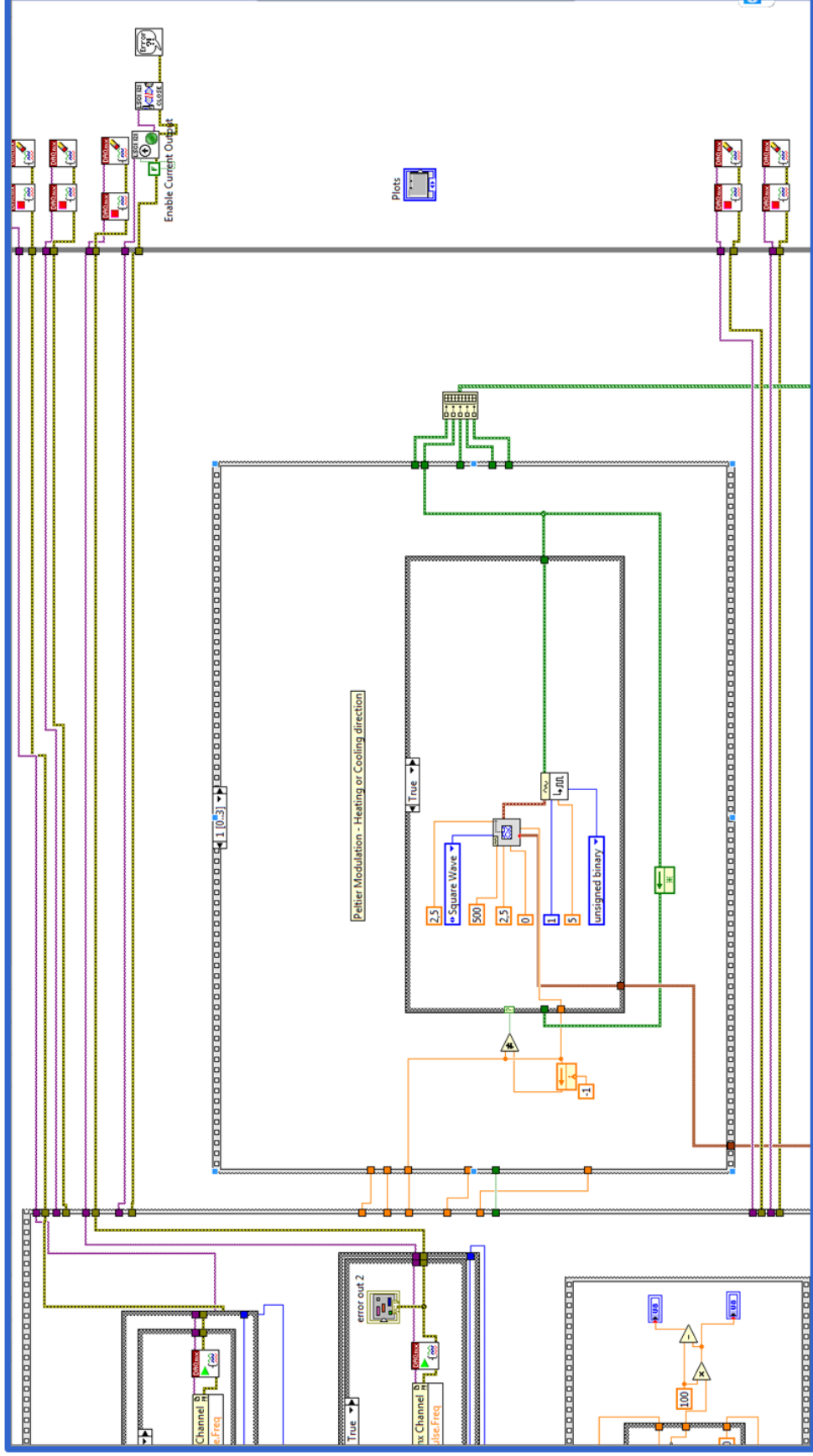


Figure 34. User graphical interface of the MSBR cultivation platform developed in LabView – Block diagram of the main control routine – the PWM digital output waveform update. Frame 1 outputs the voltage to the Peltier element (MSBR heater) controlling the direction of the heating power (heating or cooling).

## DO Frame 2: MBR stirrer speed control with PWM modulation

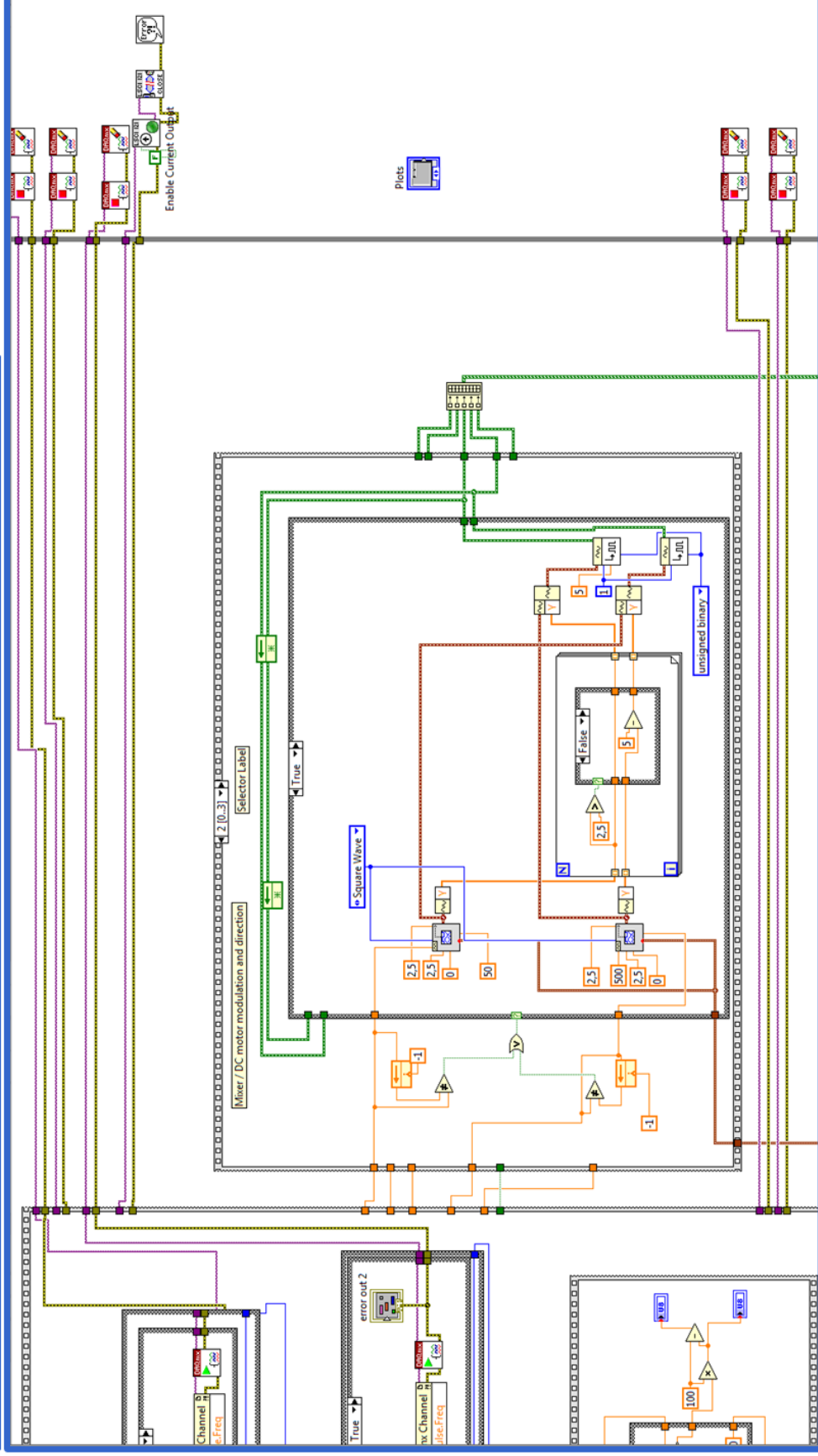


Figure 35. User graphical interface of the MSBR cultivation platform developed in LabView – Block diagram of the main control routine – the PWM digital output waveform update. Frame 2 outputs the voltage to the DC motor (MSBR stirrer) controlling the speed of the stirrer



### DO Frame 3: Humidifier temperature control with PWM modulation

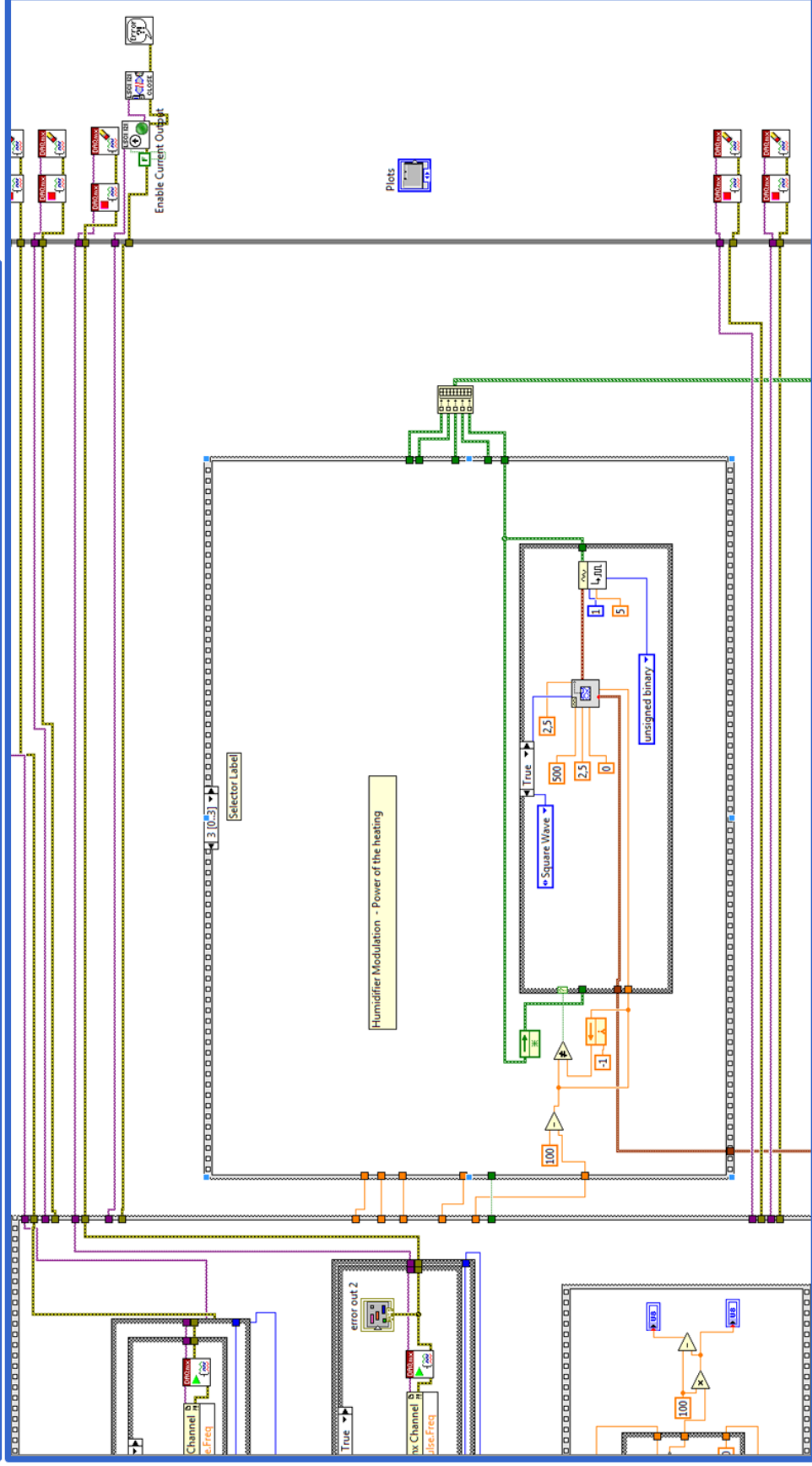


Figure 36. User graphical interface of the MSBR cultivation platform developed in LabView – Block diagram of the main control routine – the PWM digital output waveform update. Frame 2 outputs the voltage to the humidifier heater realizing the temperature control of the humidifier.

# MSBR data logging and process variables plots update

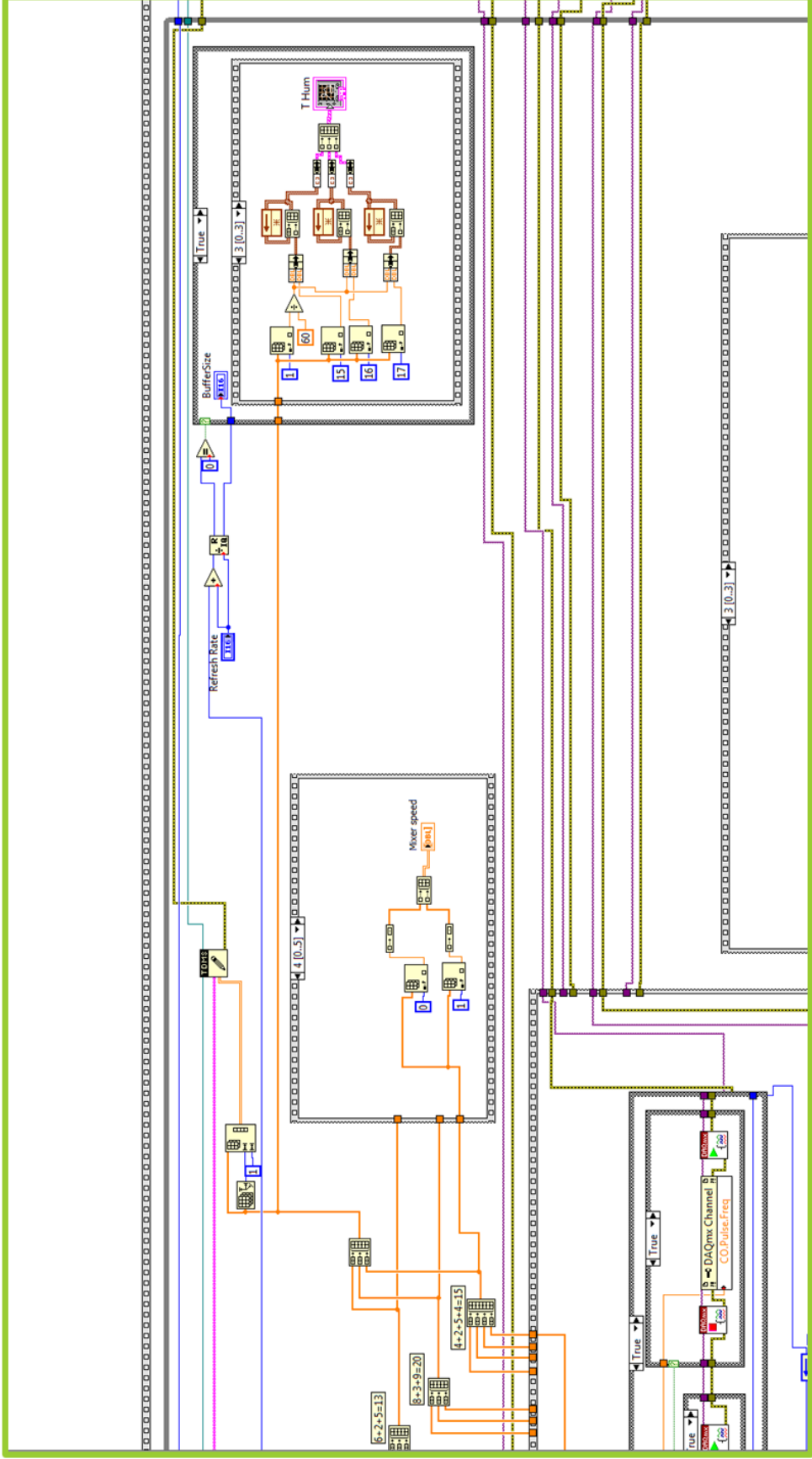


Figure 37. User graphical interface of the MSBR cultivation platform developed in LabView – Block diagram of the main control routine – the data logging and GUI plot updates.

**Process and Systems Engineering Center (PROSYS)  
Department of Chemical and Biochemical Engineering  
Technical University of Denmark**

Søltofts Plads, Building 229  
DK - 2800 Kgs. Lyngby  
Denmark

Phone: +45 45 25 28 00

Web: [www.kt.dtu.dk/forskning/prosys](http://www.kt.dtu.dk/forskning/prosys)